WELDING Journal

March 2010

Brazing and Soldering Today

Help in Choosing Shielding Gases

New Welding Wire for Thin Sheet

PUBLISHED BY THE AMERICAN WELDING SOCIETY TO ADVANCE THE SCIENCE, TECHNOLOGY, AND APPLICATION OF WELDING AND ALLIED JOINING AND CUTTING PROCESSES, INCLUDING BRAZING, SOLDERING, AND THERMAL SPRAYING

Built TOUGH in the USA by CMI for Welders around the WORLD.
Your best source for Semi-Automatic and Automatic MIG welding guns including air and water cooled, Push-Pull, and Smoke Extractor.
With us, customer support comes first: from custom designed MIG guns and consumables to rapid delivery.
For a complete range of our products, visit us online at cmindustries.com or call us toll free. 1-800-530-0032
CMI 400A
Replacement Reamer Blades
Model 2100E
CM Industries has a full line of Robotic Nozzle Cleaning Stations, Wire Cutters, and Replacement Reamer Blades to choose from. Make robotic nozzle cleaning operations easier with CMI.
CM INDUSTRIES® INC.
505 Oakwood Rd. Lake Zurich, ILLINOIS 60047
PH. 847-550-0033 FX. 847-550-0444
CMINDUSTRIES.COM EMAIL: SALES@CMINDUSTRIES.COM
For Info go to www.aws.org/ad-index

CONTENTS

March 2010 • Volume 89 • Number 3

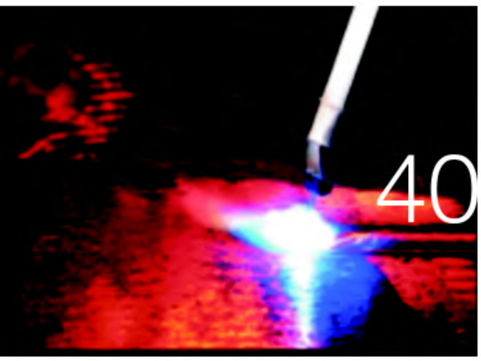

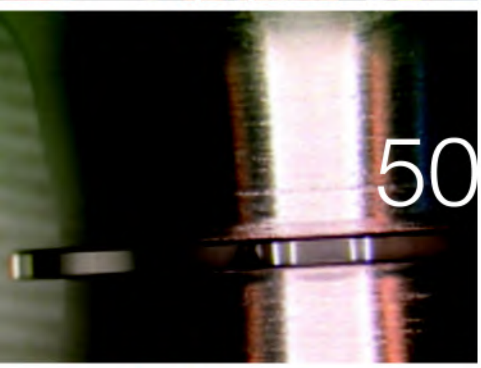

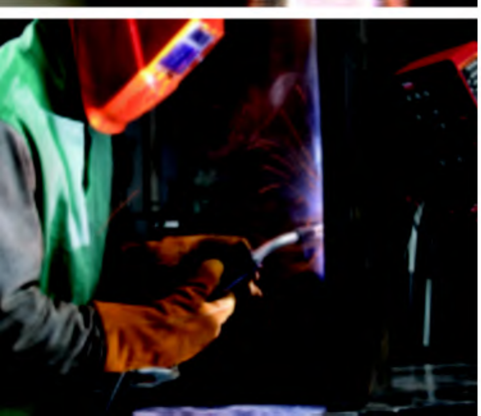

Features

Brazing & Soldering Today

Welding Research Supplement

On the cover: For users of the FCAW-G process, the choice of which shielding gas to use should be based on how it most positively influences the overall driving factors of cost, quality, and productivity to their welding operations. (Photo courtesy of The Lincoln Electric Co., Cleveland, Ohio.)

AWS Web site *www.aws.org*

Departments

Welding Journal (ISSN 0043-2296) is published monthly by the American Welding Society for $120.00 per year in the United States and possessions, $160 per year in foreign countries: $7.50 per single issue for domestic AWS members and $10.00 per single issue for nonmembers and $14.00 single issue for international. American Welding Society is located at 550 NW LeJeune Rd., Miami, FL 33126-5671; telephone (305) 443-9353. Periodicals postage paid in Miami, Fla., and additional mailing offices. **POSTMASTER:** Send address changes to Welding Journal, 550 NW LeJeune Rd., Miami, FL 33126-5671. **Canada Post:** Publications Mail Agreement #40612608 Canada Returns to be sent to Bleuchip International, P.O. Box 25542, London, ON N6C 6B2

$8 Billion Awarded to States for High-Speed Rail Projects

The U.S. Department of Transportation is awarding $8 billion to states across the country for developing America's first nationwide program of high-speed intercity passenger rail service. "Through the Recovery Act, we are making the largest investment in infrastructure since the Interstate Highway System was created, putting Americans to work rebuilding our roads, bridges, and waterways for the future," said President Barack Obama.

These awards will serve as a down payment on developing or laying the groundwork for 13 new, large-scale high-speed rail corridors across the country. The major corridors are part of a total of 31 states receiving investments. In addition, the grants are expected to have an up-front job and economic impact. It is expected this investment will create or save tens of thousands of jobs over time in areas like track laying, manufacturing, planning and engineering, plus rail maintenance and operations.

High Employee Turnover Cited for Faulty Pipe Welds at Northrop Grumman Shipbuilding

The U.S. Navy released a statement about SUPSHIP Gulf Coast (SSGC) identifying an unacceptable number of deficient welds on piping systems produced by Northrop Grumman Shipbuilding (NGSB). These defects were fixed, and SSGC issued a corrective action request that led to NGSB's plan of action for correcting process problems.

Many factors contributed to this situation, such as the high turnover rate of Northrop Grumman Shipbuilding-Gulf Coast (NGSB-GC) employees due to Hurricane Katrina, particularly in the New Orleans area. "This resulted in less-experienced production and inspection shipbuilding personnel requiring more oversight than the shipbuilder and/or SUPSHIP quality assurance organizations could supply," the statement read.

In response, SSGC hired more than 230 new employees in the past four years, and factored with high attrition, there's been a 30% increase in manning including a Navy captain assigned as the deputy supervisor for operations.

"As a result of corrective actions taken since the pipe weld problem was discovered, the first time quality defect rate of pipe welds improved from more than 15% to less than 2% (all of which are being corrected)," the statement read. "Additionally, working with SSGC, NGSB-GC engineering has reviewed and reduced the number of pipe joint designs used by production, thus simplifying the welding requirements to decrease the likelihood of deficient welds. The number of overall pipe joints has also been reduced dramatically, with emphasis on minimizing the number of joints having to be completed shipboard where it is more difficult, and instead producing them in the craft shops where conditions are optimized for the craftsman to produce a better product."

New Web Site Promotes Welding Careers

Visit www.CareersInWelding.com *to discover the importance of welding along with fun facts, people and company profiles, salary information, industry news, plus welding publications and videos.*

The American Welding Society (AWS) and National Center for Welding Education & Training (Weld-Ed) Web site, *www.CareersInWelding.com*, is now operational. An expansion of the *Careers In Welding* magazine, it contains the following details: people and companies in the welding industry; fun facts; salary information; industry news; videos; articles; and upcoming trainings, seminars, and events. Also, it features pages geared directly for students with scholarship information and a welding school locator; for welding professionals to build a résumé, find welding-related jobs, and learn about AWS certifications; and for educators to discover tips for teachers and guidance counselors, information about curricula, professional development, and resources.

This Web site serves as a valuable tool for students, parents, educators, counselors, and welding professionals. In addition, it offers an opportunity to send questions, comments, or ideas for people profiles.

WELDING journal

Publisher *Andrew Cullison*

Editorial
Editorial Director *Andrew Cullison*
Editor *Mary Ruth Johnsen*
Associate Editor *Howard M. Woodward*
Associate Editor *Kristin Campbell*
Peer Review Coordinator *Erin Adams*

Publisher Emeritus *Jeff Weber*

Graphics and Production
Production Manager *Zaida Chavez*
Senior Production Coordinator *Brenda Flores*

Advertising
National Sales Director *Rob Saltzstein*
Advertising Sales Representative *Lea Garrigan Badwy*
Senior Advertising Production Manager *Frank Wilson*

Subscriptions
Subscriptions Representative *Edalia Suarez*
esuarez@aws.org

American Welding Society
550 NW LeJeune Rd., Miami, FL 33126
(305) 443-9353 or (800) 443-9353


SAY YOU'RE
THE BEST,
WITHOUT SAYING A WORD
ONLY THE HIGHEST QUALITY MIG GUNS WILL DO.
Tweco®
TRUSTED BY AMERICAN LABOR
THERMADYNE
For Info go to www.aws.org/ad-index
WWW.TWECO.COM

D1.1: How Often Is Too Often?

How frequently should a code like D1.1, *Structural Welding Code — Steel*, be updated?

The question is simple, and over the past few years, the D1 Structural Welding Committee has asked it many times. Many issues, however, should be considered when developing an answer. During a recent discussion, a previous statement from long-time committee member William A. Milek Jr. was recalled and quoted: "The value of a standard is reflected by its longevity."

To some of us, there is wisdom in those words.

The American Welding Society published the first edition of the *Code for Fusion Welding and Gas Cutting in Building Construction* in 1928. The first bridge welding specification was published separately in 1936. AWS D1.1 was first issued in 1972 and covered both buildings and bridges. This practice continued until 1988 with the issuance of the AASHTO/AWS joint publication D1.5, whereupon welding requirements for bridge and building applications were once again separated.

In the 41-year period from the printing of the first building welding code in 1928 until the last building-only code in 1969, nine editions were issued with an average time between them of five years. In the earliest years of D1.1, it was published every three years with annual interim revisions. In the late 1970s, the interim revisions gave way to annual publication. Since 1986, D1.1 has been issued every two years.

After 24 years of this every other year tradition, it is fair to ask, "Why change?" After all, "If it ain't broke, don't fix it." However, in the minds of some of us on the D1 Committee, the publication cycle was "broke" and needed fixing. Consider the following:

- Some D1.1 purchasers have said the issue-to-issue changes are minor and not enough to justify a new edition
- Fabricators with multiple projects in their shops at the same time often find each project governed by a different edition of D1.1, adding unnecessary confusion to welding operations
- Engineers and designers cite the number of construction standards (not just welding codes) and the frequency of revisions as major factors adding complexity to their jobs.

Donald Rager, my predecessor as D1 chair, decided to challenge the status quo of the past two decades. With the support of the D1 Executive Subcommittee, a variety of presentations were made, eventually resulting in the topic being discussed by the AWS board of directors. The board commissioned an independent study — with a focus on publication frequency — to obtain the opinions of D1 purchasers.

Key findings of the study included the following:

- Fewer than one-third of the respondents (30%) recommended that D1.1 be revised on a two-year or more frequent cycle.
- More than two-thirds of the respondents indicated that D1.1 represents a fair to excellent value based on its purchase price.

The study offered the opportunity for verbatim comments to be submitted. Some not-so-bashful D1 purchasers were quite outspoken. Following are representative comments:

- "Stop making ridiculous changes in order to sell more code books."
- "Code revisions are too frequent. Once every four or five years is sufficient. It is perceived as forced to increase income."

Rather than rejecting these types of comments as simply the voice of malcontents, the AWS board welcomed the feedback, and put the issue back into the D1 Committee's hands, requesting that it review the study's findings and recommend a plan. A plan was developed and eventually adopted by both the D1 Committee and the AWS board of directors.

Starting with the 2010 edition, D1.1, *Structural Welding Code — Steel*, will be published on a five-year cycle. This frequency is consistent with that of the American Institute of Steel Construction steel specifications and the American National Standards Institute requirement that standards be reaffirmed or revised on a five-year cycle.

D1.1 users are expected to experience multiple benefits from this change, but to me, what is most important is what it represents: AWS and its leadership are committed to being responsive and to make the changes necessary to better serve the needs of our industry.

So, when you get your copy of D1.1:2010, take care of it. You'll need it for the next five years.

Duane K. Miller
Chair, D1 Structural Welding Committee

AT&F Nuclear Opens One of the First 100-Ton Nuclear Fabricating Facilities Built in Decades

The AT&F Nuclear Fabrication Building in Cleveland, Ohio, offers clean-environment fabrication, welding, and assembly.

AT&F Nuclear Inc., in coordination with its parent, The American Tank & Fabricating Co. (AT&F), recently began operations at its newly built AT&F Nuclear Fabrication Building in Cleveland, Ohio. This 32,000-sq-ft building addition is one of the first 100-ton crane capacity structures built in the United States in decades and reflects AT&F's response to the emerging global nuclear new-build market, according to company officials.

"Creating a new 100-ton high-bay facility completely dedicated to serving the nuclear industry may be seen as a bold step," said AT&F President Michael Ripich, "but the market interest shown during construction indicates we are spot-on."

The facility is used for welding and assembling nuclear components, and the clean-environment fabrication of nonsafety and safety-related metal components. It features an 18 × 15 ft assembly and inspection pit. In addition, its six certifications stamps from the American Society of Mechanical Engineers include NPT (fabrication of nuclear appurtenances and supports), N (nuclear vessels, pumps, valves), and NS (nuclear supports).

With this building, AT&F adds manufacturing capacity to the 400,000 sq ft it already utilizes. As a steel and fabricating service center, it handles dedicating, upgrading, and materials processing from carbon, high-strength low-alloy, and stainless steels to exotic alloys. Also, it offers metal forming and rolling, laser beam cutting, and robotic contour beveling.

According to the World Nuclear Association, a private-sector organization promoting peaceful uses of nuclear power, "With 30 reactors being built around the world today, another 90 or more planned to come online during the next 10 years, and over 200 further back in the pipeline, the global nuclear industry is clearly going forward strongly."

The new building comes together during its construction phase.

This 100-ton crane provides unique fabrication capabilities at AT&F's nuclear facility.

Large Linear Friction Welding Machine Designed for Use in Aerospace Applications

At Thompson Friction Welding's headquarters near Birmingham, UK, an engineer inspects what is thought to be the world's largest linear friction welding machine, the E100, jointly designed by Moog and Thompson Friction Welding.

Moog Inc., East Aurora, N.Y., and Thompson Friction Welding, UK, have developed what they believe is the world's largest linear friction welding (LFW) machine, the E100. It is capable of welding a surface area of 10,000 mm^2 and extends the use of LFW in automotive and aerospace industries.

The equipment's automatic handling systems and rapid open/close features cut production cycle times while recharging of the accumulators takes around 30 s for the largest and longest welds. Also, it opens up new possibilities for welded fabrication of parts that previously needed to be machined from solid metal, and the companies believe it is set to transform how jet engines are manufactured. Thompson manufactured the machine at its UK facility.

"The machine weighs 100 tons, is 2.5 m (100 in.) tall, and has a huge capacity of 100 tons in terms of the amount of force that it can apply to a welded joint," said Steve Darnell, Moog's regional business manager for northwest Europe.

Moog's hydraulic servo system and support for the E100 included a closed-loop control system; multiple digitally controlled servovalves; hydraulic power plant; seven 105-gal gas volume accumulators; manifold and distribution pipe work installation; plus experience in friction welding and project management, design, development, manufacturing, and installation services.

Frost & Sullivan Recognizes ESAB with Energy Generation Award

Frost & Sullivan's 2009 Global Best Partners Welding & Cutting Systems for Energy Generation Award has been presented to ESAB. The company has emerged as a leading manufacturer of welding and cutting systems for energy generation industries including power, LNG tanks, offshore, and pipelines industries in Europe. In 2009, it also accounted for nearly 18% of the global welding and cutting market for energy generation.

"Key performance drivers for ESAB have been its unique product range in response to the energy-specific needs of various industries, being a one-stop shop and having globally dis-

ESAB recently received Frost & Sullivan's 2009 Global Best Partners Welding & Cutting Systems for Energy Generation Award. Ian Muir (left), global HR director, ESAB Holdings Ltd., poses at the award ceremony with Iain Jawad, director, strategic partnerships, Frost & Sullivan.

persed manufacturing facilities," said Frost & Sullivan Senior Research Analyst Archana Chauhan. "Providing a comprehensive service portfolio at competitive prices, minimizing machine downtime, and ensuring customer focused growth has also been central to its success."

International Training Institute Awarded Nearly $5 Million for 'Green' Job Training

The International Training Institute (ITI) for the sheet metal and air-conditioning industries has been awarded nearly $5 million in Energy Training Partnership grants through the American Recovery and Reinvestment Act of 2009. These funds will be used to train approximately 1200 unemployed or underemployed sheet metal workers for energy-efficient-building construction, retrofitting, and manufacturing jobs.

While the grant will benefit areas in Michigan, Ohio, Missouri, Illinois, California, New Mexico, and Texas, this training program is available to all sheet metal workers. It will feature the following three areas of instruction: advanced building information modeling; HVAC testing, adjusting, and balancing; and phenolic installation. For more information on ITI or to take part in the program, visit *www.sheetmetal-iti.org*.

Western Enterprises Donates Welding Equipment to Great Oaks Career Campuses

Western Enterprises, Westlake, Ohio, has made a donation of its equipment to the Cincinnati-based Great Oaks Career Campuses in support of the school's welding program. This center was chosen based on its ability to train students for welding positions in various industries using processes like gas metal arc and gas tungsten arc welding, plasma cutting, and oxyfuel brazing.

The company provided a variety of equipment including shielding gas regulator/flowmeters, oxygen and acetylene regulators,

Mike Miller (left), product manager/industrial products for Western Enterprises, presents a sampling of the welding equipment donated by the company to Eric McCarthy (center) and Mike Burch, both instructors at the Great Oaks Career Campuses.

torch and regulator flashback arrestors, and quick disconnects. This donation will be used to equip the welding instruction labs in various facilities on the Great Oaks Career Campuses.

"Sponsoring students and promoting welding as a viable occupation is key to the future of this industry," said Mike Miller, product manager of industrial products for Western Enterprises.

Jet Edge Hosts AMT, NTMA Executives

Jet Edge, Inc., St. Michael, Minn., recently hosted the Association for Manufacturing Technology's (AMT) president and chief operating officer of the National Tooling and Machining Association (NTMA). AMT President Douglas K. Woods and Robert L. Akers Jr., NTMA chief operating officer, toured the company's headquarters. During this visit, they saw the waterjet manufacturer's 100,000-sq-ft manufacturing facility as well as demonstrations of its 90,000 lb/in.^{2} X-Stream® waterjet cutting

Shown during a visit to Jet Edge are (from left) Robert L. Akers Jr., NTMA chief operating officer; AMT President Douglas K. Woods; and Jet Edge President Jude Lague. (Photo courtesy of Jet Edge, Inc.)

technology. Woods and Akers also discussed the recession's impact on original equipment manufacturers with Jet Edge President Jude Lague, and they shared insight on how manufacturers can prepare for recovery.

Industry Notes

- **Adept Technology, Inc.**, Pleasanton, Calif., recently received a $3.2 million order for high-precision robots from an international manufacturer of test automation equipment.

- **Kapp Alloy & Wire**, Oil City, Pa., a solder and spraywire manufacturer, has been awarded an IT KickStart grant from the **Center for eBusiness and Advanced IT**. It will be used to update the main company and consumer ecommerce Web sites.

- **Farr Air Pollution Control**, Jonesboro, Ark., a producer of dust and fume collectors for industrial processes, now operates under the name **Camfil Farr Air Pollution Control**.

- The steel processing business segment of **Worthington Industries, Inc.**, acquired the steel processing assets of **Gibraltar Industries, Inc.**, including its Cleveland facility, the equipment/inventory in Buffalo, and a warehouse in Detroit.

- **VRSim**, East Hartford, Conn., has donated a portable SimWelder™ virtual reality welding training system to **Whittier Regional Vocational Technical High School**, Haverhill, Mass.

- The **Material Handling Industry of America** and **Automation Technologies Council** recently announced **ProMat** and **The International Robots, Vision & Motion Control Show** will colocate and be held March 21–24, 2011, at Chicago's McCormick Place.

- **Joseph T. Ryerson & Son, Inc.**, a subsidiary of Ryerson Inc., Chicago, Ill., acquired **Texas Steel Processing, Inc.**, Houston, Tex., for an aggregate purchase price of approx. $11.4 million.

- **United Tool & Die Co.**, West Hartford, Conn., joins **The Boeing Co.** as a partner of its nationwide team competing for the U.S. Air Force's contract to build a new fleet of aerial refueling tankers.

- The Accelerated Concept to Product process by **Engineering Technology Associates, Inc.**, won the 2nd Annual Society of Automotive Engineers Detroit Section/Massachusetts Institute of Technology Enterprise Forum Vehicle Innovation Competition.

- **Dresser-Rand Co.** acquired the assets of **Leading Edge Turbine Technologies, Inc.**, Houston, Tex., which operates a service and repair facility with welding, machining, and coating capabilities.

- **NASCAR, NHRA**, and other celebrity drivers recently went to Lake Placid, N.Y., for the Fifth Annual Lucas Oil Geoff Bodine Bobsled Challenge by **Whelen Engineering. The Lincoln Electric Co.** supported this event with a company-branded bobsled.

- Italian motion manufacturer **Nadella** signed **G. H. Binroth Co.**, Jackson, Mich., to distribute its linear guides and motion control components, plus provide applications support in the U.S.

- **AISI's Steel Market Development Institute** is celebrating two honors as the 2010 North American Car and Truck of the Year, the Ford Fusion hybrid and Ford Transit Connect, feature a number of lightweight, advanced high-strength steel technologies.

- **Protofab Engineering**, Blaine, Minn., a provider of machined parts and weldments, launched its new Web site at *www.protofabengineering.com* that offers an updated design.

Praxair China to Supply Welding Gases for High-Speed Railway

Praxair China recently signed a contract with Tangshan Railway Vehicle Co., Ltd., a subsidiary of China Northern Locomotive & Rolling Stock Industry Group, to supply welding gases used in the production of its newest high-speed train. The train will have a top speed of 350 km/h.

Praxair China will supply a laser welding gas mixture, which will be used during manufacture of the train's body. Prior to this contract, Praxair China had supplied welding gases for Tangshan Railway Vehicle for its 300 km/h high-speed train production.

Curtiss-Wright Flow Control to Supply Tie-Down Plates for British Aircraft Carriers

Curtiss-Wright Flow Control Co., Falls Church, Va., recently received a $6.4 million contract from BAE Systems, a member of the UK Aircraft Carrier Alliance, for the manufacture, test, and supply of more than 8500 aircraft tie-down link plates for the UK Royal Navy. The plates will be installed on board the HMS *Queen Elizabeth* and HMS *Prince of Wales*, which are the largest and most powerful surface warships ever constructed for the Royal Navy. The 65,000-ton carriers will be 280 m long and 70 m wide, capable of 250 knots maximum speed, and will have a total complement of 1500 personnel.

Tie-downs are welded onto the flight deck and hangar spaces and are used as hard points for securing the aircraft with chains or straps. Work for this contract will be performed at INDAL Technologies, a business unit of Curtiss-Wright Flow Control Co., based in Mississauga, Ont., Canada. Deliveries are scheduled between later this year and 2014.

GE Invests $1 Million at German Facility

A view of the balancing and calibration area at GE Sensing & Inspection Technologies' Odelzhausen, Germany, facility.

GE Sensing & Inspection Technologies recently announced it will spend $1 million to expand its Odelzhausen, Germany, facility, which designs and manufactures Rheonik coriolis flow meters used in the oil and gas and power-generation sectors. The expansion will create a flow meter calibration center to test and calibrate ultrasonic and coriolis flow meters. The project is expected to be in operation by the fourth quarter of this year.

The company acquired Rheonik in 2008, expanding its flow meter portfolio to include coriolis technology. The meters measure flow from 0.5 g/min to 1500 tons/h.

"The calibration center in Odelzhausen is a symbol of our investment in and commitment to expanding our global infrastructure, providing high-tech products and services for our customers," said Tim Povall, GE's general manager of measurement solutions.

Sumitomo Metal's Welded H Beam Being Used for Road Project in Japan

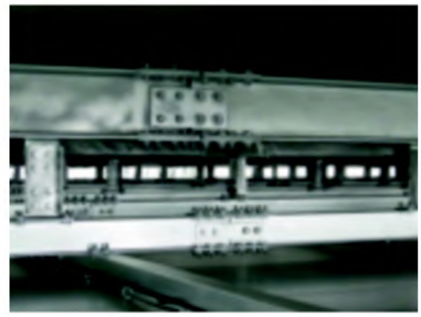

Upper side of sound-absorbing panel for underside of elevated road showing the lightweight supporting beams, which are manufactured using high-frequency resistance welding.

Sumitomo Metal Industries Ltd. SMart BEAM™ lightweight welded H beams are being used to support sound-absorbing panels for the underside of elevated portions of the Second Keihan Highway. The 28.3-km-long toll road currently under construction will link Kyoto and Osaka, Japan. It is expected to open soon.

The company has received orders for approxmately 1500 tons of the beams, which are continuously manufactured from hot-rolled coils by means of high-frequency resistance welding. Since they are thinner than standard rolled H-beams, it is possible to reduce the weight of the steel material used by up to 40%. In addition, since SMart beams are welded after the hot-rolled coils are cut to the necessary width, the company can manufacture various sizes with high dimensional precision.

PSTproducts Provides Electromagnetic Pulse Technology System to Sapa

A lightweight extruded aluminum seat structure made of Sapa extrusions joined at PSTproducts with electromagnetic pulse technology equipment.

Sapa Aluminium Sp. z o.o., Trzcianka, Poland, recently purchased an electromagnetic pulse technology (EMPT) system from PSTproducts, Alzenau, Germany. Sapa is initially using the system for testing, prototype manufacture, and small series production.

Electromagnetic pulse technology is a noncontact process for joining, welding, forming, and cutting of metals. For EMPT processing, electromagnetic coils are used to which a short but high-power electric current is applied. The coil produces electromagnetic forces that can, for example, change the diameter of tubes by compression or expansion.

Sapa Aluminium manufactures a variety of aluminum products and components for such applications as automotive instrument panel beams, furniture, cooling fins, ladders, solar collectors, yacht masts, gates, and scaffolding.

American Welding Society

Friends and Colleagues:

I want to encourage you to submit nomination packages for those individuals whom you feel have a history of accomplishments and contributions to our profession consistent with the standards set by the existing *Fellows*. In particular, I would make a special request that you look to the most senior members of your Section or District in considering members for nomination. In many cases, the colleagues and peers of these individuals who are the most familiar with their contributions, and who would normally nominate the candidate, are no longer with us. I want to be sure that we take the extra effort required to make sure that those truly worthy are not overlooked because no obvious individual was available to start the nomination process.

For specifics on the nomination requirements, please contact Wendy Sue Reeve at AWS headquarters in Miami, or simply follow the instructions on the Fellow nomination form in this issue of the *Welding Journal*. Please remember, we all benefit in the honoring of those who have made major contributions to our chosen profession and livelihood. The deadline for submission is July 1, 2010. The Committee looks forward to receiving numerous Fellow nominations for 2011 consideration.

Sincerely,

Nancy C. Cole
Chair, AWS Fellows Selection Committee

American Welding Society

Fellow Description

DEFINITION AND HISTORY

The American Welding Society, in 1990, established the honor of Fellow of the Society to recognize members for distinguished contributions to the field of welding science and technology, and for promoting and sustaining the professional stature of the field. Election as a Fellow of the Society is based on the outstanding accomplishments and technical impact of the individual. Such accomplishments will have advanced the science, technology and application of welding, as evidenced by:

* Sustained service and performance in the advancement of welding science and technology
* Publication of papers, articles and books which enhance knowledge of welding
* Innovative development of welding technology
* Society and chapter contributions
* Professional recognition

RULES

1. Candidates shall have 10 years of membership in AWS
2. Candidates shall be nominated by any five members of the Society
3. Nominations shall be submitted on the official form available from AWS Headquarters
4. Nominations must be submitted to AWS Headquarters *no later than July 1 of the year prior* to that in which the award is to be presented
5. Nominations will remain valid for three years
6. All information on nominees will be held in strict confidence
7. No more than two posthumous Fellows may be elected each year

NUMBER OF FELLOWS

Maximum of 10 Fellows selected each year.

AWS Fellow Application Guidelines

Nomination packages for AWS Fellow should clearly demonstrate the candidates outstanding contributions to the advancement of welding science and technology. In order for the Fellows Selection Committee to fairly assess the candidates qualifications, the nomination package must list and clearly describe the candidates specific technical accomplishments, how they contributed to the advancement of welding technology, and that these contributions were sustained. Essential in demonstrating the candidates impact are the following (in approximate order of importance).

1. Description of significant technical advancements. This should be a brief summary of the candidates most significant contributions to the advancement of welding science and technology.
2. Publications of books, papers, articles or other significant scholarly works that demonstrate the contributions cited in (1). Where possible, papers and articles should be designated as to whether they were published in peer-reviewed journals.
3. Inventions and patents.
4. Professional recognition including awards and honors from AWS and other professional societies.
5. Meaningful participation in technical committees. Indicate the number of years served on these committees and any leadership roles (chair, vice-chair, subcommittee responsibilities, etc.).
6. Contributions to handbooks and standards.
7. Presentations made at technical conferences and section meetings.
8. Consultancy — particularly as it impacts technology advancement.
9. Leadership at the technical society or corporate level, particularly as it impacts advancement of welding technology.
10. Participation on organizing committees for technical programming.
11. Advocacy — support of the society and its technical advancement through institutional, political or other means.

Note: Application packages that do not support the candidate using the metrics listed above will have a very low probability of success.

Supporting Letters

Letters of support from individuals knowledgeable of the candidate and his/her contributions are encouraged. These letters should address the metrics listed above and provide personal insight into the contributions and stature of the candidate. Letters of support that simply endorse the candidate will have little impact on the selection process.

Return completed Fellow nomination package to:

Wendy S. Reeve
American Welding Society
Senior Manager
Award Programs and Administrative Support
550 N.W. LeJeune Road
Miami, FL 33126

Telephone: 800-443-9353, extension 293

SUBMISSION DEADLINE: July 1, 2010

(please type or print in black ink)

CLASS OF 2011

FELLOW NOMINATION FORM

DATE_______________NAME OF CANDIDATE____

AWS MEMBER NO.______________________YEARS OF AWS MEMBERSHIP________________________________

HOME ADDRESS____

CITY_______________________________________STATE______ZIP CODE________PHONE____________________

PRESENT COMPANY/INSTITUTION AFFILIATION____

TITLE/POSITION____

BUSINESS ADDRESS____

CITY_______________________________________STATE______ZIP CODE________PHONE____________________

ACADEMIC BACKGROUND, AS APPLICABLE:

INSTITUTION____

MAJOR & MINOR____

DEGREES OR CERTIFICATES/YEAR____

LICENSED PROFESSIONAL ENGINEER: YES________NO_________ STATE__________________________

SIGNIFICANT WORK EXPERIENCE:

COMPANY/CITY/STATE____

POSITION____YEARS__________________

COMPANY/CITY/STATE____

POSITION____YEARS__________________

SUMMARIZE MAJOR CONTRIBUTIONS IN THESE POSITIONS:

____

____

____

IT IS MANDATORY THAT A CITATION (50 TO 100 WORDS, USE SEPARATE SHEET) INDICATING WHY THE NOMINEE SHOULD BE SELECTED AS AN AWS FELLOW ACCOMPANY NOMINATION PACKET. IF NOMINEE IS SELECTED, THIS STATEMENT MAY BE INCORPORATED WITHIN THE CITATION CERTIFICATE.

SEE GUIDELINES ON REVERSE SIDE

SUBMITTED BY: PROPOSER____________________________________AWS Member No.________________

Print Name______________________________

The Proposer will serve as the contact if the Selection Committee requires further information. Signatures on this nominating form, or supporting letters from each nominator, are required from four AWS members in addition to the Proposer. Signatures may be acquired by photocopying the original and transmitting to each nominating member. Once the signatures are secured, the total package should be submitted.

NOMINATING MEMBER:______________________________
Print Name______________________________
AWS Member No.____________

NOMINATING MEMBER:______________________________
Print Name______________________________
AWS Member No.____________

NOMINATING MEMBER:______________________________
Print Name______________________________
AWS Member No.____________

NOMINATING MEMBER:______________________________
Print Name______________________________
AWS Member No.____________

SUBMISSION DEADLINE July 1, 2010

Reader Praises Letter on the U.S. Economy

Lee A. Warncke recently wrote a Letter to the Editor that focused on the economy. It was published on page 14 of the January 2010 Welding Journal.

Whatever job or position Mr. Warncke holds, it's not the right one. He should be one of President Barack Obama's top economic advisors. Until our elected officials and the American people realize what Mr. Warncke is telling us, this stagnant economy isn't going to change. It is highly unlikely and very unfortunate that the average person will ever read his letter. Mr. Warncke should send a copy of his letter to a paper like *The New York Times*. My hat is off to him. Keep up the good work!

Louis Sohns
Welding Superintendent (ret.)
34-year AWS member
Fish Creek, Wis.

Reader Points out a Fourth Mechanism for Cathodic Cleaning

This comment refers to "Cathodic Cleaning of Oxides from Aluminum Surface by Variable-Polarity Arc," by R. Sarrafi and R. Kovacevic, January 2010 Welding Journal *pp 1-s to 10-s.*

On page 4-s the authors state, "Three main mechanisms are suggested in the literature of aluminum welding to describe the cathodic cleaning of oxides during the electrode positive polarity."

There is a fourth mechanism reported in the book *Welding Processes and Practices*, by Koellhoffer, Manz, and Hornberger, 1988. On page 280, POLARITY, it states the following concerning the cathode spots: "The arc current is conducted through these spots, and each spot becomes very hot. One theory of cleaning action says that the heat causes a tiny bit of aluminum to vaporize beneath the oxide layer. The vapor expands and 'pops' the oxide layer off. High-speed motion pictures show that the vaporizing takes place at each cathode spot...After the oxide layer is cleaned away at one spot, the arc moves to another place where there is more oxide; you see the dancing spots as the arc moves over the surface of the aluminum. The arc always looks for more oxide and will reach out to find it if there is none around."

The SEM images that accompany is article clearly show myriad surface pits on cathode sputtered surfaces. These pits could have been created by the instantaneous vaporization process reported by Koellhoffer, Manz, and Hornberger.

August F. Manz
AWS Fellow
Union, N.J.


American Welding Society
YOU ASKED FOR IT, AND NOW IT'S HERE... THE AMERICAN WELDING SOCIETY CLOTHING & ACCESSORY LINE
AWS Members now have access to American Welding Society shirts, hats, accessories and more at the AWS E-store. All of the products in this store are branded with the American Welding Society logo. Don't miss out on an assortment of great products.
Visit www.logodogz.net/aws
Classic Oxford Shirt
Mens Pique Knit Sport Shirt
Ladies Easy Care Twill Shirt
Beefy-T Crew Neck T-Shirt
Challenger Jacket
Ladies Pique Knit Sport Shirt
Grommeted Golf Towel
Midcity Messenger
Racing Check Panel Cap
Fashion Visor
Check out the complete product line, and order on-line at www.logodogz.net/aws

BY DAMIAN J. KOTECKI

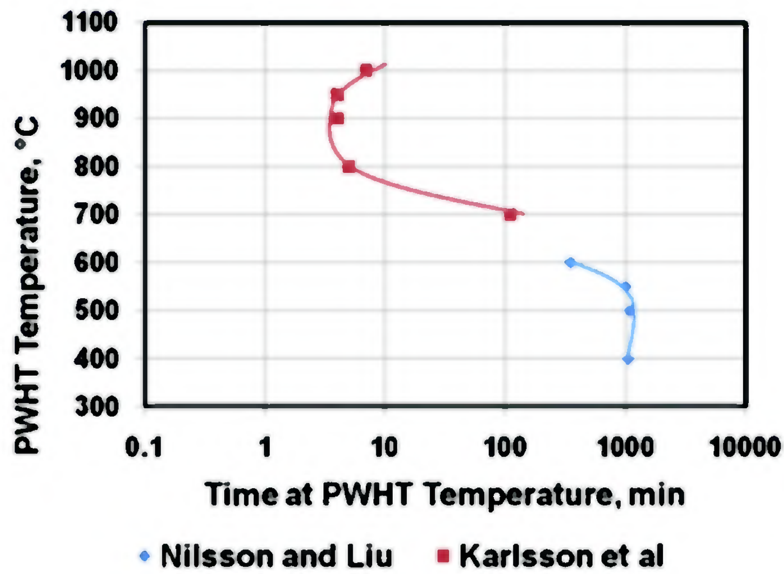

Fig. 1 — Limits of 27 J (20 ft-lbf) Charpy V-notch impact energy at room temperature after PWHT of 2209 Duplex Stainless Steel Weld Metal. Less than 27 J (20 ft-lbf) CVN was observed to the right of the two curves (Ref. 1).

Q: We have received some large valves of low-alloy steel whose interiors were weld overlaid with ER2209 duplex stainless steel in some cases, and with ER2594 superduplex stainless steel in other cases. To meet hardness limitations in the heat-affected zone (HAZ) of the low-alloy steel, the supplier performed a postweld heat treatment (PWHT) for 2 h at 620°C (1150°F) after the weld overlay was completed. It is my understanding that PWHT is not advisable for duplex stainless steel. Should we be concerned about the effects of this PWHT on the duplex stainless steel weld overlay?

A: In my opinion, you should be concerned. The 620°C PWHT temperature is within the temperature range where sigma phase and other intermetallic compounds can form from the ferrite in duplex stainless steel weld metal. Sigma is the most common, and it is rather normal to lump all the intermetallic compounds that form above 600°C under the term "sigma phase," as I do in this article. Further, in heating to that temperature, the weldment must pass through the temperature range where alpha prime (a chromium-rich ferrite) can precipitate within the ferrite of the duplex stainless steel weld metal.

Table 1 lists the chemical compositions of ER2209 and ER2594 filler metals as shown in AWS A5.9/A5.9M:2006, *Specification for Bare Stainless Steel Electrodes and Rods*. Note that ER2594 contains more chromium and generally more molybdenum than ER2209, so its weld metal will be more sensitive to precipitation of alpha prime and sigma phase (i.e., these phases tend to form more quickly in higher-alloy weld metal). You didn't indicate whether the overlay was done by gas metal arc, submerged arc, or another process, but that doesn't change the concerns to any significant extent.

Alpha prime and sigma phase have similar effects on the weld metal properties. Both, being hard, make the metal brittle. And both, because they contain more Cr than the matrix, must get that Cr from the matrix by diffusion, which reduces the corrosion resistance of the matrix. Sigma phase contains nearly 50% Cr, and alpha prime contains more than 90% Cr.

I must emphasize that I cannot be certain that the PWHT has caused significant damage, because formation of both sigma phase and alpha prime requires significant time for diffusion to take place, but the possibility is very real. You should test the welding procedure and exact PWHT thermal cycle (including both heating rate and cooling rate) for evidence of damage. There are four tests you can conduct to evaluate damage due to PWHT.

One way is to examine the microstructure using ASTM A923, *Standard Test Methods for Detecting Detrimental Intermetallic Phase in Duplex Austenitic/Ferritic Stainless Steels,* to look for intermetallic compounds. There are some shortcomings to this approach. It does not address the alpha prime possibility, only the sigma possibility. And finding traces of intermetallic compounds does not automatically mean the weld overlay is not serviceable. At the same time, you can measure the microhardness in the ferrite areas as compared to the microhardness without

Table 1 — Chemical Composition Limits (wt-%) of ER2209 and ER2594 Filler Metals

Filler Metal	C	Mn	P	S	Si	Cr	Ni	Mo	N	Cu	W
ER2209	0.03	0.50 to 2.00	0.03	0.03	0.90	21.5 to 23.5	7.5 to 9.5	2.5 to 3.5	0.08 to 0.20	0.75	—
ER2594	0.03	2.5	0.03	0.02	1.0	24.0 to 27.0	8.0 to 10.5	2.5 to 4.5	0.20 to 0.30	1.5	1.0

Note: Single values are maxima.

PWHT. A significantly harder result after PWHT would indicate alpha prime if you can't find sigma.

A second way is to conduct the ASTM G48A ferric chloride pitting test before and after PWHT. A drop in critical pitting temperature (CPT) of 10°C or more as a result of PWHT would indicate damage, as would failure to satisfy a specified CPT. The difficulty with this test is that you will need to remove all traces of substrate and diluted weld metal from the test coupon(s) before exposure, or you will be finding pits in the lower-alloyed metal without evaluating the final surface of the overlay. In service, only the final surface is exposed, so it is misleading to test lower layers of metal.

A third way is to perform longitudinal face bend tests of the overlay surface. This will assess the ductility loss due to the PWHT. I like this test because it is sensitive to low levels of both alpha prime and sigma. Failure to pass the test using the normal 2T bend radius would indicate damaged overlay material.

A fourth way is to conduct Charpy V-notch impact tests at a modest temperature — perhaps 0°C (32°F) or even at room temperature. Both ER2209 and ER2594 should comfortably exceed 27 J (20 ft-lbf) at these temperatures if they are not damaged by the PWHT. Figure 1 shows test results, from the literature, of 2209 weld metal given various PWHTs. All combinations of time and temperature to the right of the two curves in Fig. 1 produced less than 27 J at room temperature. Note that there is a gap between the two curves. The gap means that PWHT temperatures in that range were not tested. The upper curve is for sigma damage, and the lower curve is for alpha prime damage. Your PWHT temperature of 620°C for 2 h (120 min) is in the gap, so it is not certain that your material is damaged. That is why you need to test to be certain.

For future fabrication of such valves, or any other situation where duplex stainless overlay is to be applied to a substrate requiring PWHT, I suggest applying a buffer layer of 309L or similar austenitic stainless steel, then conducting the PWHT before applying the duplex stainless overlay. Then, the HAZ hardness limitation of the base metal can be met (provided that the duplex stainless application does not penetrate through the buffer layer), and the duplex stainless overlay can be put into service in the as-welded condition.

Reference

1. Karlsson, L., Ryen, L., and Pak, S. 1995. Precipitation of intermetallic phases in 22% Cr duplex stainless weld metals. *Welding Journal* 74(1): 28-s to 40-s. Who also quote data from Nilsson, J. O., and Liu, P. 1991. *Material Science and Technology,* 7(9): 853–862.

Dear Readers:

The *Welding Journal* encourages an exchange of ideas through letters to the editor. Please send your letters to the Welding Journal Dept., 550 NW LeJeune Rd., Miami, FL 33126. You can also reach us by FAX at (305) 443-7404 or by sending an e-mail to Kristin Campbell at *kcampbell@aws.org*.

BY TOM SNOW

Q: My boss assigned me the project of buying a resistance spot welding machine for welding a sheet metal part made from two pieces of 18-gauge mild steel in a production line environment. I know very little about the process. How do I begin?

A: With so many types, sizes, and brands of resistance welding machines on the market today, choosing what to buy can be a challenging assignment. However, if you start by documenting the part to be welded, the selection process should flow from there.

Although spot welding machines are traditionally compared and selected by their respective kVA ratings, this is potentially confusing because kVA (kilovolt amps) is only a thermal rating and kVA does not do the welding. To choose a spot welding machine for a particular application, it's more important to understand the variables known in the world of resistance welding as PCT (pressure, current, time).

To spot weld a part successfully, the machine must produce the proper amount of pressure (weld force) and current (amperage), which must flow for a given duration of time. I limit this discussion to single-phase AC spot welding machines, which are much more common than three-phase MFDC inverter-type welding machines. Also not addressed are any of the other resistance welding processes, which include projection welding, seam welding, and flash butt welding.

To determine what's needed to spot weld two pieces of 18-gauge sheet metal, first refer to one of the welding charts in the *Resistance Welding Handbook* available from the Resistance Welding Manufacturing Alliance (RWMA) at *www.rwma.org*. The pressure and current required to weld the two sheets are shown. If the sheets are of different thicknesses, you would size the machine for the thinner of the two sheets.

Some charts show welding schedules for Class A, Class B, and Class C welds, with different pressure and current settings for each. However, for maximum weld strength and best appearance, always select a machine that will meet Class A spot welding specifications.

For your 18-gauge application, Class A specifications in the RWMA *Handbook* call for pressure (welding force) of 650 lb, current of 10,300 A, and a relatively short weld time of 12 cycles (each cycle is 1/60th of a second).

Welding to Class B and C specifications uses lower force and current settings, plus a longer weld (current flow) time, which allows the heat-affected zone to expand and leaves the weld less attractive and not as strong as a Class A joint.

Fig. 1 — A 50-kVA rocker arm spot welding machine. A machine like this, manufactured to RWMA standards, is a good general-purpose machine. The modern control improves welding quality, and a built-in SOFT-TOUCH system protects the operator from pinch-point injury. A reputable dealer who asks lots of questions about how the machine will be used can be a great help in explaining the many machine and control options available today.

Fig. 2 — Press-type spot welding machines. Both of these press-type resistance spot welding machines are rated 100 kVA by their manufacturers, and one machine may be better suited for a particular application than the other. However, the difference in physical size illustrates why the kVA rating is not the only specification that should be considered when selecting a spot welding machine to purchase.

Part configuration is the next consideration. What throat depth and gap (arm length and shut height) are required to reach all the welds? Choose a throat configuration that reaches all the welds but is not so large that the output of the machine is compromised. Just as a drill connected to an extremely long extension cord won't work as well as one plugged directly into a wall outlet, welding current delivered to the tips is reduced due to electrical losses as the total area between the welding arms is increased.

The next major decision is to choose between a rocker arm-type spot welding machine (Fig. 1) and a vertical action press-type machine (Fig. 2). While a rocker arm usually beats a press welding machine in versatility and price, a press-type machine often produces superior weld quality and appearance, since the weld force is applied in a straight line motion instead of the inherent arc of a rocker arm design. It is important to note that this factor alone makes a rocker arm unsuitable for projection welding nuts and studs.

When choosing a spot welding machine, weld forging force is an often-overlooked variable. Since most machines are air operated, the diameter and mounting position of the air cylinder must be considered a critical factor.

The lever-type action of the rocker arm is a potential drawback of that design since, assuming that incoming air pressure remains constant, weld force decreases as the weld tips are extended farther away from the fulcrum point.

On the other hand, weld force produced by a vertical-action press-type machine is applied directly and at a ratio of one to one to the output of the cylinder.

Just as you would not drive your car at the red line for rev/min every day if you expect it to last, choosing a spot welding machine that must run wide open to weld your application in a production line environment is not advisable. Instead, select a machine that has enough "head room" available to accomplish your weld at about 60–80% of its rated capacity.

As an example, if your plant's air supply averages 80 lb/in.^{2}, choose a welding machine that can produce the required forging force at about 60 lb/in.^{2} of regulated air pressure. Just as an undersized air cylinder is undesirable, one that is oversized can also cause problems, since welding at low regulated air pressures (below about 20–30 lb on the gauge) may result in improper follow-up during the weld, which is a critical part of the forging process.

Another important welding machine performance comparison measure is the maximum rated secondary amperage available when the machine is fired short circuit or tip to tip, with no steel in the throat. This rating should be shown in the machine manufacturer's spec sheet and, again, you should choose a machine with plenty of extra capacity. Figure that the short circuit secondary amperage rating will be reduced by about 15% with a part in the throat and then allow for another 25–30% of head room.

Now comes the most confusing part: Resistance spot welding machines have always been rated in kVA, a thermal rating that can be stated in several ways depending on the duty cycle of the machine. As an example, a machine rated 100 kVA at 50% duty cycle may also be rated 141 kVA at 25% duty cycle or 224 kVA at 10% duty cycle.

Although it is unusual for a resistance spot welding machine to operate at or even close to 50% duty cycle (when current flow "on time" equals cool or "off time" between welds), it is important during the machine selection process to understand that RWMA specifications call for resistance welding machines to be rated at 50% duty cycle as a standard for comparison.

However, not all machines being sold today meet RWMA standards and the kVA rating of a spot welding machine can be inflated, as illustrated above, by citing a lower duty cycle in the fine print of the specifications or even just omitting that spec altogether.

While a light-duty spot welding machine may be adequate for occasional use or a light-duty production line application, it's important to understand the variables of PCT in order to make a wise purchase.

Now, let's choose a welding machine for your 18-gauge application. Assuming that a rocker arm machine is adequate and assuming that all the spot welding machines being considered meet RWMA standards and that a 12-in.-deep by 8-in.-high throat will reach all your weld locations, let's see if a 20-kVA machine will work.

First, let's look at welding pressure: RWMA specifications for a 20-kVA rocker arm with a 12-in. throat are 970 lb of force at 80 lb/in.^{2}. Since we want to operate the machine at about 75% of rated force capacity (60 lb/in.^{2} on the gauge), that gives us a working force range of just over 700 lb, which is okay, since our Class A weld spec calls for 650.

Now, let's look at welding current: A 20-kVA rocker arm welding machine is typically rated at 16,000 short circuit secondary amps at a 12-in. × 8-in. throat. Subtracting 15% to go from short circuit amps to usable welding amps gives us 13,600 A. Subtracting another 25% for head room leaves us with 10,200 A for welding, which is close enough to the 10,300 we're looking for.

So, a short throat 20-kVA welding machine that meets RWMA minimum specs is adequate for this application, if that's all your budget will allow.

However, a larger welding machine would probably be a better choice, since a 30-kVA machine, with 21,000 short circuit secondary amps available at a 12-in. × 8-in. throat, comes in a larger frame size with more weld force available. This would allow you to specify a longer throat depth, such as 18 or 24 in., which could be handy for future applications.

And, since an RWMA standard 50-kVA spot welding machine comes in the same frame as a 30 kVA and does not cost much more per kVA, consider investing in even more welding capacity to handle future applications.

A reputable spot welding machine dealer can be a great help to you in explaining these choices, as well as the many machine and control options available. Be ready to supply the salesperson with the following information:

1. The maximum metal thickness to be welded for each alloy
2. The deepest dimension needed from the electrode to the back of the welding machine throat (opening)
3. The highest vertical clearance needed to clear the parts being welded
4. Your available line voltage
5. If welds are to be spot, seam, projection, etc.
6. If you will be working with weld nuts or weld studs.

And remember, if a potential vendor does not ask lots of questions about your welding application, you should probably just keep on shopping.♦

TOM SNOW is chief executive officer, T. J. Snow Co., Inc., Chattanooga, Tenn. He is a member of the Resistance Welding Manufacturing Alliance (RWMA). Send your comments/questions to him at tomsnow@tjsnow.com, *or to Tom Snow, c/o Welding Journal, 550 NW LeJeune Rd., Miami, FL 33126.*

Brazing Foils for Exhaust Gas Applications Provide Corrosion Resistance

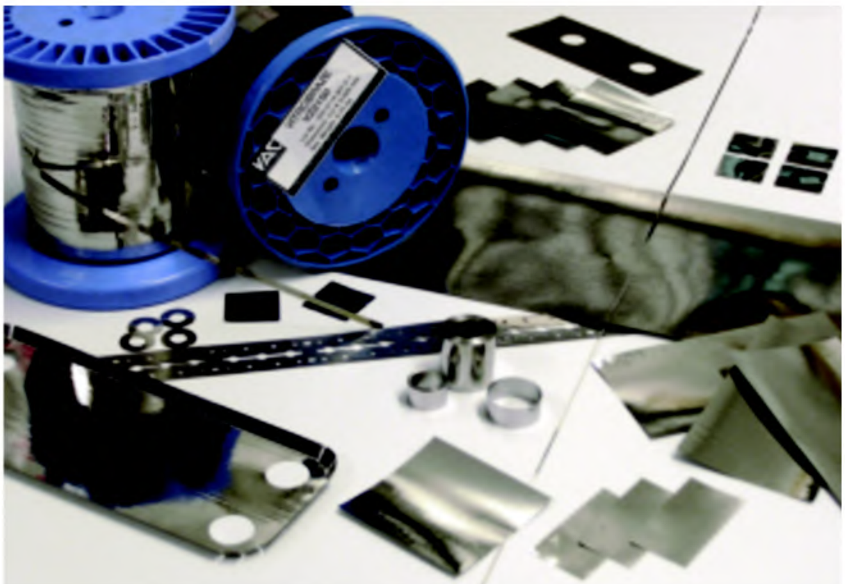

Vitrobraze brazing foils are beneficial for exhaust gas applications. They are free of all organic constituents, making them suitable for compact design configuration. Also, due to an amorphous structure, they have a homogenous composition resulting in consistent melting of the brazing filler material. The homogenous thinness of these foils enables the brazing filler material to be metered in line with the individual requirements of each brazing job. In addition, the foil can be incorporated into automated high-speed assembly lines. The VZ2106 (Fe content 35 wt-%) and VZ2099 (Fe content 51 wt-%) achieve corrosion resistance. Another feature is their optimization for joining exhaust gas recirculation coolers and metallic filters in a continuous furnace under hydrogen. The VZ2170, based on the Ni-Cr-P system, was developed to combine the low-melting temperature essential to the process (range 950°–1100°C) with good corrosion resistance, primarily achieved by adjusting chromium content to > 20 wt-%.

Vacuumschmelze GmbH & Co. KG
www.vacuumschmelze.de
+49 6181 / 38-0

Laser Soldering Useful for Connecting Self-Bonding Copper Wires

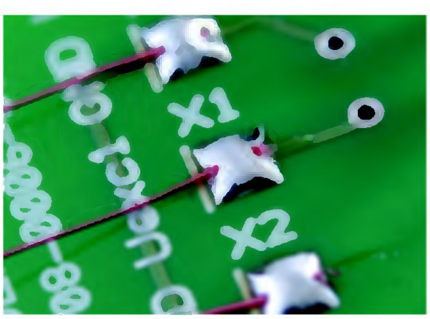

For manufacturing processes with small and medium quantities in electrical, medical, and sensor engineering, the company's automated laser soldering process increases the flexibility as well as process speed of production. Enamel removal and interconnection take place in a single process step. Reproducibility is increased through integrated process monitoring and control based on pyrometric sensors used in the laser-beam soldering process. Plus, this process allows not only a nearly free choice of connection geometries, but makes manufacturing so flexible that any number of quantities can be produced without increasing reaction time. Pictured is a demonstrator component to solder self-bonding wires on circuit boards.

Fraunhofer Institute for Laser Technology
www.ilt.fraunhofer.de/eng/100000.html
+49 241 8906-0

Gas Lenses Optimize Shielding Gas Coverage

The company's multiple styles of precision-machined gas lenses help ensure consistent GTAW performance. Available for both the company's WP Series and Crafter Series™ air- and water-cooled GTA torches, they are comprised of high-quality materials that also provide good current capacity and effectively dissipate heat for longer, trouble-free performance. These gas lenses also fit GTA torches from other manufactures. The product line consists of three main styles — standard size, large diameter, and stubby — to fit GTA torches with 10N or 13N series front-end parts and accommodate tungsten electrode diameters from 0.020 to $\frac{5}{32}$ in. Each gas lens features durable screens that consistently direct the shielding gas flow around the weld pool, minimizing weld defects and improving productivity.

Weldcraft
www.weldcraft.com
(800) 752-7620

Alumina Fixtures Handle High-Temperature Brazing

The company's custom-made alumina fixtures isolate and insulate metal components during high-temperature brazing processes. A flexible design means that both simple and intricate features, including small-diameter holes, can be machined to tight tolerances. Cleanliness is ensured through an air firing process. During the brazing process, thermal expansion of the fixture is matched to that

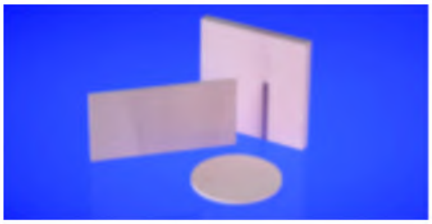

of the alumina insulator used for ceramic-to-metal seals. The alumina has a good dimensional stability at higher temperatures (greater than 800°C) and a long service life. Additionally, the alumina shows no material degradation in a wet reducing atmosphere. Contamination with foreign materials are easier to see because of its white color. There is no outgassing or material transfer to parts it is in contact with during vacuum brazing applications.

Morgan Technical Ceramics
www.morgantechnicalceramics.com
(800) 433-0638

Belt Conveyor Oven Solders Metal Parts

The No. 851, a 650°F electrically heated belt conveyor oven used for soldering metal parts, features workspace dimensions measuring 18 in. wide × 96 in. deep × 15 in. high. Its full heat processing system consists of a 2-ft-long open belt loading zone; two 4-ft-long insulated heat zones with independent recirculated airflow and temperature control; 1-ft-long open zone; 12-ft-long cooling zone; and 2-ft-long open belt unloading zone. Heat is provided by 60 kW installed in Nichrome wire heating elements while two 1000 ft^3/min, 2-hp recirculating blowers furnish downward vertical airflow to the workloads. The oven also has 5-in. insulated walls, an aluminized steel exterior, Type 304 stainless steel interior, two 16-in.-diameter tube axial fans each driven by a ¾-hp motor to push/pull air through the cooling zone, as well as a 12-in.-wide, 1- × 1-in.-high carbon steel flat wire conveyor belt with ¼-hp motor drive, variable speed from 1.3 to 25.3 in./min.

The Grieve Corp.
www.grievecorp.com
(847) 546-8225

GMA Guns, Consumables Improve Weld Quality

The customizable W™-series water-cooled GMA guns and water-cooled Centerfire™ consumables meet the needs of high-amperage, water-cooled GMA applications. These guns offer users their choice of neck style, cable length, handle style, consumables, and direct plugs. They further feature a more durable and easily replaced power pin housing with an improved coolant hose strain relief. The dedicated side-entry coolant channel and strain relief greatly reduce the potential for premature gun failure due to kinked coolant lines. A coolant channel keeps the consumables cool under high-amperage, high-heat applications. They are rated to 600 A at 100% duty cycle and offer direct plug connections to all major wire feeder brands. In addition, the consumables offer the durability, weld quality, and productivity benefits of their air-cooled counterparts. These come with a 1/8- or 1/4-in. contact tip recess and contain a spatter shield that improves shielding gas flow to better protect the weld pool and keeps spatter from clogging the shielding gas diffuser.

Bernard Welding Equipment
www.bernardwelds.com
(800) 946-2281

Induction Brazing Systems Join Auto Fuel Lines

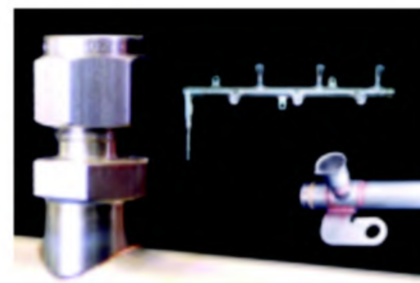

The company's controlled atmosphere induction brazing systems utilize patent pending technology to join high-pressure fittings efficiently to fuel lines, making for a greener car. This technology is integrated into systems used by automotive and aerospace suppliers to braze fittings to fuel lines and rails. Additional features and benefits include the following: reduced energy costs; repeatable processes that produce quality parts; no tube deformation; no cleaning required; ability to braze multiple parts at the same time; manual, semi, and fully automatic systems scaled to user's needs; modular, manual, and automatic tooling changes; digital controls; and strong braze joints.

Radyne Corp.
www.radyne.com
(414) 481-8360

Soldering, Rework System Offers Dual Output Ability

The MFR-2200 series soldering and rework systems provide a high-power way to perform production and touch-up soldering. SmartHeat® responds to the load, delivering the energy required for each connection, while protecting sensitive components and substrates from damage. This series features dual output capability that allows the user to select operation of one or two handpieces simultaneously. One or two handpiece operation is easily chosen through a front panel switch. Also, it contains two separate power supplies. The MFR-H1-SC cartridge handpiece offers a range of soldering and rework cartridges that provide fine-access soldering tips, SMD rework tips, and pad clean-up blade tips. A handpiece for production soldering, MFR-H2-ST, features high power and tips designed for production soldering environments. A third option for this system is the MFR-H4-TW precision tweezers handpiece.

OK International, Inc.
www.okinternational.com
(714) 799-9910

Trailing Shields Reduce Gas Consumption

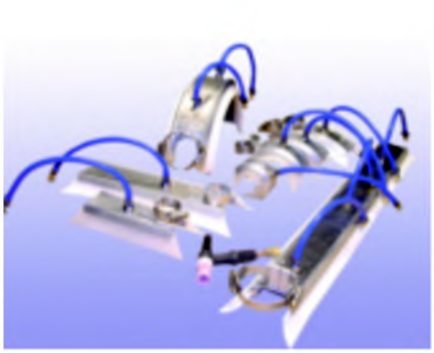

Argweld® trailing shields fit any make of GTAW, GMAW, or PAW torch for manual or automatic welding. Flat trailing shields are available for welding sheet metal or plate work. Radiused trailing shields are manufactured for every diameter of tube pipe or vessel from 1 in. upward. Along with the ones radiused for outside welding, a version for inside welding is manufactured as well. Additional trailing shield models are available for robotic welding where the shields are wider and longer for greater welding speeds. Other benefits are that gas consumption is reduced, faster welding times are obtained, and the need to use a purge enclosure is eliminated. They can be used for welding stainless steel, duplexes, and titanium.

Huntingdon Fusion Techniques Ltd.
www.huntingdonfusion.com
+44 (0) 1554 836 836

Abrasives Prepare Workpieces for Finishing

The company's surface conditioning abrasives are made from nonwoven materials impregnated with abrasives for easy removal of materials such as sealants, paints, and rust. Consisting of more than 100 products, this line features EZ strip wheels available in 2 to 8 in. diameters and an assortment of attachment styles including roll-on, ¼-in. spindle, and ½-in. arbor hole; hook and loop discs designed for quick changes but have strong attachment capacities; hand pads in premium and economy grades; plus interleaf wheels and flap discs with alternating flaps of nonwoven and coated abrasive materials for uniform surface preparation and finishes.

CGW-Camel Grinding Wheels
www.cgwheels.com
(800) 447-4248

Choosing a Shielding Gas for FCAW

Fig. 1 — Gas shielded flux cored arc welding.

Gas shielded flux cored arc welding (FCAW-G) is a popular and versatile welding process — Fig. 1. It is used with mild steel, low-alloy steel, and other alloy materials in a variety of applications and industries, such as heavy fabrication, structural, shipbuilding, and offshore. The two most common shielding gases used with the FCAW-G process are 100% carbon dioxide, commonly referred to as CO_2, and the mixture of 75–80% argon (Ar) with 20–25% CO_2, referred to as an Ar/CO_2 blend.

So which shielding gas, CO_2 or Ar/CO_2 blend, should operators choose for flux cored arc welding applications? Each type offers some advantages and disadvantages. The factors of cost, quality, and productivity should be considered when manufacturing decisions are made. The choice of shielding gas affects each of these factors, sometimes in a conflicting way. This article focuses on the merits of the two basic gas options for FCAW-G on steel applications.

Before getting into the particular advantages of the gas options, it is appropriate to review some basics. It should also be noted that this article only focuses on a few types of gases. As a more comprehensive reference, ANSI/AWS A5.32/A5.32M, *Specification for Welding Shielding Gases*, prescribes the requirements for shielding gases, defining requirements for testing, packaging, identification, and certification. Additionally, it contains helpful information on ventilation during welding, as well as general safety considerations.

Cost, overall operator appeal, and weld quality must all be considered when selecting the shielding gas for a flux cored arc welding application

BY TOM MYERS

How Shielding Gas Works

The primary function of all shielding gases is to protect the molten weld pool and electrode from the oxygen, nitrogen, and moisture in air. Shielding gases flow through the welding gun and exit the nozzle surrounding the electrode, displacing the air and forming a temporary protective pocket of gas over the weld pool and around the arc. Both CO_2 and Ar/CO_2 blend shielding gases accomplish this purpose.

Some shielding gases make it easier to create the arc plasma, providing a current path for the welding arc. The choice of shielding gas also affects the transfer of thermal energy in the arc and forces on the pool. For these issues, CO_2 and Ar/CO_2 blends behave differently.

Properties of Shielding Gases

When exposed to the heat of the welding arc, CO_2 and Ar react in different ways. Analysis of these differences is useful in understanding how the properties of each gas affect the welding process and weld deposit.

Ionization potential is a measure of the energy required to ionize the gas (i.e., transform to a plasma state in which it is positively charged), enabling the gas to conduct current. The lower the number, the easier it is to initiate the arc and maintain arc stability. The ionization potential for CO_2 is 14.4 eV vs. 15.7 eV for Ar. Thus, it is easier to initiate an arc in CO_2 than in Ar.

Thermal conductivity of a gas is its ability to transfer thermal energy. This affects the mode of transfer (spray vs. globular, for example), shape of the arc, weld penetration, and temperature distribution within the arc. Carbon dioxide has a higher thermal conductivity level than both Ar or an Ar/CO_2 blend.

Reactivity of a gas refers to whether or not it will chemically react with the molten weld pool. Gases can be divided into two groups, inert and active. Inert gases, or noble gases, are those that are unreactive with other elements in the weld pool. Argon is an inert gas. Active gases, or reactive gases, are those that combine or react with other elements in the weld pool to form compounds. At room temperature, CO_2 is inert. However, in the arc plasma, CO_2 will disassociate, forming carbon monoxide (CO), oxygen (O_2), and some monotonic oxygen atoms (O). Therefore, CO_2 becomes an active gas in the welding arc, allowing the oxygen to react with metals (i.e., oxidize) in the arc. An Ar/CO_2 blend is also an active gas, but less reactive than CO_2.

With all other welding variables being the same, different shielding gases produce different welding fume generation rates. Typically, there is a reduction in rates with an Ar/CO_2 blend, as compared to CO_2, due to the oxidizing potential of CO_2. Specific fume generation levels vary and are dependent on the particular application and procedures used.

More about Inert Gases

Although inert gases provide weld pool shielding, they are not suitable by themselves for FCAW-G on ferrous or iron-based metals (mild steel, low-alloy steel, stainless steel, etc.). For example, if only Ar was used to weld mild steel, the resulting weld characteristics would be very poor. Using an inert shielding gas causes excessive arc length and premature melting of the electrode's outer steel sheath. Wide and uncontrollable arc characteristics would lead to excessive weld buildup. Therefore, for the best results for FCAW-G on ferrous metal base materials, a blend of inert gas with active gas is used.

More about CO_2/Ar Blends

The most common blend for mild steel FCAW-G applications in North America is 75% Ar/25% CO_2. A less common blend for mild steel FCAW-G applications is 80% Ar/20% CO_2. Some gas shielded flux cored wires are designed for use with as much as 90% Ar/10% CO_2. However, less than 75% Ar in a shielding gas blend will have a diminished impact on arc characteristics, while you would still incur the cost of having Ar in the shielding gas. In addition, nonstandard percentages of Ar/CO_2 blended cylinders will typically be more difficult to obtain than standard blended cylinders, like 75% Ar/25% CO_2 or 80% Ar/20% CO_2.

Alloy Recovery and Mechanical Properties

Due to the reactive nature of CO_2, a higher level of alloy recovery from a given

TOM MYERS (tom_myers@lincolnelectric.com) is a senior application engineer, The Lincoln Electric Co., Cleveland, Ohio.

MECHANICAL PROPERTIES[1] – As Required per AWS A5.20/A5.20M: 2005

	Yield Strength[2] MPa (ksi)	Tensile Strength MPa (ksi)	Elongation %	Charpy V-Notch J (ft•lbf) @ –18°C (0°F)	Charpy V-Notch J (ft•lbf) @ –29°C (–20°F)
Requirements[3] AWS E71T-1C H8, E71T-1M H8	400 (58) min.	480 - 655 (70 - 95)	22 min.	27 (20) min.	Not Specified
AWS E71T-9C H8, E71T-9M H8				Not Specified	27 (20) min.
Typical Performance[4] As-Welded with: 100% CO_2	510 - 550 (73 - 79)	570 - 600 (82 - 87)	26 - 28	38 - 95 (28 - 70)	27 - 65 (20 - 48)
75% Ar/25% CO_2	570 - 610 (82 - 88)	620 - 660 (90 - 96)	24 - 26	62 - 111 (46 - 82)	39 - 85 (29 - 63)

DEPOSIT COMPOSITION[1] – As Required per AWS A5.20/A5.20M: 2005

	%C	%Mn	%Si	%S	%P	Diffusible Hydrogen (mL/100g weld deposit)
Requirements[3] AWS E71T-1C H8, E71T-1M H8; AWS E71T-9C H8, E71T-9M H8	0.12 max.	1.75 max.	0.90 max.	0.03 max.	0.03 max.	8 max.
Typical Performance[4] As-Welded with: 100% CO_2	0.03 - 0.04	1.28 - 1.41	0.42 - 0.49	0.01	0.01 - 0.02	3 - 8
75% Ar/25% CO_2	0.03 - 0.04	1.45 - 1.60	0.54 - 0.62	0.01	0.01 - 0.02	4 - 8

Fig. 2 — Deposition composition and mechanical properties results of a typical gas shielded flux cored wire designed for use with both CO_2 and an Ar/CO_2 blend.

electrode in the weld metal is experienced when using an Ar/CO_2 blend vs. CO_2 shielding gas. This is because CO_2 will react with alloys to form oxides, which, along with oxides from the flux, form the slag. The flux in the core of the electrode must contain reactive elements, such as manganese (Mn) and silicon (Si), which act as deoxidizers, among other purposes. A portion of these alloys react or oxidize with the free oxygen from the CO_2, ending up in the slag instead of being recovered in the weld metal. Therefore, higher levels of Mn and Si result in the weld deposit (i.e., more alloy recovery) with an Ar/CO_2 blend than with a CO_2 shielding gas (see the example in Fig. 2).

The consequences of higher levels of Mn and Si in the weld deposit are an increase in weld strength and a decrease in elongation, as well as changes to the Charpy V-notch impact toughness. By simply changing from CO_2 to an Ar/CO_2 blend, you typically get a 7–10 ksi increase in tensile and yield strength and 2% decrease in elongation — Fig. 2. This is an important concept to understand, for as the percentage of Ar in the shielding gas increases, the weld strength could become too high and ductility too low.

Knowing that shielding gases can affect the resulting properties in the weld, AWS D1.1/D1.1M:2008, *Structural Welding Code — Steel*, has a series of requirements to ensure acceptable properties are achieved. For all welding, the shielding gas must conform to the requirements of AWS A5.32/A5.32M. AWS classifications for FCAW-G welding consumables (A5.20/A5.20M and A5.29/A5.29M) put upper limits on the strength of the weld deposit . A shielding gas should be selected to ensure that these limits are not exceeded, depending on the design of the electrode and the welding procedures used. For prequalified welding procedure specifications (WPS), D1.1:2008 requires the specific filler metal and shielding gas combination used be supported with test data.

Clause 3.7.3 of D1.1:2008 provides two acceptable forms of support: either the use of shielding gas used for electrode classifications purposes, or data from the filler metal manufacturer that shows conformance with the applicable AWS A5 requirements, but with the specific shielding gas that is to be listed on the WPS. In the absence of these two conditions, D1.1:2008 requires that the combination be subject to qualification testing.

Filler Metal Classification by Gas Type

Beginning in 2005, the American Welding Society's flux cored filler metal specifications made the type of shielding gas used for classification part of the classification designation. A mild steel FCAW-G electrode's AWS classification is EXXT-XX, where the last X is the shielding gas designator. It will either be C for CO_2 or M for mixed gas, or Ar/CO_2 blends (for example, E71T-1**C** or E71T-1**M**). For a low-alloy steel electrode, the shielding gas designator follows the deposit composition designator at the end of the mandatory designators (for example, E81T1-Ni1**C**). In contrast, self shielded flux cored electrodes, which require no shielding gas, would have no shielding gas designator in its classification (for example, E71T-8).

Some electrodes are designed to be used solely with CO_2. Other electrodes are designed to be used solely with Ar/CO_2 blends. Still others are designed to be used with both types of shielding gases, CO_2 and Ar/CO_2 blends. In this latter case, the electrode must meet the requirements of both classifications.

Selecting Shielding Gases for FCAW-G

In choosing either CO_2 or an Ar/CO_2 blend shielding gas for flux cored welding, consider the following three comparison points.

1) **Shielding Gas Cost.** Total welding costs are a significant factor for many companies and controlling these welding costs is crucial to maintaining profitability. In general, 80% of total welding costs can be attributed to labor and overhead expenses and 20% to material costs, with shielding gases accounting for as much as a quarter of material costs, or 5% of total welding costs. If cost of shielding gas is the only deciding factor, then significant cost savings can be achieved by using CO_2 over an Ar/CO_2 blend. However, oftentimes other factors influence total welding costs as well and those are discussed in later sections.

Carbon dioxide costs less than Ar/CO_2 blends because it is a less costly gas to collect, and the sources are plentiful and widely available all over the world. Carbon dioxide is generally collected as a byproduct of some other process. For the welding industry, a common source is from the processing or cracking of natural gas. On the other hand, Ar can only be collected from air. With Ar constituting just less than 1% of the atmosphere, a tremendous amount of air must be processed to extract Ar in large quantities. Special air-separation plants are required to process air. Air-separation plants consume large quantities of electricity and are located in specific areas of the world.

2) **Overall Operator Appeal and Impact on Productivity.** When comparing shielding gases for use on the same type and size electrode, smoother, softer arc characteristics and lower spatter levels are seen with an Ar/CO_2 blend, resulting in an increased overall appeal to operators, vs. CO_2 shielding gas. A welding arc in CO_2 shielding gas has a more globular arc transfer with larger droplet sizes (typically larger than the diameter of wire), resulting in a harsher, more erratic arc and

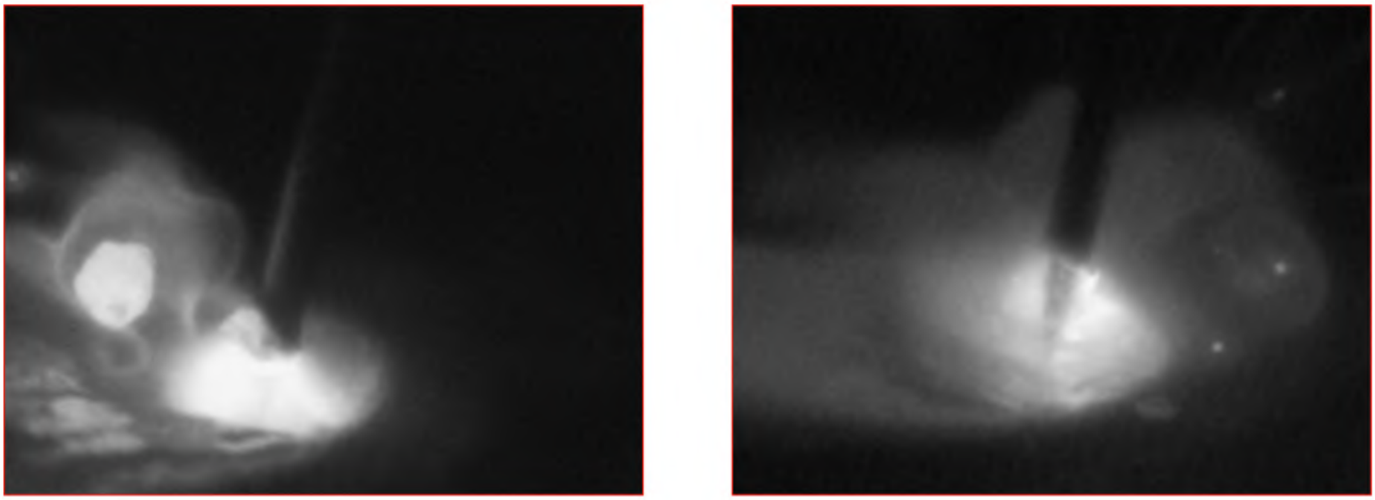

Fig. 3 — A comparison of the metal transfer through the arc with CO_2 (left) vs. 75% Ar/25% CO_2 blend using the same wire feed speed and voltage welding procedures.

higher levels of spatter. A welding arc in an Ar/CO_2 blend has more of a spray arc transfer with smaller droplet sizes (typically smaller than the diameter of wire), resulting in a smoother, softer arc and lower levels of spatter.

Another feature of an Ar/CO_2 blend that increases its overall operator appeal, with its lower level of thermal conductivity, is that it tends to keep the weld hotter or more fluid, compared to a weld produced using CO_2. This makes it easier to work the pool and wet the bead at the toes of the weld. Higher operator appeal is particularly valuable when welding out of position (i.e., uphill and overhead positions). Some fabricators find that using an Ar/CO_2 blend gives less-experienced welders more control over the welding arc, which results in the ability to weld at higher productivity levels.

Because of the high Ar content, one disadvantage of an Ar/CO_2 blend is that it radiates more heat up toward the operator than CO_2. This means that it feels hotter when welding. In addition, welding guns run hotter with an Ar/CO_2 blend (guns have a lower duty cycle rating with Ar/CO_2 blend than with CO_2). This may require the use of larger guns or potentially incur higher annual replacement costs of the same size guns and consumable parts.

3) **Weld Quality.** As discussed earlier, an Ar/CO_2 blend when compared to CO_2, tends to keep the weld pool more fluid, making it easier to work the pool and wet the bead at the toes of the weld. Some fabricators find this allows welders to improve the weld profile and resulting quality of the weld.

In addition, the welding arc in an Ar/CO_2 blend produces less weld spatter. This results in higher weld quality and reduction in weld cleaning time and cost. Lower spatter levels can also improve ultrasonic weld testing costs, as excessive spatter must first be removed to ensure proper weld inspection with ultrasonic testing equipment.

Another quality issue impacting a weld's cosmetic appearance is a shielding gas's susceptibility to gas marks. Gas marks, also referred to as worm tracks or chicken scratch, are small grooves that sometimes appear on the weld surface. They are caused by dissolved gases in the weld metal that have escaped before the pool freezes, but then are trapped underneath the slag after it has solidified.

There is a higher susceptibility to gas marks with an Ar/CO_2 blend than with a CO_2 shielding gas. The spray arc transfer characteristics of Ar/CO_2 shielding gas produce a large number of small metal droplets. This increases the total surface area of the molten droplets, resulting in a higher level of dissolved gases in the weld metal. There are factors besides shielding gas type that affect susceptibility to gas marks; however, they are outside the scope of this article.

Typical Shielding Gas Used for Some Main Applications and Industries

Over the years, the type of shielding gas used for FCAW-G has been standardized for some main applications and industries. For example, with high-deposition applications in the flat and horizontal positions only, CO_2 is preferred, as little benefit is achieved with an Ar/CO_2 blend in these positions.

Shipyards also generally prefer to use CO_2 because its arc characteristics have a greater ability to burn off primer on the base material. In the North American offshore fabrication industry, downhill final passes on T-, Y-, and K-connection groove welds require a very smooth weld contour and minimal spatter levels, making an Ar/CO_2 blend the preferred shielding gas. In some regions of the world, CO_2 is the gas of choice for all applications due to an inconsistent supply of Ar. Fabricators who use more than one gas shielded welding process in their shop, such as GMAW and FCAW-G, often standardize both processes with on type of shielding gas. In that situation, many fabricators choose an Ar/CO_2 blend to obtain the GMAW benefits of spray or pulsed arc transfer.

Conclusion

When choosing a shielding gas for your FCAW-G applications, you should consider more than just the cost of the gas. Instead, consider all three comparison points discussed in this article. How does each gas type affect your total welding costs? Which gas type reduces your total cost to make one foot or one meter of weld? Some fabricators find that the merits of an Ar/CO_2 blend allow them to improve their quality and productivity. For other fabricators, the benefits of an Ar/CO_2 blend are not realized or do not outweigh the cost savings of CO_2. And for yet other fabricators, CO_2 provides the best cost and benefits for their particular welding application. For users of the FCAW-G process, the choice of which shielding gas to use should be based on how it most positively influences the overall driving factors of cost, quality, and productivity to their welding operations. Then once the choice of shielding gas is made, the FCAW-G electrode used should be one that is designed for that particular shielding gas.♦

New Welding Wire for Thin Steel Sheet

The features of an innovative GMAW solid wire for high-speed welding of thin steel sheet are detailed

BY Y. UMEHARA, R. SUZUKI, AND T. NAKANO

Arc welding robots are used in most welding processes in automotive manufacturing. The robots weld steel sheets that have been press formed into complicated three-dimensional shapes. The press-formed sheets require high dimensional accuracies. In reality, however, the accuracies of press-forming are limited, causing problems such as variations in root openings and in gas metal arc welding (GMAW) wire target positions. The variations often cause welding discontinuities such as misalignment and melt-through, increasing the worker hours involved in fixing such discontinuities. High-speed welding is desirable for efficiency; however, excessively high speed can cause problems such as undercuts, convex beads, and insufficient bead width, which again increases repair time.

Most of these problems are solved by reducing welding speed to secure bead width; however, that solution is not feasible in terms of efficiency and cost. A means for solving the above problems in high-speed welding is to make the bead wider by adjusting the shape of the bead penetration. A wide bead width helps weld quality by reducing discontinuities, and it is desirable for welding thin steel sheets. Another aspect in weld quality assurance is to further reduce slag, which tends to peel paint coatings off.

In response to such needs, Kobe Steel developed a GMAW wire, SE-A50FS, that provides wide bead widths and generates minimal slag. The company studied ways to control the properties of the molten pool during GMAW through the composition of the wire.

Application of GMAW Wire

The new GMAW wire produces a desirable bead shape and low slag. The welding wire is suited for corner welding of lap-joints and T-joints of thin (about 2 to 4 mm) steel sheets used for automobiles and electric appliances. The welding wire is also suitable for mixed gas (Ar-CO_2) welding.

Design Concept of New Welding Wire

Wide bead widths are effectively produced from molten pools having low viscosities. Oxygen and sulfur are the elements known to significantly reduce the viscosities and surface tensions of molten metal (Ref. 1). However, these elements are also known to adversely affect the behaviors of welds. Although oxygen may be added purposely through shielding gas, the element works to cool and shrink welding arcs and thus destabilize them. In addition, oxygen reacts with steel elements having oxygen affinities, such as Si and Mn, and is discharged to the bead surfaces in large amounts as slag containing SiO_2 and MnO. The slag tends to remain on the bead surfaces and causes deterioration of the bead appearance and paintability. Furthermore, oxygen added in an acceptable amount does not exert any significant effect in improving the bead shape.

On the other hand, sulfur is known to increase the susceptibility to hot cracking (Ref. 2) and has been regarded as an impurity. Thus, its addition to GMAW wires has been avoided as much as possible. As a matter of fact, no conventional GMAW wire has a purposeful addition of S. In an attempt to significantly reduce the viscosity and surface tension, extensive studies were performed on the purposeful addition of S, which has resulted in the development of a commercially feasible GMAW wire.

The main feature of the new wire is that it contains about 0.06% S, which is several times higher than in conventional GMAW wires. The addition of S advantageously reduces slag formation, unlike in the case of O_2. The S addition serves not only to reduce the viscosity and surface tension, but also to improve the convection (Marangoni convections) (Ref. 3) in the weld pool, changing the pool's properties and yielding various merits.

The susceptibility to high-temperature cracking, which is regarded as a disadvantage of S addition, described more in detail in a later section, is considered to be affected by two factors: 1) metallurgical factors such as the segregation and discharging of low-melting-point compounds including S; and 2) morphological factors in macroscopic scale related to solidification. The new wire was designed taking these factors into consideration. If the wire use is limited to welding thin steel sheets, the wire exhibits a resistance to hot-cracking comparable to those of conventional GMAW wires.

Characteristics of New Welding Wire

Bead Shape

The new wire exhibits a stable, wide, and flat bead shape. Such welding beads reduce machining steps, and the smooth ends of the bead reduce stress concentrations.

Figure 1 depicts the relationship between the deposit height (H) divided by bead width (W) (H/W) and arc volt-

Y. UMEHARA, R. SUZUKI, and T. NAKANO are with Kobe Steel, Ltd., Fujisawa-City, Kanagawa, Japan.

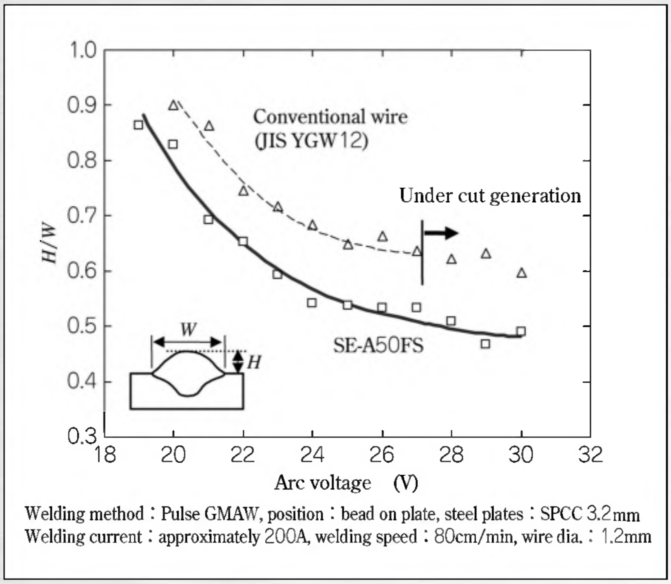

Fig. 1 — Relationship between bead shape and arc voltage.

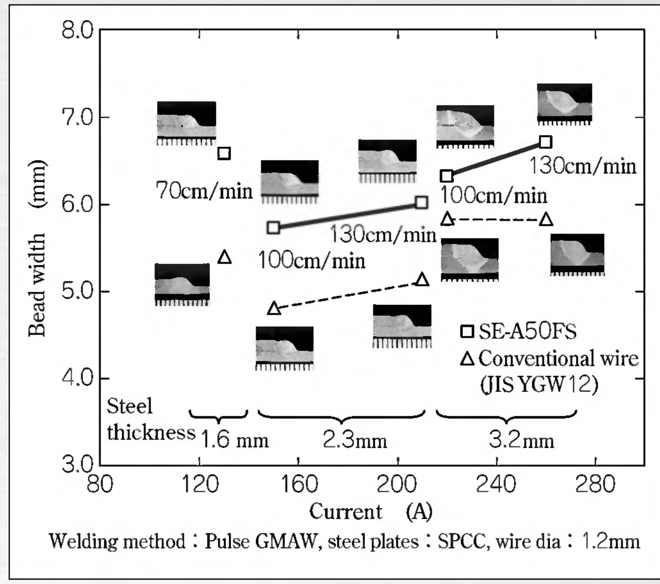

Fig. 2 — Relationship between current, bead width, steel thickness, and welding speed along lap joint.

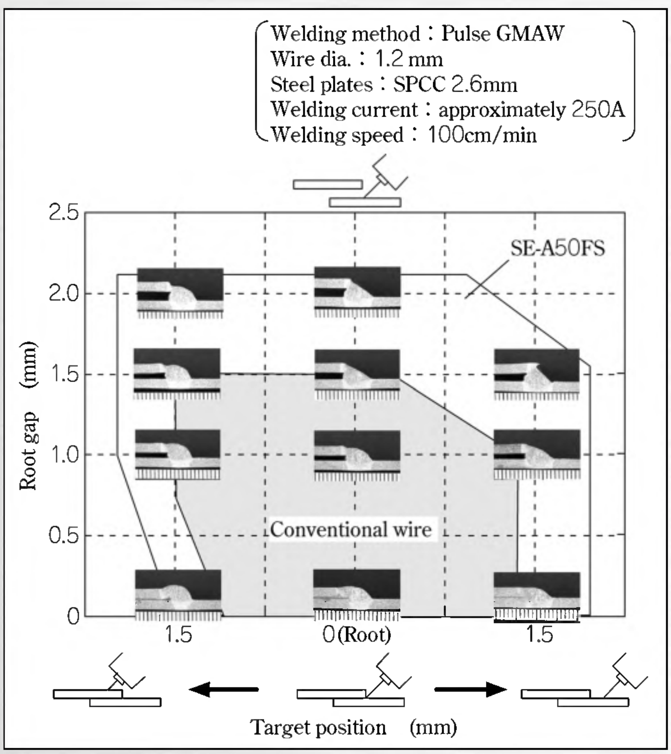

Fig. 3 — Relationship between bead shape, wire target position, and root opening along lap joint.

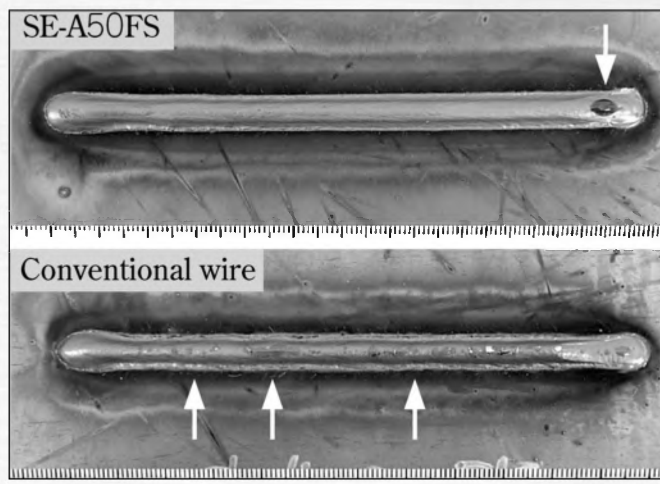

Fig. 4 — Comparison of slag distribution after welding.

age. When compared to a conventional GMAW wire (AWS A5.18 ER70S-6, JIS YGW12), the new wire exhibits smaller H/W values through all the voltage ranges. A smaller H/W value indicates the formation of a wider bead with a lower deposit height. In addition, the new wire shows bead formation without an undercut in the range higher than 28 V in which the conventional GMAW wire exhibits undercut.

When welding three-dimensional works, such as press-formed automotive panels, the current and arc length are subjected to changes due to disturbances such as the change in projection length and target position of the GMAW wire. The new wire prevents formation of misaligned beads caused by such disturbances. The stable bead shapes also serve to facilitate the condition settings during robot teaching.

Figure 2 depicts the relation between the welding current and bead width at welding speeds from 70 to 130 cm/min for lap joints of steel sheets having 1.6 to 3.2 mm thickness. The new wire produces wider beads compared to the conventional GMAW wire.

One major issue with welding thin steel sheets is melt-through discontinuities caused by the increase in arc force. The discontinuities are the result of increased current to compensate for insufficient leg length due to increased welding speed. The current also needs to be increased to bridge root openings, and the current increase causes melt through in thin sheets having a thickness of 1.6 mm or less. The new wire forms wide beads and provides sufficient leg length while bridging gaps at low currents with a small deposition.

Root Opening and Wire Target Deviation Tolerance

Figure 3 illustrates the relationship between bead shapes, wire target posi-

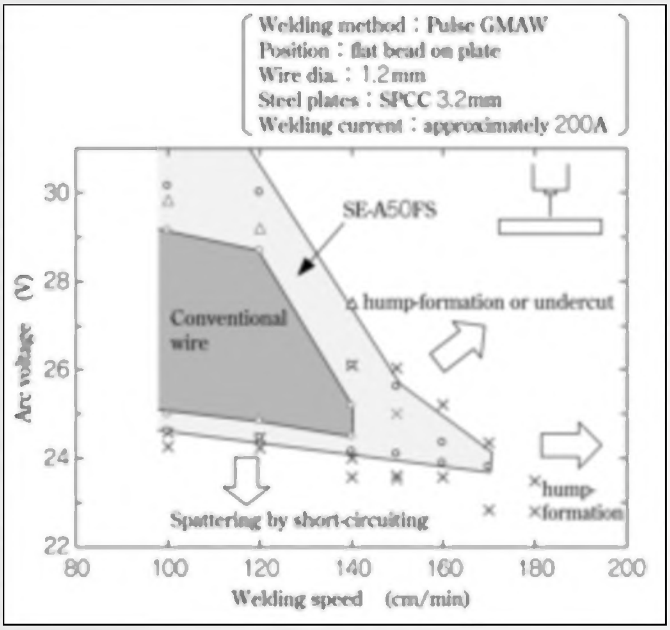

Fig. 5 — Applicable range of welding speed and arc voltage.

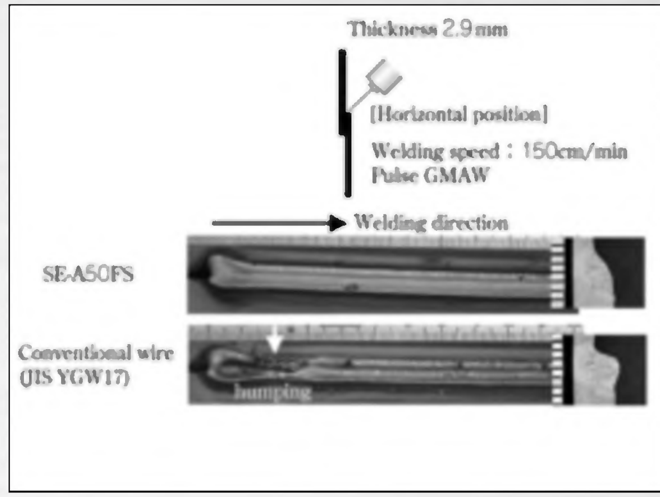

Fig. 6 — Comparison of start bead appearance with high-speed welding.

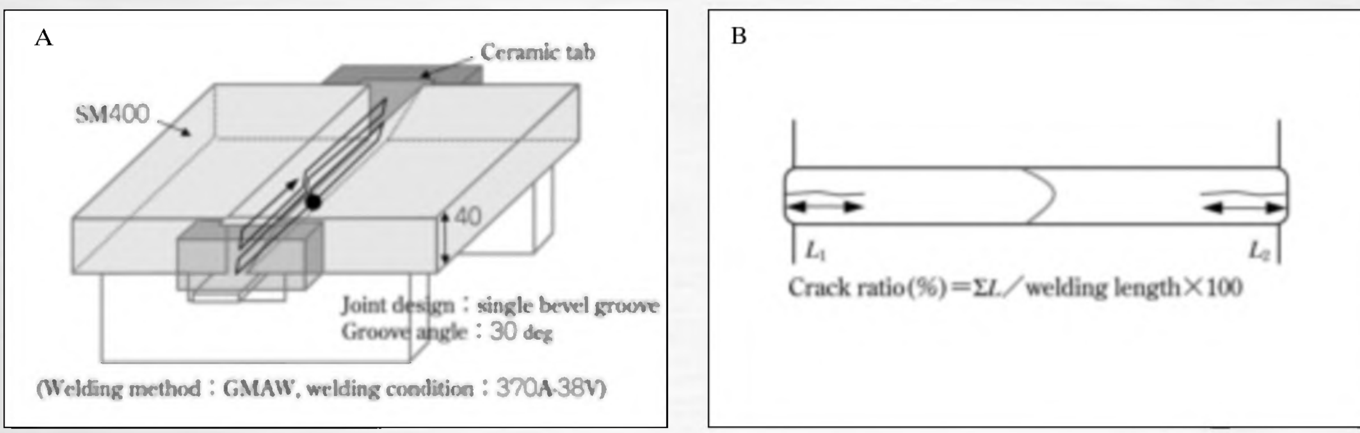

Fig. 7 — A — Welding setup; B — image of X-ray film of hot cracking test.

tions, and root openings along lap joints. When compared to the conventional GMAW wire, the new wire shows tolerance for a wide root opening range even if the GMAW wire target position is somewhat offset.

In a cross section of typical beads with wide root openings, the new wire exhibits a flat bead with a smooth end and no undercut.

Low Slag Generation

In the case of a conventional GMAW wire, the slag deposits in the rear of the molten pool, disperses thinly, and solidifies. In the case of new wire, the slag first agglomerates in spherical shapes in the vicinity of the arc, is dragged with the arc, and then solidifies in the rear of the molten pool when the agglomerates grow and coagulate. Such slag formation is possible only when the surface tension is controlled at the interface between the molten pool and slag.

Figure 4 shows the slag appearances after solidification. In the case of conventional GMAW wire, the slag is formed thinly along the surface of the bead and its distribution is inhomogeneous. In contrast, the slag of the new wire concentrates in the crater and is rarely formed in other areas. The slag generated is likely to clump together, forming a small area with preferable bead appearance. When comparing the slag area ratios (slag surface area/total bead surface area) of conventional GMAW wires (AWS A5.18 ER70S-3 or G, JIS YGW17) and of the new wire, its area ratio is ⅓ to ⅕ of those for conventional GMAW wires and is significantly lower. The slag formed by the new wire can be removed by light tapping. Residual slag on the weld bead can cause rusting of the steel sheets, which subsequently may be subjected to coating. The coating is applied to prevent corrosion of the welds; however, the slag tends to peel the coating off, increasing the chance of rusting. The slag characteristics of the new wire prevent this from happening.

High-Speed Weldability

Figure 5 compares the applicable ranges of welding speed and arc voltage between the new and conventional GMAW wires. Each range in the figure is defined for the respective wire by the welding conditions in which the number of expulsions due to short circuiting is acceptable (less than 100 times/s) and no irregular bead is formed, such as undercut and hump formation. The new wire enables welding under high-speed conditions while the conventional GMAW

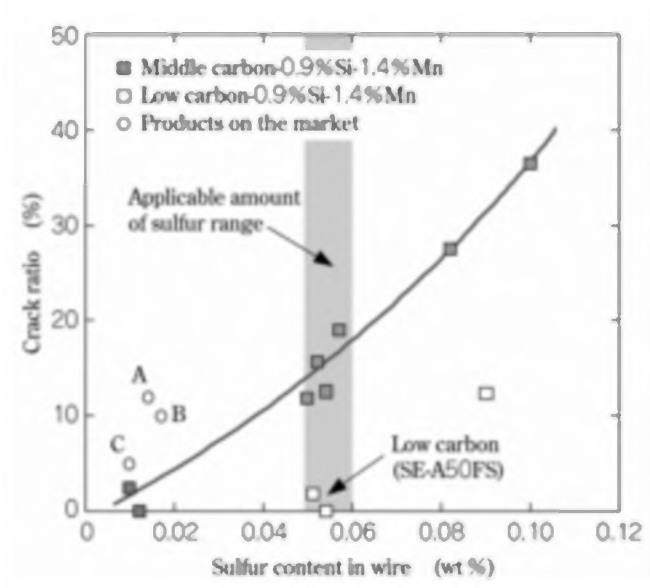

Fig. 8 — Relationship between crack ratio and sulfur content in welding wire.

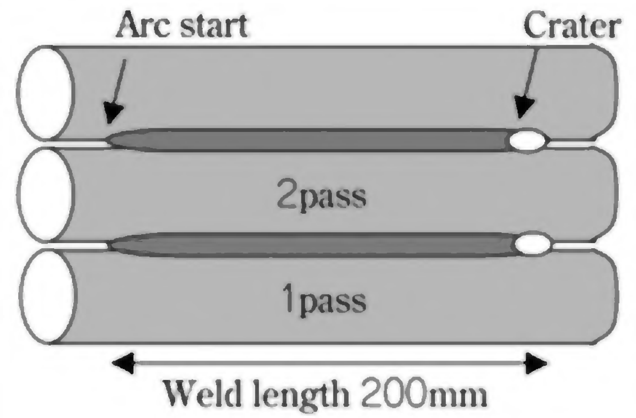

Welding method: Pulse GMAW
Wire diameter: 1.2 mm
Steel plates: STK400, diameter 40 mm, 3.2 mm
Welding speed: 40, 70, 100 cm/min

Fig. 9 — Schematic of pipe welding crack examination.

wires produced hump formation or excessive short circuiting.

Meanwhile, the new wire has a wider applicable range of voltage for lower welding speeds. The GMAW wire is effective in preventing undercut and hump formation particularly at high voltages. The result indicates that a quality bead is formed even with a long arc length. In other words, the new wire prevents the short-circuiting of molten drops and reduces the amount of expulsion to an extremely low level.

Figure 6 compares the bead-shapes of joints respectively welded with the new wire and a conventional GMAW wire at a high speed (150 cm/min). A hump is formed at the starting point of the bead of the conventional wire, while the new wire exhibits a stable bead without hump formation. The hump is considered to have been caused by a disturbed flow of molten metal at the arc start and is enhanced in high-speed welding. Conventionally, the hump formation has been prevented by applying a forward angle to the welding gun only at the time of arc start. Since no hump is formed when the new wire is used, it eliminates the need for complicated robot teaching and detailed condition setting, and thus facilitates the control. The new wire has an advantage in its bead shape since it prevents convexed shapes, insufficient width and constrictions, as well as undercut and hump, all of which tend to occur in high-speed welding. The advantage arises from the wire's intrinsic characteristics of producing wide beads with smaller deposits.

Hot-Cracking Resistance

As described previously, SE-A50FS is unique by its purposeful addition of sulfur. Generally, S is known to increase the susceptibility to hot cracking. Because of this, the addition of S is limited to 0.030% at maximum in the JIS standard for solid GMAW wires used in the welding of mild steels and high-strength steels of 490 MPa grade. The major cause of hot cracking is considered to be a low-melting-point phase being discharged from the metal during the solidification process, forming a final solidification line in the liquid phase that is unable to withstand the tensile stress induced by thermal distortion. As mentioned previously, two types of factors affect the susceptibility to hot cracking: 1) metallurgical factors and 2) morphological factors. The metallurgical factors include impurity elements with low melting points, such as P, S, and B, that form liquid phases at grain boundaries in the final stage of solidification; and elements, such as C, added in large amounts that increase the formation of γ-phase in which the low-melting-point elements have very low solubilities. As for the morphological factors, a bead having an excessive shape factor (P/W) is known to be more susceptible to hot cracking, where P is the throat thickness and W is the bead width (Ref. 4).

Thin steel sheets are less susceptible to hot cracking compared to thick steel plates, considering their binding forces and shape factors. A thick plate was used for an accelerated test to clarify the effect of sulfur on hot-cracking susceptibility. As shown in Fig. 7, hot cracking was induced on purpose in bead ends having a large shape factor (P/W). The bead was formed by continuously welding layers with no interruption in the narrow groove of the thick plates. Figure 8 shows the relationship between the crack ratio (crack length/total bead length) and S content in GMAW wires. The results indicate that higher S content in GMAW wires increases the crack ratio. The minimum S content to achieve the various properties described above has been found to be 0.05%. Such S content, if applied to conventional GMAW wires, causes cracks to occur at a ratio from 11 to 20%. The authors also found through research conducted separately on hot cracking that C has more significant influence on hot-cracking sensitivity when compared with S, P, and B in a practical composition range (Ref. 5). Thus, the new wire has a reduced carbon content to compensate for the deterioration of hot-cracking resistance. The reduction in carbon content narrows the range of solid-liquid coexisting zone and increases the volume fraction of δ phase, which has high solubility of S. As a result, the new wire exhibits a very small crack ratio of 0 to 2% despite its high S content. Commercially available wires were tested in the same manner, and their results are depicted in the figure as plots A, B, and C (crack ratios 4 to 11%). As shown in the figure, the new wire has a lower crack ratio even in comparison with commercially available GMAW wires.

Generally, the shape factor (P/W) becomes smaller for thin steel sheets compared with thick steel plates. Another test was also conducted on samples purposely having a large (P/W) to evaluate hot-cracking susceptibilities. In this test, pipes were disposed in a manner as shown in Fig. 9. The flare portions were welded and the bead cross sections were visually inspected for any cracks. Neither the conventional GMAW wire nor the new wire exhibited any cracking under any of the testing conditions.

The new wire takes appropriate measures to prevent hot cracking. From a metallurgical aspect, the increase in hot-cracking susceptibility caused by the addition of S is compensated by the reduction of C content. From a morphological aspect, the shape factor (P/W) is kept small enough by limiting the application of the wire to single-pass welding of thin steel sheets.

The Mechanical Properties of Welded Metals

Table 1 summarizes the mechanical properties of the deposited weld metal. The deposit has sufficient strength and falls in the range of a 490 MPa grade. It should be noted that thin steel sheets up to 590 MPa grade can be welded with sufficient joint strength using the developed GMAW wire.

Conclusions

The design concept and basic properties of SE-A50FS have been introduced. The wire exhibits excellence in bead shapes and provides quality welding of thin steel sheets frequently used in automotive industries. The wire shows promise to improve production efficiencies and lower defect rates.

Competition among automotive companies will make the use of the new wire more feasible as the requirements for improved technology, efficiency, and weld quality become more stringent.♦

References

1. Hagino, K., et al. 1983. *Tetsu-to-Hagane* 69(16): 1989.
2. Ohji, T., et al. 1990. *Quarterly Journal of the Japan Welding Society* 8(1): 54.
3. Shinozaki, K. 2005. Technical course for celebrating Nishiyama. *Welding of Steels* 184-185: 3.
4. Harasawa, H., et al. 1974. *JSSC* 10 (103): 31.
5. Sasakura, S., et al. 2006. Preprints of the national meeting of the Japan Welding Society 79: 32.

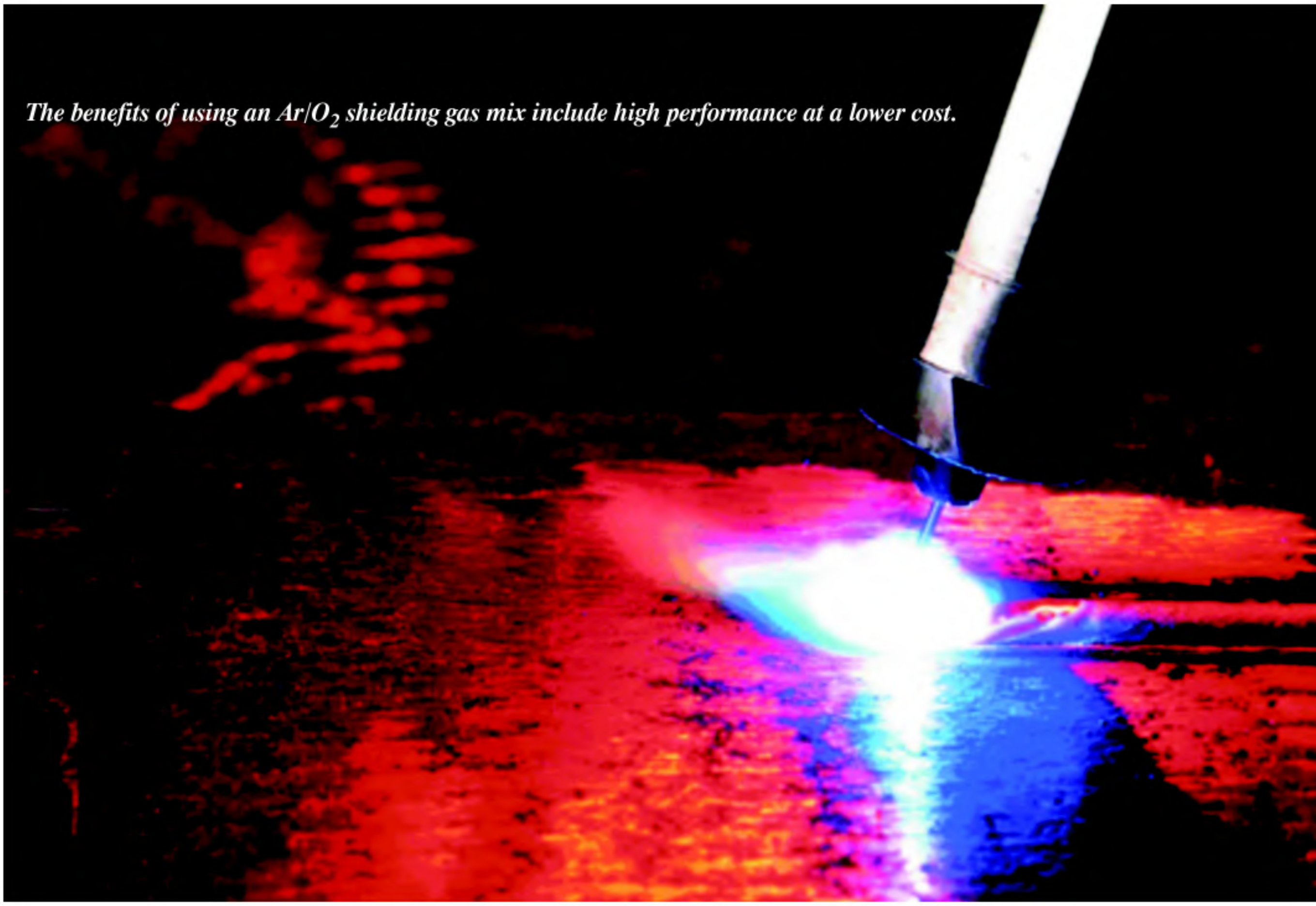

Argon/Oxygen Shielding Gases Improve Carbon Steel GMAW

These preblended gases increase welding speeds, provide good mechanical properties, and offer better weld economics

BY SCOTT LAYMON, CRAIG CHRITZ, AND FRED SCHWEIGHARDT

The most commonly used shielding gases for gas metal arc welding (GMAW) of carbon steel are various mixtures of Ar/CO_2. The most frequently encountered mixtures are 75% Ar/25% CO_2 and 90% Ar/10% CO_2. For many fabrication shops, these welding gas mixtures are delivered premixed in compressed gas cylinders. The mixing of the gases is performed under tight control at the cylinder fill plants before shipping to end users. After delivery, there is typically a significant amount of handling to get these cylinders or packs to the production areas. For volumes of gases exceeding about 30,000 ft^3/month, it is more cost effective for end users to use shielding gases from liquid bulk tank storage than the compressed gas cylinder packages. One load of 30,000 ft^3 of argon packaged in compressed cylinders could cost $3900, whereas the same volume delivered to the end user in liquid argon form typically would cost $2700, which is a 32% reduction in cost. In the case of 75% Ar + 25% CO_2 mixtures, a bulk supply solution requires two cryogenic liquid bulk tanks, one each for the argon and CO_2, plus an on-site mixer.

This shielding gas is available in a preblended bulk mixture of liquid oxygen

SCOTT LAYMON, CRAIG CHRITZ, and FRED SCHWEIGHARDT (Fred.Schweighardt@Airliquide.com) *are ALTEC welding specialists for Air Liquide Industrial US LP, Houston, Tex.*

mixed with liquid argon delivered directly to the end user tank. Since the gas is preblended and stored in a single cryogenic storage vessel, there is no need for a mixer and the secondary storage tank that are normally required for shielding gas mixtures. This reduces not only the overall gas packaging and storage equipment capital costs but also the variable costs of shielding gas — Fig. 1.

Reduction of Variable Cost, Spatter, and Fumes

Many GMAW operations can enjoy the benefits of replacing the traditional Ar/CO_2 shielding gas mixture with an Ar/O_2 mixture such as Emixal from Air Liquide. This shielding gas can provide an opportunity for cost reduction and quality when compared to the traditional gas mixtures. As more and more manufacturers and fabricators continue to search for ways to improve welding efficiencies, various analyses confirm that the primary factors contributing to the cost of a weld are wire and labor — Fig. 2.

Welding Cost Savings

The Ar/O_2 mixes are designed for automatic, semiautomatic, and robotic welding applications on most carbon steels. The characteristics of these mixes enable end users to produce high-quality welds using short arc, spray, and pulsed spray modes of metal transfer, while some of the traditional shielding gases or gas mixtures will only allow for short-circuit or globular modes of metal transfer. The spray or pulsed spray modes of metal transfer have the highest deposition efficiency and deposition rates when comparing the GMAW transfer modes — Fig. 3. Since the deposition rate is higher in spray and pulsed spray modes, weld metal is deposited at a higher rate and welding speed can be increased to reduce variable cost, which includes labor costs.

Decreased Spatter

Since spatter is reduced and often eliminated with spray transfer using Ar/O_2 mixes, the need for postweld cleanup is reduced. Since less wire is wasted through weld spatter, the deposition efficiency is increased, and thus the cost per hour is re-

A

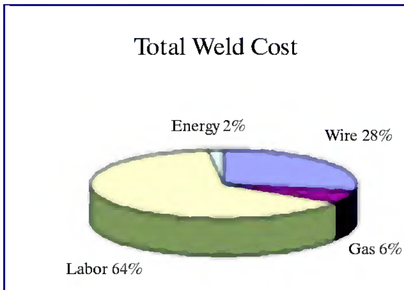

Fig. 2 — Typical hourly cost breakdowns for welding operations.

B

Solutions for more than 30,000 ft^3/month	Cylinders	Tank 1	Tank 2	On-site mixing	Index of cost per month
Ar/CO_2 shielding gas preblended in compressed cylinders	90% Ar/10% CO_2				100
Ar/CO_2 shielding gases in bulk liquid tanks		Liquid Ar	Liquid CO_2	Mixer	70
Ar/O_2 shielding gas preblended in compressed cylinders	95% Ar/5% O_2				85
Emixal shielding gas preblend of liquid Ar/liquid O_2		Premixed Liquid			55

Fig. 1 — Compared to the conventional Ar/CO_2 mixture, Ar/O_2 mixes do the following: A — Eliminate capital expenditures for one tank and one on-site mixer, as well as the foundation requirements for their installations; and B — yield lower consumables costs per month.

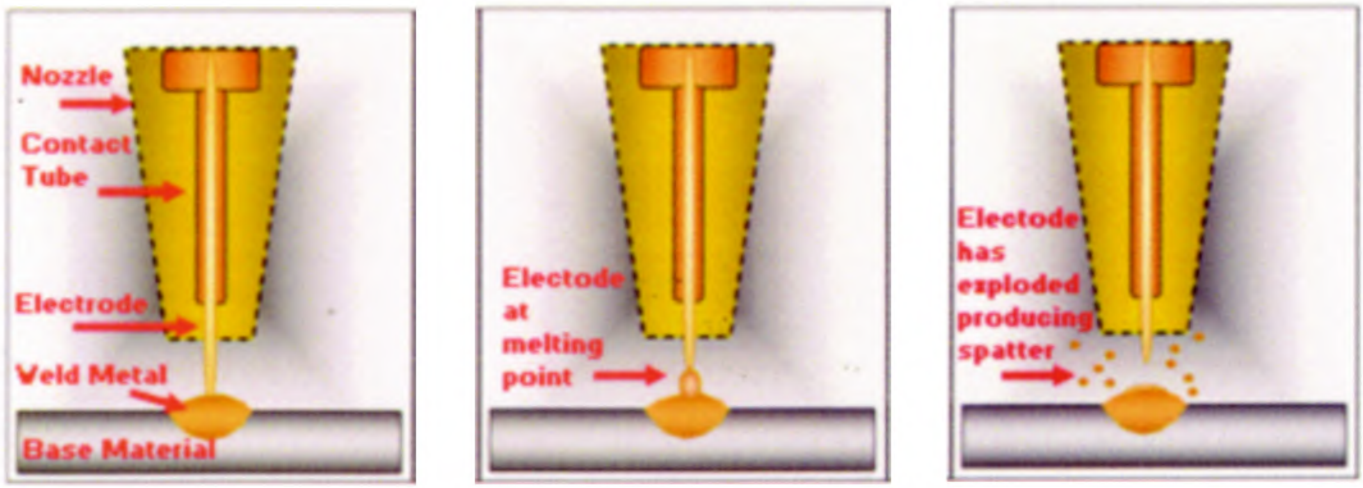

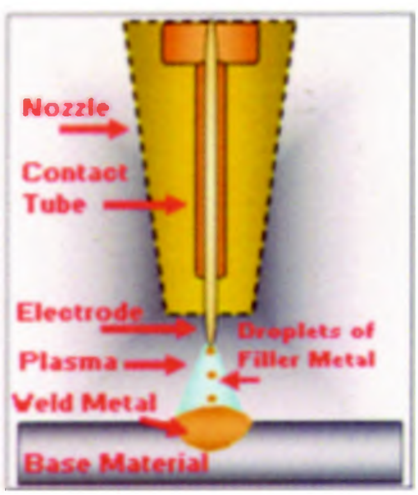

Fig. 3 — Short-circuit (top row) and spray spatter (bottom) levels.

duced. These factors significantly reduce the overall labor and wire costs, which are the top two largest contributors to the total variable cost of a weld — Fig. 4.

COST ANALYSIS		
OBJECTIVE:	Semiautomatic welding of loader arm assembly	
Shielding gas	Ar/O_2	Ar/CO_2
Labor & overhead cost ($/h)	$45.00	$45.00
Gas cost (100 ft^3)	$3.00	$2.50
Wire diameter (in.)	0.035	0.035
Wire type	ER70S-3	ER70S-3
Wire cost (lb)	$0.90	$0.90
Energy cost (kWh)	$0.07	$0.07
Welding data:		
Gas flow rate (ft^3/h)	40	40
Wire speed (ft/min)	43.29	37.39
Amperage	180	170
Voltage	25	26
Arc time (s)	32	41
Total cost	$0.48	$0.60
Percentage difference	20.11%	
Labor	$0.40	$0.51
Wire	$0.07	$0.08
Gas	$0.01	$0.01
Energy	$0.00	$0.00

Fig. 4 — Cost analysis of a shielding gas performance.

Lower Fume Levels

The results of a study comparing a 95-5% Ar/O_2 mix to a 90-10% Ar/CO_2 mix show a very favorable reduction in fume levels. The 95-5% Ar/O_2 mix showed the total fume volume generated was six times less with the 90-10% Ar/CO_2 blend. This study was conducted with copper-coated solid wire and using straight spray transfer. The fume levels were reduced even more when pulsed spray transfer was used (Ref. 1).

Mechanical Properties with Emixal

Material: A36 to A36 Carbon Steel Plate — 1 in.
Filler Metal: ER 70S-6 (0.045 in.)
Specification: ANSI/AWS D1.1:1998

Transverse Tension Test	
ANSI/AWS Minimum Values	Ar/O_2 Tensile Test
Tensile Strength, lb/in.^{2} = 58,000	88,126

All-Weld-Metal Tension Test	
ANSI/AWS Minimum Values	Ar/O_2 Tensile Test
Tensile Strength, lb/in.^{2} 70,000	82,660
Yield Point, lb/in.^{2} 58,000	65,730

Fig. 5 — Mechanical properties.

Weld Mechanical Properties

There may be concerns about the metallurgical effects of this oxygen-bearing shielding gas on the mechanical properties of the welds. All-weld-metal and transverse tensile tests have been performed on welds using 95/5 Ar/O_2 mixes, which show excellent properties — Fig. 5. This clearly shows that with proper welding techniques, mechanical properties well in excess of code requirements can be obtained.

Summary of Benefits

The Ar/O_2 mixes offer the following advantages over traditional mixes (Ref. 2):

- Reduction of weld spatter and fumes and subsequent postweld cleanup.
- Increased welding speeds.
- Higher deposition rates.
- Excellent weld profiles and mechanical properties.
- Improved weld economics.
- Achieve spray transfer at lower welding parameters than conventional Ar/CO_2 mixes.
- More consistent gas mix than mixers can provide and the components never separate.
- Single tank system eliminates the need for a mixer and second storage tank or cylinders.

Conclusion

Various factors such as gas, labor, wire, and energy should be evaluated in the selection of shielding gas. Using Ar/O_2 mixes provide an opportunity to increase welding production and reduce variable cost along with the price of owning a shielding gas supply system. With proper welding techniques, there is no reason to be concerned about loss of metallurgical properties or performance.♦

References

1. Dreon, L., Porter, K., and Wilkinson, D. 1999. Shielding gases and their effects on fume generation. *Welding Journal* 78(9): 56–58.
2. *www.us.airliquide.com/en/solutions-by-industry/solutions-products-services/automotive-and-fabrication.html*

Maximizing Your Investment in Welding Automation

The efficient operation of robotic installations depends on an effective preventative maintenance program.

Simple preventive maintenance tips are discussed that can minimize production downtime and improve the overall efficiency of robotic GMAW equipment

BY ROB RYAN AND THOMAS JAEGER

Given that the most enticing reason for companies to invest in welding automation is to improve productivity, it may seem counterintuitive to stop or slow production for any reason. But what if scheduled downtimes could save your company time, money, and trouble in the long term? Or increase your competitive edge by improving your overall efficiency? Simply put, this is the basis for implementing a preventive maintenance (PM) program.

Far too often companies fall victim to the "if it isn't broken, don't fix it" mentality when it comes to caring for automated equipment, including their robotic gas metal arc welding (GMAW) gun (Fig. 1) and consumables. Doing so, however, can have dire consequences. Not only is there a risk of losing productivity and lowering throughput if the entire system isn't functioning properly, but even the slightest malfunction could result in higher labor costs, lower weld quality, additional rework, and wasted materials. But most important, the downtime associated with troubleshooting and completing repairs can significantly lower the return on investment sought by transitioning to welding automation in the first place.

And while properly maintaining the automated welding system is important, maintenance of the robotic GMAW gun is just as important. In fact, the robotic GMAW gun (including the consumables) is often one of the most overlooked components of the system, and also one of the easiest to maintain. Fortunately, by adding a few simple steps, you can make maintenance of the robotic GMAW gun a regular part of your overall PM program to ensure consistent performance of the entire automated welding system.

Fig. 1 — Performing regular preventive maintenance on the robotic gas metal arc welding gun can help assure consistent operation and minimum downtime.

The Who, Why, and Whens of PM

Preventive maintenance programs, particularly those for robotic GMAW guns, are not just beneficial for large companies with numerous automated welding cells. All companies, regardless of their size or arc count, should regularly care for their equipment. Like the key tenets of the 5S methodology (Sort, Straighten, Shine, Standardize, and Sustain), taking proactive steps to ensure the productivity of your automated welding operations, starting with the guns (no matter how many you have), can positively affect your company's work flow, throughput, and the bottom line.

The scope of a PM program varies ac-

ROB RYAN is product manager, automation group, and THOMAS JAEGER is engineering manager, R&D and new product development, at Tregaskiss, Windsor, Ont., Canada, www.tregaskiss.com.

cording to each particular application. Specifically, the higher the risk of problems in the process — logistically and fiscally — the more frequently you should take steps to prevent them. Take, for example, a heavy-equipment manufacturer that welds thick plate and has an average welding cycle time of 4 h per part. This company stands to have greater downtime and more expensive rework to remedy a problem than a company that welds smaller, less-expensive parts in a 4-min weld cycle. Therefore, the higher-risk process needs more frequent care of its equipment, including its robotic GMAW gun, as part of an overall PM program.

Welding engineers, welding supervisors, tool and die employees, and members of the maintenance staff are all viable candidates to oversee a PM program. There is, however, one requirement for employees executing a PM program successfully: proper training. All personnel involved need to be aware of the potential problems that could arise in the weld cell and trained how to prevent them.

Getting Down to the Specifics

To make your robotic GMAW gun a central part of a PM program takes significantly less time than you might expect. In fact, most of the maintenance can be completed shift by shift with minimal off-line time. Note, however, that such in-process PM does not constitute the entirety of a PM program. There may be procedures that need to take place off-shift due to their complexity and the time necessary to complete them.

The first thing to know about maintaining your robotic GMAW gun is to always use the designated tools for the job. When changing diffusers (or retaining heads), use the proper adjustable or crescent wrench. Contact tips should also be installed with a suitable pair of pliers or welpers, or a specific tip-installation tool. Always use a sharp pair of side cutters when trimming the robotic GMAW gun liner, as any other type of tool will likely create a large burr that could wear or drag on the welding wire.

Secondly, during in-process robotic GMAW gun maintenance, always check that the connections on the gun, consumables, and cable are secure, in good working order, and that these components are as clean as possible. This task can be completed relatively quickly when the welding operator overseeing the weld cell changes out a finished part and/or during a routine contact tip changeover.

Specifically, check that the diffuser is tightly connected to the neck (or gooseneck) and that, in turn, the contact tip fits snugly in the diffuser. Similarly, be certain the nozzle and any seals around it (depending on the style you use) are secure. Tight connections from the neck through the contact tip ensure there will be a solid electrical flow through the components and that there will be minimal heat buildup that could cause a premature failure. Minimizing heat buildup also lessens the chances for troublesome occurrences like meltback, which could result in unplanned downtime to change the contact tip and diffuser, as well as poor arc stability, which could cause quality issues and rework. Note: Any change in the color of the consumables (particularly if the copper changes to a dark orange or purple) is a good indication that they are loose and require tightening.

Additionally, check that the power pin and welding cable lead are properly secured and that the cable does not rub against any part of the robot's metal casting, as this could eventually cause it to loosen or wear out the cable. A worn spot on your robot or on your tooling (e.g., the absence of paint) is a good indication that the cable is rubbing against it. Fixing such a problem must be done while the robot is off-line, because it could require repositioning the tooling or adding some form of cable management device; however, a quick in-process inspection that identifies the issue can flag it for a later, proactive solution.

Visually inspecting the contact tip, nozzle, and diffuser for spatter buildup is also a crucial part of a robotic GMAW gun PM program. Check, too, that the grounding blocks are clean and free of spatter in order to make good electrical contact.

Like loose connections between components, spatter buildup can cause excessive heat to be generated from the contact tip to the GMAW gun neck, fouling the internal and external threads — even to the point of causing the gun itself to overheat and fail. Spatter can also block the shielding gas flow, causing problems like porosity or other defects that require costly rework. It can also add to your overall costs for the consumables themselves, as spatter buildup makes it necessary to change nozzles and contact tips more frequently.

To prevent such problems, inspect your consumables regularly for spatter accumulation. Even better, consider using an automated consumables-cleaning device, often called a nozzle-cleaning station, reamer, or spatter cleaner to minimize spatter buildup. As with any part of your automated welding system, adding equipment like a spatter cleaner also adds costs to the initial capital investment; however, as with any part of a PM program, it can save money over the long term.

Like its name implies, a spatter cleaner device removes spatter (and other debris) that builds up in the nozzle and diffuser as part of the normal welding process. Using this product in conjunction with a sprayer that applies an antispatter compound provides further protection against spatter accumulation and reduces downtime needed for fixing weld defects.

Next in the PM of your robotic GMAW gun, determine how long it takes for the gun liner to become worn or fouled using your particular process, then schedule a liner replacement as required. Replacing it prior to a failure prevents unplanned downtime to remedy wire feeding or quality problems later.

As a side note, remember to cut the liner to the correct length, per the manufacturer's recommendation. A liner that is either too long or too short can lead to poor wire feeding and poor weld quality. Improper liner lengths can also lead to premature contact tip failure.

Periodically, check the force required to pull the welding wire from the feeder through the robotic GMAW gun to ensure that there isn't too much drag, which indicates a buildup of debris in the liner. To complete this task properly, the drive rolls of the feeder should be released first. Also, it is best to perform this task between shifts, as opposed to during contact tip changeover, as this operation will take a bit more time.

During this time, you should also check the force needed to pull the welding wire from the coil through the wire conduit to the feeder. While the conduit and feeder are obviously not part of your robotic GMAW gun, caring for them directly affects the performance of the gun itself. For example, debris in the wire conduit, if undetected through regular inspections, can be pulled through the length of the robotic gun, causing liner and consumable problems, especially wire stoppages that lead to meltback.

Similarly, too many twists or bends in the welding wire that feeds through the gun can also affect the longevity of the gun liner, as well as arc stability and weld quality. It is a good preventive measure to check that the wire conduit is clean, drive roll pressure is properly set, and you inspect and replace worn drive rolls and wire guides.

Parting Thoughts on PM

Maintaining your robotic GMAW gun is just part and parcel of an overall PM program, but it is significant nonetheless. Most of the robotic GMAW gun maintenance, as discussed here, can be completed on a shift-by-shift basis with minimal interference with your cycle times and with minimal labor, especially when you consider the time and cost of resolving problems instead of preventing them in the first place. Remember, PM programs don't have to be complicated, only effective. So take some time to consider the PM needs specific to your automated welding operation in order to establish the scope and frequency of your own program.♦

Measuring Contact Angles on Sessile Drop Test Samples

The contact angle comparison for a copper-stainless steel system indicated the projected area and cross-section methods presented results within a 95% confidence interval

BY DANIEL G. STROPPA, JIMY UNFRIED S., TAHIANA HERMENEGILDO, AND ANTONIO J. RAMIREZ

As a widespread technique applied to surface characterization, the sessile drop test (Ref. 1) has supported the study and improvement of innumerous systems, from protective coating films (Ref. 2) to joining technology (Ref. 3). The sessile drop test is commonly applied to brazing studies to measure the contact angle of specific systems to evaluate filler metal wettability (Ref. 4) and, consequently, its adequacy for producing successful brazed joints (Ref. 5).

The wettability evaluation of molten filler metal on base materials presents several challenges for brazing engineers due to the difficulties associated with the contact angle measurement. In-situ measurement at brazing temperature requires complex instrumentation and has inherent high costs, while optical microscopy measurement of cross-sectioned samples is a time-consuming task due to the required sample preparation. In addition, the characteristic low contact angles required for brazing processes seriously compromises the acuity of these traditional methods.

Aiming the development of a simplified approach for contact angle evaluation, this work proposes a simplified geometric model and compares its results with the optical microscopy analysis of cross-sectioned samples for the evaluation of a copper-stainless steel brazing system.

Experimental Methods

A typical brazing thermal cycle under pure hydrogen atmosphere was applied to ten samples, as shown by the time-temperature profile illustrated, which applies a peak temperature of 1150°C — Fig. 1. Each sample consisted of 50 × 50 × 3 mm AISI 304 stainless steel base metal degreased and pickled in two stages with pure hydrochloric and chromic acids, and a copper filler metal (C11000) piece with approximately 50 mg freely placed on top of the base metal.

The copper-stainless system contact angle was evaluated on the sessile drop using two different methodologies, the standard cross-sectioning and the proposed drop projected area method, which is described in the next section. For the cross-sectioning method, the samples were sectioned using a precision saw (Buehler IsoMet 4000) followed by metallographic preparation and optical microscopy (Leica DMLM 100×) observation. Finally, the contact angle was obtained from the digital images using ImageJ® software. On the other hand, for the projected area method, plain view digital images of the brazed samples were obtained using a digital camera (Nikon Coolpix 5200 5.1M). The image was digitally scaled using a reference object (caliper). The projected area of the brazed drop sitting on top of the base metal was evaluated by color contrast on the digital images using ImageJ® software.

Proposed Projected Area Measurement Method

The proposed method is based on fundamental geometry and assumes that any sessile drop can be considered as a spherical cap, which is a good approximation when the drop is small and surface tension dominates over the gravity (Ref. 6) — Fig. 2A. From this assumption, it is possible to evaluate the contact angle, when $\alpha << 90$ deg, as function of the drop total volume and its projected area on top of the base material. The total volume of a spherical cap can be achieved by integral calculus as demonstrated elsewhere (Ref. 7) and results in Equation 1:

$$V = \pi h^2 (R - h/3) \qquad (1)$$

where R represents the sphere radius and h the drop height — Fig. 2B.

The spherical cap (drop) volume, V, can be inferred from the known filler metal mass and density. R and h variables can be correlated by the Pythagoric relationship on the drop cross section, also illustrated in Fig. 2B and presented in Equation 2:

$$R^2 = A^2 + (R - h)^2 \qquad (2)$$

where A represents the projected spherical cap radius, which can be measured on the brazed sample plain view digital image.

Equations 1 and 2 constitute a two-variable system (R, h), which can be solved by numeric evaluation. On the other hand, the spherical surface curvature evaluation is presented as a function of R at a given point — Fig. 3. Therefore, considering a spherical cap model, the contact angle α can be evaluated by the derivative at $x = \pm A$ using Equation 3:

$$\alpha = arctg[A/(R^2 - A^2)^{0.5}] \qquad (3)$$

DANIEL G. STROPPA (dstroppa@lnls.br), *JIMY UNFRIED S., TAHIANA HERMENEGILDO, and ANTONIO J. RAMIREZ* (ramirez@lnls.br) *are with Brazilian Synchrotron Light Laboratory, LME–LNLS, Campinas, SP, Brazil.*

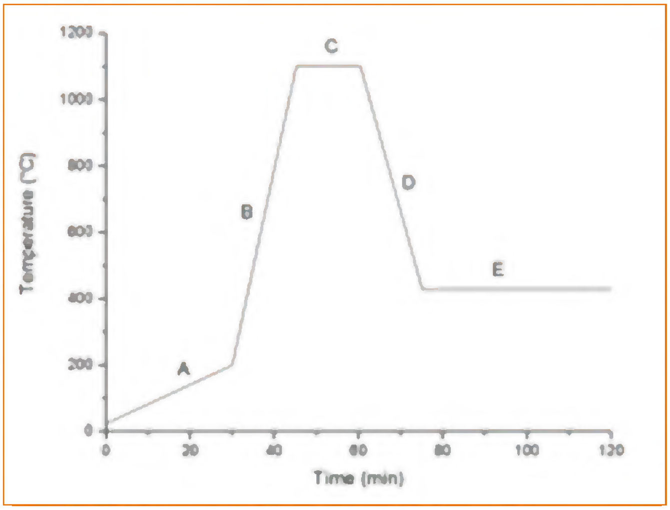

Fig. 1 — Temperature profile during sessile drop test.

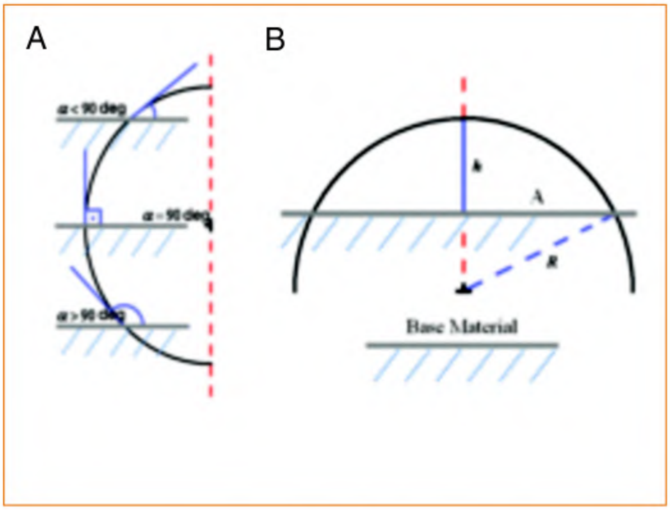

Fig. 2 — A — Illustration of contact angles for sessile drops as spherical caps; B — geometrical parameters used on proposed method. (R: sphere radius; h: spherical cap (drop) height; A: projected spherical cap.)

Table 1 — Contact Angle in Degrees Measured on Cross-Sectioned Samples Using the Optical Microscope and Calculated Using the Projected Area Method

Sample Number	Cross Section Test (deg)	Projected Area Method (deg)
1	2.9	2.7
2	4.7	4.2
3	1.9	2.4
4	3.1	2.8
5	1.9	2.5
6	2.8	2.4
7	3.4	2.4
8	2.3	2.2
9	3.5	4.1
10	2.6	2.3

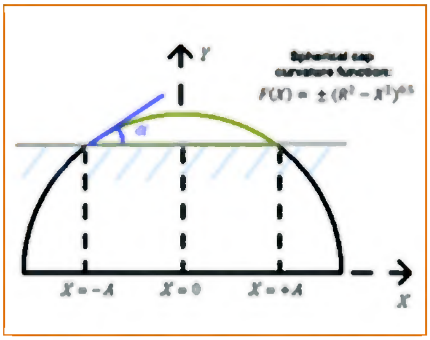

Fig. 3 — Illustration of curvature function and derivative position for the proposed model.

Table 2 — Statistical Comparison of the Standard Sessile Drop Test and the Proposed Method

Result (deg)	Cross Section Test	Projected Area Method
Standard Deviation	0.88	0.78
Value for 95% Confidence Interval	2.9 ± 1.8	2.8 ± 1.6
Max Value	4.7	4.2
Min Value	1.9	2.2

Results and Discussion

Figure 4A shows the drop plain view digital image taken after the sessile drop test, and Fig. 4B presents a detail of the drop cross-section image obtained after metallographic preparation, which was used for contact angle measurement.

The results obtained using the contact angle measurements on cross-sectioned samples and the projected area methods for the copper-stainless steel system brazed under pure hydrogen atmosphere are presented in Table 1. These results indicate very good agreement between the cross-section and projected area method results achieving a concordance value of approximately 83.5%. It should be pointed out that the cross-section method provides the contact angle just on the plane the drop has been sectioned. On the other hand, the projected area method allows calculating the contact angle based on the whole drop behavior and not just a specific region or sectioned plane of it. Therefore, this proposed method provides a quantitative and more representative measurement of the system contact angle, which is useful for actual brazing applications that are based on real and nonhomogeneous materials.

Table 2 presents a statistical comparison of standard cross-section method and

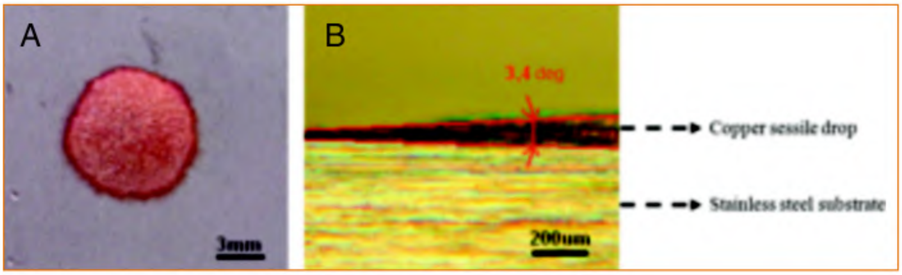

Fig. 4 — A — Plain view of an obtained sessile drop; B — cross-section image detail with measured contact angle.

the proposed projected area method results for the contact angle measurement. Such comparison indicates the quantitative equivalence of both methods to measure the contact angle within a 95% confidence interval. As expected, the projected area method shows a lower standard deviation due to the averaging effect of this method.

The projected area method is based on geometrical evaluation of a sessile drop, which can be virtually extended to any case where the drop shape can be assumed as a spherical cap. However, there are restrictions regarding the drop mass and contact angle range that can be evaluated. Large drop masses will tend to form oblate ellipsoidal caps instead of spherical ones (Ref. 8). However, as previously stated, this consideration is beyond the application of the proposed method, which is applicable to commonly used brazing systems where the contact angles tend to be very low.

A correction on total volume of the drop V must be performed in systems where the filler material is partially consumed during the brazing process by considering only the metal volume that contributes to the sessile drop formation. The use of flux cored filler material contextualizes this example.

Conclusions

The comparison of the results obtained using the very simple and easy-to-apply projected area method proposed here and the more conventional cross-sectional method to evaluate the contact angle for the copper-stainless steel (AISI 304) system brazed under a pure hydrogen atmosphere showed that fundamental geometry can be used to evaluate a sessile drop experiment, demanding only the measurement of filler metal mass and sessile drop plain-view projected area.

Experimental agreement higher than 83% was achieved when comparing both methods results for each sample. In addition, the mean value of contact angle provided by the two methods for the evaluated system was identical within a 95% confidence interval. Therefore, the presented results indicate that the proposed projected area method can be successfully applied to analyze the sessile drop test of low contact angle systems in both qualitative and quantitative manner.◆

References

1. Bashforth, F., and Adams, J. C. 1883. *An Attempt to Test the Theory of Capillary Action*. Oxford.

2. Panwar, A. K., Barthwal, S. K., and Ray, S. 2003. *J. Adhes. Sci. Technol.* 17(10): 1321–1329.

3. Chen, J. C., Hao, C. Y., and Zhang, J. S. 2006. *Sci. Technol. Weld. Join*, Vol. 11, pp. 600–605.

4. Funk, E. R., and Udin, H. 1952. Brazing hydromechanics. *Welding Journal* 6(18): 310–316.

5. *Brazing Handbook*, 5th ed. 1991. Miami, Fla.: American Welding Society.

6. Erbil, H. Y. 2006. *Surface Chemistry of Solid and Liquid Interfaces*, 1st ed.

7. Lennart, R., and Westergren, B. 1990. *Beta Mathematics Handbook*, 2nd ed. CRC Press.

8. Erbil, H. Y. 1997. *J. Phys. Chem. B*, Vol. 101, pp. 6867–6873.

Direct Brazing of Sapphire to Niobium

The mechanisms by which niobium diffuses through liquid braze filler metal to react with sapphire were examined

BY C. A. WALKER, F. R. TROWBRIDGE, AND A. R. WAGNER

The fabrication of switches and other high-voltage components often requires joining metal contacts to nonmetallic insulator materials such as ceramics. Brazing is the logical, and sometimes only, joining method available to the manufacturer due to high production volumes, material property differences, and joint performance requirements. While other high-temperature joining methods such as diffusion bonding, transient liquid phase bonding, or variants thereof have been used successfully to braze metals to nonmetals, furnace brazing processes have become the industry standard for large- and small-scale production processes. Prior to the brazing process, in many cases the nonmetal component is metalized using a molybdenum-manganese/nickel plating process (Refs. 1, 2) to promote proper wetting by the brazing filler metal. The subsequent brazing operation is performed in a manner similar to a standard metal-metal braze process. Alternative ceramic metallization methods have been proven to perform similarly (Ref. 3).

In the more recent past, however, brazing processes have been developed that allow a metal to be joined to a nonmetal without prior metallization. These brazing processes have progressed from the use of metal-hydride powders applied directly to the nonmetal faying surfaces and clad metallic strips with an "active" element layer, such as titanium, to alloys with active elements available in powder, paste, or sheet form (Refs. 4, 5). Another method for joining metals to nonmetals, known simply as direct brazing, can be made using conventional filler materials. Although useful in limited cases, the direct brazing process takes advantage of a substrate metal's limited solubility in liquid braze filler metal and oxide stability to react with the nonmetal substrate, without the need for metallization or expensive active braze filler metals (Ref. 6).

Background. In specific applications, niobium metal is joined to single crystal alumina (sapphire) or polycrystalline alumina ceramic. Because niobium metal has limited solubility in many high-temperature braze filler materials, such as copper, gold, nickel, etc., and forms relatively stable oxides, it is well suited for use in direct brazing operations. The very similar coefficients of thermal expansion (CTE) of sapphire and niobium result in minimized residual stress in brazed components. Additionally, hermetically sealed, long-life components can be made reliably without the use of more expensive active braze filler metals. These traits, as well as the lack of formation of brittle intermetallic phases with alumina ceramic or sapphire, make niobium an attractive candidate for direct brazing.

Direct Brazing. Direct brazing of niobium to alumina ceramic and sapphire has been successfully demonstrated as a manufacturing process for high-reliability components such as high-voltage switches and hermetically sealed packages (Ref. 7). The choice of metal-ceramic brazing method, brazing filler metal, atmosphere, temperature, etc., can result in a broad range of observed strengths for tensile test samples. ASTM-F19 tensile samples (Ref. 8) made from 94% alumina and brazed to Fe-29Ni-10Co interlayers showed strengths ranging from 76 to 147 MPa (11–21.3 ksi) (Ref. 9). While some of these

Fig. 1 — ASTM-F19 tensile button. (Previously published in Titanium Scavenging in Ag-Cu-Ti Active Braze Joints, by P. T. Vianco, et al., October 2003 Welding Journal.*)*

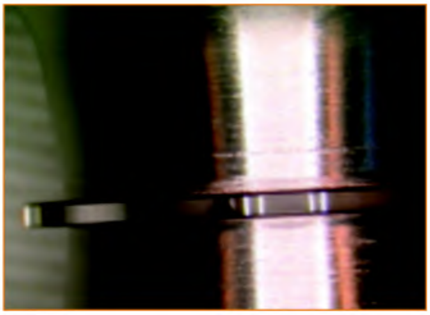

Fig. 2 — Niobium/sapphire/niobium tensile button.

C. A. WALKER (cawalke@sandia.gov)*, F. R. TROWBRIDGE, and A. R. WAGNER are with Sandia National Laboratories, Albuquerque, N.Mex.*

Sandia is a multiprogram laboratory operated by Sandia Corp., a Lockheed Martin company, for the U.S. Department of Energy under contract DE-AC04-94AL85000.

Based on a paper presented at the International Brazing & Soldering Conference, Orlando, Fla., April 26–29, 2009.

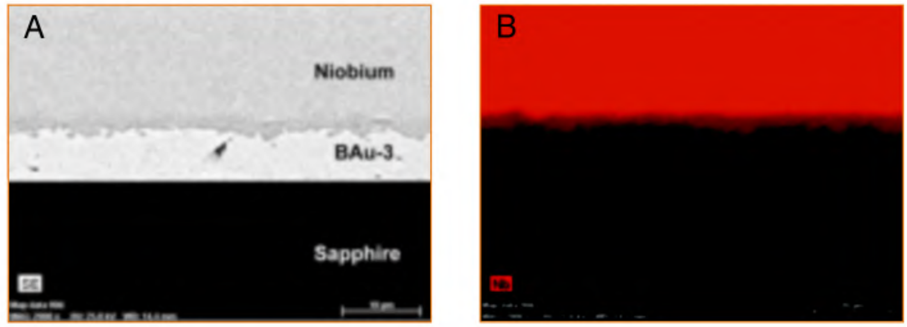

Fig. 3 — Niobium-sapphire sample brazed with BAu-3; A — SEM image; B — EDS maps showing no diffusion.

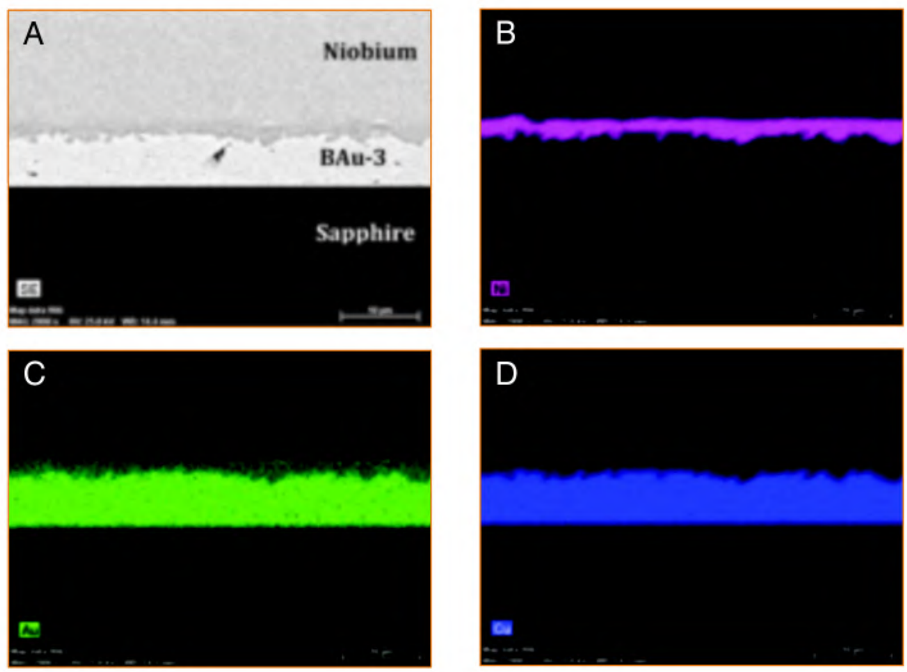

Fig. 4 — Niobium-sapphire sample brazed wih BAu-3; A — SEM image; B–D — EDS maps showing Ni, Au, and Cu distributions in the braze joint.

Table 1 — Braze Filler Metal Liquidus and Solidus Temperatures

Brazing Filler Metal	Solidus Temperature (°C)	Liquidus Temperature (°C)
BAu-3	1000	1030
35Au-62Cu-2Ti-1Ni	983	1020
Cusil-ABA	780	815
97Ag-1Cu-2Zr	940 (est.)	962 (est.)

differences can be explained by variations in the physical and mechanical properties of the braze filler metals or atmospheres used in the joining environment, the tensile strength of direct-brazed metal-nonmetal samples is consistently lower than other brazing methods when using commonly used temperature profiles. For the same brazing filler metals, Stephens et al. (Ref. 7) reported strengths 50% lower for tensile samples that were direct-brazed compared to those that had been metalized using the moly-manganese/nickel plating process, even though no notable differences in joint hermeticity were observed.

A literature search on niobium-ceramic or niobium-sapphire brazing reveals that while not exhaustively studied, the joining of ceramic or sapphire to itself using niobium alone or in combination with other filler metals by brazing, diffusion bonding, and other liquid and partially liquid processes is well documented (Refs. 10, 11). Marks et al. reported alumina to alumina four-point bend specimen strengths exceeding 240 MPa when specific sample preparation and processing conditions were followed (Ref. 10). This literature also reveals that the research laboratory joining methods, fixturing means, vacuum levels, temperature cycles, and equipment necessary to achieve the high strengths are not always practical or obtainable when the manufacturer is limited to industrial furnace equipment and standard brazing processes. Recognizing this, an effort has been made to incorporate some of the more readily achieved differences in processing with the goal of increasing the tensile strengths of direct-brazed niobium-sapphire assemblies, without affecting the joint hermeticity.

Experimental Procedure

Due to the inability to easily fabricate sapphire tensile buttons, niobium-sapphire assemblies were fabricated using niobium tensile buttons machined to ASTM-F19 ceramic tensile button dimensions. After an initial comparison of sapphire interlayer thicknesses of 0.25 and 0.41 mm (0.010 and 0.016 in.) and finding no statistical differences in strength or hermeticity, the thicker material was chosen for the remaining brazed samples (0.016 in. thick). The sapphire washers were cut 30 deg off the C-axis in what is known as the random orientation, a less-expensive crystal orientation that typically yields the most products from a sapphire boule or ingot.

The ASTM-F19 94% alumina ceramic tensile specimens were brazed using standard 0.25-mm- (0.010-in.-) thick niobium interlayers in the typical configuration. The brazing atmosphere used for all samples was ultrahigh vacuum, approximately 1.0E–07 torr at peak brazing temperature. The sample preparation, testing, and metallography techniques used for brazing with BAu-3 braze filler metal were followed for the active filler metal brazed samples, with the exception of the processing temperatures, which were adjusted for the differences in liquidus and solidus temperatures. The thermal cycle used was a typical ramp of 15°C/min to 25°C below the solidus temperature of the braze filler metal, allowed to equilibrate for 15 min, then proceed at 10°C/min to a

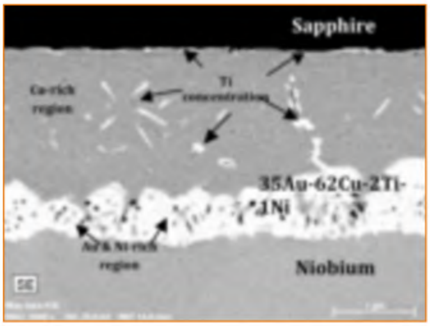

Fig. 5 — SEM image of a niobium-sapphire sample brazed with 35Au-62Cu-2Ti-1Ni.

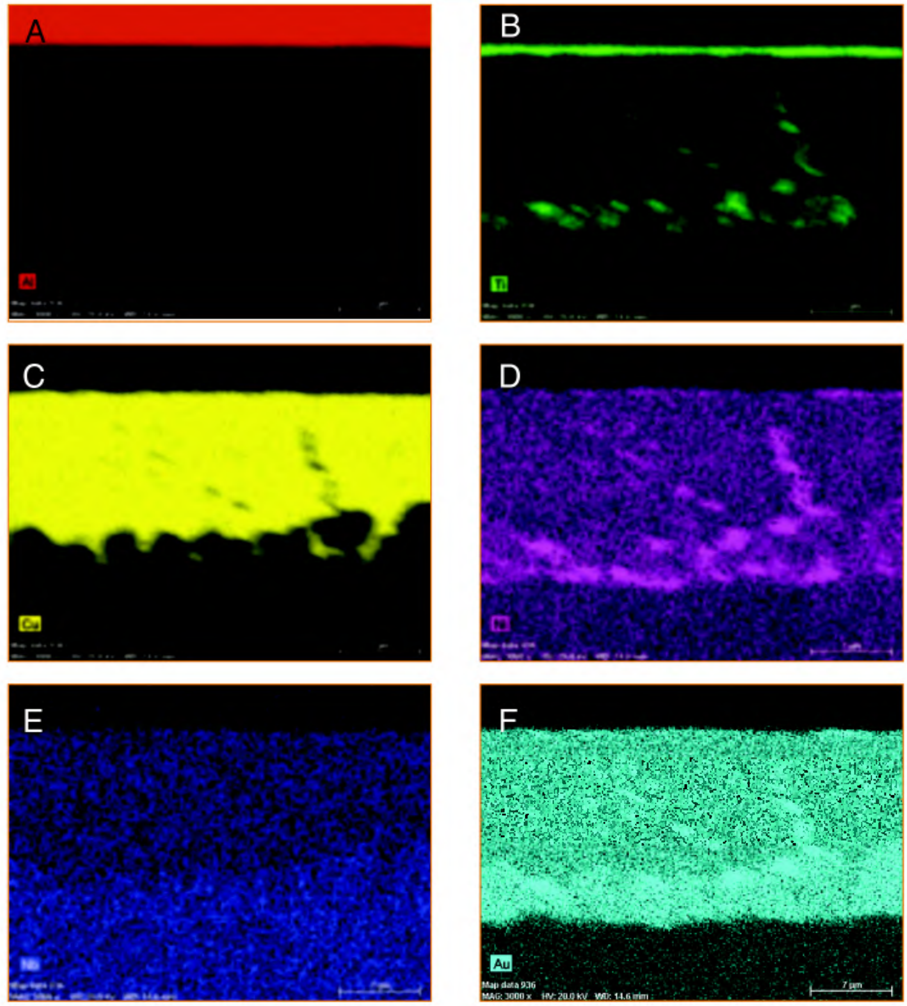

Fig. 6 — EDS maps (Al, Ti, Cu, Ni, Nb, and Au) of niobium-sapphire sample brazed with 35Au-62Cu-2Ti-1Ni.

temperature 30°C above the liquidus temperature of the braze filler metal and soaked for 2 min before cooling. The cooling profile was 25°C/min to a temperature 25°C below the braze filler metal solidus temperature, at which time the ramp was changed to 10°C/min for the remainder of the cycle. The solidus and liquidus temperatures of the brazing filler metals used are displayed in Table 1.

Completed tensile button assemblies were leak checked using a Pfeiffer Qualytest™ HT 265 helium mass spectrometer leak detector. A representative whole and fractured 94% alumina tensile button is shown in Fig. 1. Assemblies with leak rates lower than 1.0 E–10 atm-cc/s were determined to have no detectable leak. Once leak checked, the tensile buttons were tensile tested using a 22 kip MTS Servohydraulic test frame at a crosshead speed of 8.38E–06 m/s (3.3E–04 in./s). The tensile strength was determined using the cross-sectional area of the tensile button-niobium interlayer brazement area, 1.11E–04 m^2 (1.80E–01 $in.^2$). The brazing thermal cycle, helium leak test, and tensile test procedures followed were the same as used for the alumina ceramic tensile button assemblies. Additional niobium-sapphire samples for metallographic analysis were made by brazing 0.41-mm- (0.016-in.-) thick sapphire washers to 0.25-mm- (0.010-in.-) thick niobium interlayer washers using 0.051- and 0.076-mm- (0.002- and 0.003-in.-) thick BAu-3 braze filler metal preforms. Following the brazing operation, the niobium-sapphire samples were cross sectioned and analyzed. An image showing the center portion of a niobium tensile button assembly is shown in Fig. 2. Undamaged portions of the brazed niobium-alumina tensile button assemblies were utilized for further analysis using the SEM. All of the SEM samples were encapsulated prior to cross sectioning and polishing.

Results and Analysis

Displayed in Table 2 are the series of eight experimental furnace cycles performed on sapphire and 94% alumina tensile buttons and one, number 9, from a previous effort in 2005. Following the fabrication, testing, and evaluation of the first three series of samples (niobium tensile buttons with sapphire interlayers), it was determined to perform a series of runs using 94% alumina tensile buttons to determine if the process space had shifted from work performed previously. This concern was primarily due to the low average tensile strengths obtained using the conventional braze filler metal, BAu-3 (34.7 MPa), and two active filler metals, 35Au-62Cu-2Ti-1Ni (21.5 MPa) and 97Ag-1Cu-2Zr (37.9 MPa). The alumina tensile button samples in Series 4 and 5 were joined using Cusil-ABA® and BAu-3 brazing filler metal, respectively. Cusil-ABA, a low-temperature filler metal of interest, yielded the highest tensile strengths in this study, 105 MPa on average. BAu-3 is the braze filler metal currently used in a direct-brazing application by a component supplier. Series 5 closely duplicates previous direct-brazing work performed in 2005 (Series number 9 in Table 2), which is the baseline for the work presently being evaluated. The thermal cycle used for Series number 9 was the same as that used by the component manufacturer in 2005 and is comparable to Series number 5, the thermal cycle used currently by the same component manufacturer. Although different compositions of 94% alumina ce-

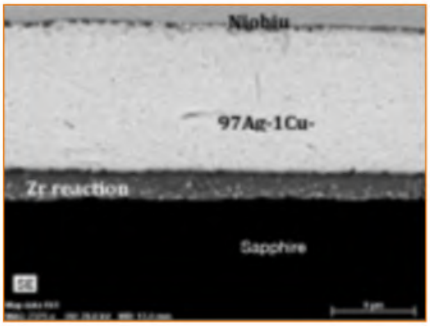

Fig. 7 — SEM image of niobium-sapphire sample brazed with 97Ag-1Cu-2Zr.

ramic were used, the average tensile strengths obtained in Series 5 (55.1 MPa) are very similar to those obtained previously (61 MPa), as reported by Stephens (Ref. 6), and would appear to indicate that the results obtained by the first three series were not anomalies. The most noteworthy difference observed is that all of the samples were hermetic in the Series 5 run while only half were hermetic in 2005.

Surprisingly, the niobium-sapphire tensile button strengths were much lower than the niobium-alumina ceramic tensile buttons. The average strength of the alumina ceramic tensile buttons brazed using BAu-3 was 55-61 MPa (Series 5 and 9) vs. only 35 MPa (Series 1) for the niobium-sapphire assemblies. While sapphire is known as a relatively strong material in the flaw-free state, with tensile strengths typically more than twice those of 94% alumina ceramic, it has a fracture toughness of approximately half that of alumina ceramic, depending on the fracture plane (Ref. 12). Notably, the tensile strengths of the niobium-sapphire tensile buttons were independent of the sapphire washer thicknesses used. A cross-section SEM image and energy-dispersive spectroscopy (EDS) map of a niobium-sapphire assembly brazed with BAu-3 can be seen in Fig. 3. As shown by the EDS map in Fig. 3B, the niobium substrate diffusion to the sapphire interface is minimal. No concentration of the niobium metal at the sapphire interface is seen. Figure 4 is a composite image showing the same SEM image displayed in Fig. 3, and EDS maps showing the distribution of the filler metal elements gold, copper, and nickel. As can be seen in Fig. 4B, the majority of the nickel has migrated to the niobium substrate surface. A comparison of the niobium EDS map (Fig. 3B) with the nickel EDS map (Fig. 4B) does show a reaction between these elements; however, that compound was not identified.

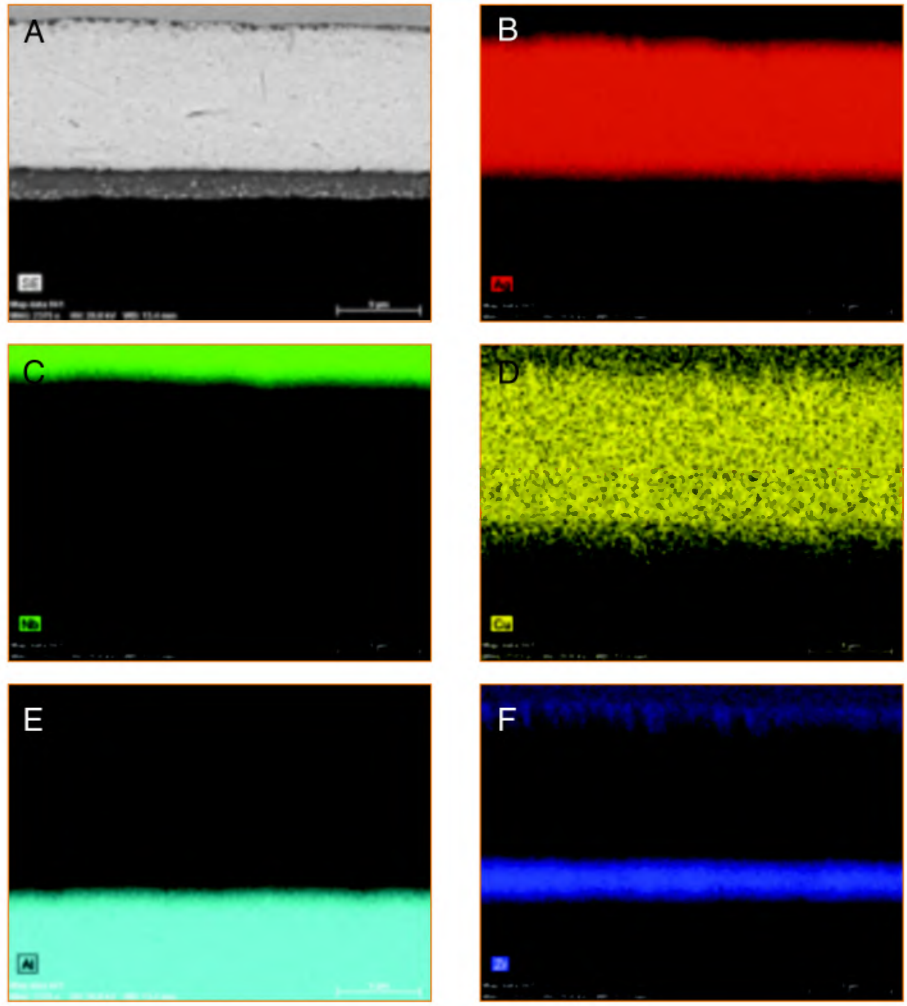

Fig. 8 — SEM image and EDS maps of niobium-sapphire sample brazed with 97Ag-1Cu-2Zr.

Figure 5 is an image of a niobium and sapphire sample brazed with active filler metal 35Au-62Cu-2Ti-1Ni. The addition of titanium to the braze filler metal results in a clearly visible reaction layer between the sapphire and filler metal. Even with this reaction layer, however, the average tensile strength of the samples was only two thirds that of the samples brazed with BAu-3, as shown in Table 2 when comparing Series 1 to Series 2. In addition to lower strength, half of the Series 2 samples failed the helium leak test. The reasons for the failures and lowered tensile strength are unknown at this time. The EDS maps in Fig. 6 portray the relative elemental compositions of the brazed cross section previously seen in Fig. 5. The reaction between the titanium in the brazing filler metal with the sapphire interface is clearly seen. Also evidenced are reactions between the niobium substrate with the nickel, gold, and titanium filler metal material, but not with the copper.

As can be seen in Table 2, a zirconium-containing braze filler metal was also evaluated (Series 3). Tensile strengths of nearly 150 MPa have been achieved using this brazing filler metal with 94% alumina tensile buttons and Fe-29Ni-17Co interlayers (Ref. 13). Because of this, it was anticipated that similarly high tensile strengths could be achieved with the sapphire and niobium components. It is believed that no attempts to braze niobium substrates to sapphire interlayers have been made using this particular braze filler metal previous to this experiment. While all of the niobium-sapphire samples made using this brazing filer metal passed the helium leak test, as can be seen in Table 2, the average tensile strengths were much less than expected for the niobium tensile buttons with the sapphire in-

Table 2 — Direct and Active Brazed Niobium and Alumina Ceramic Tensile Button Series Parameters

Series Number	Series Quantity	Material Tensile Buttons	Material Interlayer	Material Thickness	Braze Filler Metal Type	Braze Filler Metal Thickness	Peak Soak Temperature (°C)	Peak Soak Time (Min)	Leak Check Number Hermetic	Average Tensile Strength (MPa)
1	6	Nb	sapphire	0.41 mm	BAu-3	0.076 mm	1060	2	6/6	34.7
2	4	Nb	sapphire	0.41 mm	Nicoro+2% Ti	0.076 mm	1060	2	2/4	21.5
3	4	Nb	sapphire	0.41 mm	97Ag-1Cu-2Zr	0.076 mm	985	5	4/4	37.9
4	5	94ND10	niobium	0.25 mm	Cusil-ABA	0.076 mm	855	5	5/5	102.0
5	5	94ND10	niobium	0.25 mm	BAu-3	0.076 mm	1060	2	5/5	55.1
6	5	94ND10	niobium	0.25 mm	BAu-3	0.076 mm	1060	240	5/5	95.5
7	5	94ND10	niobium	0.25 mm	BAu-3	0.076 mm	1260	120	0/5	39.4
8	5	Nb	sapphire	0.25 mm	BAu-3	0.076 mm	1060	240	5/5	5.9
9*	4	Al-500	niobium	0.25 mm	BAu-3	0.076 mm	1058	3	2/4	61.0

*Series Number 9, performed in 2005, is shown for reference.

terlayers. The average tensile strengths (37.9 MPa) were, however, comparable to the baseline Series 1 samples (34.7 MPa) made using the BAu-3 braze filler metal and 50% greater than those achieved using the active braze filler metal 35Au-62Cu-2Ti-1Ni (21.5 MPa). The active element used in this filler metal, zirconium, formed a very uniform and clearly visible reaction with the sapphire interface. This is seen distinctly as the thick dark-gray line labeled "Zr reaction layer" between regions labeled "97-1Cu-2Zr" and "sapphire" in the cross-section SEM image of the brazed sample shown in Fig. 7. An SEM image of the area shown in Fig. 7, along with EDS maps showing the relative concentrations of the elements silver, niobium, copper, aluminum, and zirconium are shown in Fig. 8. A comparison of these EDS maps reveals that a slight amount of niobium is present along with the zirconium material at the sapphire (Al) interface; the silver appears to remain between the reaction zone and the niobium base material; and the copper is dispersed relatively uniformly throughout the brazement.

Modified Thermal Cycle Series

Previously mentioned, and seen in Figs. 5 and 6, is the high concentration of titanium at the sapphire interface, clearly defining the reaction layer between the braze filler metal and sapphire substrate. Similarly, Figs. 7 and 8 show a reaction interlayer between the zirconium in the braze filler metal and sapphire. These results, the lack of a clear reaction layer between the niobium and sapphire when using BAu-3, and results from previously referred to studies (Ref. 10), led to the decision to make additional samples with BAu-3 and modified thermal cycles. Using studies mentioned by Marks et al. for guidance, it was determined that two approaches would be used: 1) increasing only the peak soak time, and 2) increasing both the peak soak time and peak soak temperature. The peak soak time would be increased from 5 to 120 or 240 min while the peak soak temperature would be increased by 200°C. It should be noted that Marks adjusted a third parameter, joint preload. For this particular case, however, it was determined that the recommended preloads would be difficult to achieve in a production brazing process. ASTM-F19 94% alumina ceramic tensile buttons with a niobium interlayer 0.25 mm thick and niobium tensile buttons with a 0.41-mm-thick sapphire interlayer were prepared and brazed with BAu-3 braze filler metal.

As was expected, the extended soak times resulted in noticeable evaporation of the braze filler metal, evidenced by condensed filler metal on the metal shielding and other cooler regions in the nearby proximity of the furnace hot zone. This evaporation was rather extreme for the samples processed at the elevated peak brazing temperature of 1260°C. While recognizing that the pressure (vacuum) levels of production equipment could be one to two orders of magnitude greater than the equipment used for these experiments, there would still be excessive braze filler metal evaporation occurring. For this reason, the higher brazing temperature was deemed to be unsuitable for production processes, and the second planned high-temperature thermal cycle was canceled.

The details for these trials, designated as Series 6–8, are shown in Table 2. Lengthening the peak soak time to 240 min while keeping the joint preload and the peak soak temperature constant had the desired effect for the niobium-ceramic samples, but resulted in a greatly reduced average tensile strength decrease for the niobium-sapphire samples. The average strength of the niobium-alumina ceramic tensile samples (Series 6) was increased by 73%, while the average niobium-sapphire sample strength (Series 7) was reduced to 6 MPa, a decrease of 83%. Even with this large disparity in strengths, no differences in the joint hermeticity between the two types of samples were measured.

Series 8, the only set of alumina ceramic tensile button samples brazed with the increased peak soak time (120 min) and peak soak temperature (1260°C), had a noticeably different visual appearance from the other samples. The braze fillets were more rough and granular, had a gray color, and appeared to have a lesser fillet volume, although no measurements were made. All of these samples leaked substantially, and had an average tensile strength of 39.4 MPa, which was a decrease of about 28.5% from the baseline condition, Series 5.

Conclusions

The ability to make strong sapphire-sapphire joints using niobium and liquid-metal in well-controlled laboratory conditions has been previously demonstrated by various researchers. Attempts to understand and describe the bonding mechanisms and requisite substrate requirements have been made; however, more efforts are necessary to understand the relationship between joint strength and surface roughness for brazed niobium-sapphire structures. Less understood are the mechanisms by which niobium diffuses through liquid braze filler metal to react with sapphire in typical brazing assembly processes that use rapid thermal cycles with minimal joint loading.

Modifying a standard brazing profile by increasing the peak soak time from 5 to 240 min did result in increased tensile strength for niobium-94% alumina ceramic samples. When joining niobium to sapphire, the same modification in a thermal cycle resulted in an average strength decrease, compared to the baseline samples. No differences in sample hermeticity from the baseline samples were measured when only the peak soak time was increased.

Increasing the peak temperature by 200°C and peak soak time from 5 to 120 min resulted in a slight strength increase. Unfortunately, all of the samples processed at these conditions failed the helium leak test.

Previous research regarding the direct-brazing of niobium to alumina revealed in TEM images bonding of niobium-containing compounds to the glassy phases between the alumina grains (Ref. 14). Similarly, Hosking et al. reported for active braze filler metals that because the majority of the oxide bonds are made with the high-temperature glass materials used to join the alumina grains in the ceramic material, lower-purity alumina grades often outperform high-purity ceramics with regard to brazed joint strength and hermeticity (Ref. 15). It still remains to be determined if the niobium reaction region increased with the extended soak time.♦

Acknowledgments

The authors express their warm thanks to the following persons who made this work possible: Tom Crenshaw, Alice Kilgo, and Bonnie McKenzie.

References

1. *Brazing Handbook*, 5th Ed. 2007. Miami, Fla.: American Welding Society. pp. 462–464, 579–580.

2. Schwartz, M. M. 1990. *Ceramic Joining*. Materials Park, Ohio: ASM International. pp. 89–93.

3. Humpston, G., and Jacobson, D. M. 1993. *Principles of Soldering and Brazing*. Materials Park, Ohio: ASM International. pp. 140–143.

4. Mizuhara, H. 2000. Ceramic-to-metal joining: Past, current and future. *Advanced Brazing and Soldering Technologies*. Eds. P. T. Vianco and M. Singh. Materials Park, Ohio: ASM International. pp. 278–283.

5. Mizuhara, H., Huebel, E., and Oyama, T. 1989. High-reliability joining of ceramic to metal. *Ceramic Bulletin*, Vol. 68, No. 9, pp. 1591–1599.

6. Stephens, J. J. 2001. Metal/ceramic brazing for hermetic components. AWE presentation. Aldermasten, UK.

7. Stephens, J. J., Hlava, P. F., Walker, C. A., Headley, T. A., and Boettcher, G. E. 2005. Direct brazing process to alumina ceramic using conventional braze alloys and a niobium interlayer. Annual TMS Meeting, San Francisco, Calif., February.

8. AWS C3.2M/3.2:2008, *Standard Method for Evaluating the Strength of Brazed Joints*. Miami, Fla.: American Welding Society, pp. 17–23.

9. Walker, C. A., and Hodges, V. C. 2008. Comparison of metal-ceramic brazing methods. *Welding Journal* 87(10): 43–50.

10. Marks, R. A., Sugar, J. D., and Glaeser, A. M. 2001. Ceramic joining IV. Effects of processing conditions on the properties of alumina joined via Cu/Nb/Cu interlayers. *Journal of Materials Science,* Vol. 36, pp. 5609–5624.

11. Song, G., Remhof, A., Theis-Bröhl, K., and Zabel, H. 1997. Extraordinary adhesion of niobium on sapphire substrates. *Physical Review Letters,* Vol. 79, No. 25.

12. Lanin, A. G., et al. 2003. Thermal shock resistance and thermal-mechanical processing of sapphire. *Journal of the European Ceramic Society,* Vol. 23.

13. Stephens, J. J., Hosking, F. M., Yost, F. G., Walker, C. A., and Dudley, E. 2006. The evolution of a ternary Ag-Cu-Zr active braze filler metal for Kovar®/alumina braze joints. *Proceedings of the 3rd International Brazing and Soldering Conference.* Eds. J. J. Stephens and K. S. Weil. Materials Park, Ohio: ASM International. pp. 207–213.

14. Headley, T. 2004. TEM characterization of two Nicoro/Nb/AL500 brazes. Unpublished internal work, Sandia National Laboratories, Albuquerque, N.Mex.

15. Hosking, F. M., Cadden, C. H., Yang, N. Y. C., Glass, S. J., Stephens, J. J., Vianco, P. V., and Walker, C. A. 2000. Microstructural and mechanical characterization of actively brazed alumina tensile specimens. *Welding Journal* 79(8): 222-s to 230-s.


SIMPLIFIND
New from AWS! Tap into the incredible network of the American Welding Society with the new online AWS Welding Buyers Guide. Powered by MultiView, the Guide gives welding professionals a faster and easier way to find great vendors.
Simplifind your search today at
awsweldingbuyersguide.com
AWS
MULTIVIEW

Brazing Metal to Ceramic in an Oxygen-Containing Atmosphere

An alternative to the conventional vacuum brazing process was developed for joining metal to ceramic with brazing filler metals for the manufacture of solid oxide fuel cells

BY MICHAEL STEFAN REICHLE, THOMAS KOPPITZ, AND UWE REISGEN

Because of the different types of chemical bonding, the brazing of metals to ceramic surfaces presents various challenges. The difference in the electron configurations prevents the wetting of a liquid metal on a ceramic surface and, therefore, joining with high bond strength. For this reason, active elements like titanium or zirconium are often added to the brazing filler metal (BFM) for a vacuum brazing process. The active elements of the BFM, reacting with the ceramic surface, form a metallic/ceramic interlayer that improves the wetting behavior of the BFM on the ceramic.

The Need for Metal-Ceramic Brazements

Due to energy and CO_2 issues that are, at present, the subject of worldwide discussions, renewable energy sources and/or energy production with a favorable CO_2 balance are in greater demand than ever before. In the foreseeable future, the solid oxide fuel cell (SOFC) may play a decisive role in this field. Although a fuel cell itself does not represent an energy source, it is nevertheless capable of producing with a high efficiency electric current from a multitude of different chemical energy carriers (petroleum, natural gas, biogas, or hydrogen). The SOFC is, therefore, not only one of the options for a future energy conversion, but it may, already today, contribute toward the reduction of CO_2 emissions and the saving of valuable energy resources due to its clearly higher degree of efficiency, when compared with conventional generators in combination with heat-power machines.

The centerpiece of a SOFC stack is the ceramic cell with its three functional layers: cathode, electrolyte, and anode. The ceramic cell is inserted into a metal housing made of ferritic chromium steel, which ensures the electrical contact and the gas supply of the SOFC. The working temperature of the SOFC is higher than 600°C (normally 750°–850°C), since the ceramic cell components show significant electric conductivity only from this temperature upward. To prevent a direct reaction of the working gases, the gas compartments of the electrodes must be separated gastight from one another. This demands a gastight joint between

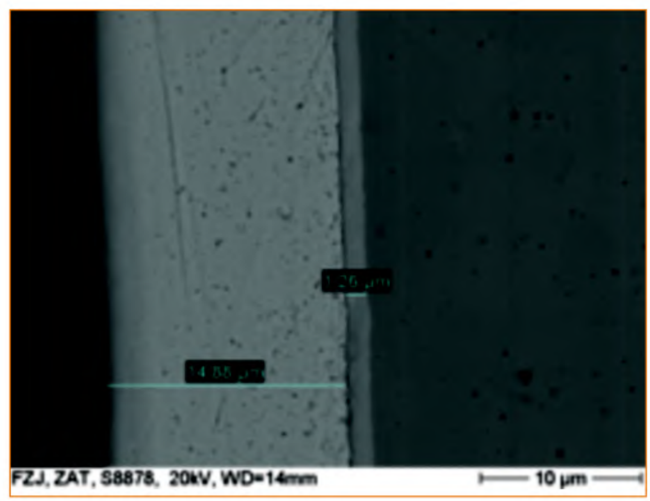

Fig. 1 — SEM image of a transverse section for the determination of the layer thickness of the PVD layers (Ag: approximately 15 µm, Zr: approximately 1.25 µm).

Fig. 2 — Schematic diagram of the PVD-layer composition.

MICHAEL STEFAN REICHLE and THOMAS KOPPITZ are with Forschungszentrum Jülich, ZAT, Jülich, Germany. UWE REISGEN is with RWTH Aachen University, Welding and Joining Institute, Aachen, Germany.

Based on a paper presented at the International Brazing and Soldering Conference, Orlando, Fla., April 26–29, 2009.

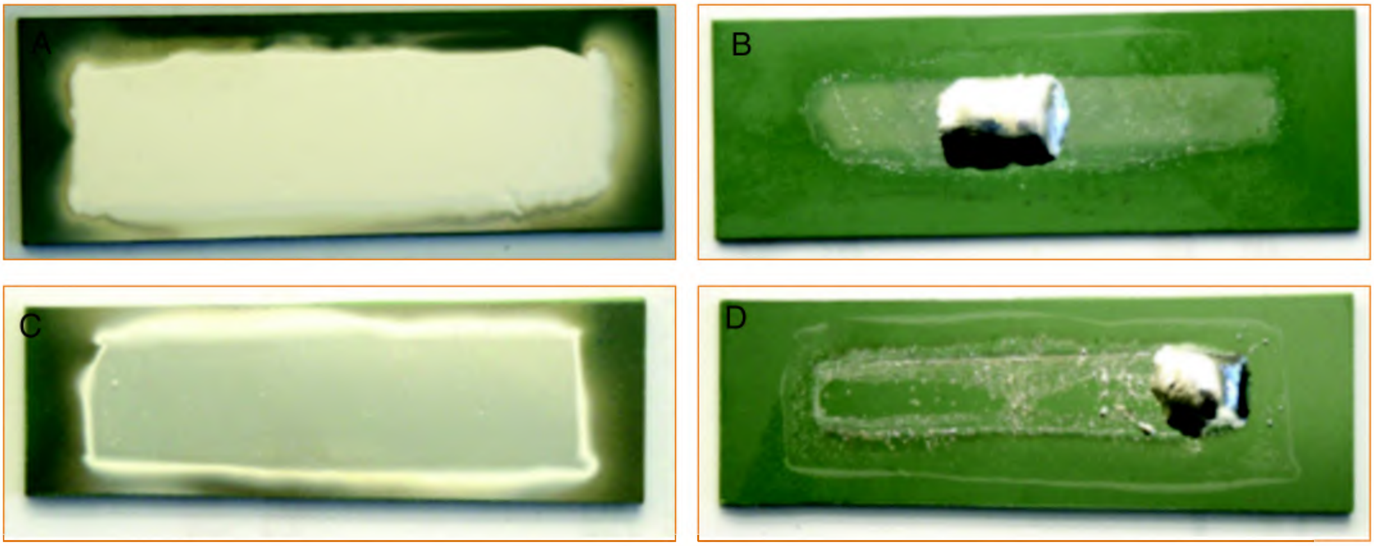

Fig. 3 — Wetting tests (sessile drop) on the 8YSZ-electrolyte of a SOFC half cell. A — Specimen with Ti as the active element before the brazing process; B — specimen with Ti as the active element after the brazing process; C — specimen with Zr as the active element before the brazing process; D — specimen with Zr as the active element after the brazing process.

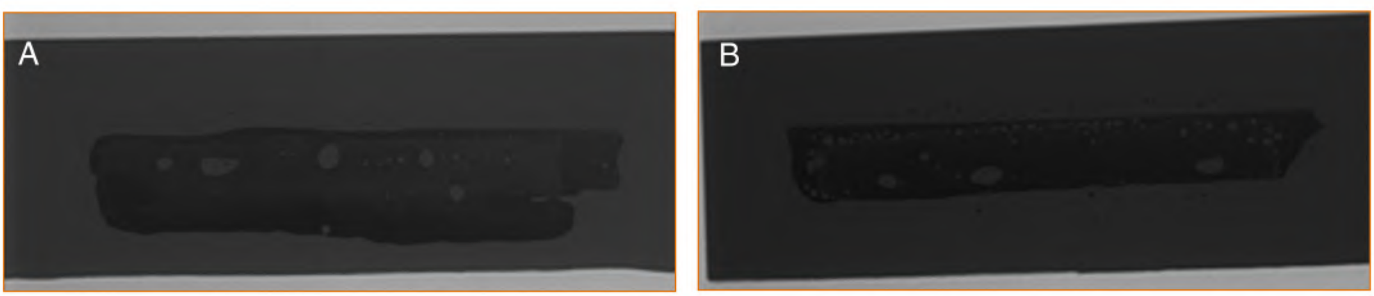

Fig. 4 — X-ray microscope radiographs of the joints of cell/Crofer 22 APU. A — Joint with Ti as the active element; B — joint with Zr as the active element.

the electrolyte and the ferritic chromium steel. Under operating conditions, the joint must be maintained gastight for several thousands of hours under reducing and oxidizing atmosphere. The joint must also be resistant to stresses that are caused by the different temperature-strain behaviors of the joining members.

Beside glass ceramics (so-called glass brazes) and high-temperature stable compressible seals (e.g., on the basis of mica), high-temperature brazing is a promising joining method for application in the field of SOFCs.

The high working temperature of 750°–850°C, the oxidizing and reducing working gases, and the material properties of the SOFC strongly restrict the selection of suitable brazing materials for a ceramic/metal joint.

Due to the vacuum incompatability of various cell components (e.g., the perovskite structure of the cathode), the vacuum active brazing method is not applicable for the conventional joining of ceramic-metal joints. A brazing process in normal atmosphere with conventional, noble metal-based vacuum solders (e.g., Ag-based solder) is also not applicable due to the high oxidation tendency of the active elements, such as Ti or Zr, that are used for the vacuum solders. Active elements support wetting of the metal-based solder material on the ceramic. If the active elements are dispensed with, the metal solder (metallic atomic bond) is no longer capable of sufficiently wetting the ceramic (covalent bond). The active elements in the solder system are, moreover, reacting with the ceramic and form an intermetallic phase that supports the wetting behavior.

One alternative is reactive air brazing with copper-oxide-bearing silver-based BFM (AgCuO). Previous examinations have shown that this joining method still requires further optimization and development (Refs. 4, 7).

For this reason, this article introduces a novel method that serves as an alternative to the conventional vacuum brazing process. In this method, the classical active elements Ti and Zr are protected against premature oxidation through the air oxygen during the furnace process. For this purpose, active elements were, by means of plasma vapor deposition (PVD) methods, precipitated on the electrolyte surface and coated via a further PVD process with the silver brazing filler metal. This protects the active element from premature oxidation and allows the active element during the brazing process right to the melting of the solder base material a wetting-promoting reaction with the ceramic surface. This method allows us to dispense with additional flux and also with a reduced or inert furnace atmosphere.

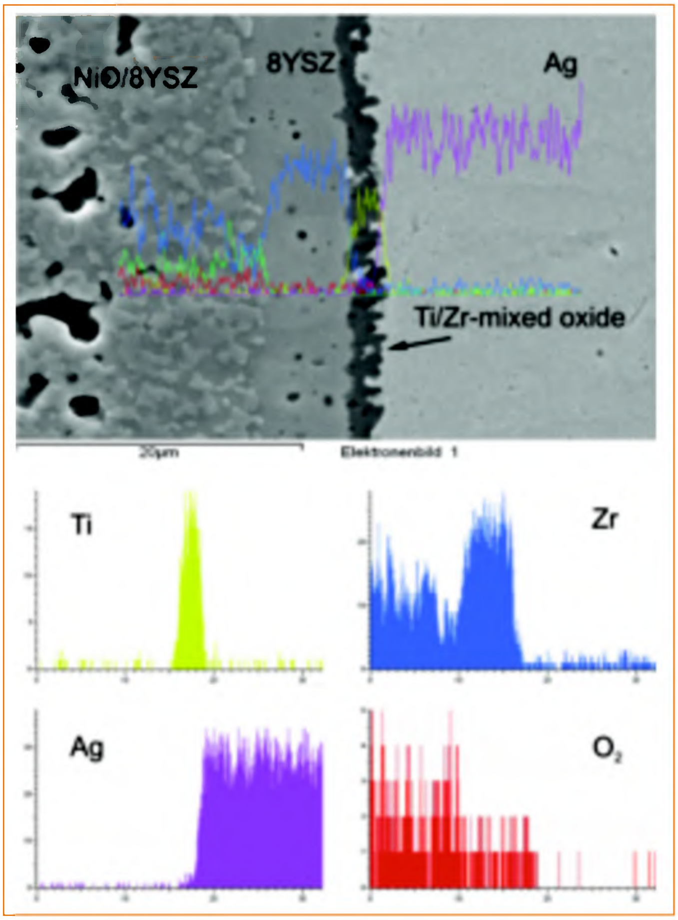

Fig. 5 — *SEM micrograph of the transverse section of the joining zone Ag/8YSZ with Ti as the active element.*

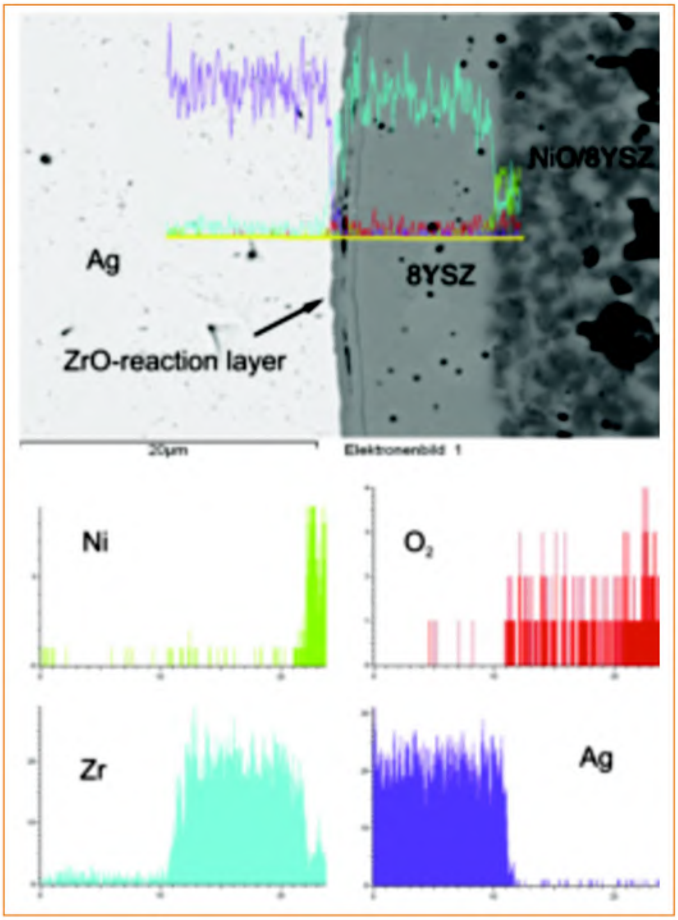

Fig. 6 — *SEM image of a transverse section of the joining zone Ag/8YSZ with Zr as the active element.*

Experimental Procedure

The joining and brazing experiments were carried out on SOFC cells without cathode-functional layers (so-called half cell, 8YSZ electrolyte and anode, made by the IEF-1 at FZJ (Ref. 1)). The metal joining partner was the ferritic chromium steel Crofer 22 APU (Ref. 2), which was developed for application with SOFCs. The noble metal silver was used as the brazing filler metal. A melting point of 962°C, and resistance to oxidizing and also in reducing atmosphere make silver highly suitable for application in SOFCs.

Zirconium (Zr) and titanium (Ti) were used as the active elements. These elements were precipitated by means of the PVD method onto the ceramic electrolyte of the SOFC half cell via a template (layer thickness approximately 1 µm, Fig. 1). In order to protect the active element against the air oxygen in the furnace atmosphere, a further PVD process was carried out where the active element received a gastight silver coating (coating thickness approximately 15 µm) — Fig. 2.

A silver foil (99.99% Ag, thickness: 100 µm) was, in addition to the BFM, used for the wetting and joining tests. Before brazing took place, all parts were cleaned using alcohol. The joining and wetting tests were made in a KS-80 muffle furnace from Linn Co. A brazing temperature of 1000°C, which was kept constant for 10 min, was selected as the temperature program. The temperature ramp was 3 k/min during heating and 5 k/min during cooling.

Subsequent to the joining process, the specimens were irradiated using microfocus X-ray equipment and then examined via metallographic sections in the scanning electron microscope. The wetting angles were determined via metallographic transverse sections.

Results and Discussions

Ti as the Active Element

Figure 3A shows the results from the wetting tests on brazing specimens. By means of the wetting angle BFM/8YSZ, the brazing specimens show if the surface tension due to the reaction of the active elements with the 8YSZ decrease and thus support the wetting process. It was, moreover, planned to examine whether the BFM was wetting exclusively within the required joining zone (the region where the active element was applied). Wetting outside the coated joining zone is, with regard to the subsequent application in the SOFC and due to the design-induced requirements that demand a joint with contour accuracy, not desired.

A zone with brownish discoloration was observed on the electrolyte surface of the specimen that was coated with Ti. The discoloring on the electrolyte surface suggests that a reaction between the electrolyte material and the titanium had occurred. The dark discoloration of 8YSZ is a sign for the removal of oxygen due to the Ti from the crystal lattice of the 8YSZ, which has a strongly reducing effect (Ref. 3). The position and size of the reaction zone complied with the original, titanium-coated area on the electrolyte surface. The silver was wetting within the reaction zone with a wetting angle of approximately 35–40 deg. Compared with pure silver, which has, on the electrolyte surface, a wetting angle of approximately 73 deg in air (Ref. 4), this stands for a significant improvement in the wetting behavior.

Figure 4A depicts the radiograph of a joint between the cell, which had been prepared with the PVD method and/or electrolyte surface, and a ferritic steel sheet made of Crofer 22 APU.

The braze filler material distribution was mainly observed in the region of the originally applied active element Ti. In places, the braze filler material ran over the zone, which was originally coated with Ti. The reason for the running of the braze filler material off the joining zone is the slight tilt of the joining weight due to missing braces in the joint clearance during the brazing process, which caused the pressing of some of the brazing filler material out of the joining zone. The cause of the defects (pores) in the joint is the oxygen that is released during the solidification process. In molten form, silver is capable of dissolving an approximately 40-fold quantity of oxygen more than it would do in a solid state (Ref. 5). Due to the fact that the brazing process is carried out in an oxygen-containing atmosphere, the superfluous oxygen is released during the silver solidification and gas pores that are filled with oxygen may develop in the joint.

Figure 5 shows the transverse section of the joining zone solder/8YSZ, recorded with a scanning electron micrograph (SEM). The titanium applied via the PVD method has developed a Ti/Zr mixed oxide with the 8YSZ surface of the cell, whereas the Zr concentration in the reactive layer is continuously decreasing with the increasing distance to the 8YSZ surface. Comparable mixed oxides develop if titanium-containing solder materials are applied in a vacuum brazing process on 8YSZ (Ref. 6). The connection of the reactive layer on the 8YSZ surface is, with the exception of a few silver-containing inclusions, complete. The silver solder also shows a good connection to the Ti/Zr mixed oxide.

Zr as the Active Element

A discoloration of the electrolyte surface (removal of oxygen off the crystal lattice) was observed on the specimen that was coated with Zr (Fig. 3D), mainly in the edge region of the coated region. The silver primarily wet within the reactive zone. The wetting angle was approximately 45–50 deg, which points to a slightly improved wetting behavior, in comparison to pure silver on the electrolyte surface (wetting angle approximately 73 deg).

Figure 4B shows the X-ray radiograph of a joint between the electrolyte surface that was prepared using the PVD method and a Crofer 22 APU sheet. The silver wet the Zr-coated specimen mainly in the region of the Zr coating — Fig. 4B. A slight spreading of the solder over the coated zone was observed at the ends. Due to the solubility differences of oxygen in the molten silver and the silver solid body, gas pores developed in the joint.

Sealing of the active element with the solder base material may protect the active element during the furnace process in normal atmosphere from premature oxidation with the air oxygen.

The SEM image of the metallographic transverse section shows an end-to-end uniform ZrO-containing reactive layer on the 8YSZ surface of the cell — Fig. 6. Few and far between, pore formation within the ZrO reactive layer was observed. The connection to the 8YSZ surface was consistently good. The silver also showed good, uniform connection to the ZrO reactive layer.

Conclusions

The tests showed that the sealing of the active element with the solder base material — in this case pure silver — may protect the active element during the furnace process in normal atmosphere from premature oxidation with the air oxygen. The active element reacts during the furnace process with the ceramic surface and forms a comparable reactive layer with the ceramic surface, as in the vacuum furnace process with a comparable vacuum solder material. Due to the reactive layers that develop during the furnace process, the wetting behavior of the metal solder material, and/or in this case the pure silver, was significantly improved.

In the future, it is planned to test the leak tightness on respective leakage test specimens that will be produced using the method specified here. These initial tests show that, using this method, leaktight joints are produced, but the quality and/or contour accuracy of the joint is not yet convincing. In this regard, further tests about the optimization of the process parameters are required.

It is, moreover, scheduled to carry out tests with regard to the strength of the joints by means of the fourpoint bending fracture test (method in accordance with Charamlabides).♦

References

1. Meulenberg, W. A., Menzler, N. H., Buchkremer, H. P., and Stöver, D. 2002. Manufacturing routes and state-of-the-art of the planar Jülich anode supported concept for solid oxide fuel cells. *Ceramic Transactions: Materials for Electrochemical Energy Conversion and Storage*, A. Manthiram, P. N. Kumta, S. K. Sundaram, and G. Ceder, eds. Westerville, Ohio: American Ceramic Society Vol. 127, pp. 99–108.

2. Crofer 22 APU. Thyssen Krupp VDM GmbH, Data Sheet No. 4046, December 2006 edition.

3. Hanson, W. B., Ironside, K. I., and Fernie, J. A. 2000. Active metal brazing of zirconia. *Acta Mater* 48(18–19): 4673.

4. Reichle, M. S., and Koppitz, T. 2008. Investigation of reactive air brazing with silver based brazing filler metals to improve the joining technology for the high temperature solid oxide fuel cell (SOFC). 8th European Fuel Cell Forum, Lucerne.

5. *Ag-O (Silver Oxygen)*. 1991. Landolt-Börnstein - Group IV Physical Chemistry, ISSN:1615-2018.

6. Singh, M., and Shpargel, T. P. 2008. Brazing of yttria-stabilized zirconia (YSZ) to stainless steel using Cu, Ag, and Ti-based brazes. *J Mater Sci* 43: 23–32.

7. Koppitz, T., Federmann, D., Reichle, M. S., Reisgen, U., Remmel, J., and Zerfass, H. R. 2007. Further development of reactive-air brazing as a joining technique for dissimilar materials with high melting temperatures. DVS-Berichte, Band 243 (ISBN: 978-3-87155-799-6): 124–129.

High-Temperature Dissimilar Joint Technology for Fission Surface Power Systems

Two joining techniques, brazing and diffusion bonding, in the context of forming the requisite stainless steel 316L to superalloy Inconel® 718 joint, were studied in the Structures and Materials Division, NASA Glenn Research Center, Cleveland, Ohio, and University of Toledo, Toledo, Ohio, including microstructures produced by brazing and diffusion bonding, the effect of brazing cycle on the mechanical tensile properties of the alloys, and the strength of several brazed joints (Ref. 1).

Joints between the superalloy IN718 and SS316L were produced by hot pressing small coupons of each material in a vacuum for 2 h at 1000 K (1340°F) or 1150 K (1610°F) with a pressure of 90 MPa. Thin sheets of Ni and V were explored as possible metal interlayers between base metals to enhance the bonding and minimize alloy-to-alloy diffusion reactions. The compatibility of several filler metals with the SS316L or IN718 were evaluated using an overlapping type brazing technique: (a) nickel-based AMDRY 790 (Ni-1.74B-3.22Si), AMDRY 108 (Ni-23Cr-11.5Fe-4.2P-6.4Si), and AMDRY 775 (Ni-15.38Cr-3.8B) and; (b) gold-based Alloys Nioro (Au-18Ni) and Palniro-7 (Au-22Ni-8Pd).

Hot press diffusion bonding trials showed that bonding occurred with and without a pure nickel interlayer. Fine porosity was detected at the new interfaces but may be reduced or eliminated with higher pressures and optimized bonding parameters. Microstructural observations indicated that gold-based brazes resulted in minimal reaction with either base metals. The chemical reaction was observed to be more extensive with any of the Ni-based brazes studied. Double-lap shear tensile specimens were successfully fabricated and tested at 830 K (1034°F).

A specific overlap, the average tensile strength observed from the brazed double-lap shear specimens for Palniro-7 and the Ni-base brazes, are higher compared to the Nioro braze; however, the higher brazing temperatures required for Palniro-7 and any of the Ni brazes may impact negatively on the properties of both base metals. The Inco718, which is extensively used in the aerospace industry, required only an aging heat treatment, after a typical Nioro brazing cycle, to regain most of its strength. The stainless steel 316L alloy, not affected from secondary phase precipitation or dissolution, maintained its ultimate tensile strength after a typical Nioro brazing cycle; however, its yield strength was more sensitive to the thermal exposures. Based on the lowest impact on the base metal strength and minimal chemical interaction, Nioro is the leading braze candidate to join the two dissimilar metals for the heat exchanger application.

Fe-Cr-Based Brazing Filler Metals as Economic Alternatives to Ni-Based Filler Metals in Automotive Applications

Now that diesel engines are in greater usage, due to their efficiency, emission-gas lowering devices such as exhaust gas recirculation systems are in greater demand. Ni-based brazing filler metals have typically been used in this application, but the market price for Ni has surged due to rightward shifting demand. An economic alternative, specifically Fe-Cr-based filler metals, have been investigated by researchers at Tokyo Braze Co., Ltd., and Tokai University, Japan (Ref. 2).

Compositions with varying amounts of Fe, Cr, Ni ranging from 30, 25, 30 to 60, 20, 5 wt-%, respectively, were tested. Solidus and liquidus temperature varied from 1010°C and 1065°C to 1090°C, 1130°C, while brazing temperature varied from 1100°–1120°C (2012°–2048°F) to 1150°–1200°C (2100°–2192°F). Joints brazed with TB-4025 at 1130°C (2066°F), a typical Fe-Cr-based filler metal, were evaluated for shear strength of stainless steel 304 lap joints. Joint failures were not observed, and the filler metals competed well with Ni-based filler metals in the application: 280 MPa (40.6 ksi) in comparison to 310 MPa (45 ksi) for BNi-5 filler metal. The addition of molybdenum, in the amount of 2 wt-%, resulted in a fine microstructure; so the 7–8 wt-% of phosphorus, present in the filler metal, did not form a brittle intermetallic layer with Fe. Also, 5–6 wt-% of silicon was present.

Due to the intended practical application of the filler metals in exhaust gas recirculation systems, corrosion resistance is a principal concern. The authors did not find significant concern for corrosion in either TB-4025 and BNi-5 after a 168-h salt spray. Corrosion resistance to dipping in H_2SO_4 (5%), NHO_3 (5%), and NH_4OH (5%) was found to be excellent, slight weight loss by HCl (5%), and very slightly affected by NaClO (5%). These characteristics altogether suggest that TB-4025 is preferable to BNi-2 and comparable with BNi-5 in its intended application.

Wettability of Different Active Brazing Alloys Ag-Cu, Ag-Cu-In, Ni-Based, and Cu-Sn (with Ti, Cr, and Si Active Elements) on CVD-Diamond Thick Films

Applications of CVD-diamond thick films in semiconductor structures and new cutting tools require a reliable method of adequate evaluation of wetting behavior and interaction of brazing filler metals on diamond surfaces. A new testing technique was developed for these purposes in the Institute of Materials Engineering, TU Dortmund, Germany

(Ref. 3). The wettability of different active brazing alloys, commercially available CB4 (Ag-26.5Cu-3Ti), Incusil ABA, BNi-2, BNi-3, BNi-6, and tailor-made Alloys Ni-3.2B-4.5Si, Cu-18Sn-1.5Ti, and Cu-18Sn-3Cr on CVD-diamond thick films were investigated using a new method of measuring the contact angle by 3D microscopy. This method is a nondestructive examination procedure delivering qualitative as well as quantitative information on the wetting mechanisms. The procedure provides opportunities for statistic analyses that go far beyond conventional approaches.

The system provides scanning the layer of brazing filler metal on a CVD-diamond surface. Contact angle profiles are being measured in eight sections around the wet area of both the outside and inside of the "halo" of the braze droplet, and besides, to study two different wetting fronts formed by the braze melt. In comparison to existing measuring methods using cross sections, this method allows multiple measuring of contact angles at different areas of the brazing filler droplet, which basically provides a better accuracy of the results without damaging the samples. Also, the samples and data sets can be used for supplemental analyses regarding the molten filler metal drop, e.g., shape, volume, and optical characteristics. This also can provide a better assessment of the wetting situation.

Most of the investigated active brazing alloys show good wetting qualities on CVD-diamond. Especially the AgCu-base and tailor-made CuSn-base fillers containing Ti or Cr as an active agent in varying concentrations obtain low contact angles between 7 and 14 deg on diamond. Some of the Ni-based fillers also show low contact angles, but as expected at elevated temperatures above 1000°C (1832°F). Incusil ABA and CB4 exhibited the lowest contact angle at 850°–950°C (1562°–1742°F) and 5-min holding time, while Cu-18Sn-1.5Ti, Cu-18Sn-3Cr, and CB4 at 10-min holding time.

New Iron-Chromium Based Brazing Filler Metal for Stainless Steel Applications

An alternative iron-chromium based brazing filler metal (marked as "FeCr" brazing alloy) containing 27% Cr, 20% Ni, 10% Cu, 5% Si, 7% P, 5% Mn, and Fe in the balance was developed and tested in Höganäs AB, Sweden, for stainless steel joints working in highly corrosive environments such as heat exchangers and exhaust gas recirculation coolers (Ref. 4). A number of tests were done including wetting, tensile and shear strengths, microstructure examination, and corrosion resistance of joints of stainless steel 316L and properties of a new alloy were compared with standard Nicrobraz Alloys BN-2 and BNi-5 filler metals, other Fe-based filler metals such as Fe-1150 and Fe-1190, and the Alloy HBNi613.

The new FeCr filler metal is manufactured by gas atomization in the form of spherical powder, and its brazing temperature is 1100°C (2012°F), which is the same as that for BNi-2 and lower for BNi-5 and Fe-1150 and Fe-1190. Wetting (spreading) was evaluated in terms of the spreading ratio S defined as $S = A_f/A_s$, where A_f is the area covered by the melted filler metal and A_s the substrate area. The spreading ability of FeCr filler metal is second only to HBNi613, while it is better than that of BNi-2 and other Fe-based alloys. The microstructure in the FeCr brazed joint contains a homogenous mixture of a hard FeCrNiP-rich phase surrounded by a ductile FeCrNi-rich phase. The tensile strength and shear strength 210 N/mm^2 (30.4 ksi) and 80 N/mm^2 (11.6 ksi), respectively, for FeCr.

Corrosion tests were conducted using T-specimens brazed and immersed in HCl, H_2SO_4, and HNO_3 solutions. The samples were placed in the corrosion solutions for four weeks, then they were cross sectioned and inspected thoroughly. In addition, joint strength of brazed bars was tested after holding in H_2SO_4 for

four weeks. The corrosion tests show that FeCr has corrosion resistance comparable to HBNi613 in H_2SO_4 solution and slightly less than that in HCl and HNO_3 solutions. It was found that Cu made a positive effect on the corrosion; FeCr has better corrosion resistance than Fe-1150, which does not contain Cu. The only material that was affected by the four weeks in H_2SO_4 solution was BNi-2. The strength of this material was reduced significantly. This correlates well with the chemical composition of the alloy: BNi-2 has low Cr content. The composition of the FeCr alloy is covered by a pending patent of Höganäs AB.

Properties of Cu-Ni-P-Zn Filler Metals Designed for Brazing Steels in the Mid-Temperature Range

Traditionally, copper-phosphorus filler metals are not recommended for brazing steel due to the formation of brittle layers of iron phosphides in the joint. Authors of JSC "ALARM," Moscow, Russia, have found out two areas of Cu-Ni-P-Zn alloy compositions that exhibit not only a low-temperature melting point of 610°C (1130°F) and 630°C (1166°F), but also a relatively high level of plasticity (elongation more than 6%) of carbon steel brazed joints manufactured for the refrigerator industry (Ref. 5).

These two near-eutectic brazing alloys are: (a) Cu 63, P 5, Ni 8, and Zn 24 wt-% (melting point 630°C) and (b) Cu 63, P 7, Ni 5, and Zn 25 wt-% (melting point 610°C). Tensile strength of steel brazed joints depends on the mass ratio of Ni, P, and Cu in the alloy. At the constant content of nickel of 5 wt-%, and phosphorus also 5 wt-%, both the tensile strength and shear strength increased as the copper percentage content becomes higher. Elongation of brazed joints is below 1% at the phosphorus content 7 wt-% and significantly improved up to 6% at the phosphorus content slightly below 5 wt-%.

Alloys containing 8 wt-% of nickel demonstrated high tensile and shear strengths with the increase of phosphorus content up to 6 wt-%, but starting from 6.5 wt-% of phosphorus, the strengths go down. The tensile strength always increases with the rise of the nickel percentage.

The Cu-Ni-P-Zn brazing alloys should be considered as brass with a high content of nickel and phosphorus. The main system properties depend on the ratio of solid solutions and complex amount of phosphides in a phase composition. The increase of solid solution content leads to the increase of the alloy plasticity. The low phosphor content and maximum nickel content result in the improvement of mechanical properties of both alloys and steel brazed joints.

References

All papers listed below are from the *Proceedings of the 4th International Brazing and Soldering Conference*, cosponsored by AWS and ASM International, held April 26–29, 2009, in Orlando, Fla. In addition, these have all been edited by A. Rabinkin, R. Gourley, and C. Walker.

1. Locci, I. E., Bowman, C. L., and Gabb, T. P. 2009. Development of high temperature dissimilar joint technology for fission surface power systems, pp. 165–174.

2. Kotaro, M., Miyazawa, Y., and Ariga, T. 2009. Development of novel Fe-Cr based brazing filler metals, pp. 130–134.

3. Tillmann, W., Osmanda, A. M., and Yurchenko, S. 2009. Investigations of contact angles of active brazing fillers on diamond-layers by optical 3D-microscopy, pp. 337–345.

4. Persson, U. 2009. New iron-chromium based brazing filler metal for demanding stainless steel applications, pp. 125–129.

5. Pashkov, I., Ilina, I., Rodin, and Baranova, I. 2009. Properties researching of Cu-Zn-P-Ni alloys to produce multipurpose mid-temperature brazing metals, pp. 153–158.

Information provided by ALEXANDER E. SHAPIRO (ashapiro@titanium-brazing.com) *and LEO A. SHAPIRO, Titanium Brazing, Inc., Columbus, Ohio.*

American Welding Society

Friends and Colleagues:

The American Welding Society established the honor of *Counselor* to recognize individual members for a career of distinguished organizational leadership that has enhanced the image and impact of the welding industry. Election as a Counselor shall be based on an individual's career of outstanding accomplishment.

To be eligible for appointment, an individual shall have demonstrated his or her leadership in the welding industry by one or more of the following:

- Leadership of or within an organization that has made a substantial contribution to the welding industry. The individual's organization shall have shown an ongoing commitment to the industry, as evidenced by support of participation of its employees in industry activities.

- Leadership of or within an organization that has made a substantial contribution to training and vocational education in the welding industry. The individual's organization shall have shown an ongoing commitment to the industry, as evidenced by support of participation of its employee in industry activities.

For specifics on the nomination requirements, please contact Wendy Sue Reeve at AWS headquarters in Miami, or simply follow the instructions on the Counselor nomination form in this issue of the *Welding Journal*. The deadline for submission is July 1, 2010. The committee looks forward to receiving these nominations for 2011 consideration.

Sincerely,

Alfred F. Fleury
Chair, Counselor Selection Committee

American Welding Society

Nomination of AWS Counselor

I. HISTORY AND BACKGROUND

In 1999, the American Welding Society established the honor of Counselor to recognize individual members for a career of distinguished organizational leadership that has enhanced the image and impact of the welding industry. Election as a Counselor shall be based on an individual's career of outstanding accomplishment.

To be eligible for appointment, an individual shall have demonstrated his or her leadership in the welding industry by one or more of the following:

- Leadership of or within an organization that has made a substantial contribution to the welding industry. (The individual's organization shall have shown an ongoing commitment to the industry, as evidenced by support of participation of its employees in industry activities such as AWS, IIW, WRC, SkillsUSA, NEMA, NSRP SP7 or other similar groups.)
- Leadership of or within an organization that has made substantial contribution to training and vocational education in the welding industry. (The individual's organization shall have shown an ongoing commitment to the industry, as evidenced by support of partici pation of its employees in industry activities such as AWS, IIW, WRC, SkillsUSA, NEMA, NSRP SP7 or other similar groups.)

II. RULES

A. Candidates for Counselor shall have at least 10 years of membership in AWS.
B. Each candidate for Counselor shall be nominated by at least five members of the Society.
C. Nominations shall be submitted on the official form available from AWS headquarters.
D. Nominations must be submitted to AWS headquarters no later than July 1 of the year prior to that in which the award is to be presented.
E. Nominations shall remain valid for three years.
F. All information on nominees will be held in strict confidence.
G. Candidates who have been elected as Fellows of AWS shall not be eligible for election as Counselors. Candidates may not be nominated for both of these awards at the same time.

III. NUMBER OF COUNSELORS TO BE SELECTED

Maximum of 10 Counselors selected each year.

<u>Return completed Counselor nomination package to:</u>

Wendy S. Reeve
American Welding Society
Senior Manager
Award Programs and Administrative Support
550 N.W. LeJeune Road
Miami, FL 33126

Telephone: 800-443-9353, extension 293

SUBMISSION DEADLINE: July 1, 2010

(please type or print in black ink)

CLASS OF 2011

COUNSELOR NOMINATION FORM

DATE________________NAME OF CANDIDATE____

AWS MEMBER NO.________________________YEARS OF AWS MEMBERSHIP____

HOME ADDRESS____

CITY____STATE________ZIP CODE_________PHONE______________________

PRESENT COMPANY/INSTITUTION AFFILIATION____

TITLE/POSITION____

BUSINESS ADDRESS____

CITY____STATE________ZIP CODE_________PHONE______________________

ACADEMIC BACKGROUND, AS APPLICABLE:

INSTITUTION____

MAJOR & MINOR____

DEGREES OR CERTIFICATES/YEAR____

LICENSED PROFESSIONAL ENGINEER: YES________NO_________ STATE________________________________

SIGNIFICANT WORK EXPERIENCE:

COMPANY/CITY/STATE____

POSITION____YEARS______________________

COMPANY/CITY/STATE____

POSITION____YEARS______________________

SUMMARIZE MAJOR CONTRIBUTIONS IN THESE POSITIONS:

____

____

____

IT IS MANDATORY THAT A CITATION (50 TO 100 WORDS, USE SEPARATE SHEET) INDICATING WHY THE NOMINEE SHOULD BE SELECTED AS AN AWS COUNSELOR ACCOMPANY THE NOMINATION PACKET. IF NOMINEE IS SELECTED, THIS STATEMENT MAY BE INCORPORATED WITHIN THE CITATION CERTIFICATE.

****MOST IMPORTANT****

The Counselor Selection Committee criteria are strongly based on and extracted from the categories identified below. All information and support material provided by the candidate's Counselor Proposer, Nominating Members and peers are considered.

SUBMITTED BY:
PROPOSER____
AWS Member No.________________
The proposer will serve as the contact if the Selection Committee requires further information. The proposer is encouraged to include a detailed biography of the candidate and letters of recommendation from individuals describing the specific accomplishments of the candidate. Signatures on this nominating form, or supporting letters from each nominator, are required from four AWS members in addition to the proposer. Signatures may be acquired by photocopying the original and transmitting to each nominating member. Once the signatures are secured, the total package should be submitted.

NOMINATING MEMBER:______________________________Print Name_______________________________
AWS Member No.____________
NOMINATING MEMBER:______________________________Print Name_______________________________
AWS Member No.____________
NOMINATING MEMBER:______________________________Print Name_______________________________
AWS Member No.____________
NOMINATING MEMBER:______________________________Print Name_______________________________
AWS Member No.____________

SUBMISSION DEADLINE JULY 1, 2010

Welding Test Positions for Groove Welds in Pipe

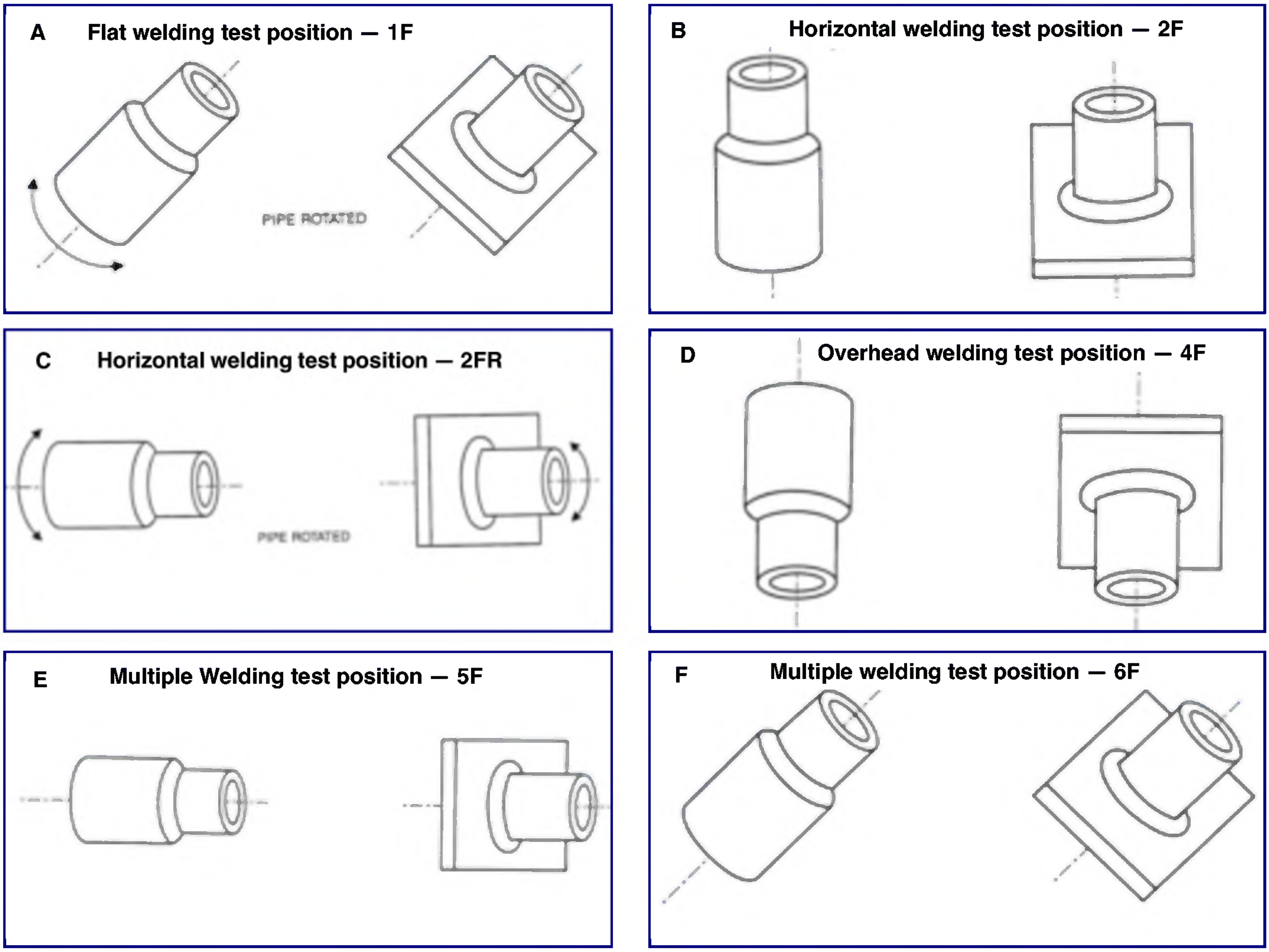

Fig. 1 — Welding test positions and their designations for fillet welds in pipe.

Welder, welding operator, and tack welder qualification tests determine the ability of the persons tested to produce acceptably sound welds with the process, materials, and procedure called for in the tests.

Following are descriptions of the various test positions for fillet welds in pipe.

1F. A welding test position designation for a circumferential fillet weld applied to a joint in pipe, with its axis approximately 45 deg from horizontal, in which the weld is made in the flat welding position by rotating the pipe about its axis — Fig. 1A.

2F. A welding test position designation for a circumferential fillet weld applied to a joint in a pipe, with its axis approximately vertical, in which the weld is made in the horizontal welding position — Fig. 1B.

2FR. A welding test position designation for a circumferential fillet weld applied to a joint in pipe, with its axis approximately horizontal, in which the weld is made in the horizontal welding position by rotating the pipe about its axis — Fig. 1C.

4F. A welding test position designation for a circumferential fillet weld applied to a joint in pipe, with its axis vertical, in which the weld is made in the overhead welding position — Fig. 1D.

5F. A welding test position designation for a circumferential fillet weld applied to a joint in pipe, with its axis approximately horizontal, in which the weld is made in the horizontal, vertical, and overhead welding positions. The pipe remains fixed until the welding of the joint is complete — Fig. 1E.

6F. A welding test position designation for a circumferential fillet weld applied to a joint in pipe, with its axis approximately 45 deg from horizontal, in which the weld is made in flat, vertical, and overhead welding positions. The pipe remains fixed until welding is complete — Fig. 1F.

Excerpted from A3.0:2001, *Standard Welding Terms and Definitions.*

NOTE: A DIAMOND (♦) DENOTES AN AWS-SPONSORED EVENT.

PICALO 2010, Pacific Int'l Conf. on Applications of Lasers and Optics. March 23–25, Shangri-La Hotel, Wuhan, P. R. China. Visit *www.laserinstitute.org.*

WESTEC 2010. March 23–25, Los Angeles Convention Center, Los Angeles, Calif. Visit *www.westeconline.com.*

Aluminum Association's 2010 Spring Meeting. April 12, 13, The Westin Alexandria, Alexandria, Va. Visit *www.aluminum.org.*

METEF-FOUNDEQ Int'l Aluminum Expo and Int'l Foundry Equipment Expo. April 14–17, Garda Exhibition Centre, Montichiari, Brescia, Italy. Visit *www.foundeq.com.*

Micromanufacturing & Nanomanufacturing Conf. and Exhibits. April 14, 15, Hilton Phoenix East/Mesa, Mesa, Ariz. Visit *www.sme.org.*

GAWDA Spring Management Conf. April 18–20, Hyatt Regency, Chicago, Ill. Visit Gases and Welding Distributors Assn. *www.gawda.org.*

Composites Manufacturing 2010. April 20–22, San Diego Marriott Mission Valley, San Diego, Calif. Visit *www.sme.org.*

The Japan Int'l Welding Show 2010. April 21–24, Tokyo Big Sight, Tokyo, Japan. Organized by The Japan Welding Engineering Society and Sampo Publications. Visit *www.weldingshow.jp/english.*

ITSC 2010, Int'l Thermal Spray Conf. & Expo. May 3–5, Republic of Singapore. Visit *www.asminternational.org.*

Offshore Technology Conf. and Expo. May 3–6, Houston, Tex. Visit *www.otcnet.org.*

♦AWS Detroit Sheet Metal Welding Conf. XIV. May 11–14, VisTaTech Center, Livonia (Detroit), Mich. Contact American Welding Society Detroit Section at *smwc@awsdetroit.org,* or visit *www.awsdetroit.org.*

♦AWS Weldmex, Metalform Mexico, FABTECH Mexico. May 11–13, Centro Banamex, Mexico City, Mexico. Visit *www.awsweldmex.com.*

Expo Mecanica. May 11–15, São Paulo, Brazil. Visit *www.biztradeshows.com.*

Laser Additive Manufacturing Workshop. May 11, 12, Houston Airport Marriott, Houston, Tex. Visit *www.laserinstitute.org.*

AISC National Steel Construction Conf. and Expo. May 12–15, Gaylord Palms Conf. Center, Orlando, Fla. Visit *www.aisc.org.*

Montreal Manufacturing Technology Show. May 17–19, Place Bonaventure, Montreal, Que., Canada. Visit *www.mmts.ca.*

Rapid Conf. & Expo and 3-D Imaging Conf. May 18–20, Disneyland Resort Anaheim, Anaheim, Calif. Visit *www.sme.org/rapid.*

EASTEC 2010. May 25–27, Eastern States Exposition, West Springfield, Mass. Visit *www.easteconline.com.*

Int'l Symposium on Surface Hardening of Corrosion-Resistant Alloys. May 25, 26, Case Western Reserve University, Cleveland, Ohio. Visit *www.asminternational.org.*

♦Beijing Essen Welding & Cutting Fair. May 27–30, New China Int'l Exhibition Centre, Beijing, China. Cosponsored by AWS, and other societies. Visit *www.beijing-essen-welding.de.*

SME Annual Conf. — "Bridging the Gaps." June 6–8, Sheraton Music City, Nashville, Tenn. Visit *www.sme.org/conference.*

♦LÖT 2010, 9th Int'l Conf. on Brazing, High-Temperature Brazing, and Diffusion Bonding. June 15–17, Aachen, Germany. Sponsored by DVS (German Welding Society), cosponsored by AWS, ASM Int'l, and other societies. Visit *www.dvs-ev.de/loet2010.*

SkillsUSA, 46th Annual National Leadership and Skills Conf. June 20–25, Kansas City, Mo. Visit *www.skillsusa.org.*

63rd Annual Assembly and Int'l Conf. of the Int'l Institute of Welding (IIW). July 11–17, Swissôtel The Bosphorus, Istanbul, Turkey. Leading researchers to share recent advances in welding and joining sciences and technologies to achieve cost-effective, environment-friendly, safe, and long-lasting welded systems in construction, energy, and transporation. Visit *www.iiw2010.com.*

♦Trends in Welding Conf. Aug. 2–5, Cherry Valley Lodge, Newark, Ohio. Cosponsored by American Welding Society and Edison Welding Institute. Contact George Ritter (614) 688-5199; *gritter@ewi.org.*

Educational Opportunities

ASME Section IX Seminars. March 1–3, Amsterdam, The Netherlands; March 15–17, Las Vegas, Nev. Presented by Walter J. Sperko. Visit *www.asme.org.*

AWS CWI Seminar and Exam. Offered July 25–31, Oct. 17–23. Call Lincoln Electric Welding School (216) 383-8325, or visit *www.lincolnelectric.com.*

Basics of Nonferrous Surface Preparation. Online course, six hours includes exam. Offered on the 15th of every month during 2010 by The Society for Protective Coatings. Members $145, nonmembers $245. Register online at *www.sspc.org/training.*

Basic Plate and Sheet Metal Welding. A six-week course offered March 29–May 7, May 10–June 18, June 21–July 30, Aug. 2–Sept. 10, Sept. 13–Oct. 22, Oct. 25–Dec. 3. Call Lincoln Electric Welding School (216) 383-8325, or visit *www.lincolnelectric.com.*

Blodgett Welding Design Technical Training Course. April 20–23, June 15–18, Oct. 12–15. Call Lincoln Electric Co. (216) 383-2409, or visit *www.lincolnelectric.com.*

Brazing Course. May 11–13, Wall Colmonoy Brazing Engineering Center, Cincinnati, Ohio. Brazing design, furnace brazing, material selection, quality control, and hands-on experience provided. Call Lydia Lee (248) 585-6400, ext. 252; or visit *www.wallcolmonoy.com/brazingschool.html.*

Building the Lean Fulfillment Stream: Supply Chain and Logistics Management. March 23. The Kendall Hotel, Cambridge, Mass. Contact Lean Enterprise Institute, *www.lean.org.*

Comprehensive Arc Welder Training. A 15-week course offered March 29–July 30, May 10–Sept. 10, June 21–Oct. 22, Aug. 2–Dec. 3, Sept. 13–Jan. 28, Oct. 25–March 11. Call Lincoln Electric Welding School (216) 383-8325, or visit *www.lincolnelectric.com.*

Flux Cored Arc Welding/Semiautomatic. A one-week course offered weeks of May 3, June 14, July 26, Sept. 7, Oct. 18, Nov. 29. Call Lincoln Electric Welding School (216) 383-8325, or visit *www.lincolnelectric.com.*

Fundamentals of Brazing Seminar. March 16–18, Crowne Plaza, Memphis, Tenn. Call Lucas-Milhaupt (800) 558-3856.

Gas Tungsten Arc Welding. A one-week course offered weeks of Mar. 22, April 19, May 17, June 1, June 21, July 12, Aug. 2, Aug. 23, Sept. 13, Oct. 4, Nov. 15, Dec. 6, Dec. 13. Call Lincoln Electric Welding School (216) 383-8325, or visit *www.lincolnelectric.com.*

♦Green Welding: The Future Is Now, Advanced Welding Technology Workshop. March 30–April 1. Arizona Western College, Institute of Welding Technology, AWS Student Chapter, Yuma, Ariz. Call Samuel Colton (928) 580-7104; (928) 344-7570, or e-mail *samuel.colton@azwestern.edu.*

Gas Metal Arc Welding/Semiautomatic. A one-week course offered weeks of March 15, April 5, April 26, May 24, June 7, June 28, July 19, Aug. 30, Sept. 27, Oct. 11, Nov. 1, Nov. 22, Dec. 6, Dec. 13. Call Lincoln Electric Welding School (216) 383-8325, or visit *www.lincolnelectric.com.*

Introduction to Welding. One-week course beginning April 12, June 7, July 19, Oct. 18. Call Lincoln Electric Welding School (216) 383-8325, or visit *www.lincolnelectric.com.*

AWS Certification Schedule

Certification Seminars, Code Clinics and Examinations

Application deadlines are six weeks before the scheduled seminar or exam. Late applications will be assessed a $250 Fast Track fee.

Certified Welding Inspector (CWI)

Location	Seminar Dates	Exam Date
Dallas, TX	Apr. 11-16	Apr. 17
Miami, FL	Apr. 11-16	Apr. 17
Knoxville, TN	EXAM ONLY	Apr. 17
Springfield, MO	Apr. 18-23	Apr. 24
Mobile, AL	EXAM ONLY	Apr. 24
St. Louis, MO	EXAM ONLY	Apr. 24
Portland, ME	Apr. 25-30	May 1
Las Vegas, NV	Apr. 25-30	May 1
Waco, TX	EXAM ONLY	May 1
Baton Rouge, LA	May 2-7	May 8
San Francisco, CA	May 2-7	May 8
Nashville, TN	May 9-14	May 15
Jacksonville, FL	May 9-14	May 15
Baltimore, MD	May 9-14	May 15
Corpus Christi, TX	EXAM ONLY	May 15
Detroit, MI	May 16-21	May 22
Miami, FL	May 16-21	May 22
Albuquerque, NM	May 16-21	May 22
Long Beach, CA	EXAM ONLY	May 29
Spokane, WA	Jun. 6-11	Jun. 12
Oklahoma City, OK	Jun. 6-11	Jun. 12
Birmingham, AL	Jun. 6-11	Jun. 12
Miami	EXAM ONLY	Jun. 17
Hartford, CT	Jun. 13-18	Jun. 19
Pittsburgh, PA	Jun. 13-18	Jun. 19
Beaumont, TX	Jun. 13-18	Jun. 19
Corpus Christi, TX	EXAM ONLY	Jul. 10
Miami	EXAM ONLY	Jul. 15
New Orleans, LA	Jul. 11-16	Jul. 17
Phoenix, AZ	Jul. 11-16	Jul. 17
Orlando, FL	Jul. 18-23	Jul. 24
Milwaukee, WI	Jul. 18-23	Jul. 24
Los Angeles, CA	Jul. 18-23	Jul. 24
Sacramento, CA	Jul. 18-23	Jul. 24
Kansas City, MO	Jul. 25-30	Jul. 31
Cleveland, OH	Jul. 25-30	Jul. 31
Louisville, KY	Jul. 25-30	Jul. 31
Denver, CO	Aug. 1-6	Aug. 7
Philadelphia, PA	Aug. 1-6	Aug. 7
Chicago, IL	Aug. 8-13	Aug. 14
San Diego, CA	Aug. 8-13	Aug. 14
Miami, FL	Aug. 8-13	Aug. 14
Charlotte, NC	Aug. 15-20	Aug. 21
San Antonio, TX	Aug. 15-20	Aug. 21
Bakersfield, CA	Aug. 15-20	Aug. 21
Rochester, NY	EXAM ONLY	Aug. 21
Portland, ME	Aug. 22-27	Aug. 28
Salt Lake City, UT	Aug. 22-27	Aug. 28
Seattle, WA	Aug. 22-27	Aug. 28
Corpus Christi, TX	EXAM ONLY	Sept. 4
Pittsburgh, PA	Sept. 12-17	Sept. 18
Houston, TX	Sept. 12-17	Sept. 18
Minneapolis, MN	Sept. 12-17	Sept. 18
St. Louis, MO	Sept. 19-24	Sept. 25
Miami, FL	Sept. 19-24	Sept. 25
New Orleans, LA	Sept. 19-24	Sept. 25
Anchorage, AK	EXAM ONLY	Sept. 25
Nashville, TN	Oct. 3-8	Oct. 9
Tulsa, OK	Oct. 3-8	Oct. 9
Long Beach, CA	Oct. 3-8	Oct. 9
Newark, NJ	Oct. 3-8	Oct. 9

For information on any of our seminars and certification programs, visit our website at **www.aws.org/certification** or contact AWS at (800) 443-9353, Ext. 273 for Certification and Ext. 455 for Seminars. Please **apply early** to save Fast Track fees. **This schedule is subject to change without notice.** Please verify the dates with the Certification Dept. and confirm your course status before making final travel plans.

9-Year Recertification Seminar for CWI/SCWI

Location	Seminar Dates	Exam Date
Miami, FL	Apr. 12-17	NO EXAM
Sacramento, CA	May 3-8	NO EXAM
Pittsburgh, PA	Jun. 7-12	NO EXAM
San Diego, CA	Jul. 12-17	NO EXAM
Orlando, FL	Aug. 23-28	NO EXAM
Denver, CO	Sept. 20-25	NO EXAM
Dallas, TX	Oct. 4-9	NO EXAM

For current CWIs and SCWIs needing to meet education requirements without taking the exam. If needed, recertification exam can be taken at any site listed under Certified Welding Inspector.

Advanced Visual Inspection

Location	Seminar Dates	Exam Date
Miami, FL	Apr. 16	Apr. 17
Dallas, TX	Apr. 16	Apr. 17
San Francisco, CA	May 7	May 8

Seminar designed to prepare for 9-Year Recertification Part B Exam and CWI candidates taking Part B re-exam.

Certified Welding Supervisor (CWS)

Location	Seminar Dates	Exam Date
New Orleans, LA	Apr. 19-23	Apr. 24
Minneapolis, MN	Jul. 19-23	Jul. 24
Miami, FL	Sept. 13-17	Sept. 18
Norfolk, VA	Oct. 4-8	Oct. 9

CWS exams are also given at all CWI exam sites.

Certified Radiographic Interpreter (CRI)

Location	Seminar Dates	Exam Date
Miami, FL	Apr. 19-23	Apr. 24
Allentown, PA	May 17-21	May 22
Miami. FL	Jun. 21-25	Jun. 26
Miami, FL	Jul. 26-30	Jul. 31

Radiographic Interpreter certification can be a stand-alone credential or can exempt you from your next 9-Year Recertification.

Certified Welding Sales Representative (CWSR)

Location	Seminar Dates	Exam Date
Houston, TX	Mar. 24-26	Mar. 26
Miami, FL	May 5-7	May 7
Chicago, IL	Jun. 9-11	Jun. 11
Miami, FL	Aug. 25-27	Aug. 27
Indianapolis, IN	Sept. 22-24	Sept. 24

CWSR exams will also be given at CWI exam sites.

Certified Welding Educator (CWE)

Seminar and exam are given at all sites listed under Certified Welding Inspector. Seminar attendees will not attend the Code Clinic portion of the seminar (usually first two days).

Senior Certified Welding Inspector (SCWI)

Exam can be taken at any site listed under Certified Welding Inspector. No preparatory seminar is offered.

Certified Robotic Arc Welding (CRAW)

Location	Week of:	Contact
ABB, Inc., Auburn Hills, MI	Apr. 5	(248) 391-8421
Wolf Robotics, Ft. Collins, CO	Apr. 19	(970) 225-7736
ABB, Inc., Auburn Hills, MI	May. 3	(248) 391-8421
ABB, Inc., Auburn Hills, MI	Jun. 7	(248) 391-8421
ABB, Inc., Auburn Hills, MI	Aug. 2	(248) 391-8421
ABB, Inc., Auburn Hills, MI	Oct. 4	(248) 391-8421

International CWI Courses and Exams

Please visit *http://www.aws.org/certification/inter_contact.html*

American Welding Society®

BY HOWARD M. WOODWARD

AWS Participates in Weld India and National Welding Seminar

The Indian Institute of Welding, Kolkata Branch, presented its National Welding Seminar, Welding and Fabrication in India — Present Status & Future Directions, Dec. 10–12, 2009, and the welding exhibition, Weld India 2009–2010, Dec. 11–13, in association with the American Welding Society, Welding Technology Institute of Australia, and the Indian Society for Non-Destructive Testing.

AWS President **Victor Matthews** had the honor to light the lamp to officially open the seminar.

R. Ravi, president, IIW-India, said, "We in India use welding extensively both for fabrication and for repair and maintenance. A tremendous wealth of knowledge is available with us for tackling the most critical welding challenges. IIW-India's National Welding Seminar is the ideal platform to share this knowledge and your institute is doing a wonderful service to the industry by organizing this seminar."

P. K. Das, vice president, IIW-India, and convenor for the event, said, "The National Welding Seminar has once again generated keen interest among the welding fraternity and nearly 75 authors including about ten from abroad will be presenting high-quality technical papers on contemporary welding topics."

S. K. De, chairman, The India Institute of Welding, Kolkata Branch, said "Over 300 delegates have registered for the seminar and representatives from six countries will be participating in the deliberations. Seventy-eight technical papers will be presented at the seminar in four parallel sessions. The concurrent event, Weld India 2009–2010, will provide an excellent opportunity to the welding industry to showcase products. The participation of over 70 exhibitors speaks well of the success of this event."

The *Indian Welding Journal* is published quarterly in technical association with AWS. It showcases technical papers by Indian authors plus an AWS Section featuring papers, articles, and departments reprinted from *Welding Journal*.

AWS President Victor Matthews lights the lamp at the inaugural ceremony to officially open the National Welding Seminar held Dec. 10–12, 2009, in Kolkata, India.

Shown from left are Victor Matthews, AWS president; R. Ravi, president IIW-India; and Subrata Gupta, managing director, West Bengal Industrial Development Corp., Ltd.

Official Interpretation D1.5

Subject: RT requirements for butt joints
Code Edition: D1.5/D1.5:2008, *Bridge Welding Code*
Code Provision: Clause 6.7.1
AWS Log No.: D1.5-08-I04

Inquiry: Is RT on butt joints merely a suggestion or a manadatory requirement by the Bridge Welding Code?

Response: *RT is required by Clause 6.7.1 unless otherwise provided (e.g., subsequent code provisions like ESW, which requires both UT and RT or agreement between supplier and owner for alternate acceptance verification). Clause C6.7.1 provides clarification for this code provision.*

Official Interpretation D17.1

Subject: Inspection and examination requirements
Code Edition: D17.1:2001, *Specification for Fusion Welding for Aerospace Applications*
Code Provision: Paragraph 4.3.8.1
AWS Log No.: D17.1-01-I01

Inquiry: Paragraph 4.3.8.1 states that test welds for welder qualification shall be inspected to Class A requirements. The paragraph further defines the inspection methods (i.e., visual and X-ray for groove welds with alternative methods of bend testing and metallographic for fillet welds). The suggested record from Figure 4.1 also only defines visual, radiographic, and metallographic in the test results section.

Neither paragraph 4.3.8.1 nor Figure 4.1 defines that penetrant testing (PT) or magnetic particle inspection (MPE) is required.

Class A inspection is, however, required. In paragraph 6.4, which defines the inspection criteria, PT/MPI are mandated for Class A welds.

For Welder Qualification Tests, is PT for nonferrous or MPI for ferromagnetic materials required to be performed?

Response: *Requirements in paragraph 4.3.8.1 specify both the methods of inspection and acceptance criteria of Class A welds shall be performed for welder and welding operator qualification. Figure 4.1 contains suggested content and format that are provided as an example only.*

Revised Standard Approved by ANSI

A5.11/A5.11M:2010, *Specification for Nickel and Nickel-Alloy Welding Electrodes for Shielded Metal Arc Welding.* Revision approved 12/15/2009.

New Standards Projects

Development work has begun on the following two new standards. Affected individuals are invited to contribute to the development of these standards. Those wanting to participate should contact Annette Alonso, ext. 299. Participation on AWS Technical Committees and Subcommittees is open to all persons.

J1.1/J1.1M:20XX, *Specification for Resistance Welding Controls.* This standard provides nomenclature pertaining to the design, construction, and programming of resistance welding controls. Standard calibration and performance parameters, as well as labeling and documentation requirements, are also outlined. The purpose is to promote standardization, safety, and proper application of resistance welding controls. Stakeholders: Manufacturers and users of resistance welding controls to establish standard nomenclature and promote functional consistency and elements of safety.

J1.2/J1.2M:20XX, *Guide to Installation and Maintenance of Resistance Welding Machines.* This guide provides general instructions for the installation, operation, and maintenance of common types of resistance welding equipment. Generic preventative maintenance schedules and equipment troubleshooting recommendations are provided, as is an overview of common weld qualification techniques and corrective actions to common weld conditions. Stakeholders: It has been customary practice for some equipment manufacturers to include a copy in their machine documentation package or to promote the publication to equipment users who have no manual for their equipment and no means to get one.

ISO Draft Standards for Public Review

Copies of the following draft international standards are available for review and comment through your national standards body, which in the United States is ANSI, 25 W. 43rd St., Fourth Fl., New York, NY 10036; (212) 642-4900. Comments regarding ISO documents should be sent to your national standards body.

In the United States, if you wish to participate in the development of International Standards for welding, contact A. Davis, ext. 466; *adavis@aws.org.* Otherwise contact your national standards body.

ISO/DIS 10882-1, *Health and safety in welding and allied processes — Sampling of airborne particles and gases in the operator's breathing zone — Part 1: Sampling of airborne particles*

ISO/DIS 15011-5, *Health and safety in welding and allied processes — Sampling of fume and gases — Part 5: Identification of thermal-degration products generated when welding or cutting through products composed wholly or partly of organic materials using pyrolysis-gas chromatography-mass spectrometry*

Technical Committee Meetings

March 8, A5H Subcommittee on Filler Metals and Fluxes for Brazing. Phoenix, Ariz. Contact S. Borrero, ext. 334.

March 9, 10, C3 Committee and Subcommittees on Brazing and Soldering. Phoenix, Ariz. Contact S. Borrero, ext. 334.

March 12, J1 Committee on Resistance Welding Equipment. Palm Beach Gardens, Fla. Contact A. Alonso, ext. 299.

March 22, A5B Subcommittee on Carbon and Low-Alloy Steel Electrodes and Fluxes for Submerged Arc Welding. Orlando, Fla. Contact R. Gupta, ext. 301.

March 23, A5 Committee on Filler Metals and Allied Materials. Orlando, Fla. Contact R. Gupta, ext. 301.

March 23–26, D1 Committee on Structural Welding. Kansas City, Mo. Contact S. Morales, ext. 313.

April 6–8, B2 Committee on Procedure and Performance Qualifications. Pittsburgh, Pa. Contact S. Morales, ext. 313.

April 20, D14I Subcommittee on Hydraulic Cylinders. Cincinnati, Ohio. Contact M. Rubin, ext. 215.

April 21, D14B Subcommittee on General Design and Practice. Cincinnati, Ohio. Contact M. Rubin, ext. 215.

April 21, D14E Subcommittee on Welding of Presses and Industrial and Mill Cranes. Cincinnati, Ohio. Contact M. Rubin, ext. 215.

April 21, D14G Subcommittee on Welding of Rotating Equipment. Cincinnati, Ohio. Contact M. Rubin, ext. 215.

April 21, D14J Subcommittee on Armament Systems. Cincinnati, Ohio. Contact M. Rubin, ext. 215.

April 21, SH4 Subcommittee on Labeling and Safe Practices. Columbus, Ohio. Contact S. Hedrick, ext. 305.

April 22, D14 Committee on Machinery and Equipment. Cincinnati, Ohio. Contact M. Rubin, ext. 215.

April 22, D14C Subcommittee on Earthmoving and Construction Equipment. Cincinnati, Ohio. Contact M. Rubin, ext. 215.

Technical Committee Volunteer Opportunities

Labeling and Safe Practices

Volunteers are needed to participate on the SH4 Subcommittee on Labeling and Safe Practices. Its documents include F2.2, *Lens Shade Selector,* F4.1, *Safe Practices for the Preparation of Containers and Piping for Welding and Cutting,* and the AWS Safety and Health Fact Sheets. For additional information about this committee's work, contact Steve Hedrick, *steveh@aws.org,* (800/305) 443-9353, ext. 305; or submit a technical committee application online at *www.aws.org/1UQ4.*

Welding Sales Representatives

AWS established a new certification program for welding sales representatives in 2009. Volunteers are invited to be part of the technical subcommittee responsible for setting the qualification requirements, **AWS B5.14,** *Specification for the Qualification of Welding Sales Representatives,* that this program is based on. Contact John Gayler, *gayler@aws.org,* (800/305) 443-9353, ext. 472; or visit *www.aws.org/1UQ4.*

Robotic and Automatic Welding

Volunteers are sought to contribute their expertise to the D16 Committee on Robotic and Automatic Welding. Its documents include **D16.1,** *Specification for Robotic Arc Welding Safety;* **D16.2,** *Guide for Components of Robotic and Automatic Arc Welding Installations;* **D16.3,** *Risk Assessment Guide for Robotic Arc Welding;* **D16.4,** *Specification for Qualification of Robotic Arc Welding Personnel.* Persons engaged in robotic welding operations and suppliers of equipment who want to contribute their expertise to the preparation of one or more of these documents are urged to contact Matt Rubin, *mrubin@aws.org;* (800/305) 443-9353, ext. 215, or visit *www.aws.org/1UQ4* to submit your member application online.

Magnesium Alloy Filler Metals

Volunteers are invited to participate on the A5L Subcommittee on Magnesium Alloy Filler Metals. This subcommittee is responsible for updating **AWS A5.19-92 (R2006),** *Specification for Magnesium Alloy Welding Electrodes and Rods.* For complete information, contact Subcommittee Secretary Rakesh Gupta at *gupta@aws.org,* or call (800/305) 443-9353, ext. 301; or visit *www.aws.org/1UQ4* to submit your member application online.

Thermal Spraying

Volunteers are invited to participate on the C2 Committee on Thermal Spraying. Several of its documents include **C2.16,** *Guide for Thermal-Spray Operator Qualification*; **C2.18,** *Guide for the Protection of Steel with Thermal Sprayed Coatings of Aluminum and Zinc and their Alloys and Composites;* **C2.19,** *Machine Element Repair*; **C2.23,** *Specification for the Application of Thermal Spray Coatings (Metallizing) of Aluminum, Zinc, and Their Alloys and Composites for the Corrosion Protection of Steel.* Contact Reino Starks, *rstarks@aws.org,* (800/305) 443-9353, ext. 304, for information, or visit *www.aws.org/1UQ4* to submit your application online.

Candidates Sought for the Prof. Masubuchi Award

November 2, 2010, is the deadline for submitting nominations for the 2011 Prof. Koichi Masubuchi Award, sponsored by the Dept. of Ocean Engineering at Massachusetts Institute of Technology.

This award is presented each year to one person who has made significant contributions to the advancement of materials joining through research and development. It includes a $5000 honorarium.

The candidate must be 40 years old or younger, may live anywhere in the world, and need not be an AWS member.

The nomination package should be prepared by someone familiar with the research background of the candidate. It should include the candidate's résumé listing background, experience, publications, honors, and awards, plus at least three letters of recommendation from fellow researchers.

The award was established to recognize Prof. Koichi Masubuchi for his numerous contributions to the advancement of the science and technology of welding, especially in the fields of fabricating marine and outer space structures. E-mail your nominations to Prof. John DuPont at *jnd1@lehigh.edu.*

AWS Publications Sales

Purchase AWS standards, books, and other publications from WEX (World Engineering Xchange, Ltd.); *orders@awspubs.com; www.awspubs.com.* Call toll-free (888) 935-3464 (U.S. and Canada); (305) 824-1177; FAX (305) 826-6195.

Copies of *Welding Journal* articles may be purchased from Ruben Lara, (800/305) 443-9353, ext. 288; *rlara@aws.org.*

Custom reprints of *Welding Journal* articles, in quantities of 100 or more, may be purchased from Claudia Stachowiak, at FosteReprints, *claudia@fostereprints.com,* (866) 879-9144, ext. 121.

AWS Mission Statement

The mission of the American Welding Society is to advance the science, technology, and application of welding and allied processes, including joining, brazing, soldering, cutting, and thermal spraying.

D17 Committee Publishes Standard for Friction Stir Welding of Aluminum Alloys

Developed by the D17 Committee on Welding in the Aircraft and Aerospace Industries, AWS D17.3/D17.3M:2010, *Specifiction for Friction Stir Welding of Alumninum Alloys for Aerospace Applications,* states the requirements for weldment design, qualification of personnel and procedures, fabrication, and inspection.

The well-illustrated, 54-page document includes 28 figures and six tables, and uses both U.S. Customary Units and SI International System of Units.

The section headings include terms and definitions, general requirements, design of weld joints, development and qualification of a welding procedure, welding operator qualification, fabrication, and inspection. The standard lists for $64, $48 for AWS members.

Purchase this and all AWS publications from WEX, Ltd., *www.awspubs.com;* or call toll-free (888) 935-3463; FAX (305) 826-6195; *orders@awspubs.com.*

Member-Get-A-Member Campaign

Listed below are the AWS members who are participating in the 2009–2010 campaign. See page 85 in this *Welding Journal* or visit *www.aws.org/mgm* for the campaign rules and prize list.

The following standings are as of Jan. 15, 2010. Call the AWS Membership Dept. (800/305) 443-9353, ext. 480, for information on your member-proposer status.

Winner's Circle

Sponsored 20+ new members.

The superscript indicates the number of times the member has achieved Winner's Circle status since June 1, 1999.

J. Compton, San Fernando Valley[7]
E. Ezell, Mobile[7]
J. Merzthal, Peru[2]
G. Taylor, Pascagoula[2]
L. Taylor, Pascagoula[2]
S. Esders, Detroit[1]
B. Mikeska, Houston[1]
W. Shreve, Fox Valley[1]
M. Karagoulis, Detroit[1]
S. McGill, NE Tennessee[1]
T. Weaver, Johnstown/Altoona[1]
G. Woomer, Johnstown/Altoona[1]
R. Wray, Nebraska[1]
M. Haggard, Inland Empire[1]

President's Guild

Sponsored 20+ new members.

V. Craven, Pascagoula — 59
B. Chin, Auburn — 24

President's Roundtable

Sponsored 9–19 new members.

R. Ellenbecker, Fox Valley — 17
A. Sumal, British Columbia — 11
H. Thompson, New Orleans — 9

President's Club

Sponsored 3–8 new members.

D. Berger, New Orleans — 5
J. Ciaramitaro, N. Central Florida — 5
L. Taylor, Pascagoula — 5
J. Hope, Puget Sound — 4
S. Keskar, India Int'l — 4
E. Ravelo, International — 4
T. Baber, San Fenando Valley — 3
G. Burrion, South Florida — 3
B. Cebery, Fox Valley — 3
J. Compton, San Fernando Valley — 3
T. Morris, Tulsa — 3

President's Honor Roll

Sponsored 2 new members.

J. Barber, Connecticut — 2
G. Callender, San Fernando Valley — 2
K. Carter, Tri-River — 2
R. Davis, Utah — 2
G. Euliano, Northwestern Pa. — 2
M. Haynes, Niagara Frontier — 2
K. Hurst, Kansas City — 2
D. Mandina, New Orleans — 2
V. Matthews, Cleveland — 2
J. Medina, International — 2
P. Newhouse, British Columbia — 2
F. Nguni, New Jersey — 2
T. Rowe, Tulsa — 2
M. Rudden, Colorado — 2
J. Sims, Syracuse — 2

3+ Student Member Sponsors

C. Rogers, San Antonio — 49
H. Hughes, Mahoning Valley — 40
D. Berger, New Orleans — 38
D. Ketler, Willamette Valley — 34
C. Lindquist, Central Michigan — 32
J. Morash, Boston — 28
M. Anderson, Indiana — 28
D. Saunders, Lakeshore — 28
J. Carney, Western Michigan — 27
R. Durham, Cincinnati — 26
D. Kowalski, Pittsburgh — 26
S. Miner, San Francisco — 26
S. Siviski, Maine — 24
A. Baughman, Stark Central — 23
T. Gerber, Allegheny — 22
R. Wahrman, Triangle — 22
D. Aragon, Puget Sound — 21
T. Geisler, Pittsburgh — 21
S. Burdge, Stark Central — 20
A. Duron, New Orleans — 20
R. Evans, Siouxland — 20
E. Norman, Ozark — 20
G. Marx, Tri-River — 20
C. Donnell, NW Ohio — 19
J. Durbin, Tri-River — 19
V. Facchiano, Lehigh Valley — 19
K. Rawlins, Columbia — 19
J. Theberge, Boston — 19
M. Arand, Louisville — 18
J. Boyer, Lancaster — 18
K. Carter, Tri-River — 17
G. Smith, Lehigh Valley — 17
N. Baughman, Stark Central — 16
A. Reis, Pittsburgh — 16
G. Seese, Johnstown-Altoona — 16
D. Zabel, SE Nebraska — 16
J. Daugherty, Louisville — 15
A. Stute, Madison-Beloit — 15
M. Vann, South Carolina — 15
R. Vann, South Carolina — 15
B. Benyon, Johnstown-Altoona — 14
J. Ciaramitaro, N. Central Florida — 14
J. Gerdin, Northwest — 14
J. Kline, Northern New York — 14
R. Munns, Utah — 14
D. Vranich, North Florida — 14
R. Hutchison, Long Bch/Or. Cty. — 12
S. Mattson, North Florida — 12
J. Stallsmith, South Carolina — 11
T. Garcia, New Orleans — 10
W. Harris, Pascagoula — 10
S. Kuntz, Pittsburgh — 10
R. Rummel, Central Texas — 10
C. Schiner, Wyoming — 10
P. Swatland, Niagara Frontier — 10
W. Galvery, Long Bch./Or. Cty. — 9
V. Harthun, Northern Plains — 8
J. Hill, Puget Sound — 8
W. Garrett, Olympic — 7
A. Mattox, Lexington — 7
J. Fitzpatrick, Arizona — 6
M. Hayes, Puget Sound — 6
R. Jones, Puget Sound — 6
A. Badeaux, Washington, D.C. — 5
D. Howard, Johnstown-Altoona — 5
S. Liu, Colorado — 5
S. Colton, Arizona — 4
R. Davis, Syracuse — 4
J. Grossman, Central Michigan — 4
S. Hansen, SE Nebraska — 4
S. Henson, Spokane — 4
E. Hinojosa, L.A./Inland Empire — 4
A. Kitchens, Olympic Section — 4
J. Lynn, Idaho/Montana — 4
S. MacKenzie, Northern Michigan — 4
J. Smith, Greater Huntsville — 4
M. Stevenson, J.A.K. — 4
J. Boyd, San Diego — 3
N. Carlson, Idaho/Montana — 3
B. Chin, Auburn — 3
J. Compton, San Fernando Valley — 3
W. Davis, Syracuse — 3
C. Gilbertson, Northern Plains — 3
G. Kimbrell, St. Louis — 3
S. McDaniel, Inland Empire — 3
R. Madrigal, L.A./Inland Empire — 3
G. Moore, San Diego — 3
D. Newman, Ozark — 3
S. Robeson, Cumberland Valley — 3
A. Rodden, West Tennessee — 3

SECTION NEWS

New York Section members are shown at the December meeting.

District 1

Thomas Ferri, director
(508) 527-1884
tferri@thermadyne.com

GREEN & WHITE MOUNTAINS

JANUARY 14
Activity: The Section's executive board met at Thermadyne in West Lebanon, N.H. Chair **Geoff Putnam** presided. Participating were Vice Chair **Garry Buckley, John Steel,** Treasurer **Philip Witteman, Ernie Plumb, Jennifer Eastley, Pearly Lund, Ray Hendersen,** and **Jim Reid.**

Shown at the Green and White Mountains meeting are, from left, (front row) Chair Geoff Putnam, Garry Buckley, and John Steel; (center row) Philip Witteman, Ernie Plumb, Jennifer Eastley, and Pearly Lund; and (back row) Ray Hendersen and Jim Reid.

District 2

Kenneth R. Stockton, director
(908) 412-7099
kenneth.stockton@pseg.com

LONG ISLAND

OCTOBER 14
Speaker: **Tom Gartland,** consultant
Affiliation: Trilogy Lab, LLC
Topic: Designing the cooler for the Magnum welding machine
Activity: The program was held at The Nook Restaurant in Wantagh, N.Y.

Shown at the Long Island Section program are (front, from left) Chair Brian Cassidy and Harland Thompson; (standing, from left) Tony Greco, Alex Duchere, Ken Messemere, speaker Tom Gartland, Barry McQuillen, and Ray O'Leary.

NEW YORK

DECEMBER 8
Speakers: **Bob Wiswesser,** director; **Jeff Wiswesser,** manager
Affiliation: Welder Training and Testing Institute

Steve Ringler accepts the Reading Section scholarship from Merilyn McLaughlin.

Speaker Warren Price (right) receives a speaker gift from Robert Brewington, chair, Florida West Coast Section.

Warren Price demonstrated his cryogenic method for making ice cream for the receptive Florida West Coast Section members.

Al Sedory, past chair of the Florida West Coast Section, and wife, Jan, perform quality control tests on Warren Price's ice cream.

Brad McAllister receives a speaker gift from Dusti Jones, Chattanooga Section chair.

Topic: Welder qualification and certification using the QC-4/QC-7 program
Activity: This New York Section meeting was held at Buckley's Restaurant in Brooklyn, N.Y.

District 3

Michael Wiswesser, director
(610) 820-9551
mike@welderinstitute.com

READING

JANUARY 10
Activity: The Section presented its annual $500 scholarship award to **Steve Ringler. Merilyn McLaughlin** presented the award in the welding lab at Berks Career & Technology Center West, in Leesport, Pa.

District 4

Roy C. Lanier, director
(252) 321-4285
rlanier@email.pittcc.edu

District 5

Steve Mattson, director
(904) 260-6040
steve.mattson@yahoo.com

FLORIDA WEST COAST

JANUARY 13
Speaker: **Warren Price,** regional sales manager
Affiliation: Chart, Inc.
Topic: Properties of cryogenic gases and the construction of bulk storage tanks
Activity: The program was held at Frontier Steakhouse in Tampa, Fla. Price demonstrated the cooling effect of liquid nitrogen by making a batch of ice cream that he served to the attendees.

District 6

Kenneth Phy, director
(315) 218-5297
KAPhyInc@gmail.com

District 7

Don Howard, director
(814) 269-2895
howard@ctc.com

COLUMBUS

JANUARY 20
Speaker: **Jim Hookey,** national resource specialist, powerplants
Affiliation: National Transportation Safety Board
Activity: The Columbus Section members met with members of the local chapters of SWE, ASME, ASM Int'l, IIE, AIAA, ISA, and NACE. ASM hosted this program at Arlington Banquets in Columbus, Ohio. Seventy-five people attended the event.

District 8

Joe Livesay, director
(931) 484-7502, ext. 143
joe.livesay@ttcc.edu

CHATTANOOGA

JANUARY 19
Speaker: **Brad McAllister,** consultant
Affiliation: WAP Sustainability Consulting
Topic: Sustainability solutions for both businesses and local governments
Activity: The program was held at Komatsu America Corp. in Chattanooga, Tenn.

District 9

George D. Fairbanks Jr., director
(225) 473-6362
fits@bellsouth.net

BATON ROUGE

OCTOBER
Activity: The Section participated in a career day for students at Zachary High School in Zachary, La. Speakers included **Davis Rayborn,** District 9 Director **George Fairbanks,** and **Mike Templet.** The topic was industrial jobs and career opportunities for welding students. The event included a tour of the school's new welding facility and some of its welding projects, including a bleacher stand and the Hard Work Café. Fairbanks Inspection sponsored the event, with door prizes provided by TNT Welding Supply.

District 10

Richard A. Harris, director
(440) 338-5921
richaharris@windstream.net

CLEVELAND

DECEMBER 8
Activity: The Section hosted its annual Christmas party and fund-raising event at

Members of the Baton Rouge Section are shown at the Hard Work Café.

St. Paul's Hellenic Center in Cleveland, Ohio. This year, the auction added $5200 to the Section's scholarship fund. More than 130 AWS and ASNT members and guests participated.

JANUARY 12
Speaker: **Bob Dissauer,** welder trainer
Affiliation: The Lincoln Electric Co.
Topic: Decisions contractors must make when laying pipe cross-country
Activity: This Cleveland Section program was held at St. Paul's Hellenic Center in Cleveland, Ohio, for 35 attendees.

DRAKE WELL

JANUARY 12
Activity: The Section members toured the Airgas Great Lakes facilities in Franklin, Pa. **Steve Goss** conducted the program. **Marty Siddall,** technical sales representative with Lincoln Electric, presented a PowerPoint talk on how shielding gases affect welds, followed by a welding demonstration.

District 11

Eftihios Siradakis, director
(989) 894-4101
ft.siradakis@airgas.com

DETROIT

JANUARY 14
Speaker: **Scott Frasso,** sales manager
Affiliation: Cor-Met, Inc.
Topic: Die repair using coated electrodes as filler metal
Activity: The Section held its patrons' appreciation night program at the Ukrainian Cultural Center in Warren, Mich., hosted by Cor-Met. Celebrated for their support of the Section and its scholarship fund were Cor-Met; Lincoln Electric; Dengensha of America; Obara Corp.; Industrial Control Repair; Luvata Ohio, Inc.; American Iron & Steel; Sastha Com, Inc.; MJM

Zachary High School students greet the photographer at the Baton Rouge Section event.

Shown at the Drake Well Section program are (from left) Fred Adelman, Treasurer Ward Kiser, Steve Goss, David Burnstein, Vice Chair Jason Fry, Chair Mike Owens, Secretary Travis Crate, and Marty Siddall.

Scott Frasso (left), representing Cor-Met, accepts a Detroit Section host-appreciation award from Don Maatz.

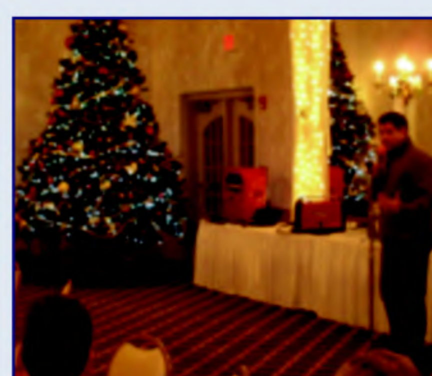

Auctioneer Scott Mahalaic kept the bids coming to benefit the Cleveland Section's scholarship fund.

Shown at the Indiana Section program are (from left) Phil Bedel, Gary Dugger, Gary Tucker, Bennie Flynn, Dave Jackson, Chair Tony Brosio, Ricky Ferguson, Mike Anderson, Eric Cooper, and Dick Alley, a past AWS president.

Iowa Section members toured Montezuma Manufacturing in January.

The Detroit Section honored its patrons in January. Representatives of the various supporting companies are shown above.

Shown at the Lakeshore Section program are (from left) Chairman Chuck Frederick, Jason Kushner, and Rob Stinson.

Sales, Inc.; ARO Welding Technologies, Inc.; Motoman, Inc.; Matuschek Welding Products; RoMan Manufacturing, Inc.; Grossel Tool; Pro Spot International, Inc.; Fusion Welding Solutions; and Centerline (Windsor), Ltd.

District 12

Sean P. Moran, director
(920) 954-3828
sean.moran@hobartbrothers.com

LAKESHORE

JANUARY 14

Activity: The Section members met at Lakeshore Technical College in Cleveland, Wis., for a lecture and demonstration of hardfacing and a second talk on maintenance and repair techniques followed by hands-on demonstrations. The presenters included Lincoln Electric sales engineer **Rob Stinson** and **Bob Dempsey,** Milwaukee district sales manager; and Eutectic Corp. technical sales representative **Jason Kushner.** Twenty-six members participated in the event.

District 13

W. Richard Polanin, director
(309) 694-5404
rpolanin@icc.edu

District 14

Tully C. Parker, director
(618) 667-7795
tparke@millerwelds.com

INDIANA

JANUARY 9

Activity: The Section held its annual organizational meeting at Jonathan Byrds Cafeteria in Indianapolis, Ind. Chair **Tony Brosio** from Lift-a-Loft Corp. conducted the program. The incoming slate of Section officers was chosen. **Gary Tucker** will serve as chairman for 2010. Plans were set for the upcoming Mid-West and SkillsUSA welding contests.

District 15

Mace V. Harris, director
(612) 861-3870
macevh@aol.com

District 16

David Landon, director
(641) 621-7476
dlandon@vermeermfg.com

IOWA

JANUARY 12

Activity: The Section members toured the Montezuma Manufacturing facility in Montezuma, Iowa, to study its operations. The facility designs and builds car parts, and performs metal forming using 200 robots for welding, parts handling, and inspection operations.

MID PLAINS

OCTOBER 6

Speaker: **Victor Matthews,** AWS president
Affiliation: The Lincoln Electric Co. (ret.)
Topic: Careers in welding
Activity: This was a joint meeting with members of the Central Nebraska Section. The program was held at Linweld Inc. in Kearney, Neb. **David Landon,** District 16 director, presented the Section an award for achieving the best increase in membership in the District. Landon cited Chairman **Dan Rucker** for his leadership of the Section during the year.

DECEMBER 12

Activity: The Section members and spouses visited the Golden Spike Observation Tower in North Platte, Neb., at the Bailey Yards of the Upper Peninsula Railroad. The tower offers a spectacular view of the sprawling railroad complex. The dinner was held at The Depot Restaurant.

District 17

J. Jones, director
(940) 368-3130
jjones@thermadyne.com

Oklahoma City Section bowling champs pose with their trophies. Shown (from left) top photos are Chris George, Dick Wigger, Terry Songer, Justin Fite, Roger Cohee, and Cary Reeves. Center photo are Dan Andrews, Dee Lawson, Rick Lawson, and Bob Strohmeyer; bottom photo are Ray Hendricks, Johnny Day, Carl Drum, and Haily Drum.

EAST TEXAS

DECEMBER 3

Speaker: **Charles 'Mike' Igo**
Affiliation: OSHA outreach trainer
Topic: Welding fume extraction and developing safety habits
Activity: The program was held at Caddo Career Center in Shreveport, La.

OKLAHOMA CITY

JANUARY 14

Activity: The Section hosted its bowling tournament at Penn 44 Lanes in Oklahoma City, Okla. **Roger Cohee** received the award for highest individual score.

District 18

John Bray, director
(281) 997-7273
sales@affiliatedmachinery.com

HOUSTON

OCTOBER 24

Activity: The Section hosted its annual fall educational program in Houston, Tex. The event raised nearly $2500 for the Section's scholarship fund. This one-day program included five speakers discussing preparation of a preliminary welding procedure specification (pWPS). The presenters included **David Berridge** of C&J Cladding;

Spokane Section members participated in demonstrations of the safe use of grinding wheels at the January program.

Shown at the Houston Section seminar in October are presenters (from left) David Berridge, Robert Huddleston, Grant Peltier, Tom Myer, and Barney Burks.

Speaker Edward Dalder (right) chats with Tom Smeltzer, San Francisco Section chair.

Houston Section seminar attendees are shown at the October event.

Robert Huddleston of Acute Technological Services; **Grant Peltier** of TWSCO; **Tom Myer** of ABS; and **Barney Burks** of SOWESCO. Fifty-five people participated in the seminar. Part two of this Houston Section seminar series will be presented in early 2010. Visit *www.awshouston.org* for details.

November 20
Activity: The Houston Section held a welder qualification testing program in Houston, Tex. Chair **John Stoll** opened the program. **John Husfeld** presented an overview of the day's activities and how the certification process works and is typically used in the fabrication process. Sixteen members participated, eight passed the test. The volunteers included **Billy Herrell, Grant Peltier, Danny Castro, Dan Jones, Barney Burks Jr., John Stoll, Fred Schweighardt,** and **John Husfeld.**

RIO GRANDE VALLEY

January 17
Speaker: **Rene Hernandez,** sales representative
Affiliation: Miller Electric
Topic: Characteristics of the new digital technology for controlling welding wire feeders
Activity: The program was held at Golden Corral in Harlingen, Tex. **John Bray,** District 18 director, attended the program.

District 19

Neil Shannon, director
(503) 419-4546
neilshnn@msn.com

SPOKANE

January 12
Speaker: **Mark Riley**
Affiliation: Flexovit USA
Topic: Grinding wheel safety
Activity: Following the PowerPoint presentation, Riley demonstrated the proper mounting and use of grinding wheels. The program was held at Oxarc Training Center in Spokane, Wash.

District 20

William A. Komlos, director
(801) 560-2353
bkoz@arctechllc.com

District 21

Nanette Samanich, director
(702) 429-5017
Nan07@aol.com

District 22

Dale Flood, director
(916) 288-6100, ext. 172
flashflood@email.com

SAN FRANCISCO

January 6
Speaker: **Edward Dalder**
Affiliation: Dalder Materials Consulting
Topic: FCAW on austenitic stainless steels used for liquid helium service
Activity: The program was held at Spenger's Restaurant in Berkeley, Calif.

Win Great Prizes in the **2009-2010 AWS** Member-Get-A-Member Campaign*

ABOUT: AWS is looking for individuals to become part of an exclusive group of AWS Members who get involved and win. Give back to your profession, strengthen AWS and win great limited-edition prizes by participating in the 2009-2010 Member-Get-A-Member Campaign. By recruiting new members to AWS, you're adding to the resources necessary to expand your benefits as an AWS Member. Year round, you'll have the opportunity to recruit new members and be eligible to win special contests and prizes. Referrals are our most successful member recruitment tool. Our Members know first-hand how useful AWS Membership is, and with your help, AWS will continue to be the leading organization in the materials joining industry.

To recruit new Members, use the application on the reverse, or visit www.aws.org/mgm

PRIZE CATEGORIES

President's Honor Roll: Recruit 1-2 new Individual Members and receive an AWS key chain.

President's Club: Recruit 3-8 new Individual Members and receive an AWS hat and an AWS key chain.

President's Roundtable: Recruit 9-19 new Individual Members and receive an AWS polo shirt, hat and an AWS key chain.

President's Guild: Recruit 20 or more new Individual Members and receive an AWS watch, an AWS polo shirt, a one-year free AWS Member-ship, the "Shelton Ritter Member Proposer Award" Certificate and membership in the Winner's Circle.

Winner's Circle: All members who recruit 20 or more new Individual Members will receive annual recognition in the *Welding Journal* and will be honored at FABTECH International & AWS Welding Show.

SPECIAL PRIZES

Participants will also be eligible to win prizes in specialized categories. Prizes will be awarded at the close of the campaign (June 2010).

Sponsor of the Year: The individual who sponsors the greatest number of new Individual Members during the campaign will receive a plaque, a trip to the 2010 FABTECH International & AWS Welding Show, and recognition at the AWS Awards Luncheon at the Show.

Student Sponsor Prize: AWS Members who sponsor two or more Student Members will receive an AWS key chain.

The AWS Member who sponsors the most Student Members will receive a free, one-year AWS Membership, an AWS polo shirt, hat and an AWS key chain.

International Sponsor Prize: Any member residing outside the United States, Canada and Mexico who sponsors the most new Individual Members will receive a complimentary AWS Membership renewal.

LUCK OF THE DRAW

For every new member you sponsor, your name is entered into a quarterly drawing. The more new members you sponsor, the greater your chances of winning. Prizes will be awarded in November 2009, as well as in February and June 2010.

Prizes Include:

★ Complimentary AWS Membership renewal
★ AWS t-shirt
★ AWS hat

SUPER SECTION CHALLENGE

The AWS Section in each District that achieves the highest net percentage increase in new Individual Members before the June 2010 deadline will receive special recognition in the *Welding Journal*.

The AWS Sections with the highest numerical increase and greatest net percentage increase in new Individual Members will each receive the Neitzel Membership Award.

*The 2009-2010 MGM Campaign runs from June 1, 2009 to May 31, 2010. Prizes are awarded at the close of the campaign.

American Welding Society
Visit www.aws.org

New AWS Supporters

Sustaining Company

Malin Int'l Ship Repair & Drydock, Inc.
320 77th St.
Galveston, TX 77554
www.malinshiprepair.com
Representative: **Andrew M. Yancy**

Malin International Ship Repair & Drydock, Inc., is a first response repair company with vast experience in maritime work. The company ensures minimum downtime for vessels under repair with work shifts that run 24 hours a day and 7 days a week. The company is ASME and National Board certified for pressure vessel fabrication and repair.

Welding Distributor

OASA/Welding and Auto Supply
206B W. Sherman St.
Calexico, CA 92231

Supporting Companies

Aceros Arquitectonicos Grupo Ferroso, S.A.
Km. 26.4 Carretera a Amatitlan
Guatemala City 01063
Guatemala

Hose Master
1233 E. 222nd St.
Cleveland, OH 44117

Miller Mechanical Services, Inc.
51 Walnut St.
Glens Falls, NY 12801

Affiliate Companies

Kentucky Machine and Engineering
590 Glenwood Mill Rd.
PO Box 619, Cadiz, KY 42211

M C Welding Services, Ltd.
5506 238 St.
Langley, BC V2Z 2P1, Canada

Ohio Valley Steel Co.
PO Box 911, Wheeling, WV 26003

Pacific Steel Fabricators
7969 W. Mossy Cup St.
Boise, ID 83709

SkyTesting Services, Inc.
100-G Knickerbocker Ave.
Bohemia, NY 11716

SteelCraft Products, LLC
2610 Fire Tower Rd.
Rockhill, SC 29730

Educational Institutions

Klaipeda University
Biyunu 17
Klaipeda, LT 91225, Lithuania

Metro Technology Center
4901 S. Bryant Ave.
Oklahoma City, OK 73129

Montana State University–Great Falls
College of Technology
2100 16th Ave. S.
Great Falls, MT 59405

Membership Counts

Member Grades	As of 02/01/10
Sustaining	506
Supporting	314
Educational	514
Affiliate	459
Welding distributor	45
Total corporate members	**1,838**
Individual members	53,171
Student + transitional members	7,514
Total members	**60,685**

Honorary Meritorious Awards

The Honorary Meritorious Awards Committee makes recommendations for the nominees presented to receive the Honorary Membership, National Meritorious Certificate, William Irrgang Memorial, and the George E. Willis Awards. These honors are presented during the FABTECH International & AWS Welding Show held each fall. The deadline for submissions is December 31 prior to the year of the awards presentations. Send candidate materials to Wendy Sue Reeve, secretary, Honorary Meritorious Awards Committee, *wreeve@aws.org;* 550 NW LeJeune Rd., Miami, FL 33126. Descriptions of these awards follow.

William Irrgang Memorial Award

Sponsored by The Lincoln Electric Co. in honor of William Irrgang, the award, adminstered by AWS, is given each year to the individual who has done the most over the past five years to enhance the Society's goal of advancing the science and technology of welding. It includes a $2500 honorarium and a certificate.

Honorary Membership Award

The honor is presented to a person of acknowledged eminence in the welding profession, or to one who is accredited with exceptional accomplishments in the development of the welding art, upon whom the Society deems fit to confer an honorary distinction. Honorary Members have full rights of membership.

National Meritorious Certificate Award

This certificate award recognizes the recipient's counsel, loyalty, and dedication to AWS affairs, assistance in promoting cordial relations with industry and other organizations, and for contributions of time and effort on behalf of the Society.

International Meritorious Certificate Award

This honor recognizes recipients' significant contributions to the welding industry for service to the international welding community in the broadest terms. The awardee is not required to be an AWS member. Multiple awards may be given. The award consists of a certificate and a one-year AWS membership.

George E. Willis Award

Sponsored by The Lincoln Electric Co. in honor of George E. Willis, the award, adminstered by AWS, is given each year to an individual who promoted the advancement of welding internationally by fostering cooperative participation in technology transfer, standards rationalization, and promotion of industrial goodwill. It includes a $2500 honorarium and a certificate.

Guide to AWS Services

550 NW LeJeune Rd., Miami, FL 33126; (800/305) 443-9353; FAX (305) 443-7559; *www.aws.org*
Staff extensions are shown in parentheses.

AWS PRESIDENT

John C. Bruskotter
jbruskotter@eplweb.com
Bruskotter Consulting Services
14254 Hwy. 23, Belle Chasse, LA 70037

ADMINISTRATION

Executive Director
Ray W. Shook.. *rshook@aws.org* ....(210)

Deputy Executive Director
Cassie R. Burrell.. *cburrell@aws.org* .....(253)

Senior Associate Executive Director
Jeff Weber.. *jweber@aws.org* ....(246)

Associate Executive Director Accounting
Gesana Villegas.. *gvillegas@aws.org* .....(252)

Executive Assistant for Board Services
Gricelda Manalich.. *gricelda@aws.org* ....(294)

Administrative Services

Managing Director
Jim Lankford.. *jiml@aws.org* ....(214)

IT Network Director
Armando Campana.*acampana@aws.org*...(296)

Director
Hidail Nuñez.*hidail@aws.org*..............(287)

Database Administrator
Natalia Swain.*nswain@aws.org*............(245)

Human Resources

Director, Compensation and Benefits
Luisa Hernandez.. *luisa@aws.org* ....(266)

Director, Human Resources
Dora A. Shade.. *dshade@aws.org* ....(235)

INT'L INSTITUTE of WELDING

Senior Coordinator
Sissibeth Lopez .. *sissi@aws.org* ....(319)
Provides liaison services with other national and international professional societies and standards organizations.

GOVERNMENT LIAISON SERVICES

Hugh K. Webster. . . *hwebster@wc-b.com*
Webster, Chamberlain & Bean, Washington, D.C., (202) 785-9500; FAX (202) 835-0243. Identifies funding sources for welding education, research, and development. Monitors legislative and regulatory issues of importance to the welding industry.

CONVENTION and EXPOSITIONS

Senior Associate Executive Director
Jeff Weber.. *jweber@aws.org* ....(246)

Corporate Director, Exhibition Sales
Joe Krall.. *jkrall@aws.org* ....(297)
Organizes the annual AWS Welding Show and Convention, regulates space assignments, registration items, and other Expo activities.

Director, Convention and Meeting Services
John Ospina.. *jospina@aws.org* ....(462)

Brazing and Soldering Manufacturers' Committee

Jeff Weber.. *jweber@aws.org* ....(246)

RWMA — Resistance Welding Manufacturing Alliance

Manager
Susan Hopkins.. *susan@aws.org* ....(295)

WEMCO — Welding Equipment Manufacturers Committee

Manager
Natalie Tapley.. *tapley@aws.org* ....(444)

PUBLICATION SERVICES

Department Information ....(275)

Managing Director, Publication Services
Andrew Cullison.. *cullison@aws.org* .....(249)

Welding Journal

Publisher
Andrew Cullison.. *cullison@aws.org* .....(249)

Editor
Mary Ruth Johnsen.. *mjohnsen@aws.org* (238)

National Sales Director
Rob Saltzstein.. *salty@aws.org* ....(243)

Society and Section News Editor
Howard Woodward..*woodward@aws.org* .(244)

Welding Handbook

Editor
Annette O'Brien.. *aobrien@aws.org* .....(303)
Publishes *Welding Journal*, *Inspection Trends*, *Welding Handbook*, *Welding Journal en Español*.

MARKETING COMMUNICATIONS

Director
Ross Hancock.. *rhancock@aws.org* .....(226)

Public Relations Manager
Cindy Weihl..*cweihl@aws.org* ....(416)

Webmaster
Jose Salgado..*jsalgado@aws.org* ....(456)

MEMBER SERVICES

Department Information ....(480)

Deputy Executive Director
Cassie R. Burrell.. *cburrell@aws.org* .....(253)

Director
Rhenda A. Mayo... *rhenda@aws.org* .....(260)
Serves as a liaison between Section members and AWS headquarters. Informs members about AWS benefits and activities.

CERTIFICATION SERVICES

Department Information ....(273)

Managing Director, Certification Operations
John Filippi..*jfilippi@aws.org* ....(222)

Managing Director, Technical Operations
Peter Howe.. *phowe@aws.org* ....(309)
Manages and oversees the development, integrity, and technical content of all certification programs.

Director, Int'l Business & Certification Programs
Priti Jain.. *pjain@aws.org* ....(258)
Directs all int'l business and certification programs. Is responsible for oversight of all agencies handling AWS certification programs.

EDUCATION SERVICES

Managing Director
Dennis Marks.. *dmarks@aws.org* ....(449)

AWS AWARDS, FELLOWS, COUNSELORS

Senior Manager
Wendy S. Reeve.. *wreeve@aws.org* ......(293)
Coordinates AWS awards and AWS Fellow and Counselor nominees.

TECHNICAL SERVICES

Department Information ....(340)

Managing Director
Andrew R. Davis.. *adavis@aws.org* ......(466)
Int'l Standards Activities, American Council of the Int'l Institute of Welding (IIW)

Director, National Standards Activities
John L. Gayler.. *gayler@aws.org* ....(472)
Personnel and Facilities Qualification, Computerization of Welding Information

Manager, Safety and Health
Stephen P. Hedrick.. *steveh@aws.org* ....(305)
Metric Practice, Safety and Health, Joining of Plastics and Composites, Welding Iron Castings

Senior Manager, Technical Publications
Rosalinda O'Neill.. *roneill@aws.org* .....(451)
AWS publishes about 200 documents widely used throughout the welding industry.

Staff Engineers/Standards Program Managers
Annette Alonso.. *aalonso@aws.org* ......(299)
Automotive Welding, Resistance Welding, Oxyfuel Gas Welding and Cutting, Definitions and Symbols, Sheet Metal Welding

Stephen Borrero.. *sborrero@aws.org* .....(334)
Joining of Metals and Alloys, Brazing and Soldering, Brazing Filler Metals and Fluxes, Brazing Handbook, Soldering Handbook

Rakesh Gupta.. *gupta@aws.org* ....(301)
Filler Metals and Allied Materials, Int'l Filler Metals, Instrumentation for Welding, UNS Numbers Assignment

Brian McGrath . *bmcgrath@aws.org* .....(311)
Methods of Inspection, Mechanical Testing of Welds, Welding in Marine Construction, Piping and Tubing

Selvis Morales.....*smorales@aws.org* .....(313)
Welding Qualification, Structural Welding

Matthew Rubin.....*mrubin@aws.org* ......(215)
Aircraft and Aerospace, Machinery and Equipment, Robotics Welding, Arc Welding and Cutting Processes

Reino Starks...*rstarks@aws.org* ....(304)
Welding in Sanitary Applications, High-Energy Beam Welding, Friction Welding, Railroad Welding, Thermal Spray

Note: Official interpretations of AWS standards may be obtained only by sending a request in writing to the Managing Director, Technical Services, Andrew R. Davis, at *adavis@aws.org*.
Oral opinions on AWS standards may be rendered. However, such opinions represent only the personal opinions of the particular individuals giving them. These individuals do not speak on behalf of AWS, nor do these oral opinions constitute official or unofficial opinions or interpretations of AWS. In addition, oral opinions are informal and should not be used as a substitute for an official interpretation.

AWS Foundation

Chairman, Board of Trustees
Gerald D. Uttrachi

Executive Director, AWS
Ray Shook, ext. 210, *rshook@aws.org*

Executive Director, Foundation
Sam Gentry, ext. 331, *sgentry@aws.org*

Solutions Opportunity Squad (SOS)

Corporate Director
Monica Pfarr, ext. 461, *mpfarr@aws.org*

Director
Connie Bowling, ext. 308, *cbowling@aws.org*

General Information
(800) 443-9353, ext. 689; *vpinsky@aws.org*

AWS Foundation, Inc., is a not-for-profit corporation established to provide support for educational and scientific endeavors of the American Welding Society. Further the Foundation's work with your financial support. Call for information.

First Friction Stir Welding Specification Published

AWS D17.3/D17.3M:2010, *Specification for Friction Stir Welding of Aluminum Alloys for Aerospace Applications,* includes the requirements for weldment design, qualification of personnel and procedures, fabrication, and inspection. The well-illustrated document includes 28 figures and six tables. It was developed by the American Welding Society's D17 Committee on Welding in the Aircraft and Aerospace Industries. The section headings are terms and definitions, general requirements, design of weld joints, development and qualification of a welding procedure, welding operator qualification, fabrication, and inspection. The standard uses both U.S. Customary Units and SI International System of Units. The 54-page document lists for $64, $48 for American Welding Society members.

WEX, Ltd. (World Engineering Xchange)
www.awspubs.com
(888) 935-3464 (toll-free U.S. and Canada)

Terminology for Additive Manufacturing Published

ASTM F2792 - 09, *Standard Terminology for Additive Manufacturing Technologies,* is a result of a collaboration between the Society of Manufacturing Engineers and ASTM International. It has been published in an effort to eliminate the confusion over terminology, design, testing methods, materials, and processing differences in the additive manufacturing technology sector. This new standard will allow manufacturers to compare and contrast the performance of different additive processes and enable researchers and process developers to provide repeatable results. The scope reads, "This terminology includes terms, definitions of terms, descriptions of terms, nomenclature, and acronyms associated with additive-manufacturing (AM) technologies in an effort to standardize terminology used by AM users, producers, researchers, educators, press/media and others." The two-page standard may be ordered or downloaded online for $33. For more information or to order, visit the Web site, then enter "ASTM F2792" in the search window.

ASTM International
www.astm.org
(610) 832-9585

AWS Publications Catalog Updated for 2010

The 36-page, full-color *2010 AWS Catalog* offers a pocket-sized reference of all of the Society's publications. The contents are well indexed and detailed to simplify finding the documents you need. New to this edition are ASTM standards for welding, A3.0: 2010, *Standard Welding Terms and Definitions;* A5.29: 2010, *Specification for Low-Alloy Steel Electrodes for Flux Cored Arc Welding;* B1.10: 2009, *Guide for the Nondestructive Examination of Welds;* B5.15: 2010, *Specification for the Qualification of Radiographic Interpreters;* C4.2: 2009, *Recommended Practices for Safe Oxyfuel Gas Cutting Torch Operation;* D1.7: 2010, *Guide for Strengthening and Repairing Existing Structures;* D1.8: 2009, *Structural Welding Code — Seismic Supplement;* and D17.3: 2010, *Specification for Friction Stir Welding of Aluminum Alloys for Aerospace Applications.* The catalog can be downloaded free from the Web site. Click the "Bookstore" tab, then scroll down to locate the catalog. Click the button to download the PDF edition to your computer's desktop.

American Welding Society
www.aws.org
(800/305) 443-9353

Welding and Soldering Equipment Report Updated

The *Welding and Soldering Equipment Manufacturing Industry in the U.S. and Its International Trade (Q4 2009 Edition)* provides the latest information and analysis on the industry's key financial data, costs and pricing, competitive landscape, industry structure, and trends and opportunities. Included are foreign trade statistics on the top 25 countries the United States exported to and their respective export values. The growth in international trade is analyzed in the section covering major trade partners. The 176-page report, with more than 150 charts and tables, includes information on the domestic market, global market, and overseas growth opportunities. Updated quarterly, the report includes sophisticated forecasts to 2013 accounting for the effects of the current economic recession. The list price is $599. For full table of contents information or to order, visit the Web site then enter the document title in the search window.

Research and Markets
www.researchandmarkets.com
U.S.A. FAX: (646) 607-1907 or (646) 964-6609

Laser Proceedings Available Online

The company has recently archived all of its conference abstracts and papers online for reference by academic and indus-

— continued on page 93

New Welding Technologies — The Key to Higher Productivity Ft. Lauderdale, Fla. June 15, 16

This conference will showcase some of the most promising new technologies. Heading the list will be presentations on arc welding, laser beam welding, friction stir welding, resistance welding, and heat treating, all aimed at generous improvements in productivity and quality. Many are already finding applications in various industries. Others are next in line for acceptance. The keynote speaker will be Mike Russell from The Welding Institute in the UK who will discuss many of the new developments in friction stir welding. Discussing the subject from another vantage point will be Jeff Ding from NASA, Huntsville, Ala., who will cover thermal stir processing and ultrasonic stir processing. Matt Short from Edison Welding Institute will describe EWI's efforts in ultrasonic additive manufacture. Another speaker who will address additive manufacture will be Scott Poepel from Joining Technologies. In this case the process involves the use of a laser to apply powder metal. In arc welding, presentations will be made on short-circuiting transfer GMAW and hot wire/cold wire GTAW cladding. Information about the use of fiber lasers for welding, cutting, and cladding will be presented as will some of the newer nondestructive examination technologies. Among them are phased array, computerized X-ray, and time-of-flight testing technologies. The subject of heat treating will also be of interest to the audience. One presentation will address the monitoring that takes place in the surveillance of heat treating.

The World of Energy — Welding's Greatest Challenge San Diego, Calif. August 31, September 1

This conference will examine many avenues, including the important aspects of coal-powered plants, the present and future states of nuclear power, activities in pipeline construction, land-based and offshore work in liquefied natural gas (LNG), solar energy, and wind power. Metals will be emphasized, especially Grade 91 steel, 2205 and the many other duplex stainless steels, and nickel-based alloys. New welding processes are already playing major roles in this arena and cladding is becoming more important than ever. Some of the world's largest operations, like the $10 billion, 3000-MW solar-powered facility in India and the expansive Gorgon gas fields in Australia, are expected to be on the agenda. Much of welding's future depends on industry's ability to adapt and promote its technologies to that cause.

13th Aluminum Welding Conference Seattle, Wash. September (date to be announced)

A panel of aluminum industry experts will survey the state of the art in aluminum welding technology and practice. Attendees will also have the opportunity to network with speakers and other participants, as well as to visit an exhibition showcasing products and services available to the aluminum welding industry.

Aluminum lends itself to a wide variety of industrial applications because of its light weight, high strength-to-weight ratio, corrosion resistance, and other attributes. However, because its chemical and physical properties are different from those of steel, welding of aluminum requires special processes, techniques, and expertise.

2010 FABTECH International & AWS Welding Show Conference Schedule Atlanta, Ga.

National Welding Education Conference November 2

What's New in Weld Consumables? November 2

A low-hydrogen weld deposit is obviously the result of proper use of low-hydrogen filler metals. Much has been done and is still being done in the development of low-hydrogen manual arc electrodes. It has become imperative that the relatively new Grade 91 steel be welded using low-hydrogen filler metals, and much is under way in the development of new chemistries for these electrodes. Many of the gas metal arc welding technologies also produce low-hydrogen weld deposits, as does submerged arc welding. Industry still has to learn to store these electrodes in rod ovens when not in use, a practice not always observed in fabricating plants throughout America. The main thrust here is in ASME code work, shipbuilding, off-highway equipment, and in the chemical industry and power plants. The introduction of duplex stainless steels and the higher-strength versions of same require new filler metals that answer the needs of many plants that deal with corrosion-resistant materials. The roles of heat treatment and shielding gases will also be discussed.

The Tools and Roadways to Effective Weld Repairs November 3

New Developments in Thermal Spray Coatings, Processes, and Applications November 3

This one-day event organized by the American Welding Society and the International Thermal Spray Association will introduce the process and its uses to new potential users with sessions focusing on actual applications and new developments in thermal spray technology. It will include a half-day tutorial on thermal spray fundamentals titled "What Is Thermal Spray" sponsored by the International Thermal Spray Association.

The Welding and Cutting of Pipe and Tubing November 4

For more information, please contact the AWS Conferences and Seminars Business Unit at (800) 443-9353, ext. 462. You can also visit the Conference Department at *www.aws.org/conferences* for upcoming conferences and registration information.

Lincoln Electric Names Two VPs

Richard J. Seif

Anthony Battle

Lincoln Electric Holdings, Inc., Cleveland, Ohio, has appointed **Richard J. Seif** senior vice president, global marketing and product development, and elected **Anthony Battle** as a company officer and vice president, internal audit, with responsibility for Lincoln's worldwide audit process and staff. Battle, who joined the company in 2003, previously was director, internal audit. Seif, with the company since 1971, most recently was senior vice president, global marketing and automation. His new role adds responsibility for directing the company's international product strategy and development programs in its market regions around the world to his current global marketing and automation strategy duties.

Aluminum Assn. President Named to Council Board

Steve Larkin

Steve Larkin, president, Aluminum Association, Arlington, Va., has been elected to serve on the board of directors of the National Association of Manufacturers Council of Manufacturing Associations. The mission of the 225-member council is to promote legislative, regulatory, and economic policies that enhance manufacturing. Larkin previously served on the board as council chair.

Motoman's Elkins Elected to Lead RIA

Dean Elkins, senior general manager of Motoman, Inc., West Carrollton, Ohio, has been elected chairman of Robotic Industries Association (RIA) for 2010. Elkins succeeds **Richard Litt,** founder and chairman of Genesis Systems Group, LLC, Davenport, Iowa, who served as RIA chairman in 2008 and 2009. Elkins has served on the RIA board of directors since 2000, and most recently was first vice chair. The other members of the RIA executive committee include **Jeff Burnstein,** RIA president; **Catherine Morris** of ATI Industrial Automation as first vice chair; **Stuart Shepherd** of KUKA Robotics as second vice chair; and **Michael Kunkle** of Harley-Davidson Motor Co. as secretary and treasurer.

Dean Elkins

Member Milestone

Boes Named Chair of ASTM Copper Alloys Committee

Eric R. Boes

Eric R. Boes, corporate quality engineer for Delta Faucet Co., Indianapolis, Ind., has been named chair of ASTM Committee B05 on Copper and Copper Alloys.

Boes, a member of the AWS Indiana Section, is a member of the AWS A5H Subcommittee on Filler Metals and Fluxes for Brazing. Currently, he is serving a three-year term on the ASTM board of directors, leads Subcommittee B05.91 on Editorial and Publications, and serves as secretary of B05.93 on Terminology.

Committee B05 recognized Boes's contributions to the standardization of copper and copper alloy products with an ASTM International Award of Merit and its accompanying title of ASTM Fellow in 2003. In 2004, Boes became founding chair of Subcommittee B05.94 on Strategic Planning. Boes is user vice chair of Committee A01 on Steel, Stainless Steel, and Related Alloys and a member-at-large on Committee B02 on Nonferrous Metals and Alloys. He participates on a number of other ASTM committees, including B07 on Light Metals and Alloys; E01 on Analytical Chemistry for Metals, Ores and Related Materials; E11 on Quality and Statistics; F17 on Plastic Piping Systems; G01 on Corrosion of Metals; and the Joint ASTM/NACE Committee on Corrosion. He served a term on the ASTM Committee on Standards for which he received a Service Award.

Boes assumed his role at Delta Faucet Co. in 1998 where he is concerned with supplier quality assurance and product development, auditing, metallurgical engineering, technical service, and standards development. He is an ASQ certified quality engineer, a certified quality auditor, a certified quality improvement associate, and a certified manager of quality/organizational excellence. He received his degree in metallurgical engineering from Michigan Technological University in Houghton, Mich.

SME Elects Its First Woman President

Barbara Fossum

The Society of Manufacturing Engineers (SME), Dearborn, Mich., has elected **Barbara M. Fossum** president for the 2010 term. Fossum is a senior research fellow of the IC2 Institute of the University of Texas at Austin where she works in economic development projects worldwide. A member of SME since 1989, she was elected an SME Fellow in 1996. She is the first woman to hold the office of president in the society's 78-year history.

Named as SME president-elect is **Paul D. Bradley.** Bradley is managing director for Peterson Industries, where he has worked since 1980.

Sutor Appoints Audit Committee Chair

Sutor Technology Group, Ltd., Dongbang Town, China, a private manufacturer of finished steel products, has appointed **Gerry Pascale** to serve as an independent director on its board of directors, and also serve as chair of the audit committee. Most recently, Pascale served as president and CEO of SC Financial Group, LLC, where he specialized in advising both U.S. and international clients on valuation, financial modeling, and the responsibilities of publicly traded U.S. companies.

AK Steel Names General Manager Global Steel Sales

Lisa A. Vensel

Lisa A. Vensel has been named general manager of electrical steel sales for AK Steel, West Chester, Ohio, responsible for global sales of its electrical steel products. Vensel, with the company since 1986, most recently served as general manager of manufacturing planning.

Doneski Retires from LORS Machinery

J. Gerard Doneski has retired from LORS Machinery, Inc., Union, N.J., after serving as president since 2000. Doneski, an AWS member since 1989, is affiliated with the AWS New Jersey Section and is a member of the Resistance Welder Manufacturing Alliance (RWMA). Doneski is succeeded as president by former vice president **Edmundo Narvaez.**

Change of Address? Moving?

Make sure delivery of your *Welding Journal* is not interrupted. Contact the Membership Department with your new address information — (800) 443-9353, ext. 217; *smateo@aws.org*.

NEW LITERATURE

— continued from page 90

trial professionals, practitioners, end-users, scientists, engineers, and technicians who could benefit from accessing the latest in laser technology on a wide spectrum of today's most relevant topics. Posted are more than 1500 proceedings and papers that can be quickly located by searching keywords. Proceedings list for $28, $25 for institute members. Visit the Web site, click the "Store" tab, then select "Conference Proceedings" to locate the documents of interest.

Laser Institute of America
www.laserinstitute.org
(407) 380-1553

CAREER OPPORTUNITIES

Top Notch Marketing Director/Manager Available

B2B marketing director looking for employment or contract work. Experienced in manufacturing and related fields, including senior level welding, occupational health and safety and commercial and residential building. Managed all marketing duties for two division manufacturers, including detailed planning through strategy and creative development and implementation. Expertise in corporate and brand identity, advertising, print, packaging, displays, trade shows and websites.

Contact tbarr5@comcast.net or call 847.414.7553 direct.

KISWEL

Kiswel Inc. is looking for a Regional Sales Manager based in the Houston, TX area.

Kiswel Inc. is a worldwide manufacturer of welding filler metals. Our newest plant is in Florence, KY.

We will review resumes from candidates with the following qualifications:

Strong interpersonal relationship skills.
Ten years of technical welding sales experience.
Self starter with the drive to succeed.
Has an established customer base in the Texas, Louisiana, Oklahoma, Arkansas region.

Please e-mail, mail or fax your resume to:

Walter Shields, National Sales Manager/Kiswel USA Inc.
7950 Dixie Highway
Florence, KY 41042
wjshields@kiswelusa.com
Phone: 859-371-0070
Fax: 859-371-5210

SERVICES

ORANGE COAST TESTING INC.
www.orangecoasttesting.com

Digital Radiography
Real-Time Radiography
Wet Film Radiography
Field/Lab Radiography
Penetrant Inspection
Magnetic Particle Inspection
Eddy Current Testing

Pressure Testing
Weld Procedure &
Welder Qualification
Metallurgical &
Hardness Testing
Bend & Tensile Testing
Chemical Analysis
Positive Material Identification

Classroom Training: MT, PT, RT
State Approved: Radiation Safety
Training, Industrial Radiography
& IRRSP (40 hr)

Calibration of Radiation
Detection Equipment

Used Equipment Sale,
Service & Rental

FAA Repair Station
AWS QC-1 CWI (86060911)
PT, MT, RT (Lvl 3) EN473 TUV Cert
NDT Consulting Lvl. 3 Services
Boeing, Pratt Whitney, Honeywell &
ASNT Professional Lvl. 3
General Contractor Lic. #537050

1305 E. Saint Gertrude Pl. Ste J
Santa Ana, CA , USA
Phone (714) 557-5844
Fax (714 557-5461
octi@orangecoasttesting.com

Marketing Communications Adviser
Make Good Brands Better and New Brands Known

Sometimes it just takes an objective outside agent to inspire a well thought-out communications plan with a full understanding of what it takes to execute that plan. Leverage the expertise gained as global communications director for a publicly traded manufacturer of welding and cutting equipment and countless other businesses.

Wesley A. Morgan
Morgan Studio/East
St. Louis, MO
morganwes@aol.com
cell 314 402-1202

EQUIPMENT FOR SALE OR RENT

CERTIFICATION & TRAINING

ADVERTISER INDEX

IFC = Inside Front Cover
IBC = Inside Back Cover
OBC = Outside Back Cover

Visit Our Interactive Ad Index: www.aws.org/ad-index

PROFESSIONAL PROGRAM ABSTRACT SUBMITTAL
Annual FABTECH International & AWS Welding Show
Atlanta, GA - November 2 – 4, 2010

Submission Deadline: March 31, 2010
(Complete a separate submittal for each paper to be presented.)

Primary Author (Full Name):
Affiliation:
Mailing Address:

City: **State/Province** **Zip/Mail Code** **Country:**
Email:

Co-Author(s):

Name (Full Name): Affiliation Address: City: State/Province Zip/Mail Code Country: E-Mail:	Name (Full Name): Affiliation: Address: City: State/Province: Zip/Mail Code: Country: E-Mail:
Name (Full Name): Affiliation: Address: City: State/Province: Zip/Mail Code: Country: E-Mail:	Name (Full Name): Affiliation: Address: City: State/Province: Zip/Mail Code: Country: E-Mail:

Answer the following about this paper
Original submittal? Yes ☐ No☐ Progress report? Yes ☐ No☐ Review paper? Yes ☐ No☐ Tutorial? Yes ☐ No☐
What are the welding/Joining processes used?
What are the materials used?
What is the main emphasis of this paper? Process Oriented ☐ Materials Oriented ☐ Modeling ☐
To what industry segments is this paper most applicable?
Has material in this paper ever been published or presented previously? Yes ☐ No☐
If "Yes", when and where?
Is this a graduate study related research? Yes ☐ No☐
If accepted, will the author(s) present this paper in person? Yes ☐ Maybe ☐ No☐

Keywords: Please indicate the top four keywords associated with your research below

______________________ ______________________
______________________ ______________________

Guidelines for abstract submittal and selection criteria:

- Only those abstracts submitted on this form will be considered. Follow the guidelines and word limits indicated.
- Complete this form using MSWord. Submit electronically via email to techpapers@aws.org

Technical/Research Oriented
- New science or research.
- Selection based on technical merit.
- Emphasis is on previously unpublished work in science or engineering relevant to welding, joining and allied processes.
- Preference will be given to submittals with clearly communicated benefit to the welding industry.

Applied Technology
- New or unique applications.
- Selection based on technical merit.
- Emphasis is on previously unpublished work that applies known principles of joining science or engineering in unique ways.
- Preference will be given to submittals with clearly communicated benefit to the welding industry.

Education
- Innovation in welding education at all levels.
- Emphasis is on education/training methods and their successes.

Papers should address overall relevance to the welding industry.

☑ Check the category that best applies:

☐ Technical/Research Oriented ☐ Applied Technology ☐ Education

Proposed Title (max. 50 characters):
Proposed Subtitle (max. 50 characters):

Abstract:

Introduction (100 words max.) – Describe the subject of the presentation, problem/issue being addressed and its practical implications for the welding industry. Describe the basic value to the welding community with reference to specific communities or industry sectors.

Technical Approach, for technical papers only (100 words max.) – Explain the technical approach, experimental methods and the reasons why this approach was taken.

Results/Discussion (300 words max.) – For technical papers, summarize the results with emphasis on why the results are new or original, why the results are of value to further advance the welding science, engineering and applications. For applied technology and education papers, elaborate on why this paper is of value to the welding community, describe key aspects of the work developed and how this work benefits the welding industry and education.

.

Conclusions (100 words max.) – Summarize the conclusions and how they could be put to use – how and by whom.

NOTE: Abstract must not exceed one page and must not exceed the recommended word limit given above

Note: The Technical Program is not the venue for commercial promotions of a company or a product. All presentations should avoid the use of product trade names. The Welding Show provides ample opportunities for companies to showcase and advertise their processes and products.

Return this form, completed on both sides, to

AWS Education Services
Professional Program 2010
550 NW LeJeune Road
Miami FL 33126
FAX 305-648-1655

MUST BE RECEIVED NO LATER THAN MARCH 31, 2010

POSTER ABSTRACT SUBMITTAL
Annual FABTECH International & AWS Welding Show
Atlanta, GA – November 2-4, 2010
(Complete a separate submittal for each poster.)

Primary Author (Full Name):
School/Company:
Mailing Address:

City:	**State/Province:**	**Zip/Mail Code:**	**Country:**

Email:
Poster Title (max. 50 characters):
Poster Subtitle (max. 50 characters):

Co-Author(s):

Name (Full Name):	Name (Full Name):
Affiliation:	Affiliation:
Address:	Address:
City:	City:
State/Province:	State/Province:
Zip/Mail Code:	Zip/Mail Code:
Country: **Email:**	Country: **Email:**

Poster Requirements and Selection Criteria:

- Only those abstracts submitted on this form will be considered. Follow the guidelines and word limits indicated. Complete this form using MSWord. Submit electronically via email to techpapers@aws.org or print and mail.
- Any technical topic relevant to the welding industry is acceptable (e.g. welding processes & controls, welding procedures, welding design, structural integrity related to welding, weld inspection, welding metallurgy, etc.).
- Submittals that are incomplete and that do not satisfy these basic guidelines will not be considered for competition.

Posters accepted for competition will be judged based on technical content, clarity of communication, novelty/relevance of the subject & ideas conveyed and overall aesthetic impression.

Criteria by category as follows:

(A) Student
- Students enrolled in 2 yr. college and/or certificate programs at time of submittal.
- Presentation need not represent actual experimental work. Rather, emphasis is placed on demonstrating a clear understanding of technical concepts and subject matter.
- Practical application is important and should be demonstrated.

(B) Student
- For students enrolled in baccalaureate engineering or engineering technology programs at the time of submittal.
- Poster should represent the student's own experimental work. Emphasis is place on demonstrating a clear understanding of technical concepts and subject matter.
- Practical application and/or potential relevance to the welding industry is important and should be demonstrated.

(C) Student
- For students enrolled in graduate degree programs in engineering or engineering technology at time of submittal.
- Poster should represent the student's own experimental work. Poster must demonstrate technical or scientific concepts. Emphasis is placed on originality and novelty of ideas presented.
- Potential relevance to the welding industry is important and should be demonstrated.

(D) Professional
- For anyone working in the welding industry or related field.
- Poster must demonstrate technical or scientific concepts. Emphasis is placed on original contributions and the novelty of the presentation.
- Potential relevance to the welding industry is important and should be demonstrated.

(E) High School
- Junior or Senior high school students enrolled in a welding concentration at the time of submittal.
- Presentation should represent technical concepts and application to the welding industry.
- Practical application and creativity are important and should be demonstrated.

Check the category that applies:

☐ (A) Student 2-yr. or Certificate Program ☐ (B) Student 4-yr. Undergraduate ☐ (C) Graduate Student ☐ (D) Professional ☐ (E) High School

Poster Title (max. 50 characters):

Poster Subtitle (max. 50 characters):

Abstract:

Introduction (100 words) – Describe the subject of the poster, problem/issue being addressed and it's practical implications for the welding industry.

Technical Approach & Results (200 words) – Explain the technical approach. Summarize the work that was done as it relates to the subject of the poster.

.

Conclusions (100 words) – Summarize the conclusions and how they could be used in a welding application.

Return this form, completed on both sides, via email to techpapers@aws.org

MUST BE RECEIVED NO LATER THAN April 16, 2010

SUPPLEMENT TO THE *WELDING JOURNAL,* MARCH 2010
Sponsored by the American Welding Society and the Welding Research Council

Effect of Pulse Current on Shrinkage Stress and Distortion in Multipass GMA Welds of Different Groove Sizes

The pulsed gas metal arc process was found to be beneficial in reducing shrinkage stress and distortion in welds on 16-mm-thick HSLA steel

BY P. K. GHOSH, K. DEVAKUMARAN, AND A. K. PRAMANICK

ABSTRACT

Multipass butt joining of 16-mm-thick microalloyed high-strength low-alloy (HSLA) steel plates was carried out by gas metal arc welding (GMAW) with and without pulsed current on different sizes of conventional and narrow grooves. Effect of welding parameters, thermal behavior, and groove size on shrinkage stress, distortion, and bending stress were suitably measured or estimated in appropriate occasions. It was observed that the use of pulsed current with controlled parameters can improve the characteristics of the weld joint with respect to its distortion and stresses, especially in the case of suitable narrow groove welds. Influence of the concerned functions on the weld characteristics studied are appropriately correlated and discussed.

Introduction

The distortion and shrinkage stress giving rise to thermal straining of a weld joint largely results from differential contraction of the weld and neighboring base metal arising out of the cooling cycle of the welding process. The thermal strain produced along the direction of welding results from the longitudinal shrinkage, whereas the strain produced in the component normal to the direction of welding is caused by the transverse shrinkage (Refs. 1–3). A combined stress resulting from the thermal strains reacting to develop internal forces causes weld distortion, commonly observed as bending (Refs. 1, 3). Welding distortion has a negative effect on the dimensional accuracy of assembly as well as external appearance and mechanical properties of the weld joint, which can add additional cost to rectify in commercial practices. Depending upon length of the weld, the linear bending stress may be due to longitudinal shrinkage (Refs. 1, 2). However, the transverse bending always remains significant in reference to plastic upsetting in the zone adjacent to the weld. As a consequence of the in-homogeneous permanent deformation of the weld and its adjacent area, some residual stresses develop in the weld joint (Refs. 4–6). The presence of residual stresses in the weld joint may adversely affect the fatigue, stress corrosion cracking, and fracture mechanics properties of the weld joint depending upon characteristics of the material (Refs. 5–8). Thus, a critical look into the development of shrinkage indulging distortion in welding depending upon the process, procedure, and parameter has always been felt imperative to produce welds of superior quality. A significant amount of experiments and numerical analyses have been carried out for measurement and estimation of shrinkage and deformation of the weld joint, which explore basic understanding of this area (Refs. 9–11). But hardly any systematic work has been reported on estimation and measurement of welding deformation in thick plate with different sizes of weld grooves and welding parameters using the gas metal arc welding (GMAW) process. This is especially true in the case of pulsed current gas metal arc welding (GMAW-P), where the situation becomes more complex due to involvement of a relatively large number of simultaneously interactive pulse parameters, such as mean current (I_m), pulse current (I_p), base current (I_b), pulse time (t_p), base time (t_b), and pulse frequency (f) at different arc voltages (V). However, a solution to the critical control of pulse parameters for the desired operation of the GMAW-P process has been well addressed by considering a summarized influence of pulse parameters defined by a dimensionless hypothetical factor $\phi = (I_b/I_p) \times f t_b$ derived on the basis of energy balance concept (Refs. 5, 8, 12–14) where, t_b is expressed as $[(1/f) - t_p]$. Thus, the control of thermal and metal transfer behavior as well as efficiency of the process, which may largely depend on interactive pulsed parameters, can be accomplished in consideration of the factor ϕ.

In view of the above, an effort has been made in this work to estimate transverse shrinkage stress and bending stress by measurement of transverse shrinkage and distortion under different welding processes, procedures, and parameters during welding of 16-mm-thick controlled-rolled high-strength low-alloy (HSLA) steel plates. At a given heat input and weld groove size the effect of welding processes,

KEYWORDS

Welding Processes
Weld Groove Size
Weld Distortion
Shrinkage Stresses
Bending Stresses
Pulsed Current
GMAW

P. K. GHOSH (prakgfmt@gmail.com), *K. DEVAKUMARAN* (devaa2001@gmail.com), *and A. K. PRAMANICK* (ajitpramanick@gmail.com) *are with Department of Metallurgical & Materials Engineering, Indian Institute of Technology Roorkee, Roorkee, India.*

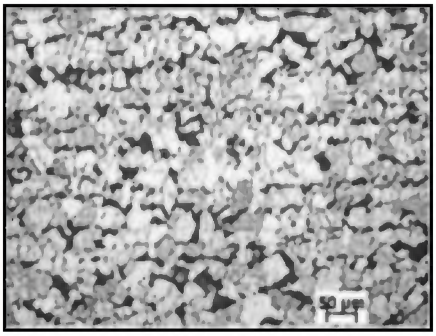

Fig. 1 — Typical microstructure of base metal.

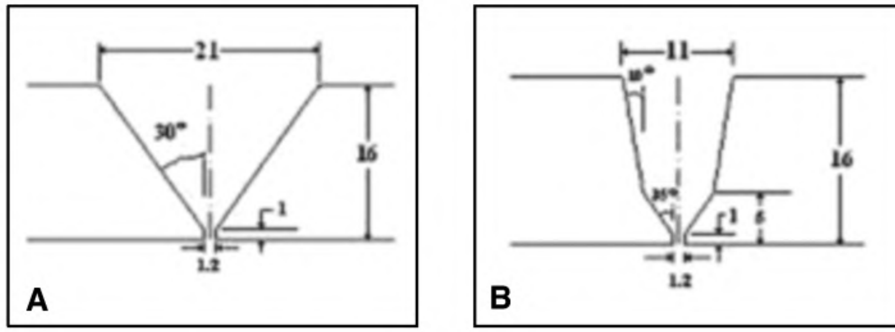

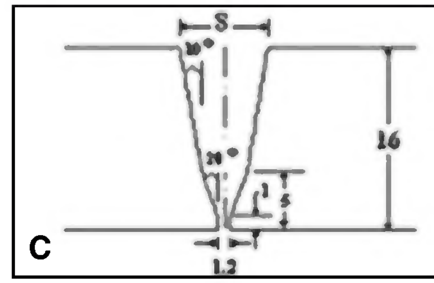

Fig. 2 — Schematic diagram of single (A) V-groove, (B) narrow groove of 11-mm opening (NG-11), and (C) narrow groove of 8-mm opening (NG-8).

procedures, and parameters on variation of estimated shrinkage stresses in the weld deposit causing bending of the weld joint were corroborated by the estimation of bending stresses developed in the weld joint through the measurement of plate bending during welding. This provides an opportunity to physically confirm the effect of various welding processes and procedures on the stress generation in the weld joint. These observations may be beneficial for using the GMAW-P process to produce desired weld quality, and also may form a basis for improvement in its automation.

Experimentation and Analysis

Welding

Controlled-rolled 16-mm-thick micro-alloyed HSLA steel plates of specification SAILMA-350 HI/SA533 grade having the chemical composition given in Table 1 were used in this work. Typical microstructure of the base metal is shown in Fig. 1. The plates in size of 110 × 110 mm were butt joint welded by multipass deposition technique using a single V-groove with an included angle of 60 deg, which conformed to AWS specification (Ref. 15), and also by using a suitably designed narrow groove with 11- and 8-mm groove openings, designated by NG-11 and NG-8, respectively, as schematically shown in Fig. 2A–C. The plates were welded by continuous current gas metal arc welding (GMAW) and pulsed current gas metal arc welding (GMAW-P) processes at direct current electrode positive (DCEP). The welding was performed by using 1.2-mm-diameter mild steel welding wire of specification AWS/SFA 5.18ER-70S-6 under argon (99.97%) gas shielding at a flow rate of 16–18 L/min. During welding the distance between the nozzle to workpiece was maintained within 17–18 mm. A relatively long electrode extension was used to facilitate welding gun manipulation in the narrow groove for weld deposition with satisfactory root and groove wall fusion. Welding of the plates was carried out using semiautomatic welding with a mechanized welding gun travel. The details of the welding parameters used in this work are presented in Table 2. Prior to welding, the plates were preheated to about 125–130°C, and after each pass, the deposit was allowed to cool down to room temperature followed by reheating to maintain an interpass temperature similar to that of preheating for subsequent weld passes. The welding was carried out by rigid clamping of one side of the weld joint, where the other side of it was left free to respond to any distortion resulting from weld deposition, as schematically shown in Fig. 3. During multipass GMA welding, the deflection of the free end of the weld joint per weld pass was measured using a dial gauge having least count of 0.01 mm placed at a given distance of 100 mm from weld centerline (L_C) — Fig. 3. The transverse shrinkage was measured at the center of the weld groove at a given strain length (L_S) (Ref. 2) of 100 mm — Fig. 3. After each pass of welding at any heat input, the transverse shrinkage and deflection of the plate from its initial position as well as the amount of weld deposition were measured, followed by an estimation of transverse shrinkage stress and bending stress using standard mathematical expressions below. The amount of weld deposition was estimated by measuring the weight gain of the plate after each weld pass. To maintain reliability in the study for weld characteristics, experiments were carried out on three to six welds for each welding parameter.

Estimation of Heat Input (Ω)

The heat input (Ω) of GMAW and GMAW-P processes were estimated with consideration of the heat generated by the welding arc as a function of welding or mean current (I or I_m), arc voltage (V), welding speed (S), and its efficiency (η_a) as follows (Refs. 15, 16):

$$\Omega = \frac{\eta_a \times V \times [I(or)I_m]}{S} \qquad (1)$$

The mean current (I_m) of the GMAW-P process may be expressed (Refs. 2, 17) as

$$I_m = \frac{(I_b t_b + I_p t_p)}{(t_b + t_p)} \qquad (2)$$

The η_a of the GMAW process using mild steel filler metal under argon gas shielding has been considered as 70% (Ref. 18) whereas, according to the earlier statment, the η_a in the case of the GMAW-P process operating at different pulsed parameters has been worked out as a function of ϕ and I_m as follows (Ref. 19).

$$\eta_a = 94.52 - 0.118 I_m - 107.61\phi$$

Table 1 — Chemical Composition (wt-%) of Base Metal

C	Si	Mn	Cr	Ni	Cu	Nb+Ti+V	Al	P	S
0.178	0.37	1.57	0.003	—	0.037	0.25 max	0.08	0.012	0.002

$$+ 0.348 I_m \phi \tag{3}$$

Estimation of Total Heat Transferred to Weld Pool (Q_T)

The total heat transfer to the weld pool (Q_T) of the GMAW and GMAW-P processes was estimated (Ref. 12) with consideration of the arc heat transfer to the weld pool (Q_{AW}), heat of the filler metal transferred to the weld pool (Q_f), and welding speed (S) as follows.

$$Q_{rT} = \frac{\left(Q_{AW} + Q_f\right)}{S} \tag{4}$$

The Q_{AW} of the GMAW-P process is estimated as

$$Q_{AW} = (VI_{eff} - \psi\, I_{eff})\eta_a \tag{5}$$

Where ψ and I_{eff} are the effective melting potential at anode and effective current (root mean square value of the pulsed current wave form), respectively. The Q_{AW} of the GMAW process was estimated by substituting I_{eff} of Equation 5 with welding current (I). The I_{eff} is estimated (Refs. 2, 20) by the following expression:

$$I_{eff} = \sqrt{\left[k_p \cdot I_p^2 + \left(1-k_p\right) \cdot I_b^2\right]} \tag{6}$$

Where, the pulse duty cycle is

$$k_p = t_p/t_{pul} \tag{7}$$

The Q_f for the GMAW and GMAW-P processes was estimated (Refs. 12, 13, 17) as follows:

For GMAW: $Q_f = Q_{de}\, m_t$ (8)

For GMAW-P: $Q_f = Q_{de}\, m_t\, f$ (9)

Where m_t is mass of filler metal transferred per pulse (kg), Q_{de} is heat content per unit mass of the welding wire (Jkg^{-1}) at the time of deposition, and f is pulse frequency (Hz). The modeling detail for estimating Q_f of the GMAW-P process has been reported elsewhere (Refs. 12, 13).

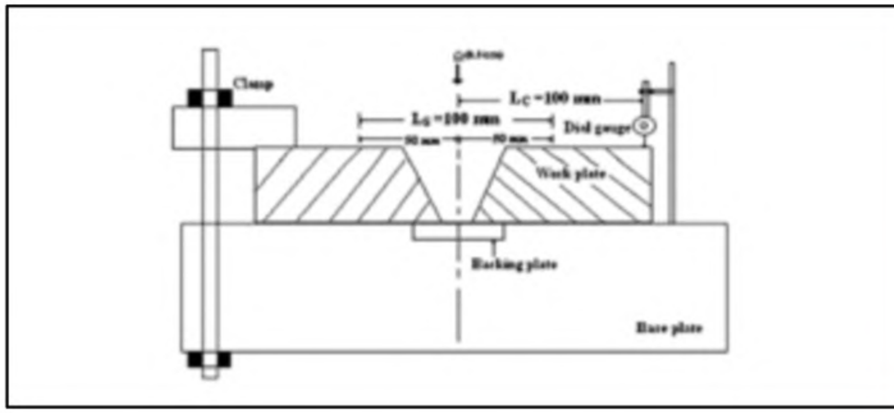

Fig. 3 — Schematic diagram of welding fixture.

The calorimetrically measured values of Q_{de} per unit mass of a deposited droplet in the GMAW process using 1.2-mm-diameter mild steel filler metal and covering the array of globular to spray metal transfer have been reported (Refs. 21, 22) by earlier workers.

Studies on Geometrical Characteristics of Weld Joint

A transverse section of the weld collected from the central part of the weld joint, assuring an area of stable welding, was polished by standard metallographic procedure and etched in 2% nital solution to reveal the weld geometry. Typical macrographs of the weld joints of V-groove, NG-11, and NG-8 produced by using the GMAW and GMAW-P processes are, respectively, shown in Fig. 4A–C and Fig. 5A–C. The geometrical characteristics of weld joint such as total area of weld deposit (A_{WD}) including the joint root opening (G), area of top (A_{TR}) and root (A_{RR}) reinforcement, area of base metal fusion (A_{BF}), and dilution ($\%D_L$) of base plate, as schematically shown in Fig. 6, was measured by graphical method. The estimation of A_{WD}, A_{BF}, and D_L was carried out as follows:

$$A_{WD} = A_{WA} + A_{TR} + A_{BF} + A_{RR} \tag{10}$$

$$A_{BF} = A_{WD} - A_{WA} - A_{TR} - A_{RR} \tag{11}$$

$$\%D_L = \frac{A_{BF}}{A_{WD}} \times 100 \tag{12}$$

Estimation of Transverse Shrinkage Stress

The transverse shrinkage stress (σ_{tr}) developed in the weld joints during their preparation under the varied thermal behaviors of different welding processes, procedures, and parameters was estimated with the help of measured transverse shrinkage (Δ_{tr}) as follows (Refs. 2, 23):

$$\sigma_{tr} \frac{R \times \Delta_{tr} \times E}{L_S} \tag{13}$$

Where E is the Young's modulus of base material (210×10^9 Nm^{-2}), R is the shape factor considered as 0.1 (Ref. 2), and L_S is the straining length of 100 mm (Fig. 3).

Estimation of Bending Stress

The bending stress (σ_b) developed through physically observed distortion of weld joints during their preparation under

Table 2 — Estimated Thermal Behavior of Welding at Different Parameters

Welding Process	Measured Welding Parameters									Estimated Thermal Behavior				
	V	S (cm/min)	$I^{(a)}/I_m$ (A)	ϕ	Pulse Parameters I_p (A)	I_b (A)	f (Hz)	t_b (s)	t_p (s)	Ω (kJ/cm)	Q_{AW} (J/s)	Q_{de} (J/kg)	Q_f (J/s)	Q_T (kJ/cm)
GMAW	24±1	28	240±4[a]	—	—	—	—	—	—	8.28 ± 0.5	2930	1834000	2156	10.89
GMAW-P		24	230±3	0.15	420	104	50	0.012	0.008	7.45 ± 0.4	4294	1755157	2059	13.61
				0.23	440	140	100	0.007	0.003	7.22 ± 0.5	4145	1702060	1996	13.16
			182±4	0.15	372	88	100	0.006	0.004	7.1 ± 0.6	3789	1677370	1731	13.67
				0.23	420	128	50	0.015	0.005	6.77 ± 0.5	3673	1625076	1677	13.38

WELDING RESEARCH

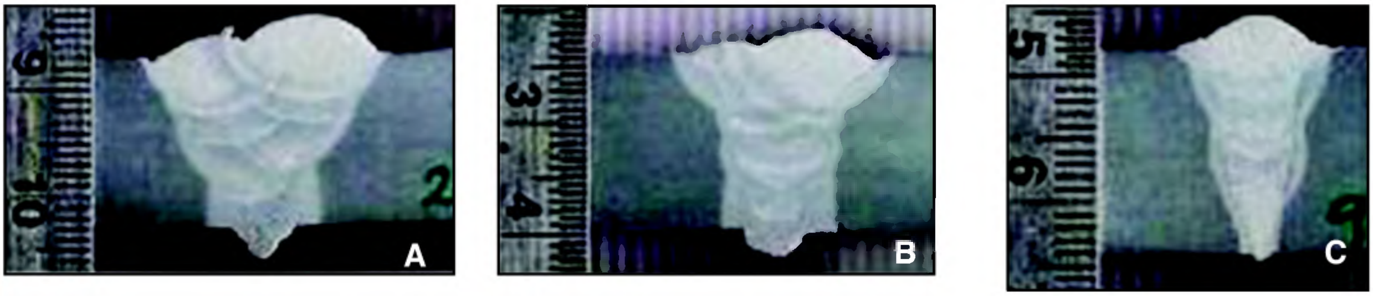

Fig. 4 — Typical macrograph of GMA weld joints having different sizes of weld grooves produced at a given Ω of 8.28 ± 0.5 kJ/cm. A — V-groove; B — NG-11; C — NG-8.

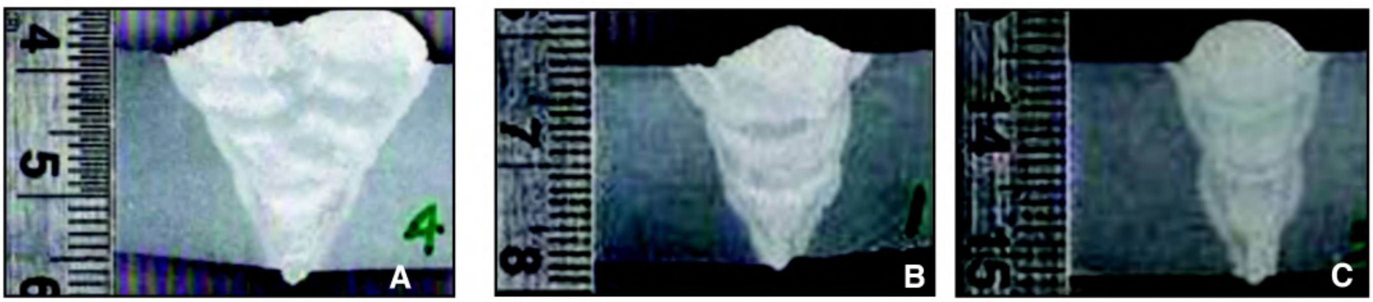

Fig. 5 — Typical macrograph of pulsed GMA weld joints having different sizes of weld grooves produced at a given I_m = 230 ± 3 A, ϕ = 0.23, and Ω = 7.22 ± 0.5 kJ/cm. A — V- groove; B — NG-11; C — NG-8.

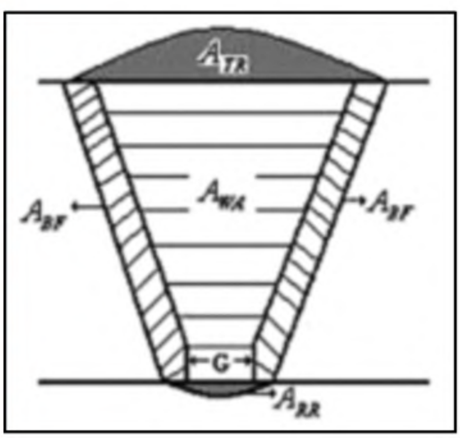

Fig. 6 — Schematic view of different locations of weld joint considered in graphical measurement of area of weld deposit (A_{WD}) and area of base metal fusion (A_{BF}).

varied thermal behavior of different welding processes and procedures was also estimated (Ref. 23) as follows:

$$\sigma_b = \frac{R \times M \times t}{2 \times I^m} \quad (14)$$

Where M is the bending moment, I^m is the moment of inertia, and t is plate thickness. The M and I^m are estimated (Ref. 23) as follows:

$$M = F \times L_C \quad (15)$$

$$I^m = \frac{b_w \times t^3}{12} \quad (16)$$

Where L_C is the distance of the measuring point (dial gauge tip, Fig. 3) from the central axis of the weld joint, and b_w is the plate width. The force (F) generated due to distortion of the plate was estimated (Ref. 23) with the help of measured deflection (δ) by considering it as a case satisfying cantilever beam theory in view of one end of the plate is fixed and other end is free to deflect as explained earlier (Fig. 3).

$$F = \frac{3\delta E I^m}{L_C^3} \quad (17)$$

The F has been appropriately estimated under different welding processes, procedures, and parameters.

Results and Discussion

GMAW

Geometrical Characteristics of Weld Joint

At a given heat input (Ω) of 8.28 ± 0.5 kJ/cm and a similar amount of weld deposition of 2.5 gm/cm per pass, the effect of welding procedure on geometrical characteristics of the weld with respect to its total area of weld deposit (A_{WD}), total area of base metal fusion (A_{BF}), and dilution of base metal (D_L) is shown in Fig. 7A–C. Figure 7A and B shows that the V-groove weld joint gives comparatively higher A_{WD} and A_{BF} than those of narrow groove weld joints. It may be due to the comparatively higher amount of weld deposition required in filling a V-groove weld joint than that of filling a narrow groove weld joint. However, it is further observed that A_{BF} of the comparatively narrower weld joint (NG-8) is relatively higher than that of NG-11, but lower than V-groove weld joints. It is possibly attributed to a comparatively larger amount of base metal fusion on both sides of the groove wall in the root region of the narrower groove width of NG-8 than that of the V-groove and NG-11 welds at a given Ω and similar order of metal deposition. This may have caused more dilution of weld metal with base metal in the NG-8 weld compared to the NG-11 and V-groove weld joints as shown in Fig. 7C. The variation in extent of base metal fusion may also significantly affect the temperature of the weld pool and consequently its solidification behavior, influencing transverse shrinkage and deflection of weld joints.

Transverse Shrinkage Stress

At a given welding current (I) and heat input (Ω) of 230 ± 4A and 8.28 ± 0.5 kJ/cm respectively, resulting in a similar rate of weld deposition (2.5 gm/cm), the effect of the number of weld passes on the cumulative transverse shrinkage (Δ_{tr}) measured during multipass GMA welding in different size grooves is shown in Fig. 8. The variation of results shown in the figure maintains a standard deviation (SD) lying in the range of ± 0.09–0.2. The figure shows that at a given heat input the increase in the number of weld passes enhances the cumulative transverse shrinkage of the weld joint due to increase in the amount of weld metal deposition.

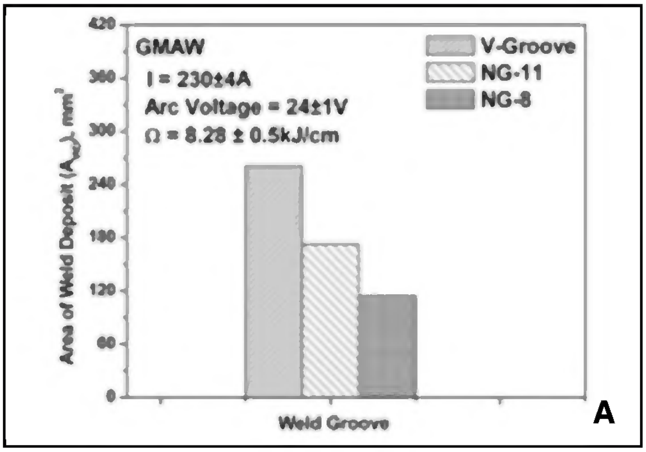

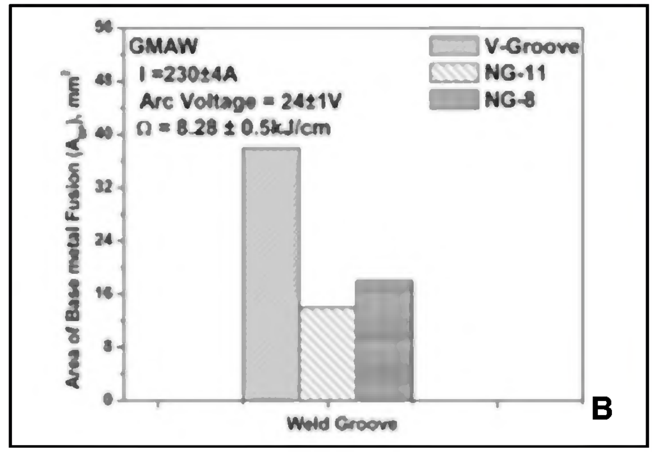

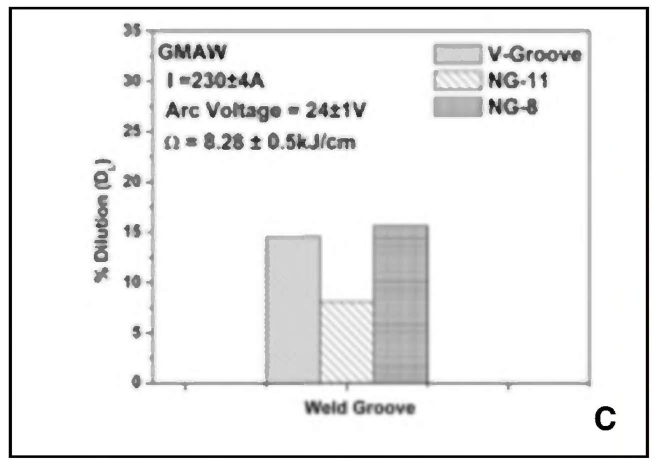

Fig. 7 — At a given Ω, $I_{m\Omega}$, and arc voltage, the effect of different weld grooves. A — Measured area of weld deposit; B — measured area of base metal fusion; C — dilution (%) of GMA weld deposit.

The figure further reveals that at a given Ω, the influence of weld pass on transverse shrinkage appreciably reduces as one proceeds from the root pass to subsequent filling passes. However, at a given weld pass, the cumulative shrinkage of the weld joint was found to be more in the NG-8 weld, but relatively less in the NG-11 weld with respect to that of the V-groove weld. On the basis of these observations, the change in estimated (Equation 13) transverse shrinkage stress (σ_{tr}) with the variation in weld groove size of GMA weld joint was studied and is shown in Fig. 9. The figure shows that the V-groove weld joint has a comparatively higher transverse shrinkage stress than that of the narrow groove weld joints, with the NG-11 weld having the lowest among them.

Deflection and Bending Stress

In line with the earlier observation (Fig. 8) on cumulative shrinkage (Δ_{tr}), the variation in cumulative deflection (δ) of the weld joint in the same range of given Ω and I with the increase in number of weld passes in multipass GMA weld deposition in different weld grooves was found to follow a similar trend as shown in Fig. 10. It was further observed that the δ gradually increases with the progress in number of weld passes from the root pass and at a given number of weld passes, it is relatively more in the NG-8 weld, but less in the NG-11 weld than that of the V-groove weld. On the basis of measured deflection of the weld joints as discussed above, it is a measure of bending of the plate from its neutral axis. At a given order of Ω, the effect of welding procedure on variation of shrinkage stresses in the weld deposit causing distortion of the weld joint can be corroborated by estimation of bending stress developed in the weld joint through measurement of degree of bending of the plate. This may provide a physical confirmation of the effect of welding process on the stress generation in the weld joint. At a given Ω, the effect of welding procedure on estimated bending stress is shown in Fig. 11. It was observed that the estimated bending stress of narrow groove welds is always considerably lower than that of the V-groove weld. However, the estimated bending stress of the NG-11 was found to be marginally lower than that of the NG-8 weld, which is in agreement with the observed trend of estimated transverse shrinkage stress (Fig. 9) with respect to variation in groove size. In this context, it is further noted that the magnitude of the estimated transverse shrinkage lies in close approximation to the bending stress estimated on the basis of distortion generated in weld joints (Figs. 9 and 11) of different groove sizes.

GMAW-P

Geometrical Characteristics of Weld Joint

At a given I_m and close range of Ω of 230 ± 3A and 7.22–7.45 kJ/cm, respectively, and a similar amount of weld deposition of 2.5 gm/cm per pass, the effect of welding procedure using different weld grooves at varied ϕ of 0.15 and 0.23 on weld deposit, base metal fusion, and dilution of weld are shown in Fig. 12A–C. In agreement with those observed in GMAW, it was found that V-groove weld joints showed comparatively higher A_{WD} and A_{BF} but lower dilution than that of the narrow groove NG-8 weld joint. However, the NG-11 weld joint shows comparatively higher A_{WD} but lower A_{BF} and D_L than that of the NG-8 weld joint. It is also interestingly observed that at a given Ω and I_m, the measures of aforesaid geometrical characteristics of all the V-groove, NG-11, and NG-8 weld joints reduce with the increase of ϕ. This may have primarily happened due to a decrease in total heat transfer to the weld pool (Q_T) (Table 2) with the increase of ϕ (Ref. 24). The lowering of Q_T with the increase of ϕ may reduce the weld groove shrinkage and A_{BF}, thus, decreases the A_{WD} and D_L. At a given welding or mean current (I or I_m), arc voltage, and welding speed, the Ω is relatively lower (Table 2) with GMAW-P than the GMAW process due to comparatively low process efficiency (η_a) of the former one causing rather low heat content per unit mass of the filler metal (Q_{de}) at the time of deposition. This behavior considerably reduces the A_{WD}, A_{BF}, and D_L of a pulsed GMA weld compared to the GMA weld at a higher ϕ of 0.23, but at the same I_m, arc voltage, and welding speed, a decrease of ϕ to 0.15 makes the above-mentioned geometrical characteristics of the pulsed GMA weld comparable

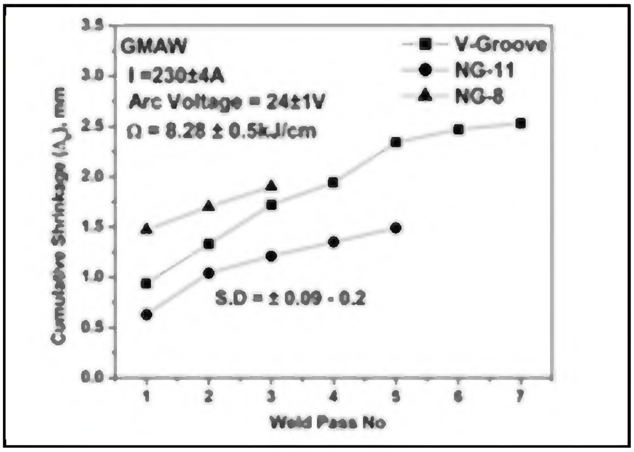

Fig. 8 — The effect of number of weld passes on measured cumulative transverse shrinkage during GMA weld deposition in different sizes of weld grooves at a given Ω, I_m, and arc voltage.

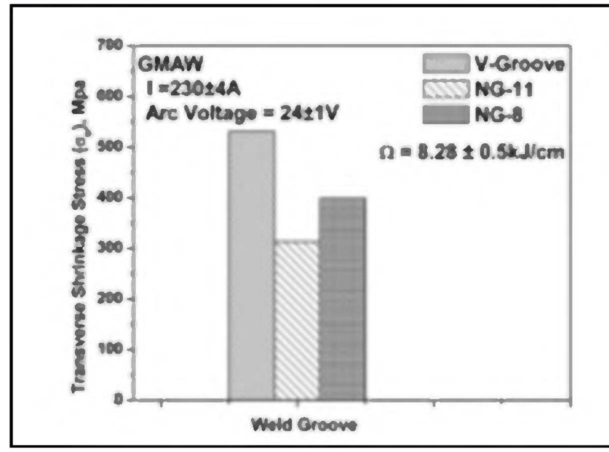

Fig. 9 — The effect of different weld grooves on estimated transverse shrinkage stress in GMA weld joints at a given Ω, I_m, and arc voltage.

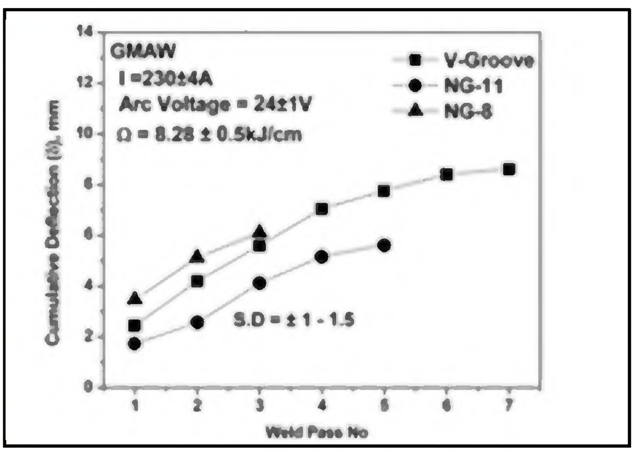

Fig. 10 — The effect of number of weld passes on measured cumulative deflection during GMA weld deposition in different sizes of weld groove at a given Ω, I_m, and arc voltage.

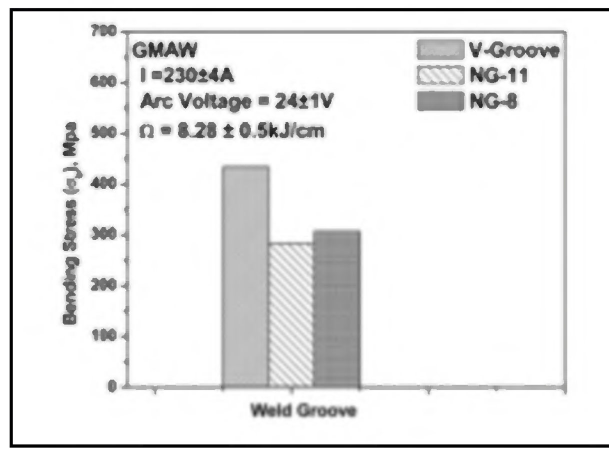

Fig. 11 — The effect of different weld grooves on estimated bending stress of GMA weld joints at a given Ω, I, and arc voltage.

to those of the GMA weld.

Similar observations on the variations in A_{WD}, A_{BF}, and D_L of the narrow groove NG-11 and NG-8 weld joints with a change in pulse parameters were noted as shown in Fig. 13A–C during welding at a relatively lower range of Ω and I_m of 6.77–7.1 kJ/cm and 182 ± 4A, respectively, with a weld deposition of 2.5 gm/cm per pass at different ϕ of 0.15 and 0.23. However, a comparison of Figs. 12 and 13 shows that at a given ϕ the A_{WD}, A_{BF}, and D_L of NG-11 and NG-8 weld joints reduces significantly with a decrease of I_m from 230 to 182 A. This may have primarily happened due to a comparatively low heat content per unit mass of weld deposition (Q_{de}) at lower I_m (Table 2), which can consequently make a difference in transverse shrinkage and deflection of the weld joint.

<u>Transverse Shrinkage Stress</u>

At a given I_m and close range of Ω of 230 ± 3 A and 7.22–7.45 kJ/cm, respectively, at different ϕ of 0.15 and 0.23, the effect of number of weld passes on cumulative transverse shrinkage (Δ_{tr}) measured during multipass pulsed GMA welding in different sized weld grooves is shown in Fig. 14. In order to maintain reliability in comparitive observations on relatively small variations in Δ_{tr}, a statistical analysis was made. In agreement to the earlier observations on cumulative transverse shrinkage of the GMA weld joints at different weld groove sizes (Fig. 8), here also it was observed that the transverse shrinkage of the pulsed GMA weld joints increased with the increase of weld passes. However, at a given weld pass and similar order of I and I_m of about 230 A, the use of GMAW-P in place of GMAW appreciably lowers the transverse shrinkage. In spite of a similar rate of weld deposition (2.5 gm/cm per pass), this may be primarily attributed to the phenomena of heat buildup (Refs. 5, 8, 25) with GMAW-P, which with the influence of interruption in metal deposition results in a comparatively milder thermal behavior of weld joints. At a given weld pass, the cumulative transverse shrinkage of the weld joint was found to be more in the NG-8 weld and relatively less in the NG-11 weld with respect to that of the V-groove weld. But, it was further observed that at a given I_m and Ω, the cumulative transverse shrinkage in all the V-groove, NG-11, and NG-8 weld joints reduced with the increase of ϕ — Fig. 14. This may have primarily happened due to the decrease in total heat transfer to the weld pool (Q_T) (Table 2) with the

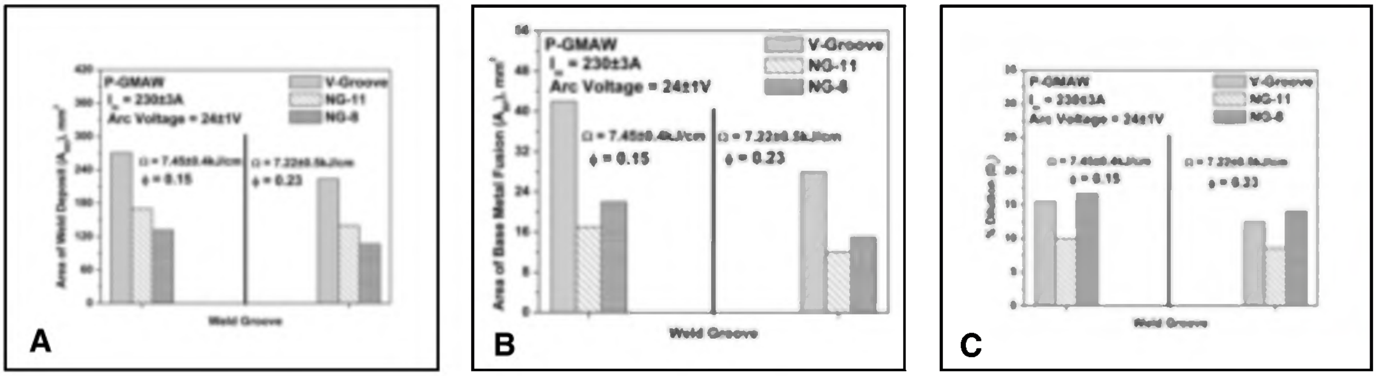

Fig. 12 — The effects of different weld grooves at a given Ω, I_m, and arc voltage of GMAW-P. A — Onmeasured area of weld deposit; B — area of base metal fusion; C — dilution of weld deposit.

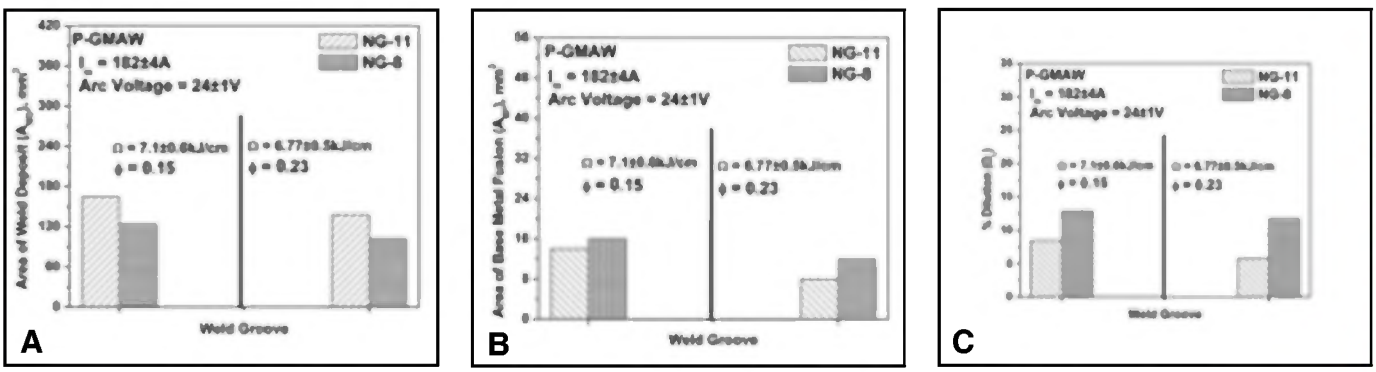

Fig. 13 — The effect of different weld grooves at a given relatively lower range of Ω and I_m of GMAW-P. A — On measured area of weld deposit; B — area of base metal fusion; C — dilution of weld deposit.

increase of ϕ as explained earlier. On the basis of these observations, the change in estimated (Equation 13) transverse shrinkage stress (σ_{tr}) with the variation in weld groove size of pulsed GMA weld joints at different ϕ has been studied as shown in Fig. 15. The figure shows that the V-groove weld joint is having comparatively higher transverse shrinkage stress than that of the narrow groove weld joints, where the NG-11 weld depicts the lowest shrinkage among them. However, Fig. 15 further shows that the transverse shrinkage stress developed in the weld joint prepared by the GMAW-P process with different weld groove sizes is comparatively lower than that observed in GMA weld joints — Fig. 9. This may be primarily attributed to the lower thermal intensity of the pulsed GMA weld due to a reduction in heat buildup in the weld deposit as a result of the interruption in weld deposition under pulsed current. It is interesting to note that at a given I_m and Ω, the transverse shrinkage stress of all the V-groove, NG-11, and NG-8 weld joints reduced with the increase of ϕ — Fig. 15.

At the comparatively lower range of I_m and Ω of 182 ± 4 A and 6.77–7.1 kJ/cm, respectively, the variation in cumulative transverse shrinkage with the increase of weld passes in different sizes of narrow groove welds observed at relatively lower and higher ϕ of 0.15 and 0.23 is shown in Fig. 16. In order to study the effect of I_m at different ϕ on transverse shrinkage of pulsed GMA welds, the observations in Figs. 14 and 16 were compared. It is observed that at a given ϕ, the decrease of I_m from 230 to 182 A at a close range of Ω significantly reduces the transverse shrinkage of both the NG-11 and NG-8 welds, possibly due to a comparatively low heat content per unit mass of the filler wire (Q_{de}) at the time of deposition (Table 2) as explained earlier. The figures further depict that at a given I_m and Ω, the increase of ϕ relatively reduces the transverse shrinkage, especially in narrower weld NG-8. However, at a given weld pass, the cumulative shrinkage of the weld joint was found comparatively more with an NG-8 weld than with an NG-11 weld. On the basis of these observations, the variation in estimated (Equation 13) transverse shrinkage stress (σ_{tr}) with the change in groove size of pulsed GMA weld joints at relatively lower range of I_m and Ω at different ϕ was studied and is shown in Fig. 17. The figure shows that at a given ϕ of 0.15, the NG-8 weld has a comparatively higher transverse shrinkage stress than that of the NG-11 weld, whereas at the higher ϕ of 0.23, an opposite trend is observed. However, Fig. 17 further depicts that the transverse shrinkage stress developed in the weld prepared by GMAW-P using different weld groove sizes is comparatively lower than that observed (Fig. 15) in the pulsed GMA weld produced at relatively higher I_m and Ω of 230 ± 3 A and 7.22–7.45 kJ/cm, respectively. In view of the results depicted in Figs. 9, 15, and 17, the significant role different weld groove sizes plays on transverse shrinkage stress developed during welding is clearly understood, along with some further critical observations at varying Ω, I_m, and ϕ. It is noted that the NG-8 weld gives the lowest transverse shrinkage stress among all the welds of different groove sizes studied,

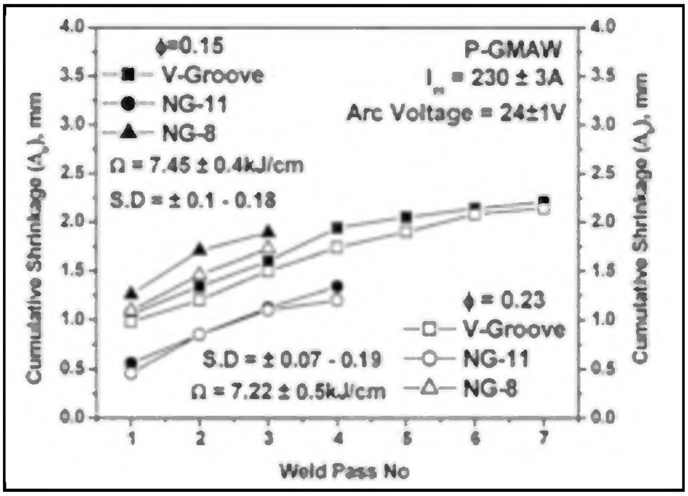

Fig. 14 — *The effect of number of weld passes at a given Ω, I_m, and arc voltage of GMAW-P on measured cumulative transverse shrinkage of weld deposit under different sizes of weld groove at different f.*

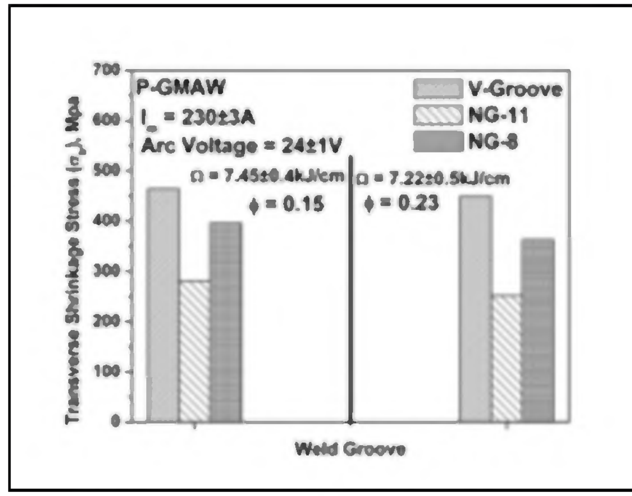

Fig. 15 — *At a given Ω, I_m, and arc voltage of GMAW-P, the effect of different weld grooves on estimated transverse shrinkage stress of weld joints at different ϕ.*

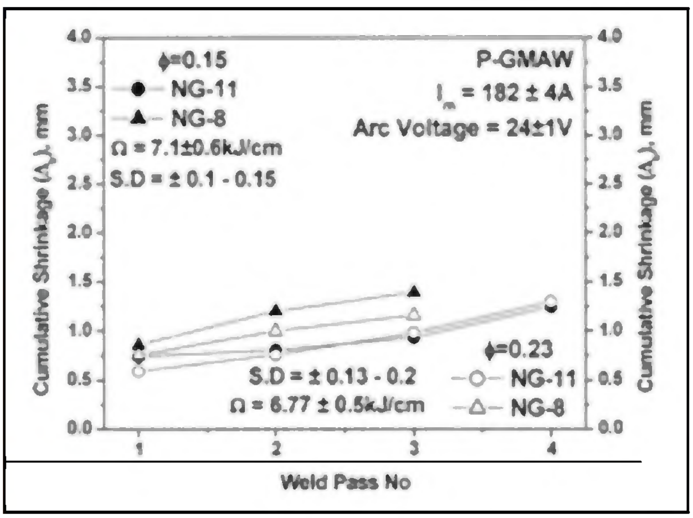

Fig. 16 — *At a relatively lower range of Ω and I_m of GMAW-P, the effect of number of weld passes on measured cumulative transverse shrinkage of weld deposition in different sizes of weld groove at different ϕ.*

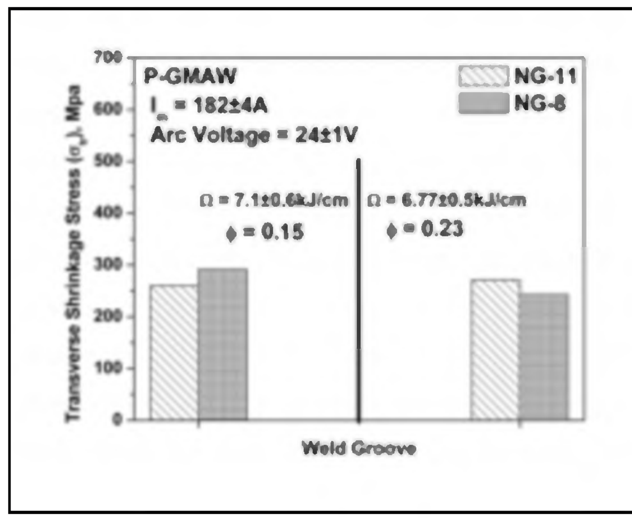

Fig. 17 — *At a relatively lower range of Ω and I_m of GMAW-P, the effect of different weld grooves on estimated transverse shrinkage stress weld joints at different ϕ.*

when a relatively higher ϕ of 0.23 is used at relatively lower range of I_m and Ω of 182 ± 4 A and 6.77–7.1 kJ/cm, respectively. However, to have a clearer understanding of all the phenomena regarding the influence of welding process, procedure, and parameters on transverse shrinkage stress developed during welding, it should be studied further in detail using primarily more variation of ϕ at different groove sizes and plate thicknesses.

Deflection and Bending Stress

In line with earlier observation (Fig. 14) on cumulative shrinkage (Δ_{tr}), the variation in cumulative deflection (δ) of the weld joint with an increase in number of weld passes using GMAW-P in different sized weld grooves in the same range of given Ω, I_m, and ϕ was found to follow a similar trend as shown in Fig. 18 for different ϕ of 0.15 and 0.23, respectively. The figure shows that the deflection developed in the weld joint prepared by GMAW-P, especially at higher ϕ of 0.23, is significantly lower than that observed (Fig. 10) in the GMA weld joint prepared with similar current voltage and heat input. This may be primarily understood by the comparatively lower estimated shrinkage stress (Fig. 15) of the pulsed GMA weld deposit, which generates comparatively lower bending force in the weld joint as a result of relatively smaller heat buildup than that noted (Fig. 11) in the GMA weld joint. However, at a given weld pass, the cumulative deflection of the weld joint was found to be more with the NG-8 weld, but relatively less with the NG-11 weld with respect to the V-groove weld. It was further observed that at a given Ω and I_m, the cumulative deflection of the weld joint with all the V-groove, the NG-11 and NG-8 welds reduced with the increase of ϕ — Fig. 18. At a given range of I_m and Ω of 230 ± 3 A and 7.22–7.45 kJ/cm, respectively, and a different ϕ of 0.15 and 0.23, the effect of welding procedure on bending stress developed in the weld joint estimated (Equation 14) on the basis of

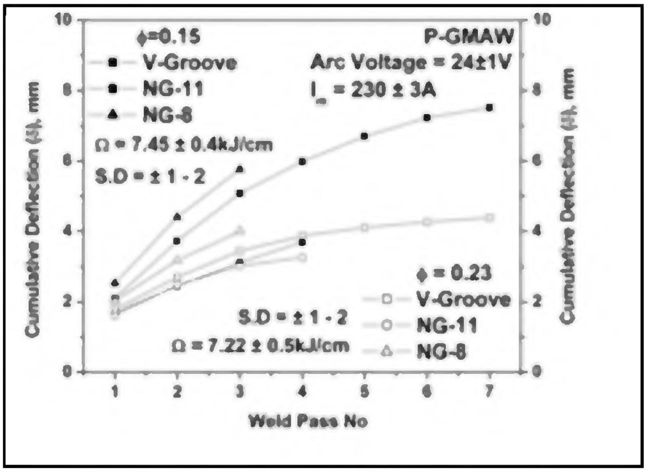

Fig. 18 — At a given Ω, I_m, and arc voltage of GMAW-P, the effect of number of weld passes on measured cumulative deflection of weld deposition under different sizes of weld groove at different ϕ.

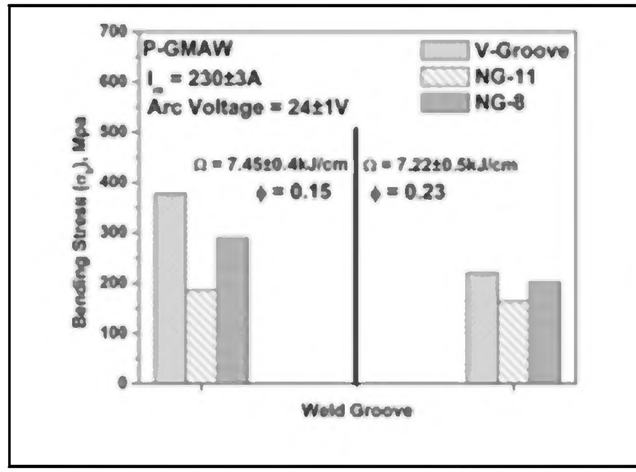

Fig. 19 — At a given Ω, I_m, and arc voltage of GMAW-P, the effect of different weld grooves on estimated bending stress of weld joints at different ϕ.

measured bending during multipass pulsed GMA welding in different weld groove sizes is shown in Fig. 19. It was observed that the estimated bending stress is marginally lower in the NG-11 weld than the NG-8 weld, but in both cases it is considerably lower than the V-groove weld, which follow a similar trend of estimated transverse shrinkage stress — Fig. 15. In this context, it was further corroborated that the estimated transverse shrinkage is well in agreement to the bending stress estimated on the basis of distortion generated in weld joints — Figs. 15 and 19.

At the comparatively lower range of I_m and Ω of 182 ± 4 A and 6.77–7.1 kJ/cm, respectively, the increase in cumulative deflection with the increase of weld passes in different sizes of narrow grooves observed at relatively lower and higher ϕ of 0.15 and 0.23 is shown in Fig. 20. The figure shows a similar trend of variation in transverse shrinkage as explained earlier (Fig. 16) in the case of variation in cumulative shrinkage under the same conditions of welding. But, it is observed that at any ϕ, the cumulative deflection is marginally lower in NG-11 than NG-8 weld. However, it was noted that at a given ϕ, the decrease of I_m from 230 to 182 A reduces the deflection significantly, and the effect is comparatively more with NG-11 weld as revealed in Figs. 18 and 20, respectively. On the basis of these observations, the variation in estimated (Equation 14) bending stress (σ_{tr}) with the change in weld groove size of pulsed GMA weld joints at the relatively lower range of I_m and Ω at different ϕ was studied as shown in Fig. 21. In line with earlier observations on the change in transverse shrinkage stress (Fig. 17) with an increase of ϕ under the same conditions of welding, a similar trend was observed concerning bending stress of the weld joints especially at a lower ϕ of 0.15.

In view of the above discussions regarding transverse shrinkage stress and bending stress generated under different welding processes and weld groove sizes, it is understood that the NG-8 weld develops comparatively higher transverse shrinkage stress and bending stress than the NG-11 weld, especially at higher thermal influence of more Ω or lower ϕ (Refs. 12, 13, 25). This may have happened due to a comparatively larger proportion of groove filling during the root pass deposition in the comparatively narrower groove of NG-8 than NG-11 weld — Fig. 23. Accordingly, the force (F_R) generated in the weld contributing to development of bending moment (M_R) in the groove wall causing its distortion resulting from root pass deposition in different sizes of weld grooves using different welding processes have been estimated by using Equations 15 and 17, respectively. The variation in F_R and M_R with respect to the welding process, groove size, and welding parameters is shown in Fig. 22 A and B, respectively. The figure shows that through the root pass the NG-8 weld generates relatively higher F_R and M_R than that observed with the V-groove and NG-11 weld joints, where the NG-11 weld is the lowest among them. Mechanism of the force (F_R) and bending moment (M_R) generated during root pass weld for V-grooves as well as NG-11 and NG-8 grooves is schematically shown in Fig. 23A–C. Figure 23 clearly shows that a decrease in weld groove size significantly enhances the proportionate filling of the weld groove by root pass, adversely affecting the shrinkage stress and bending stress of the weld. However, this phenomenon has to be studied further in order to exploit the use of narrow groove welding of thick plates with appropriate amount of weld deposition per pass.

Conclusions

The investigation revealed that the use of GMAW-P in multipass butt joining of thick (16-mm) steel plate is beneficial to reduce the shrinkage stress of the weld deposit as well as distortion and bending stress of the weld joint compared to using conventional GMAW at a given welding heat input. During GMAW-P at a given heat input, a control of pulse parameters gives rise to a relatively higher ϕ and further improves the weld characteristics in this regard. The use of a narrow weld groove instead of a conventional V-groove also improves the situation in this respect. The variation of weld characteristics in question with a change of pulse parameters primarily happens due to decrease in total heat transfer (Q_T) to the weld pool as a function of the transfer of arc heat (Q_{AW}) and heat of the filler metal (Q_f) to it with a change in ϕ at a given welding speed (S), where the increase of ϕ decreases the Q_T. The change in said weld characteristics with groove size is largely dictated by the amount of weld deposit. However, the use of a too narrow weld groove, where the root pass can fill the groove more than half of its depth, may restrict the beneficial effect of narrow groove to minimize the bending stress of weld joint.

Acknowledgments

The author thankfully acknowledges

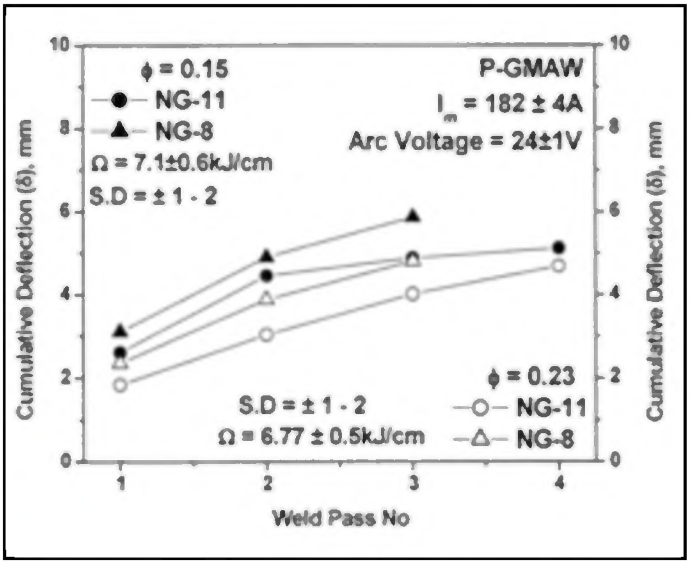

Fig. 20 — At a relatively lower range of Ω and I_m of GMAW-P effect of number of weld passes on measured cumulative deflection of weld deposition in different sizes of weld groove at different ϕ.

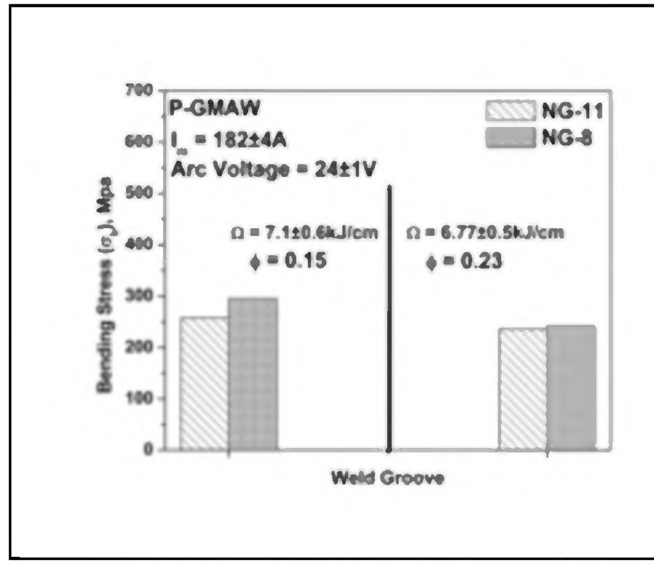

Fig. 21 — At a relatively lower range of Ω and I_m of GMAW-P effect of different weld grooves on estimated bending stress of weld joint at different ϕ.

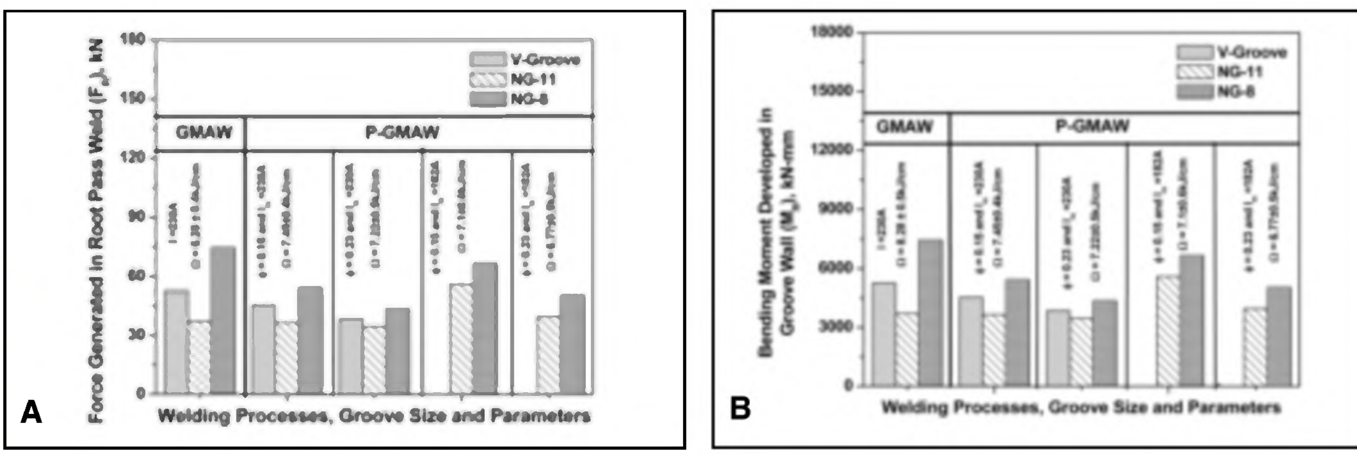

Fig. 22 — Effect of root pass deposition using different welding processes and weld groove sizes. A — Force (F_R) generated in weld; B — bending moment (M_R) developed in groove wall.

the Council of Scientific and Industrial Research (CSIR), India, and for financial support to K. Devakumaran, research associate during analysis of the work.

References

1. Masubuchi, K. 1980. *Analysis of Welded Structures*. New York, Pergamon Press, p. 235.
2. Radaj, D. 1992. *Heat Effects of Welding*. Berlin, Springer-Verlag, p. 182.
3. Parmer, R. S. 1997. *Welding Engineering and Technology*. New Delhi, Khanna Publishers, p. 214.
4. Teng, T. -L., and Chang, P. -H. 2004. Effect of residual stresses on fatigue crack initiation life for butt welded joints. *J Mater Process Technol* (145): 325–335.
5. Ghosh, P. K., and Ghosh, A. K. 2004. Control of residual stresses affecting fatigue life of pulsed current gas metal arc weld of high-strength aluminum alloy. *Met. Mater. Trans. A* (35A): 2439–2446.
6. Deng, D., and Murakawa, H. 2008. Prediction of welding distortion and residual stress in a thin plate butt welded joint. *Comp Mater Sc* (43): 353–365.
7. Deng, D., Murakawa, H., and Liang, W. 2008. Numerical and experimental investigations on welding residual stress in multi pass butt welded austenitic stainless steel pipe. *Comp Mater Sc* (42): 234–244.
8. Kulkarni, S. G., Ghosh, P. K., and Ray, S. 2008. Improvement of weld characteristics by variation in welding processes and parameters in joining of thick wall 304LN stainless steel pipe. *ISIJ Int.* (48): 1560–1569.
9. Sattari Far, I., and Javadi, Y. 2008. Influence of welding sequence on welding distortions in pipes. *Int J Pressure Vessel and Piping* (85): 265–274.
10. Tang, T. L., and Lin, C. C. 1998. Effect of welding conditions on residual stresses due to butt weld. *Int J of Pressure Vessel and Piping* (75): 857–864.
11. Panin, V. N. 2007. Experimental calculation estimation of residual welding distortion in shells of turbine penstocks at hydraulic power stations. *The Paton Welding J*, pp. 7–11.
12. Goyal, V. K., Ghosh, P. K., and Saini, J. S. 2008. Analytical studies on thermal behavior and geometry of weld pool in pulsed current gas metal arc welding. *J Mater Process Technol* (209): 1318–1336.
13. Ghosh, P. K., Goyal, V. K., Dhiman, H. K., and Kumar, M. 2006. Thermal and metal

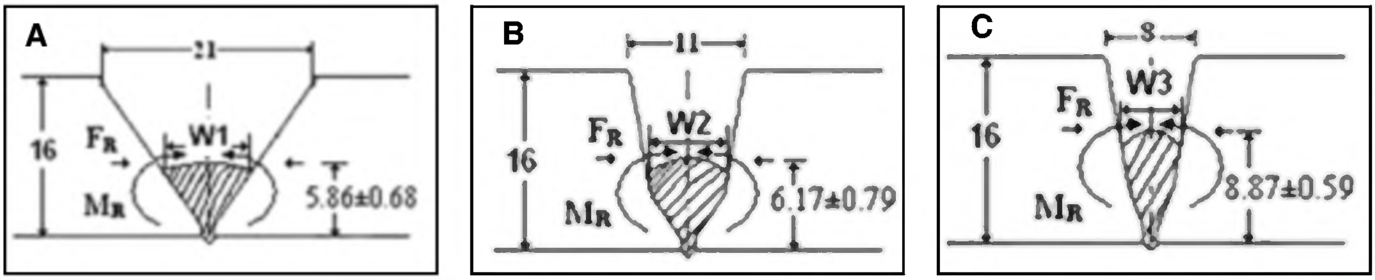

Fig. 23 — Schematic diagram showing the proportionate filling of groove with the root pass contributing to force generated and bending moment developed in weld with different groove sizes. A — V-groove; B — NG-11; C — NG-8.

transfer behavior in pulsed current GMA weld deposition of Al-Mg alloy. *Sci. Technol. Weld. Joining* 11(2): 232–242.

14. Ghosh, P. K., Randhawa, H. S., and Gupta, S. R. 2000. Characteristics of a pulsed-current vertical up gas metal arc weld in steel. *Met. Mater. Trans. A* 31A(12): 2247–2259.

15. Jenney, C. L., and O'Brien, A., eds. 2001. *AWS Welding Handbook*. 9th ed. Vol. 1, p. 110, American Welding Society, Miami, Fla.

16. Messler, Jr., R. W. 1999. *Principles of Welding*. New York, John Willey & Sons, p. 181.

17. Lancaster, J. F. 1984. *The Physics of Welding*. New York, International Institute of Welding, p. 109.

18. Christensen, N., de L. Davis, V., and Gjermundsen, K. 1965. Distribution of temperature in arc welding. *British Welding J* 12(2): 54–75.

19. Ghosh, P. K., Devakumaran, K., and Bhaskarjyoti, S. 2009. Arc efficiency in pulsed current gas metal arc welding of ferrous and non ferrous materials. *Australian Welding J*., 4th quarter.

20. Joseph, A., Harwig, D., Farson, D., and Richardson, R. 2003. Measurement and calculation of arc power and heat transfer efficiency in pulsed gas metal arc welding. *Sci. Technol. Weld. Joining* 8(6): 400–406.

21. Essers, W. G., and Walter, R. 1981. Heat transfer and penetration mechanisms with GMA and plasma GMA welding. *Welding Journal* 60(2): 37-s to 42-s.

22. Ueguri, S., Hara, K., and Komura, H. 1985. Study of metal transfer in pulsed GMA welding. *Welding Journal* 64(8): 242-s to 250-s.

23. Khurmi, R. S. 2002. *Strength of Materials*. 467, India, S. Chand & Company.

24. Goyal, V. K., Ghosh, P. K., and Saini, J. S. 2008. Influence of pulse parameters on characteristics of bead on plate weld deposits of aluminium and its alloy in P-GMA welding process. *Met. Mater. Trans. A* (39A): 3260–3275.

25. Ghosh, P. K., Ravi Reddy, M., and Devakumaran, K. 2006. Distortion and transverse shrinkage stress in butt welds of steel plates under different welding procedure and parameters of GMAW and SMAW processes. *Indian Welding J*. 38(4): 15–23.

Nomenclature

Symbol	Description
A_{WD}	Total area of weld deposit (mm^2)
A_{WA}	Initial area of weld groove (mm^2)
A_{TR}	Area of top reinforcement (mm^2)
A_{BF}	Area of base metal fusion (mm^2)
A_{RR}	Area of root reinforcement (mm^2)
b_W	Plate width (mm)
D_L	Dilution (%)
E	Young's modulus (MPa)
F	Force generated due to distortion (N)
F_R	Force generated at the root pass weld due to distortion (N)
f	Pulse frequency (Hz)
G	Root opening (mm)
I	Welding current (A)
I_{eff}	Effective current (A)
I_p	Peak current (A)
I_b	Base current (A)
I_m	Mean current (A)
I^m	Moment of inertia (mm^4)
k_p	Pulse duty cycle
L_S	Straining length (mm)
L_C	Distance of the measuring point (mm)
M	Bending moment (N-mm)
M_R	Bending moment developed in groove wall (kN-mm)
m_t	Mass of filler metal transferred per pulse (kg)
Q_T	Total heat transferred to weld pool (kJ/cm)
Q_{AW}	Arc heat transferred to the weld pool (Js^{-1})
Q_{de}	Heat content per unit mass of the filler metal at the time of deposition (J kg^{-1})
Q_f	Heat of the filler metal transferred to the weld pool (Js^{-1})
R	Shape factor
S	Welding speed (m/min)
SD	Standard deviation
t	Thickness of the base plate (mm)
t_p	Pulse on time (s)
t_b	Pulse off time (s)
V	Arc voltage (V)
ϕ	Summarized influence of pulse parameters factor
η_a	Arc efficiency (%)
ψ	Effective melting potential at anode (mild steel = 5.8 V)
Ω	Heat input (kJ/cm)
σ_{tr}	Transverse shrinkage stress (MPa)
σ_b	Bending stress (MPa)
Δ_{tr}	Measured transverse shrinkage (mm)
δ	Measured deflection (mm)

SMAW, FCAW, and SAW High-Strength Ferritic Deposits: The Challenge Is Tensile Properties

Consistently satisfying the minimum requirements for tensile strength demanded a rigorous approach to welding parameter selection in order to obtain repeatable results

BY E. S. SURIAN, N. M. RAMINI DE RISSONE, H. G. SVOBODA, R. REP, AND L. A. DE VEDIA

ABSTRACT

The objective of this work was to analyze the influence of chemical composition and welding parameters on microstructure and mechanical properties of medium- and high-strength steel all weld metals of both C-Mn-Ni-Mo and C-Mn-Ni-Mo-Cr ferritic types produced with coated electrodes, flux cored arc welding electrodes, and wire/flux combinations for submerged arc welding and compare these results with AWS requirements. Chemical composition of the deposits was varied and welding parameters were changed in the production of all-weld-metal samples according to the relevant AWS standards of the consumables employed. Tensile properties, hardness, and Charpy-V impact toughness of the all-weld-metal specimens were assessed and metallographic studies were conducted with light microscopy in order to correlate mechanical properties with resulting microstructures. From the analysis of the results it was concluded that achieving the toughness required by the standards was not a problem. On the contrary, consistently satisfying the minimum requirements for tensile strength turned out to be much more difficult, demanding a rigorous approach to welding parameter selection in order to obtain repeatable results. On the other hand, for a given type of weld deposit, the requirements to be met differ according to the welding process employed, thus adding another variable to the difficulties in satisfying the tensile requirements of the different standards.

E. S. SURIAN is with Research Secretariat, Faculty of Engineering, National University of Lomas de Zamora, Buenos Aires, and Deytema-Center of Material Development and Technology, Regional Faculty San Nicolás, National Technological University, San Nicolás, Buenos Aires, Argentina. N. M. RAMINI DE RISSONE is with Deytema-Center of Material Development and Technology, Regional Faculty San Nicolás, National Technological University, San Nicolás, Buenos Aires. H. G. SVOBODA is with Laboratory of Materials and Structures, Department of Mechanical Engineering, University of Buenos Aires. R. REP is with Development Department, Conarco-ESAB, Buenos Aires. L. A. DE VEDIA is with Institute of Technology Professor Jorge A. Sabato, National University of San Martín-CNEA, CIC, Buenos Aires.

Introduction

It is well known that when selecting a C-Mn steel as an alloy base, in order to increase tensile strength it becomes necessary to add to the alloy base alloying elements such as Ni, Mo, and/or Cr, which will modify other properties as well (Refs. 1, 2). It is also known that an increase in tensile strength is frequently accompanied by a loss in toughness, particularly at low temperatures (Refs. 3, 4). For this reason, when designing an electrode formulation starting with C-Mn consumables, the main concern is devoted to maintaining the toughness requirement and the achievement of adequate tensile properties is seldom of concern.

The AWS standards that currently classify the welding consumables for C-Mn-Ni-Mo and C-Mn-Ni-Mo-Cr medium- and high-strength alloy steels are AWS A5.5/A5.5M:2006 (Ref. 5) for shielded metal arc electrodes (SMAW), ANSI/AWS A5.29/A5.29M:2005 (Ref. 6) for flux cored arc welding electrodes (FCAW), and AWS A5.23/A5.23M:2007 (Ref. 7) for flux/wire combinations for submerged arc welding (SAW). According to these standards, all weld metal must meet chemical composition, tensile properties, and Charpy V-notch impact test requirements, among others.

KEYWORDS

High-Strength Steels
Tensile Properties
Weld Metal Impact Toughness
Weld Metal Hardness
Weld Deposit Microstructures
SMAW
FCAW
SAW

Tables 1 and 2 present the all-weld-metal chemical composition and mechanical properties requirements for the consumables employed in this work. It can be observed that there are several types of consumables corresponding to different welding processes that exhibit approximately similar properties, which would suggest the same type of application. Nevertheless, while, for example, manual electrodes of the E11018M type (Ref. 5) require 760 MPa of minimum tensile strength and yield strength in the range 680–760 MPa, for the equivalent tubular electrode E111T5-K3 (Ref. 6), there is a single minimum yield strength requirement of 680 MPa and an extended tensile strength range of 760–900 MPa. The minimum elongation requirement is also different for both consumables: 20% for the manual electrode and 15% for the tubular electrode. On the other hand, the toughness requirements are the same for all these consumables: a mean value of 27 J at –51°C (–60°F) with 20 J minimum for each individual value. It is important to take into account that for SMAW consumables the specifications are military ones, then with special requirements; it is not so for the rest of the welding consumables used.

The general objective of this work was to analyze and compare mechanical properties measured at different stages of the study program on the performance of high-strength ferritic all-weld metals conducted by the authors. The specific objective was to analyze the influence of chemical composition and welding parameters on microstructure and mechanical prop-

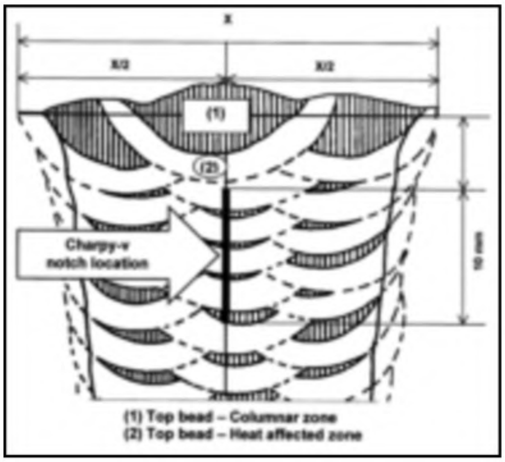

Fig. 1 — Charpy V-notch location.

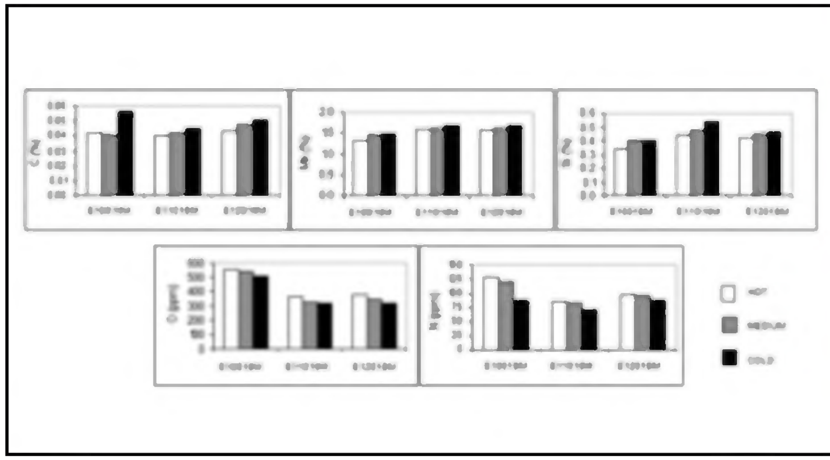

Fig. 2 — Heat input influence on all-weld-metal chemical composition (SMAW).

Table 1 — All-Weld-Metal Chemical Requirements According to the Corresponding AWS Standards: SMAW, A5.5-81 and A5.5-96; FCAW, A5.29-98 and A5.29/29M:2005; SAW, A5.23-97

Process	Classification	C	Mn	P	S	Si	Ni	Cr	Mo
SMAW	E10018M	0.10	0.75–1.70	0.030	0.030	0.60	1.40–2.10	0.35	0.25–0.50
SMAW	E11018M	0.10	1.30–1.80	0.030	0.030	0.60	1.25–2.50	0.40	0.25–0.50
SMAW	E12018M	0.10	1.30–2.25	0.030	0.030	0.60	1.75–2.50	0.30–1.50	0.30–0.55
FCAW	E91T5-K2 E101T5-K3	0.15	0.50–1.75	0.03	0.03	0.80	1.25–2.60	0.15	0.35
FCAW	E111T5-K3	0.15	0.75–2.25	0.03	0.03	0.80	1.25–2.60	0.15	0.25–0.65
FCAW	E120T5-K4	0.15	1.20–2.25	0.03	0.03	0.80	1.75–2.60	0.20–0.60	0.20–0.65
SAW	F9/10/11/12 A6-ECM2-M2	0.10	0.90–1.80	0.030	0.040	0.80	1.40–2.10	0.35	0.25–0.65

Single values are maximums.

Table 2 — All-Weld-Metal Mechanical Property Requirements According to the Corresponding AWS Standards: SMAW, A5.5-81 and A5.5-96; FCAW, A5.29-98 and A5.29/29M:2005; SAW, A5.23-97

Process	Classification	TS (MPa)	YS (MPa)	E (%)	Ch-V at – 51°C
SMAW	E10018M	690	610–690	20	27
SMAW	E11018M	760	680–760	20	27
SMAW	E12018M	830	745–830	18	27
FCAW	E91T5-K2	620–760	540	17	27
FCAW	E101T5-K3	690–830	610	16	27
FCAW	E111T5-K3	760–900	680	15	27
FCAW	E120T5-K4	830–970	750	14	27
SAW	F9A6-ECM2-M2	620–760	540	17	27
SAW	F10A6-ECM2-M2	690–830	610	16	27
SAW	F11A6-ECM2-M2	760–900	680	15*	27
SAW	F12A6-ECM2-M2	830–970	750	14*	27

Single values are minimums.
* Elongation may be reduced by one percentage point for both classifications weld metals in the upper 25% of their tensile strength range.

erties of medium- and high-strength steel all-weld metals. The weld deposits were of the C-Mn-Ni-Mo and C-Mn-Ni-Mo-Cr ferritic types produced with different welding consumables. These consumables were coated electrodes, flux cored arc welding electrodes, and wire/flux combinations for submerged arc welding. The purpose behind this selection was to identify the difficulties to satisfy all-weld-metal mechanical property requirements of the respective AWS standards since, contrary to common perception, achieving the required level of all-weld-metal tensile strength is in general more difficult than impact properties due to the limitations imposed by the standard requirements on yield strength and to some extent, by the required welding procedure variables.

Experimental Procedure

Consumables

The welding consumables employed were SMAW electrodes of the ANSI/AWS A5.5-81 (Ref. 8) E10018M, E11018M, and E12018M commercial type; FCAW electrodes of the ANSI/AWS A5.29-98 (Ref. 9) E91T5-K2/E101T5-K3, E111T5-K3, and E120T5-K4 commercial types; and SAW flux/wire experimental combinations of the ANSI/AWS A5.23-97 (Ref. 10) F9/F10/F11 and F12A6-ECM2-M2 types, with a basic flux of BI = 2.5, Boniszewski basicity index (Ref. 11), for all cases. All-weld-metal test coupons in the flat welding position, varying the welding procedure but always within the requirements of the corresponding standards were produced with all the consumables studied.

For the analysis, results from submerged arc weldments specifically produced for this work were used together with those generated by the authors in previous research on SMAW (Refs. 12, 13) and FCAW (Refs. 14–16) processes.

Weldments

SMAW. With each one of the mentioned consumables, three all-weld-metal test pieces were produced (cold: 1.2–1.5 kJ/mm, medium: 1.6–2.0 kJ/mm, hot: 2.0–2.2 kJ/mm) varying the welding parameters according to Table 3 within the allowable range of the corresponding standard. The specimens were identified as E10018M c (cold), m (medium), h (hot); E11018M c (cold), m (medium), h (hot); and E12018M c (cold), m (medium), h (hot).

FCAW. All-weld-metal test pieces were produced with four FCAW wires varying the shielding gas composition (CO_2 and Ar 80%/CO_2 20%) and the number of passes per layer (2 or 3). Identification: with flux cored wire "Fa," samples FaC2, FaC3, FaA2, and FaA3, with flux cored wire "Fb," samples FbC2, FbC3, FbA2, and FbA3, with flux cored wire F1, samples F1C3 and F1C2, and with flux cored wire F2, only sample F2C3; C meaning CO_2 shielding and A corresponding to 80%Ar/20%CO_2 mixture shielding and the numbers following C or A, depict the number of passes per layer (Table 3).

SAW. Eight all-weld-metal samples were produced employing four 3.2-mm-diameter wires of different composition varying the interpass temperature in one case, in combination with the previously mentioned flux, according to Table 3.

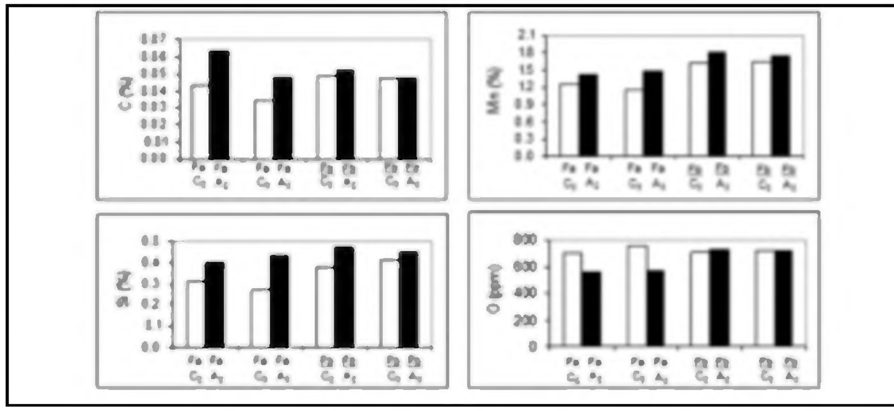

Fig. 3 — Gas shielding type influence on all-weld-metal chemical composition (FCAW).

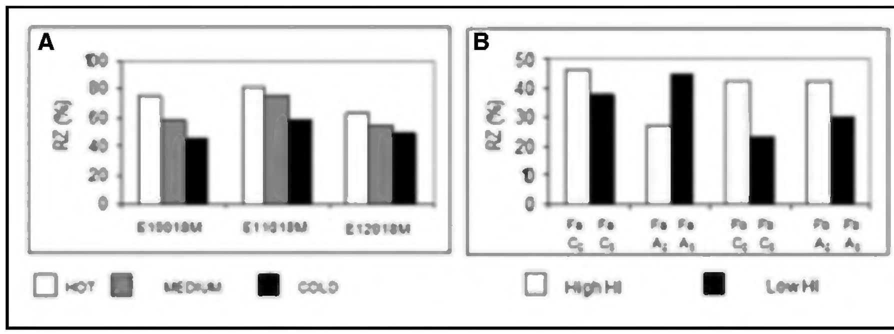

Fig. 4 — Heat input influence on reheated zone: A — SMAW; B — FCAW.

Metallographic Study

Precisely due to the circumstance of having done the welds on different occasions, the methodologies employed for the microstructural analysis differed somewhat. In the case of the manual electrodes, to identify the microconstituents in the columnar zone, the technique previously applied by Evans in his first papers on the C-Mn system (E7018) (Refs. 17, 18) was used, in which the following three components were quantified: acicular ferrite [AF], lamellar components [LC], and primary ferrite [PF]. In the other samples the following constituents were identified: AF, ferrite with nonaligned second phase [FS(NA)], ferrite with aligned second phase [FS(A)], intragranular polygonal ferrite [PF(I)], and grain boundary ferrite [PF(G)], according to IIW Doc. IX-1533-88 (Ref. 19).

This study was conducted on the weld cross section in the columnar zone of the last bead and in the fine and coarse grain heat-affected zones, using Nital 2% and according to the description in Ref. 19. The proportion of reheated zones was measured at 500× in the region corresponding to the location of the Charpy V-notch — Fig. 1. The austenitic primary grain width (PAGW) was measured on the last bead of the samples at 100×. In order to quantify the microconstituents in the columnar zone, 10 fields of 100 points each were taken at 500×.

Mechanical Properties

After radiographic testing of all the test welds, an AWS tensile test specimen was machined out from SMAW, F1CAW (FCAW with F1 wire), F2CAW (FCAW with F2 wire), and SAW test coupons. On the other hand, a Minitrac (Ref. 20) tensile specimen (total length = 55 mm, gauge length = 25 mm, reduced section diameter = 5 mm, ratio of gauge length to diameter = 5:1) from the FaCAW (FCAW with Fa wire) and FbCAW (FCAW with Fb wire) specimens was extracted. A cross section for metallographic analysis, chemical analysis, and hardness survey was also obtained from each coupon as well as five Charpy-V specimens to measure the absorbed energy at –51°C (–60°F).

Table 3 — SMAW, FCAW, and SAW AWS Test Specimen Identification and Welding Parameters Used. SMAW: A5.5-81; FCAW: A5.29-98; SAW: A5.23-97

Sample	Shielding gas	Interpass T (°C)	Number of passes per layer	Total No. of passes/ No. layers	Current (A)	Tension (V)	Welding speed (mm/s)	Heat input (kJ/mm)
E10018M h	—	107	2	14/7	185	25	2.2	2.1
E10018M m	—	101	2	16/8	160	24	2.3	1.7
E10018M c	—	93	2	16/8	140	22	2.4	1.3
E11018M h	—	107	2	14/7	180	25	2.0	2.2
E11018M m	—	101	2	16/8	160	24	1.9	2.0
E11018M c	—	93	2	16/8	140	23	2.0	1.6
E12018M h	—	107	2	14/7	180	23	2.0	2.1
E12018M m	—	101	2	16/8	160	23	2.3	1.6
E12018M c	—	93	2	17/9	130	22	2.4	1.2
AWS req.	**—**	**107 to 93**	**2**	**NS/ 7 to 9**	**NS**	**NS**	**NS**	**NS**
FaC2	CO_2	140–150	2	12/6	238	29	3.6	2
FaC3	CO_2	140–150	3	18/6	193	26	4.1	1.5
FaA2	Ar/CO_2	140–150	2	12/6	234	28	3.4	2.2
FaA3	Ar/CO_2	140–150	3	18/6	197	25	4.6	1.2
FbC2	CO_2	140–150	2	12/6	265	27	4.1	1.9
FbC3	CO_2	140–150	3	18/6	241	26	6.4	1.1
FbA2	Ar/CO_2	140–150	2	12/6	260	27	4	1.9
FbA3	Ar/CO_2	140–150	3	12/6	235	26	5.6	1.2
F1C3	CO_2	150	3	18/6	150	25	2.9	1.3
F1C2	CO_2	150	2	12/6	150	25	1.9	2.0
F2C3	CO_2	150	3	12/6	230	27	6.2	1.0
AWS req.		**150**	**2 or 3**	**NS/ 5 to 8**	**NS**	**NS**	**NS**	**NS**
wire P3-D009	—	150	2	17/8	450	29	7	1.86
wire P4-D010	—	150	2	15/7	450	29	7	1.86
wire P4-D012	—	100	2	17/8	450	29	7	1.86
wire P14-D011	—	150	2	15/7	450	29	7	1.86
wire P18-D018	—	150	2	15/7	450	29	7	1.86
wire P18-D020	—	135	2 and 3	22/8	450	29	8.3	1.60
wire P20-D014	—	150	2	15/7	450	29.5	7	1.90
AWS req.	**—**	**150 ± 15**	**2 or 3**	**NS/ 5 to 8**	**450 ± 25**	**30 ± 1**	**6.0 ± 0.5**	**NS**

c: cold; m: medium; h: hot specimens. The plates were buttered with the same electrode used as filler and preset to avoid restraining. FCAW: electrode extension was 20 mm; gas flow: 20 L/min. SAW: all the wires in diameter 3.2 mm. NS: not specified.

The tensile properties were determined in the as-welded condition at room temperature, after baking the samples at 100°C (212°F) for 48 h to eliminate hydrogen. Toughness was also measured in the as-welded condition.

Results and Discussion

Chemical Composition

Table 4 shows the chemical composition corresponding to the weld metal samples employed to determine mechanical properties. The following can be seen:

SMAW. All the chemical requirements were satisfied for all the welding conditions employed. Figure 2 shows that as the heat input decreased higher values of C,

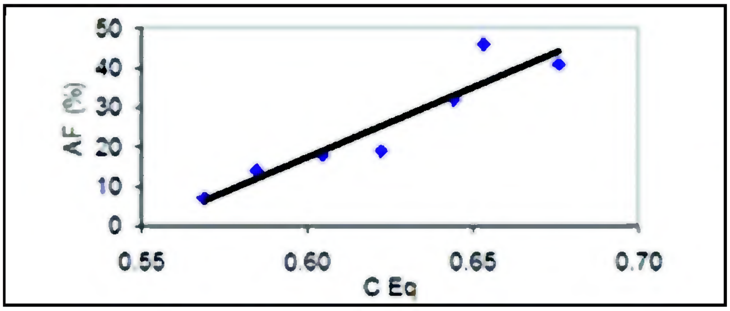

Fig. 5 — Acicular ferrite content vs. carbon equivalent.

$$\left(Ceq = C + \frac{Mn}{6} + \frac{(Cr+Mo+V)}{5} + \frac{(Cu+Ni)}{15}\right)$$

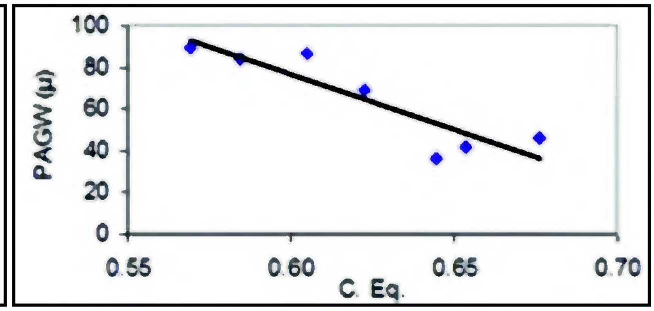

Fig. 6 — Primary austenite grain width vs. carbon equivalent.

$$\left(Ceq = C + \frac{Mn}{6} + \frac{(Cr+Mo+V)}{5} + \frac{(Cu+Ni)}{15}\right)$$

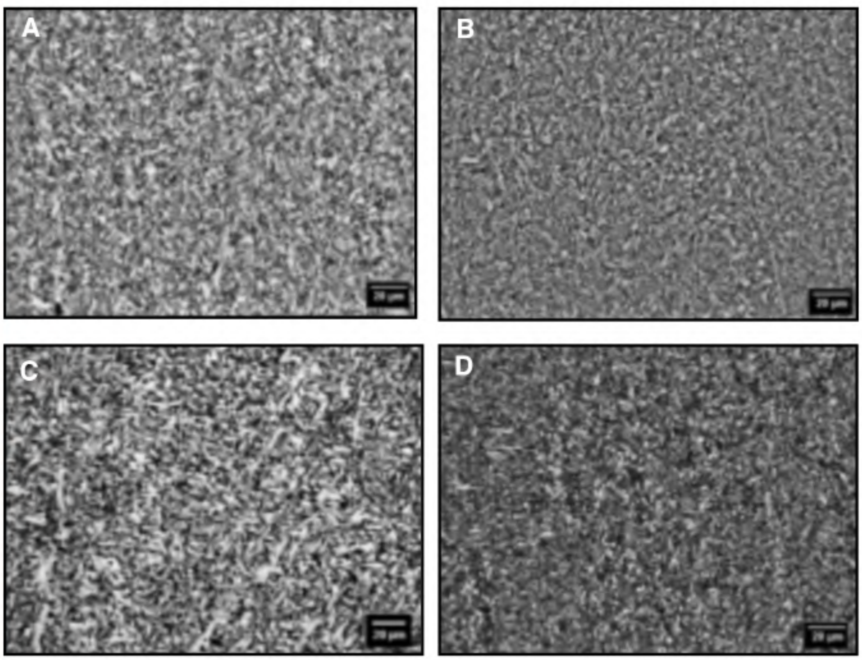

Fig. 7 — Optical micrograph of all-weld-metal columnar zones from different welding processes. A — E12018Mm; B — FbC3; C — F1C2; D — D018. Magnification: 500×. Metallographic etchant: Nital 2.

Mn, and Si were obtained, and oxygen and nitrogen levels were reduced, as previously found (Refs. 21, 22). Here, a trend in the chemical composition to vary with the heat input becomes apparent. Although the differences in the values obtained for the different elements probably were within the measurement error of the method, the systematic variations found could hardly be attributed to this error (around 5%).

FaCAW and FbCAW. Figure 3 shows that with both wires Mn and Si levels increased when the weld was done under the Ar-CO_2 gas mixture shielding, as compared to those made employing CO_2. For both wires Fa and Fb, the oxygen values were higher when using CO_2, this effect being slightly less marked for the wire Fb. The chemical composition of deposits made with wire Fa satisfied the requirements of the E101T5-K3 classification, but presented an excess in Mo according to E91T5-K2. In the case of wire Fb, Mo was above the required maximum, with the rest of the elements in agreement with E111T5-K3.

F1CAW and F2CAW. In the three test pieces the chemical requirements of the applicable standard were satisfied. The oxygen values were similar to those obtained in the manual electrode deposits E11018M and E12018M and significantly less than those corresponding to the weld deposits produced with wires Fa and Fb. The nitrogen values were surprisingly high and no explanation can be offered (Table 4).

SAW. Table 4 shows that the chemical requirements of the applicable standards were satisfied in all cases, these requirements being the same because they corresponded to the same wire M2.

The test conducted can be classified in four groups:

a) Cr free, low C, medium Mn: D009

b) Cr bearing, low C, medium Mn: D011, D012, and D010

c) Cr bearing, medium C, medium Mn: D018 and D020

d) Cr bearing, medium C, high Mn: D014

The oxygen values were similar to those found in the manual electrode deposits E11018M and E12018M and in those corresponding to wires F1 and F2.

Metallographic Study

SMAW. In Table 5A and Fig. 4A, it was observed that increasing the heat input an increase in the area fraction of the reheated zone at the expense of the columnar zone and an increase of the PAGW where this measurement was possible (samples E10018M and E11018M) took place. PAGW measurement in E12018M sample was not carried out due to the almost complete disappearance of the PF(G). For the three samples, the volumes of AF and LC increased at the expense of PF, as previously found by Evans (Ref. 17). It can be seen that the values of AF were much higher than those found in deposits of similar composition made with other welding processes; it is possible that the measurement of AF using this method included also FS(NA). The results of determinations made on two weld deposits from manual electrodes are presented in Table 5B. It is seen that when FS(A) and FS(NA) were discriminated, the AF levels were reduced leading to a percentage of microconstituents similar to those found in the samples of welds made with flux cored and submerged arc welding that were assessed using IIW Document (Ref. 19).

FaCAW and FbCAW. In Table 6 and Fig. 4B it is seen that, similarly to what was found for manual electrodes, an increase in heat input led to an increase in the reheated zone area fraction for both wires, as a general tendency. An increase in the PAGW of the columnar zone was determined when heat input increased for wire Fa, since for wire Fb this measurement was not possible due to the disappearance of PF(G). The values obtained for the PAGW were of the

Table 4 — All-Weld-Metal Chemical Composition from SMAW, FCAW, and SAW (all the elements expressed in wt-% except O and N, which are in ppm)

	C	Mn	P	S	Si	Ni	Cr	Mo	O	N	C. Eq.
E10018M h	0.042	1.34	0.025	0.013	0.34	1.90	0.08	0.38	552	129	0.48
E10018M m	0.041	1.45	0.028	0.013	0.40	1.97	0.08	0.40	538	120	0.51
E10018M c	0.056	1.49	0.029	0.013	0.40	1.97	0.09	0.40	511	87	0.53
Req. AWS	**0.10**	**0.75–1.70**	**0.030**	**0.030**	**0.60**	**1.40–2.10**	**0.35**	**0.25–0.50**	**NS**	**NS**	
E11018M h	0.040	1.58	0.015	0.007	0.44	1.94	0.30	0.33	360	86	0.56
E11018M m	0.042	1.63	0.016	0.007	0.48	1.97	0.31	0.35	321	84	0.58
E11018M c	0.045	1.68	0.016	0.008	0.54	1.98	0.31	0.34	315	71	0.59
Req. AWS	**0.10**	**1.30–1.80**	**0.030**	**0.030**	**0.60**	**1.25–2.50**	**0.40**	**0.25–0.50**	**NS**	**NS**	
E12018M h	0.043	1.56	0.022	0.016	0.43	2.25	0.45	0.43	377	98	0.63
E12018M m	0.048	1.62	0.018	0.013	0.45	2.20	0.43	0.42	349	95	0.63
E21018M c	0.051	1.68	0.020	0.012	0.46	2.13	0.46	0.40	314	87	0.65
Req. AWS	**0.10**	**1.30–2.25**	**0.030**	**0.030**	**0.60**	**1.75–2.50**	**0.30–1.50**	**0.30–0.55**	**NS**	**NS**	
FaC2	0.043	1.26	0.010	0.009	0.31	1.86	0.04	0.45	693	31	0.48
FaC3	0.035	1.14	0.010	0.009	0.27	1.90	0.04	0.45	755	28	0.45
FaA2	0.063	1.43	0.010	0.009	0.40	1.79	0.04	0.42	558	40	0.51
FaA3	0.048	1.47	0.010	0.009	0.43	1.79	0.04	0.44	573	26	0.51
FbC2	0.049	1.62	0.010	0.012	0.38	2.17	0.04	0.71	707	73	0.61
FbC3	0.047	1.66	0.010	0.012	0.41	2.17	0.04	0.73	715	65	0.62
FbA2	0.052	1.81	0.010	0.012	0.47	2.13	0.04	0.70	734	63	0.64
FbA3	0.047	1.76	0.010	0.011	0.45	2.16	0.03	0.71	716	58	0.63
E91T5-K2 req.	**0.15**	**0.50–1.75**	**0.03**	**0.03**	**0.80**	**1.25–2.60**	**0.15**	**0.35**	**NS**	**NS**	
E101T5K3/ E111T5-K3 req.	**0.15**	**0.75–2.25**	**0.03**	**0.03**	**0.80**	**1.25–2.60**	**0.15**	**0.25–0.65**	**NS**	**NS**	
F1C3	0.058	1.80	0.021	0.009	0.49	2.43	0.53	0.48	376	127	0.72
F1C2	0.054	1.64	0.020	0.009	0.40	2.38	0.53	0.47	398	132	0.69
F2C3	0.066	1.86	0.021	0.009	0.56	2.37	0.53	0.47	419	152	0.73
E120T5-K4 req.	**0.15**	**1.20–2.25**	**0.03**	**0.03**	**0.80**	**1.75–2.60**	**0.20–0.60**	**0.30–0.65**	**NS**	**NS**	
D009	0.07	1.63	0.015	0.011	0.18	1.67	0.06	0.52	*	*	0.57
D011	0.05	1.66	0.016	0.012	0.16	1.83	0.21	0.47	360	80	0.58
D012	0.07	1.67	0.017	0.009	0.29	1.89	0.18	0.56	340	70	0.62
D010	0.06	1.66	0.016	0.010	0.29	1.89	0.18	0.53	350	90	0.60
D018	0.10	1.74	0.022	0.008	0.37	1.79	0.20	0.52	*	*	0.65
D020	0.09	1.73	0.023	0.008	0.37	1.80	0.19	0.54	*	*	0.64
D014	0.08	1.86	0.018	0.011	0.43	2.04	0.21	0.54	*	*	0.68
F9/10/11/12A6- ECM2-M2 req.	**0.10**	**0.9–1.8**	**0.030**	**0.040**	**0.80**	**1.4–2.1**	**0.35**	**0.25–0.65**	**NS**	**NS**	

In all cases Sn, As, Sb, Co, Nb, and Al were lower than 0.01 wt-%.
* Without data.

$$Ceq = C + \frac{Mn}{6} + \frac{(Cr + Mo + V)}{5} + \frac{(Cu + Ni)}{15}$$

WELDING RESEARCH

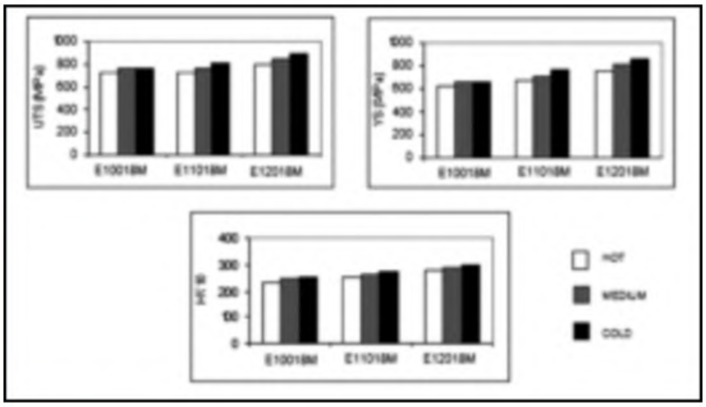

Fig. 8 — Heat input influence on UTS, YS, and HV of SMAW all-weld metal.

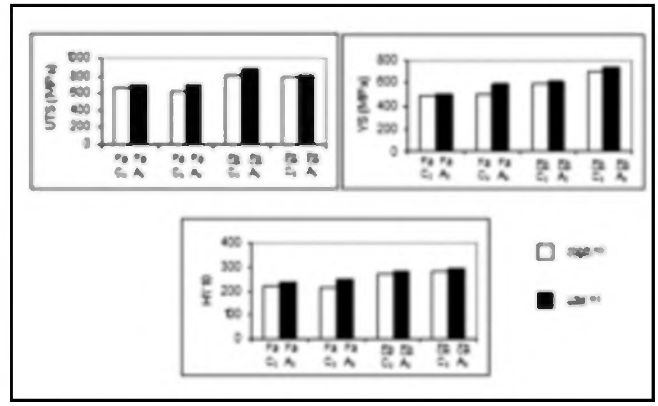

Fig. 9 — Heat input influence on UTS, YS, and HV of FCAW all-weld metal.

same order as those measured in samples E11018M of comparable oxygen content. For wire Fa, under gas mixture shielding, the largest proportion of AF and the lowest values of FS were obtained. For wire Fb under both shielding gases, the AF volumes were similar. In all samples, the main component was ferrite with second phase aligned or not.

The difference found between the microstructures of weld deposits from manual electrodes and flux cored wires may be due to the difference in oxygen level, which was significantly higher in the deposits made with the latter consumables. It is determined that AF increases when the oxygen is reduced within the ranges found in this work (Refs. 23–25).

F1CAW and F2CAW. Table 6 shows that sample F2C3 (low heat input obtained via an increment in the welding current and high welding speed) exhibited a higher columnar zone than F1C3 (low heat input and low welding current) and F1C2 (high heat input and low welding current); no important variation was found between F1C3 and F1C2 due to the difference in heat input. The PAGW was measured only in sample F1C3 (due to the disappearance of PF veins in deposits F2C3 and F1C2), and it was observed that it amounted approximately to deposits from SAW with similar oxygen levels.

Ferrite with second phase was the major component in the deposits of the three flux cored wires, due most certainly to the high Cr and Mo contents (Refs. 26, 27) presenting around 20% acicular ferrite.

SAW. Table 6 shows that the proportions of columnar zone did not disclose any relationship with the welding parameters. The AF values were very low in sample D009, with low C, Mn, and Ni, and without Cr addition, with the highest proportion of PF(G). Chromium-bearing samples D011, D012, and D010, all of which, with low carbon content, presented intermediate values of AF and PF(G). The largest proportion of AF and the lowest values of PF(G) corresponded to samples D018, D020, and D014 with higher C and Mn levels in agreement with previous findings (Refs. 16, 28, and 29). As a general tendency as the Ceq increased, there was an increase of AF (Fig. 5) and a decrease of the PAGW (Fig. 6), probably due to the simultaneous effects of C, Mn, and Cr (Refs. 16, 28–31). Sample D020, welded with low heat input and lower interpass temperature, showed the lowest PAGW due to the fact that the higher cooling rate limited its growing. This sample also showed the highest values of FS(NA).

Figure 7 shows typical columnar zone microstructures achieved with the different welding processes used in this work, where little difference among them can be observed.

Tensile Properties and Hardness

Table 7 presents the tensile properties obtained with all the welding processes employed.

SMAW. Figure 8 shows that for the three electrodes, as the heat input increases, a reduction in hardness, tensile strength, and yield strength took place in agreement with the chemical analysis, as was to be expected (Ref. 21). In all the samples corresponding to the three electrodes, the elongation values were above the required minimum.

In the case of the E10018M electrode, all the tensile and yield strength requirements were satisfied for the three samples, which mean that within the variation imposed on heat input, the change in tensile properties maintained satisfactory values. On the other hand, with electrode E11018M, the required minimums in tensile and yield strengths were not met by the "hot" sample, while yield strength was above the maximum with the "cold" sample. Only with the intermediate sample was it possible to satisfy the standard spec-

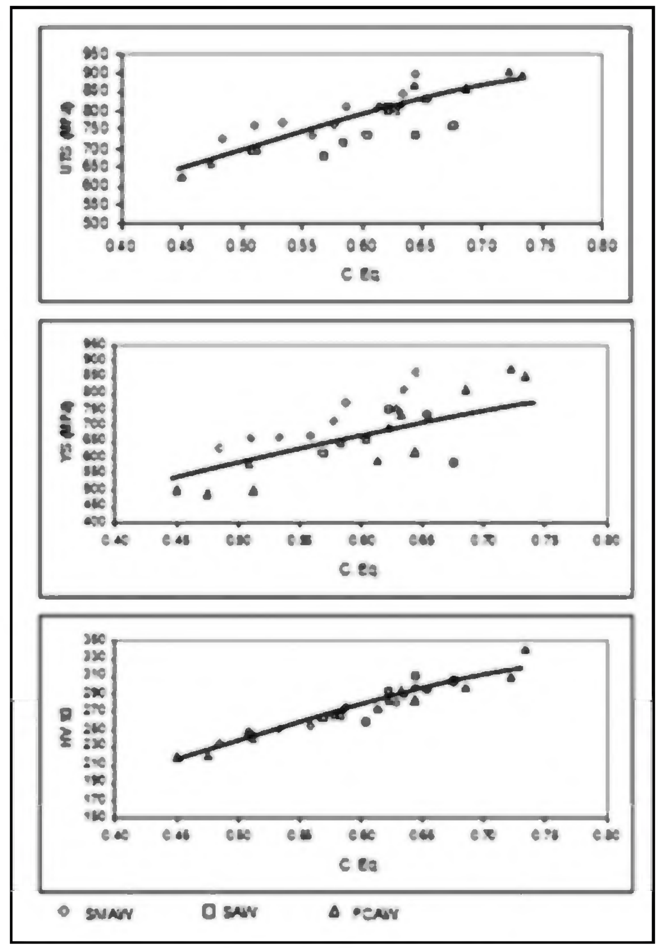

Fig. 10 — Carbon equivalent influence on UTS, YS, and HV of all-weld metals from all the welding processes. $\left(C_{eq} = C + \frac{Mn}{6} + \frac{(Cr + Mo + V)}{5} + \frac{(Cu + Ni)}{15}\right)$

Table 5A — Results of Metallographic Studies, Carried Out According to the Methodology Used by Evans (Refs. 13 and 14)

Electrode	Heat input (kJ/mm)	CZ (%)	RZ (%)	PAGW (μ)	AF (%)	LC (%)	PF (%)
E10018M h	2.1	25	75	140	62	20	18
E10018M m	1.7	42	58	125	58	16	26
E10018M c	1.3	55	45	110	56	14	30
E11018M h	2.2	18	82	216	74	20	6
E11018M m	2.0	25	75	189	72	19	9
E11018M c	1.6	42	58	159	66	17	17
E12018M h	2.1	36	64	(*)	64	26	10
E12018M m	1.6	45	55	(*)	62	25	13
E12018M c	1.2	50	50	(*)	59	22	19

(*) It was not possible to perform this measurement due to the loss of the grain boundary ferrite veins.
CZ: columnar zone; RZ: reheated zone; PAGW: prior austenite grain width.
Columnar zone microconstituents: AF: acicular ferrite; PF: primary ferrite; LC: lamellar components.

Table 5B — Results of Metallographic Studies Performed with the Two Methodologies on the Same Samples

	New results (Ref. 15)					Previous results (Refs. 13 and 14)		
Electrode	AF	PF(G)	PF(I)	FS(A)	FS(NA)	AF	LC	PF
E11018M m	36	8	15	2	39	72	19	9
E12018M m	36	13	14	3	34	62	25	13

AF: acicular ferrite; PF(G): grain boundary ferrite; intragranular polygonal ferrite; FS(A): ferrite with second phase, aligned; FS(NA): ferrite with second phase, not aligned; LC: lamellar components; PF: primary ferrite.

Table 6 — Results of Metallographic Studies Perfomed According to IIW Doc. IX-1533-88 (Ref. 19)

Electrode	Heat input (kJ/mm)	CZ (%)	RZ (%)	PAGW (μ)	AF (%)	FS(A) (%)	FS(NA) (%)	Total FS (%)	PF(G) (%)	PF(I) (%)	Total PF (%)
FaC2	2.0	54	46	107	15	3	53	56	22	7	29
FaC3	1.5	62	38	97	7	15	37	52	36	5	41
FaA2	2.2	73	27	120	45	2	28	30	13	12	25
FaA3	1.2	55	45	103	37	6	31	37	12	14	26
FbC2	1.9	58	42	(*)	26	3	48	51	5	18	23
FbC3	1.1	77	23	(*)	23	4	56	60	3	14	17
FbA2	1.9	58	42	(*)	16	0	75	55	0	9	9
FbA3	1.2	70	30	(*)	21	2	80	82	1	16	17
F1C3	1.3	50	50	46	23	8	63	71			6
F1C2	2.0	47	53	(*)	9	8	73	81			10
F2C3	1.0	70	30	(*)	29	8	53	61			10
D009	1.86	80	20	89	7	11	36	47	37	9	46
D011	1.86	51	49	84	14	26	42	68	12	6	18
D012	1.86	40	60	69	19	23	36	59	13	9	22
D010	1.86	39	61	87	18	13	43	56	16	10	26
D018	1.86	30	70	42	46	4	37	41	3	10	13
D020	1.60	52	48	36	32	2	50	52	2	14	16
D014	1.90	40	60	46	41	9	38	47	5	7	12

(*) It was not possible to perform this measurement due to the loss of the grain boundary ferrite veins.
CZ: columnar zone; RZ: reheated zone; PAGW: prior austenite grain width.
Columnar zone microconstituents: AF: acicular ferrite; PF(G): grain boundary ferrite; PF(I): intragranular polygonal ferrite; PF: primary ferrite; FS: ferrite with second phase; FS(A): ferrite with second phase, aligned; FS(NA): ferrite with second phase, not aligned.

ification. With electrode E12018M, the "hot" sample did not meet the minimum of tensile strength and the "cold" sample exceeded yield strength requirements, while only the intermediate sample satisfied the requirements.

These results show that mechanical properties of the weld metal deposited by the last two electrodes were sensitive to the heat input, which in this case was essentially modified with moderate changes in current intensity (Table 3). It is worth noting that there was a narrow range of heat input within which mechanical property requirements were met. These variations in the heat input influenced the microstructural development, affecting mostly the fraction of reheated zone (RZ) and the PAGW. The hardness level in the RZ was lower than in the columnar zone (CZ), as was observed previously (Ref. 21). This could explain the reduction in tensile and yield strength results as the heat input increased.

Table 7 — All-Weld-Metal Mechanical Property Results

Electrode	Heat Input (kJ/mm)	UTS (MPa)	YS (MPa)	E (%)	Ch-V at –51°C (J)	Average Hardness (HV 10)
E10018M h	2.1	724	632	23.4	53	234
E10018M m	1.7	760	660	22.8	56	246
E10018M c	1.3	766	665	22.0	73	251
AWS req.		**690 min.**	**610–690**	**20 min.**	**27 min.**	**NS**
E11018M h	2.2	734	669	23.1	55	255
E11018M m	2.0	764	715	23.6	60	264
E11018M c	1.6	810	770	21.6	45	275
AWS req.		**760 min.**	**680–760**	**20 min.**	**27 min.**	**NS**
E12018M h	2.1	796	754	20.7	55	281
E12018M m	1.6	845	814	19.7	50	289
E12018M c	1.2	895	866	19.0	54	297
AWS req.		**830 min.**	**745–830**	**18 min.**	**27 min.**	**NS**
FaC2	2.0	661	492	28	74	221
FaC3	1.5	625	502	20	47	219
FaA2	2.2	699	503	20	83	239
FaA3	1.2	699	587	21	59	248
E91T5-K2 req.	**NS**	**620–760**	**540 min.**	**17 min.**	**27 min.**	**NS**
E101T5-K3 req.	**NS**	**690–830**	**610 min.**	**16 min.**	**27 min.**	**NS**
FbC2	1.9	812	594	18.8	61	274
FbC3	1.1	801	695	18.8	44	283
FbA2	1.9	866	619	17.2	54	284
FbA3	1.2	815	739	18.4	64	293
E111T5-K3 req.	**NS**	**760–900**	**680 min.**	**15 min.**	**27 min.**	**NS**
F1C3	1.3	903	879	19	59	309
F1C2	2.0	856	813	20	39	298
F2C3	1.0	891	854	18	31	341
E120T5-K4 req.	**NS**	**830–970**	**750 min.**	**14 min.**	**27 min.**	**NS**
D009	1.86	680	615	23	71	262
D011	1.86	715	647	24	60	265
D012	1.86	810	749	23.4	101	292
D010	1.86	735	655	25	99	258
D018	1.86	827	734	23	66	295
D020	1.60	735	—	5.2	79	310
D014	1.90	757	586	NO	84	305
F9A6-ECM2-M2 req.	NS	**620–760**	**540 min.**	**17 min.**	**27 min.**	**NS**
F10A6-ECM2-M2 req.	NS	**690–830**	**610 min.**	**16 min.**	**27 min.**	**NS**
F11A6-ECM2-M2 req.	NS	**760–900**	**680 min.**	**15 min.**	**27 min.**	**NS**
F12A6-ECM2-M2 req.	NS	**830–970**	**750 min.**	**14 min.**	**27 min.**	**NS**

UTS: ultimate tensile strength, YS: yield strength, E: elongation, Ch-V: Charpy-V impact, NS: not specified.

The welding current range employed (between 140 and 180 A) is within what is usually adopted for these types of electrodes in 4 mm diameter, and it is slightly lower than that indicated in Table A.3 of Annex A of the corresponding AWS Standard (Ref. 1) of 135–185 A. Consequently, if samples are welded using this allowable current range, larger differences in tensile properties will be obtained making the satisfaction of the tensile property standard requirements even more difficult.

FaCAW and FbCAW. Figure 9 shows that for both wires the tensile and yield strengths, as well as hardness values, decreased with the protection of CO_2 with respect to the Ar-CO_2 gas mixture in agreement with the chemical composition. All the samples satisfied the elongation requirements. Nevertheless, for both wires, only with heat inputs of 1.2 kJ/mm or less, the minimum yield strength requirements for E91T5-K2 and E111T5-K3 classifications were reached. In the case of the latter, hardness in CZ was higher than in the RZ. The larger proportion of CZ and the probably lower PAWG could explain the increase in the yield strength for these samples.

With wire Fa, under Ar/CO_2 shielding and with three passes per layer, the requirements of classification E91T5-K2 were satisfied (but not those of chemical composition, since the Mo content was above the maximum specified). The sample welded with two passes per layer under the same shielding did not meet the yield strength requirement. On the other hand, no weld deposit reached the tensile requirements of the E101T5-K3 classification, notwithstanding the fact that they satisfied the chemical requirements. These deposits showed a reasonable variation in tensile strength (625 to 699 MPa), but a large variation in yield strength (492 to 587 MPa), which would prevent the satisfaction of the narrow specification range for the equivalent manual electrode

(E10018M) that in this work met the requirement. For this wire, in order to increase the tensile strength without exceeding the allowed Mo maximum, or alternatively to satisfy the tensile requirements of the E101T5-K3 classification without modification in the Mo content, an increase in Mn could be explored but since this element is furnished not only by the core material but also by the steel sheath, there is danger of overalloying and going over the allowed range of 1.75% Mn with a possible deterioration in toughness. Something similar took place with wire Fb. Tensile requirements of E111T5-K3 classification were satisfied (although not that of chemical composition due to an excess in Mo) with the weld samples produced with both shielding gases using three passes of layer. Tensile strength in these samples resulted somewhat lower, but the yield strength was higher and over the required minimum. The variations found in tensile strength values when the heat input was changed was reasonable (801 to 866 MPa) but the range in yield strength values was ample (594 to 739 MPa). This implies that this consumable would have not met the yield requirements of the equivalent manual electrode E11018M (range = 80 MPa, Table 2).

F1CAW and F2CAW. The three deposits obtained with this process satisfied the tensile requirements of E120T5-K4 classification. Chemical composition was close to the upper limit of the standard, which is at least a potentially dangerous condition taking into consideration the usual variations in composition found in electrode manufacturing. Hardness values were the highest obtained comparing all the processes, in correlation with tensile values.

SAW. Weld D009 did not meet tensile requirements in any of the two classifications: F10A6-ECM2-M2 and F11A6-ECM2-M2. The alloying achieved was not enough for this procedure. It would have satisfied the requirements of F9A6-ECM2-M2 with tensile strength 620 to 760 MPa and yield strength of 540 MPa minimum.

Weld D011 did not satisfy the requirements of classification F11 but did those of F10, which stresses the necessity of Cr additions to raise the tensile strength. However, with the same wire and reducing the interpass temperature without any change in heat input, weld D012, F11 requirements were satisfied. These results confirm that by using lower interpass temperatures higher tensile strength values can be obtained as previously found (Ref. 32).

Weld D010, of a chemical composition close to that of D011, but with higher Si and Mo levels, gave similar results although with somewhat higher tensile and yield strengths.

With weld D018, with higher C and with the same Cr level, the requirements of F11 were comfortably satisfied, so it was necessary to raise the tensile strength through an increase in C content. When using the same wire to weld a test piece with lower heat input, weld D020, the tensile test was invalid and the results were consequently discarded.

With the high-Mn wire, weld D014 failed the tensile test since it broke in a completely brittle manner, with virtually no elongation, and the results were again discarded (although this was not the case for impact test results obtained from these last two samples).

These results show that as was expected, when the alloy content increases, tensile strength also increases up to a point close to the upper limit of the M2 wire specification (see Table 4), thus leaving little margin for further increase via alloy content. The marked sensitivity to welding procedure parameters was also made apparent for these deposits.

As tensile strength increased, hardness increased except for the samples that failed in the tensile test, which presented maximum hardness values.

For all the welding processes, as International Institute of Welding-IIW Carbon Equivalent-CE (Ref. 33) increased, hardness, tensile strength, and yield strength increased, as can be seen in Fig. 10.

Charpy V-Notch Impact Properties

Table 7 shows Charpy-V impact test result obtained at –51°C (–60°F), since this is the specified temperature by the relevant standards for this type of deposits obtained with all the processes considered in this work.

SMAW. Impact test requirements were comfortably satisfied in all cases for any condition of welding procedure. High values of toughness had already been found by the authors in previous studies on this system in which the effects of variations in Mn (Ref. 28), C (Ref. 31), Cr for two different levels of Mn (Ref. 30), and Mo for two different levels of Mn (Ref. 34) were analyzed, and in which it was observed that individually, Mn level could be increased up to 1.7%, C level up to 0.10%, Cr level up to 0.5%, and Mo level up to 0.5% without deleterious effect on toughness.

FaCAW and FbCAW. All the welded samples with these consumables also satisfied comfortably the impact requirements. No single value under the required minimum of 27 J was found. The lowest average value, corresponding to wire Fb, was 44 J, obtained with CO_2 shielding and three passes per layer.

F1CAW and F2CAW. The three welded samples met the standard requirements in spite of the very high tensile values and nitrogen contents exhibited by these welds. The lowest impact value was 27 J for weld F2C3; this result may be related to the highest hardness and percentage of columnar zone measured in this sample.

SAW. All the welds tested comfortably met the minimum impact requirements for any of the welding conditions considered, including those welds that failed to pass the tensile test. The lowest Charpy-V impact value obtained was 53 J in welded samples D011 and D018, and the lowest average was 60 J for weld D011. For all the procedure variations analyzed, the mean and individual impact values obtained in all these samples were within the range reported by the consumables manufacturers (Refs. 35–38).

AWS Standard Requirements Corresponding to the Different Welding Processes for the Same Type of Weld Deposit

Table 2 presents the tensile and impact property requirements for the deposits considered. It can be seen that for a given type of weld metal (see chemical composition, Table 1) the requirements differ notwithstanding the fact that the minimum values for tensile and yield strength are the same but differing the ranges within which these values must fall.

Besides the example mentioned in the Introduction (E11018M and E110T5-K3 or F11A6-ECM2-M2), E12018M and E120T5-K4 or F12A6-ECM2-M2 are also presented. Although it is nearly the same type of deposit according to their chemical composition, the manual electrode must satisfy a minimum of tensile strength (830 MPa) and a yield strength range (745–830 MPa) of only 85 MPa while the FCAW electrode or the combination flux/wire for SAW have a wide range for tensile strength requirement (830–970 MPa) and a single minimum value for yield strength (750 MPa). The same applies to E10018M and E101T5-K3 or F10A6-ECM2-M2.

The elongation requirements are not the same for different processes for the same type of deposit. So, how to interpret that a given welded joint in a welded fabrication requires 20% minimum elongation for manual electrodes and 15% for FCAW tubular electrodes, or for the wire/flux combination in SAW?

On the other side, impact requirements of AWS standards for these type of materials impose exactly the same requirement of 27 J minimum at –51°C (with no single value under 20 J), which as has already been shown, were comfortably satisfied by all the welding processes analyzed.

This implies that if it is necessary to replace SMAW EXXX18M consumables with FCAW or SAW ones, to increase efficiency, in order to produce similar weld metal it may not be advisable to switch to a chemical composition equivalent consumable for SAW or FCAW, due to the less stringent requirements they present. (It is necessary to take into account that the SMAW consumables used in this work respond to military special requirements; military specifications for FCAW and SAW consumables of this type do not exist in AWS filler metal standards.)

Conclusions

From the analysis of the results obtained in this work, it is seen that with all the processes and welding procedures considered, the impact requirements of the appropriate standards were comfortably satisfied. However, fulfillment of tensile properties proved to be much more difficult. In several cases, it became necessary to exceed the specified chemical composition in order to achieve the required minimum tensile strength.

On the other side, it is not only about the manual electrode deposits being more sensitive to heat input as shown by the tensile test results, but rather that for these consumables the tensile requirements are more stringent (as they are military special specifications) than for the equivalent consumables in chemical composition employed in the other welding processes.

An important practical implication of the observed variation of mechanical properties as function of welding conditions is that frequently the welding conditions used for welding procedure qualification are different from those used for consumable classification as required by the different AWS specifications. Therefore, the user of the welding consumable needs to be aware of this fact when selecting consumables and when conducting qualification of the welding procedure.

Acknowledgments

The authors want to express their recognition to Conarco-ESAB Argentina and to Air Liquide Argentina SA-SAF for furnishing the consumables and facilities to weld the test pieces; to the Latin American Welding Foundation, Argentina, for welding facilities, machining, and testing of test pieces; to ESAB, Sweden, to the Centre Téchnique des Applications de Soudure, France; and to Siderca, Argentina, for the O and N determinations; and to ANPCyT, Argentina, for the financial support.

References

1. Pickering, F. B. 1977. *Microalloying' 75.* pp. 9–30. N.Y.: Union Carbide Corp.
2. Widgery, D. J. 1976. Deoxidation practice for mild steel weld metal. *Welding Journal* 55(3): 57-s to 68-s.
3. Dolby, R. E. 1976. Factors controlling weld toughness — The present position, Part 2 — Weld metals. *Research Report 14/1976/M* Abington, UK: The Welding Institute.
4. Abson, D. J., and Pargeter, R. J. 1986. Factors influencing as-deposited strength, microstructure, and toughness of manual metal arc welds suitable for C-Mn steel fabrications. *International Metals Reviews* 31(4): 141–194.
5. AWS A5.5/A5.5M:2006, *Specification for Low-Alloy Steel Electrodes for Shielded Metal Arc Welding*. 2006. Miami, Fla.: American Welding Society.
6. ANSI/AWS A5.29/A5.29M:2005, *Specification for Low-Alloy Steel Electrodes for Flux Cored Arc Welding*. 2005. Miami, Fla.: American Welding Society.
7. AWS A5.23/A5.23M:2007, *Specification for Low Alloy Steel Electrodes and Fluxes for Submerged Arc Welding*. 2007. Miami, Fla.: American Welding Society.
8. AWS A5.5-81, *Specification for Low Alloy Steel Covered Arc Welding Electrodes.* 1981. Miami, Fla.: American Welding Society.
9. ANSI/AWS A5.29-98, *Specification for Low-Alloy Steel Electrodes for Flux Cored Arc Welding.* 1998. Miami, Fla.: American Welding Society.
10. ANSI/AWS A5.23-97, *Specification for Low-Alloy Steel Electrodes and Fluxes for Submerged Arc Welding.* 1997. Miami, Fla.: American Welding Society.
11. Tuliani, S. S., Boniszewski, T., and Eaton, N. F. 1969. Notch toughness of commercial submerged arc weld metal. *Welding Met. Fab.*, 37, pp. 327–339.
12. Vercesi, J., and Surian, E. 1996. The effect of welding parameters on high-strength SMAW all-weld-metal — Part 1: AWS E11018M. IIS-IIW Doc II-A-915-94. *Welding Journal* 75(6): 191-s to 196-s.
13. Vercesi, J., and Surian, E. 1997. The effect of welding parameters on high-strength SMAW all-weld-metal. Part 2: AWS E10018M and E12018M. IIW-IIS Doc II-A-934-94. *Welding Journal* 77(4): 164-s to 171-s.
14. Ramini de Rissone, M., Svoboda, H., Surian, E., and de Vedia, L. 2005. Influence of procedure variables on C-Mn-Ni-Mo metal cored wire ferritic all-weld metal. *Welding Journal* 84(9): 139-s to 148-s.
15. Surian, E., and Vercesi, J. 1997. The effect of welding parameters on high strength flux cored arc welding (FCAW) all-weld metal. Presented at the 78th AWS Annual Meeting, April 13–17, Los Angeles, Calif.
16. Surian, E., Svoboda, H., Ramini de Rissone, N. M., and de Vedia, L. 2005. Influence of procedure variables on C-Mn-Ni-Mo ANSI/AWS A5.29-98 E111T5-K3/K4 metal cored wire ferritic all-weld metal. *Proceedings of the 7th International Conference Trends in Welding Research*, Pine Mountain, Ga.
17. Evans, G. 1980. Effect of Mn on the microstructure and properties of all-weld-metal deposits. *Welding Journal* 59(3): 67-s to 76-s.
18. Evans, G. M. 1986. Effect of silicon on the microstructure and properties of C-Mn all-weld-metal deposits. *Metal Construction* 18(7): 438R–444R.
19. Guide to the light microscope examination of ferrite steel weld metals. 1988. IIW Doc. IX-1533-88.
20. Schnadt, H. M., and Leinhard, E. W. 1963. Experimental investigation of the sharp-notch behavior of 60 steels at different temperature and strain rates. IIW-IIS Doc. 196-343-63.
21. Evans, G. M. 1979. The effect of heat input on the microstructure and properties of C-Mn all-weld-metal deposits. *Welding Journal* 61(4): 125-s to 132-s.
22. Ramini de Rissone, N. M., de S. Bott, I., de Vedia, L., and Surian, E. 2003. Effect of welding procedure (welding position, number of layers, arc energy, and shielding gas type) on ANSI/AWS A5.20-95 E71T1 flux cored wire deposits. *Science and Technology of Welding and Joining* 8(2): 113–122.
23. Ramini de Rissone, N. M., de S. Bott, I., Jorge, C. F. I., Corvalan, P., and Surian, E. 1997. AWS A5.1-91 E6013 Rutile electrodes: The effect of Wollastonite Part 1: on diffusible hydrogen, operational behavior and all-weld metal properties. *Welding Journal* 76(11): 1-s to 4-s.
24. Boniszewski, T., and Malsingh, I. 1996. Studies of AWS E6013 rutile electrodes. Part 6: Generation of acicular ferrite. IIW Doc. II-A-975-96.
25. Surian, E. 1997. ANSI/AWS E7024 SMAW electrode: The effect of coating magnesium additions. Part 1: on operational behavior, diffusible hydrogen and all-weld-metal mechanical properties and microstructure. *Welding Journal* 76(10): 404-s to 411-s.
26. Evans, G. M. 1988. The influence of molybdenum on the microstructure and properties of C-Mn all-weld-metal deposits. *Join. Mat.* 1(5): 239-s to 246-s.
27. Evans, G. M. 1989. The effect of chromium on the microstructure and properties of C-Mn all-weld-metal deposits. *Weld. Met. Fab.* 57(7): 346–358.
28. Surian, E., Trotti, J., Cassanelli, A. N., and de Vedia, L. 1987. Influence of Mn content on mechanical properties and microstructure of a high strength SMA electrode weld metal. IIW-IIS Doc. II-A-724-87.
29. Evans, G. L. 1983. Effect of carbon on the microstructure and properties of C-Mn all-weld-metal deposits. *Welding Journal* 62(11): 313-s to 320-s.
30. Surian, E., Trotti, J., Cassanelli, L. A., and de Vedia, L. A. 1994. Influence of chromium on mechanical properties and microstructure of weld metal from a high strength SMA electrode. *Welding Journal* 73(3): 45-s to 53-s.
31. Surian, E., Trotti, J., Herrera, R., and de Vedia, L. A. 1991. Influence of C on mechanical properties and microstructure of weld metal from a high-strength SMA electrode. *Welding Journal* 70(6): 133-s to 140-s.
32. Evans, G. M. 1983. Effect of interpass temperature on the microstructure and properties of C-Mn all-weld-metal deposits. *Welding Res Abroad* 29(1): 13–23.
33. Dearden, J., and O'Neill, H. 1940. Guide to the selection and welding of low alloy structural steels. *Trans. Inst. Wel.* 3: 203–214.
34. Surian, E., Ramini de Rissone, M., and de Vedia, L. 2001. Influence of molybdenum on ferritic high-strength SMAW all-weld metal properties. *Welding Journal* 84(4): 53-s to 62-s.
35. Catalog of Conarco Manual Electrodes (F-C-CO-001-001).
36. Welding Consumables ESAB SeAH Corp., Catalog. SS-03-E, Rev. 7, 0101.
37. SAF Welding Consumable Catalog, edition 2000.
38. Welding Consumables. Catalog, Kobe Steel, Kobelco.


ULTRACORE
Stainless
I CHOOSE LINCOLN℠...
FOR UNPARALLELED WELDING PERFORMANCE ON
STAINLESS STEEL FABRICATION PROJECTS
New ULTRACORE® stainless flux-cored wires feature:
• All Position and Flat & Horizontal Welding Capability
• Enhanced Operator Appeal
• Superior Weld Performance
• Q2 Lot® Controlled and Tested
• ProTech® Foil Bag
Visit www.lincolnelectric.com/products/stainless for more information.
www.lincolnelectric.com
© The Lincoln Electric Co. All Rights Reserved.
AR10-07
For info go to www.aws.org/ad-index
LINCOLN® ELECTRIC
THE WELDING EXPERTS®